T2R2 東京科学大学 リサーチリポジトリ
Science Tokyo Research Repository

論文 / 著書情報
Article / Book Information

題目(和文)	
Title(English)	Miniaturized Olfactory Display Using Electroosmotic Flow SAW Streaming for Instantaneous Multi-component Odor Presentation
著者(和文)	ｱｰﾘﾔｸﾝ ﾖｯｼﾘ
Author(English)	Yossiri Ariyakul
出典(和文)	学位:博士（学術）, 学位授与機関:東京工業大学, 報告番号:甲第9338号, 授与年月日:2013年9月25日, 学位の種別:課程博士, 審査員:中本 高道,岩本 光正,中川 茂樹,間中 孝彰,長谷川 晶一,柳田 康幸
Citation(English)	Degree:Doctor (Academic), Conferring organization: Tokyo Institute of Technology, Report number:甲第9338号, Conferred date:2013/9/25, Degree Type:Course doctor, Examiner:,,,,,
学位種別(和文)	博士論文
Type(English)	Doctoral Thesis

Powered by T2R2 (Science Tokyo Research Repository)

Miniaturized Olfactory Display Using Electroosmotic Flow and SAW Streaming for Instantaneous Multi-component Odor Presentation

by
Yossiri Ariyakul

A dissertation submitted to
The Department of Physical Electronics
in partial fulfillment of the requirements
for the degree of
Doctor of Philosophy
in the subject of Engineering

Tokyo Institute of Technology
August 2013

Doctoral Committee

Advisor:

Takamichi Nakamoto, Dr.Eng.

Professor, Department of Computational Intelligence and Systems Science, Tokyo Institute of Technology

Members:

Mitsumasa Iwamoto, Dr.Eng.

Professor, Department of Physical Electronics, Tokyo Institute of Technology

Shigeki Nakagawa, Dr.Eng.

Professor, Department of Physical Electronics, Tokyo Institute of Technology

Takaaki Manaka, Dr.Eng.

Associate Professor, Department of Physical Electronics, Tokyo Institute of Technology

Shoichi Hasegawa, Dr.Eng.

Associate Professor, Department of Computational Intelligence and Systems Science, Tokyo Institute of Technology

Yasuyuki Yanagida, Dr. Eng.

Professor, Department of Information Engineering, Meijo University

© 2013 – Yossiri Ariyakul

All rights reserved.

Abstract

Incorporating the sense of smell into media like the sense of seeing and the sense of hearing is one of the rising challenge researches. Despite the fact that olfaction is rather difficult to be handled than those two senses since it depends on chemical substances, enabling the odor stimuli into media can cause massive benefits in a variety of applications, such as entertainment, arts, education, advertisement, and medicine. For this reason, an odor presenting device or olfactory display is indispensable.

The olfactory display for all general purpose should be able to present all kinds of smells vividly and reproducibly, start and stop the odor presentation as fast as possible, adjust the intensity and amount of the presented odor precisely and in real time, and blend smells to present a variety of odors from a limited number of odor components. Additionally, it should be miniaturized and does not produce any disturbance such as noise or heat. Even though a variety of olfactory displays have been developed based on various techniques and standards, the olfactory display that can be used appropriately in all general usage still does not exist.

In this study, electroosmotic pumps and a SAW (Surface Acoustic Wave) device were utilized to propose the olfactory display that presents scents by atomization. The electroosmotic pump conveyed tiny odorant droplets onto the SAW device so that the droplet can be atomized into smell. At the first stage of the research, the approaches to use the electroosmotic pumps and the SAW device effectively were investigated individually. The experimental results showed that the SAW device can atomize odorant droplets into vapor and its atomization capability can be enhanced by increasing the number of its IDT pairs. Besides, the pump should be driven by a one shot pulse or DC voltage so that the amount of a droplet can be adjusted by varying the pulse width or amplitude of the applied voltage.

The preliminary olfactory display was developed by cooperating the electroosmotic pumps and SAW device together. Its capability to present odor using SAW atomization was confirmed through an odor sensing system. The odor sensing system was then improved to

be more suitable to measure the intensity of a vapor released by SAW atomization. The capability to control odor intensity by adjusting pulse width of the driving pulse applied to the electroosmotic pump was confirmed. However, it was found that the atomization performance was still not sufficient to atomize a droplet of an odorant with low volatility completely. Thus, the SAW device with higher performance was then developed.

Subsequently, the device structure was improved by using two metal blocks to maintain the device structure. The device consists of six electroosmotic pumps and a SAW device. Very thin stainless tubes were placed closely to the SAW propagation path to supply the liquid droplets to be atomized. Based on this configuration, the repeatability of the released odor was improved from the preliminary device. According to the experimental results, this six-component olfactory display can present even the scents of low volatile substances rapidly and it its capability to control the intensity of the released odor were also confirmed.

Subsequently, in order to further miniaturize the dimension of the entire device, the new structure of the olfactory display was developed on a single PCB (Printed Circuit Board). Even though the device was composed of eight electroosmotic pumps, its size is rather smaller than any other odor blender and compact enough to be equipped on a headset. Its atomization performance was also enhanced by developing a higher-performance SAW device. As a result, it can atomize some odorants that the previous olfactory display cannot such as, vanilla flavor and some odorants in perfumes. The capability to blend smells was also confirmed by using the odor sensing system.

However, due to the fact that the sensor response obtained from the gas sensor did not return to the baseline, sensory evaluation technique was also performed to verify whether it was caused by the odor residue on the device or in the sensor cell. As a result, the participants did not feel any smell remaining on the device. Subsequently, a visual-olfactory system was developed to verify the proposed olfactory display in practical use. An experiment was performed to verify whether participants can feel the fragrant of Eau de Givenchy, a perfume

with relatively low volatility, presented by the system. The result shows that all participants could feel the smell when it is presented. The validity of the proposed olfactory display was confirmed.

In conclusion, the proposed device can present odors abruptly even the scents of low volatile substances. It can adjust the intensity and amount of the presented odor and can blend smells without producing heat to the nearby environment. Thus, the purpose of this research was achieved.

Thesis advisor: Dr. Takamichi Nakamoto

Professor, Department of Computational Intelligence and Systems Science

Acknowledgements

This doctoral dissertation is the result of my research for many years in Nakamoto Laboratory in the Department of Physical Electronics at Tokyo Institute of Technology. Having started as a research student here in 2008, I certainly did not imagine completing a Ph.D. degree with these impressive achievements. This task is uneasy and very time-consuming but fulfilling at last. It would not have been accomplished without help and support from many people along this long journey. I would like to express my sincere gratitude to all of them.

First and foremost I would like to express my deeply gratitude to my academic advisor, Prof. Takamichi Nakamoto, who welcomed me to his laboratory in 2008. Without his patiently guidance, his helpful discussions, his generous support, his careful attention, and his inspirational encouragements during these past five and a half years, I could never finish this work. I have learned a lot from him how a good advisor should be. Our discussions have been very helpful not only for my doctoral study but also for the development of my professional career.

I also would like to express my appreciation to Prof. Yasuyuki Yanagida of the Meijo University, Prof. Shoichi Hasegawa, Prof. Mitsumasa Iwamoto, Prof. Shigeki Nakagawa, and Prof. Takaaki Manaka of Tokyo Institute of Technology for taking the time to be members of the doctoral committee for this thesis. I wish to thank Prof. Makoto Konagai and Prof. Akira Yamada for taking the time to attain my preliminary examination as well. All of their detailed and insightful comments broadened my perspective on the development of this work.

This research would not have been possible without funding support from Royal Thai Government Scholarship which has covered all of my personal expenses until I pursue the doctoral degree. I am deeply indebted to all Thai people whose taxes have been contributed to help me doing this work smoothly and competently. I would like to express my honest appreciation to all of them. I also would like to thank the Office of Educational Affairs at the Royal Thai Embassy in Tokyo, the National Science and Technology Development Agency,

and the Office of the Civil Service Commission of Thailand for their great assistance and facilitation.

This research was partially supported by the Japan Society for the Promotion of Science, Grant-in-aid for Scientific Research No. 2230073 and 25540120, which I gratefully acknowledge. Some expenses relating with this research was also supported by Global COE Photonics Integration-Core Electronics. My deeply thanks to Prof. Fumio Koyama and Prof. Shunri Oda, the former and present person in charge of this program respectively. I am also very grateful to my mentor in this program, Prof. Kiyomichi Araki of Tokyo Institute of Technology. Our discussion broadened my viewpoint on the practical application of this work.

Members of Nakamoto Laboratory also deserve my gratitude. I give my heartfelt thanks to Dr. Bartosz Wyszynski who kindly provided me with the QCM gas sensors, Mr. Yuki Harada who recommended an appropriate odorant for the experiment in this study to me, Mr. Masaaki Iseki, Mr. Yushi Hosoda and Mr. Tomoyuki Aizawa who worked with me professionally and patiently, Mrs Kazuko Makiyama who supported my work tidily. A number of current and former members of Nakamoto Laboratory also helped me in various ways. I give my sincere thanks to all of them. In particular, thank Mr. Kim Dae-ho, a colleague who shared the best and worst moments of my journey during 2008 - 2012.

From April 2011 to March 2012, I was a student secretary at the Doctoral Student Forum (DSF) in Global COE Photonics Integration-Core Electronics. The program leader Prof. Fumio Koyama, Managing Professor Masayuki Izutsu and Prof. Tetsuya Mizumoto gave us a lot of good advice for DSF activities. I have also learned a lot from working with other DSF secretaries including Dr. Masao Yamagishi, Dr. Takayuki Nozaki, Dr. Hayato Sano, Dr. Daisuke Tanaka, Dr. Ryo Miyazawa, Mr. Shuichi Kondo, Ms. Wang Cui, and Mr. Liu Xuan. Although the activity was not directly related to my research, the experience of managing the forum provided me with good leadership and interpersonal skill trainings. I would like to thank all of them.

I also would like to thank Prof. Atsushi Saitoh of Shibaura Institute of Technology for his generosity. He did provide me with the first SAW device and gave me valuable advice when I had a problem in the initial state of my research. I am also grateful to Prof. Hiroshi Ishida of Tokyo University of Agriculture and Technology for his accurate advice which helped me solving a problem about unstable airflow in an air pump. I also thank Mr. Junichi Ide of T. Hasegawa Co., Ltd. Most of the odorants I used were provided by him.

I would like to pay respect to all of my former teachers for encouraging me to be disciplined, prompt, diligent, and gentle. They not only sharpened my knowledge, but also taught me how to live virtuously and generously. I will forever be thankful to all of them.

Finally, I would like to dedicate this work to my family. They have provided me with unconditional love and indescribable support throughout my life. I am indebted to my father, Thanachoti Ariyakul. He worked industriously and wholeheartedly to provide the best possible environment for me to grow up and attend the best possible school. I am very grateful to my mother, Siriwan Ariyakul. She always understands me, trusts in me, encourages me, and supports me with her everlasting love. I also thanks my aunt, Pornpim Ariyakul, my grandmother, Muisim Sae-ao, and my grandfather, Hiangjue Sae-tie. All of them worked hard and lived frugally to build a wealthy family in which their descendants would live comfortably. They looked after me since I was born and always taught me to be principled and honest. I remember their warm love and my grandmother's delicious dishes well. Although my grandfather is no longer with us, his goodness is forever remembered.

Contents

Abstracts iii
Acknowledgements vi
Contents ix

Chapter 1 Introduction
1.1 Background 1
1.2 Structure of Smell 2
1.2.1 Lucretius's philosophy
1.2.2 Wright's vibrational theory
1.2.3 Amoore's stereochemical theory
1.2.4 Turin's spectroscopic theory
1.2.5 Proposed theories on primary smells
1.3 Importance of Smells 13
1.4 Human Olfactory System 14
1.2.1 Odorant receptor
1.2.2 Signal transduction
1.2.4 Sensory test
1.5 Basics of Olfactory Display 25
1.6 Fundamental Technologies in Olfactory Display 26
1.6.1 Scent generation method
1.6.2 Scent delivery method
1.7 Case Studies of Olfactory Displays 35
1.7.1 Magnum opus Sensorama
1.7.2 iSmell
1.7.3 Olfactory display using high speed switching solenoid valves
1.7.4 Olfactory display using inkjet devices
1.7.5 Olfactory display using temperature responsive gel
1.7.6 Olfactory display using air cannon

1.7.7 Wearable olfactory
1.7.8 Scent Collar
1.7.9 Odor presentation on a LCD screen
1.7.10 Micro aroma shooter (MAS)
1.7.11 Olfactory display connected with smartphone
1.7.12 Olfactory display using on-off switchable device
1.7.13 Olfactory display using MEMS actuator
1.7.14 Comparison
1.8 Research Purpose 60

Chapter 2 Development of a SAW Device for Liquid Droplet Atomization Using SAW Streaming
2.1 Introduction 63
2.2 Principles of SAW Device.....64
2.3.1 Surface acoustic wave (SAW)
2.3.2 SAW device
2.3.3 SAW streaming
2.3 Development of 11 x 11 *mm* SAW Device 71
2.4 Evaluation of 11 x 11 *mm* SAW Device.....74
2.4.1 Resonant frequency measurement
2.4.2 Evaluation of the atomization performance
2.5 Development of 11 x 19 *mm* SAW Device 77
2.6 Liquid Atomization Using 11 x 19 *mm* SAW Device 79
2.6.1 Investigation on threshold voltage of liquid droplet atomization
2.6.2 Observation of liquid residue after atomization
2.7 Summary 83

Chapter 3 Study on Conveying Liquid Odorant Using an Electroosmotic Pump
3.1 Introduction 84
3.2 Basics of Electroosmotic Pump 85

3.2.1 Electroosmotic flow
3.2.2 Electroosmotic pump
3.3 Characteristics of electroosmotic pump in this study 92
3.4 Investigation on Effective Approach to Use Electroosmotic Pump in Olfactory Display 94
3.4.1 Investigation on pump driving method
3.4.2 Investigation on method to suppress droplet volume
3.5 Measurement of Parameters Affecting Odor Presentation.....98
3.5.1 Measurement of start-up time
3.5.2 Measurement of droplet's volume
3.6 Summary 102

Chapter 4 Fundamental Study of an Olfactory Display Using Electroosmotic Pumps and a SAW Device
4.1 Introduction 104
4.2 Concept of Olfactory Display Using Electroosmotic Pump and SAW Device 105
4.3 Preliminary Development of Olfactory Display Using Electroosmotic Pump and 11 x 19 *mm* SAW Device 108
4.3.1 Preparation of 11 x 19 *mm* SAW device
4.3.2 Consideration on method to drive the SAW device
4.3.3 Consideration on solvent for odorant dilution
4.3.4 Arrangement of electroosmotic pumps and SAW device in preliminary olfactory display
4.4 Evaluation of Olfactory Display Using Electroosmotic Pumps and 11 x 19 *mm* SAW Device Based on Odor Sensing System 115
4.4.1 Principle of odor sensing system using QCM gas sensor
4.4.2 Measurement of odor vapor released from SAW atomization
4.4.3 Investigation on methods to control intensity of odor vapor
4.5 Evaluation of Olfactory Display Using Electroosmotic Pumps and 11 x 19 *mm* SAW Device Based on Improved Odor Sensing System 122

4.5.1 Improvement of odor sensing system using QCM gas sensor
4.5.2 Investigation on atomization performance at different positions
4.5.3 Evaluation of method to control intensity of odor vapor
4.5.4 Measurement of odor vapor of substance with low volatility generated from SAW atomization
4.6 Summary 131

Chapter 5 Development of a Miniaturized Six-component Olfactory Display Using Electroosmotic Pumps and a SAW Device for Presenting Scents of Low-volatile Substances
5.1 Introduction 132
5.2 Development of Miniaturized Six-component Olfactory Display Using Electroosmotic Pumps and SAW Device 133
5.3 Development of 14 x 25.5 *mm* SAW Device 139
5.4 Investigation on Appropriate Condition to Drive SAW Device 144
5.5 Evaluation of Olfactory Display Using Electroosmotic Pumps and 14 x 25.5 *mm* SAW Device Based on Improved Odor Sensing System 145
5.5.1 Evaluation of capability to control odor intensity
5.5.2 Evaluation of capability to blend multiple of odors
5.5.3 Evaluation of dynamic range and resolution
5.6 Summary 153

Chapter 6 Development of an Eight-component Wearable Olfactory Display Using Electroosmotic Pumps and SAW Device for Presenting Scents of Low-volatile Substances
6.1 Introduction 155
6.2 Problem of Insufficient Atomization Performance 156
6.3 Development of 14 x 27.5 *mm* SAW Device 157
6.4 Investigation on Appropriate Condition to Drive SAW Device 161

6.5 Development of Wearable Eight-component Olfactory Display Using Electroosmotic Pumps and SAW Device 162
6.6 Evaluation of Olfactory Display Using Electroosmotic Pumps and 14 x 27.5 *mm* SAW Device Based on Improved Odor Sensing System 168
6.6.1 Evaluation of dynamic range and resolution of moderate-volatile odor presentation
6.6.2 Evaluation of dynamic range and resolution of low-volatile odor presentation
6.6.3 Evaluation of capability to blend multiple of odors
6.7 Summary 174

Chapter 7 Evaluation of an Eight-component Wearable Olfactory Display Using Electroosmotic Pumps and a SAW Device Based on Sensory Evaluation
7.1 Introduction 176
7.2 Evaluation of Timing of Odor Presentation Based on Sensory Evaluation 177
7.2.1 Preliminary experiment
7.2.2 Main experiment
7.3 Evaluation of Timing of Odor Presentation Using Sensory Evaluation 181
7.4 Development of Visual-olfactory Presentation System 183

7.5 Evaluation of Visual-olfactory Presentation System Based on Sensory Evaluation ..184
7.6 Summary 186

Chapter 8 Conclusions
8.1 Conclusions 188
8.2 Future Perspective 190

Publications 191
Bibiography 194

Chapter 1
Introduction

1.1 Background

This dissertation describes about the development of a miniaturized multi-component olfactory display using electroosmotic pumps and SAW (Surface Acoustic Wave) device. In this first chapter, the reviews of basics of olfactory display, related technologies, and relevant researches are described.

As olfactory displays are the devices presenting smells to human's nose, understanding about the structure of odors and human olfactory system are necessary for the reader to be comprehended. Thus, Section 1.2 in this chapter starts with the descriptions about theories on structure of odors, including Lucretius's theory, Wright's vibrational theory, Amoore's stereochemical theory, and Turin's spectroscopic theory. In Sections 1.3 and 1.4, the details about importance of odors and human olfactory system are described, respectively.

The detail about basics of olfactory displays is introduced in Section 1.5 in order to help the reader who might not be familiar with this research field. In Section 1.6, the related technologies which can be used to generate and delivery smells are described. In Section 1.7, various types of olfactory displays which have been developed and their comparison are described. Lastly, the purpose of this research is described in Section 1.8.

1.2 Structure of Smell

Even though the sense of smell is both ancient and ubiquitous, mechanism of smell remains the most poorly understood among all our senses. The first description of molecular theory of smell interaction was provided two thousand years ago. Since then, various assumptions have been suggested and rejected. At present, even though the chemistry of smell is still not fully understood, various useful models have been developed to explain the interaction. The detail about Lucretius's philosophy is described in Section 1.2.1 and the details on useful theory in the last fifty years including Wright's vibrational theory, Amoore's stereochemical theory, and Turin's spectroscopic theory are described chronologically in Sections 2.2.2 to 2.2.4.

1.2.1 Lucretius's philosophy

The nature of smell was firstly explained two thousand years ago by Titus Lucretius Carus, a Roman poet and philosopher [Lucretius47BC]. According to the fourth book of his famous poem, De rerum natura (On the Nature of Things), there are plenty of things we can't see but nevertheless know existence, such as wind, smells, heat and cold. There are many smelling objects which flow out and roll along. These objects are emitted, flowing out and scattering in all directions along the wind. The smells are varied by their shapes. Some smells are easier to be identified by some animals, such as scent of honey that is sensitive to bees or scents of wild-animals that are sensitive to hunting-dogs, respectively. Some smells can travel longer than others. However, none of them travels as far as sound.

Even though his explanation is simple without more detail about how our nostrils feel smells and how the smell particles look like, it is considered as the first beginning opinion about smells [Philip2009].

1.2.2 Wright's vibrational theory

The basic assumption of the chemistry of smells was proposed by Wright [Wright1964-1]. He claimed that the essential quality of odors mainly depend on their vibrational movement of the odorous molecules with some minor effect on the strength of odors from volatility, water-or-lipid-solubility, adsorbability, and so on. He also supposed that the molecular vibrations would be at frequencies below about 300 to 400 cm^{-1} but not below about 50 to 60 cm^{-1}. This provides about 25 primary odors which can be combined in a various ways. Most of odorous substances are complex and do not contain only one primary odor. He performed an experiment using musk and nonmusk perfumes to verify his hypothesis. In the experiments, the positions of the so-far observed infrared absorption peaks were observed by using a Far Infrared Spectrophotometer. The obtained results of musk-like odors and nonmusk-like odor are shown in Figs. 1.1 and 1.2, respectively.

The result in Fig. 1.1 shows the monotonous consistency of the infrared spectra to the structure of sample which similarly consists of large closed loops of $-CH_2-$ groups whereas it could not be observed in the result in Fig. 1.2. However, these results still were not sufficient to establish the vibrational theory unequivocally. Even though, this hypothesis explained why some molecularly dissimilar molecules had similar smells, Wright did not explain the mechanism by which the olfactory cells detect the vibrations of odorous molecules.

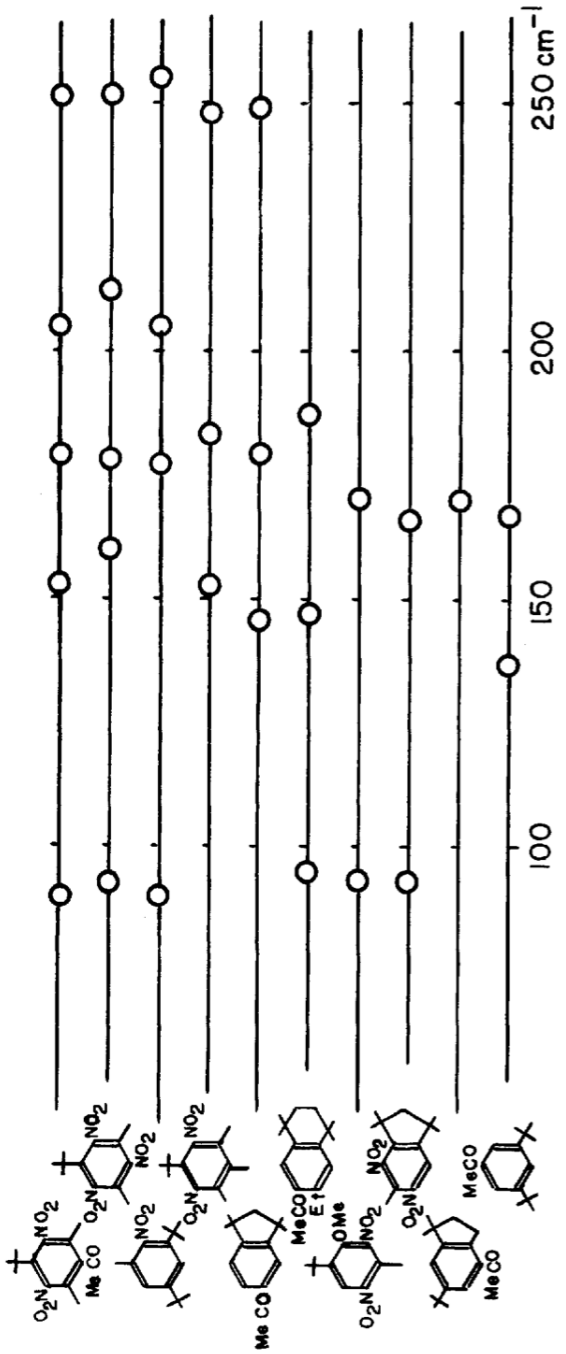


Fig. 1.1 Musk perfumes (top to bottom); musk ketone, musk xylol, 2-nitro-3,5-di-tert.-butyl toluene, musk tibetene, 5-acetyle1-1,1,1,3-tetra-methyl indane, versalide, musk ambrette, moskene, 4-acetyl-1,1-di-methyl-6-tert.-butyl indame, 3,5-di-tert.butyl acetophenone [Wright1964-2].

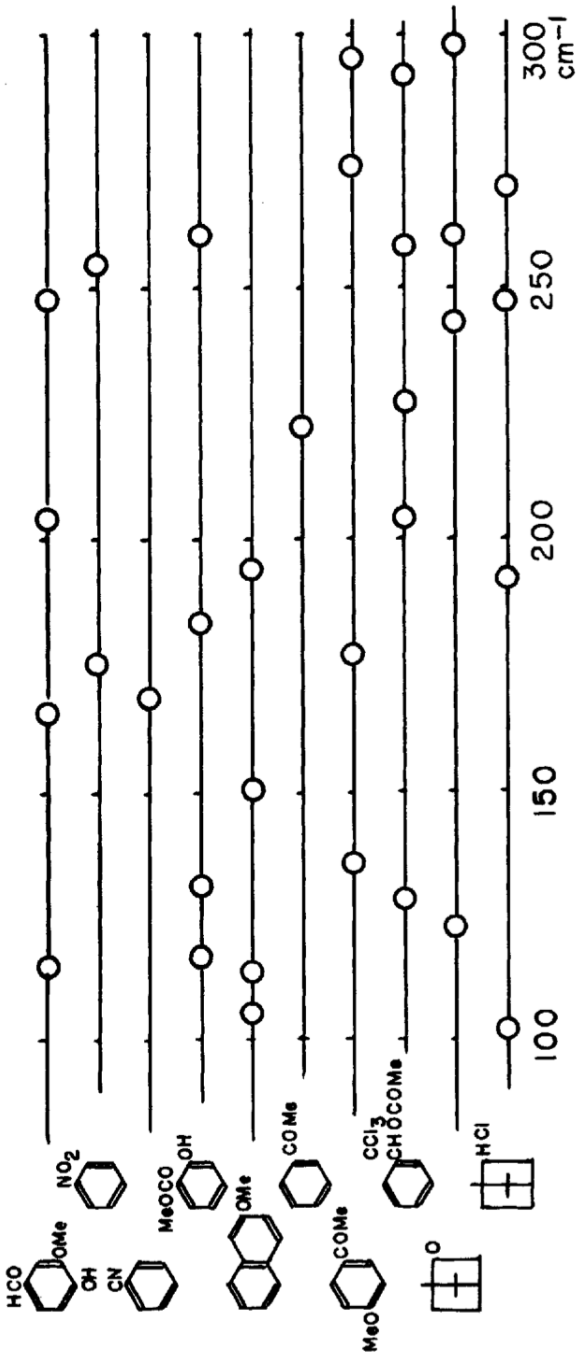


Fig. 1.2 Nonmusk perfumes (top to bottom); vanillin, nitrobenzene, benzonitrile, methyl salicylate, methyl-beta-naphthyl ether, acetophenone, p-methoxy acetophenone, rosetone, camphor, bornyl chloride [Wright1964-2].

1.2.3 Amoore's stereochemical theory

This theory was first proposed by Amoore. It states that quality of odors are determined primarily by its molecular dimension [Amoore1963]. Thus, the similar odors are likely to have similar molecular size and shape, and the different odors represents the distinct molecular profile. The theory also states that the odorous molecule can be classified into two categories; rigid and flexible ones. The former is unlikely to fit snugly into more than one kind of olfactory receptor, whereas the latter can rearrange their contours to fit more kinds of olfactory receptor. Amoore proposed that there are seven different types of primary odors which are ethereal, camphor-aceous, musky, floral, minty, pungent, and putrid. All of them have corresponding olfactory receptors. Thus, this mechanism is also called a "lock and key" mechanism by which a scent molecule fits into olfactory receptors in the nasal epithelium.

The first three primary odors depend mainly upon molecular size. The ethereal site is a narrow slot that accepts only very small or thin molecules. The camphor site is a roughly hemispherical basin. The musky site is a larger, elliptical, and flat bottomed pan which requires a big disk-shaped molecule to fill it adequately. The next two primary odors result from molecular shapes rather than size. The floral receptor site is roughly keyhole shaped into which the notably kite-shaped molecules can be expected to fit. The minty site is for wedge-shaped molecules. The final two primary odors depend not at all upon molecular size or shape but on the electrical status of the odorous molecule. Thus, the pungent odor is caused by strongly electrophilic molecules, and the putrid odor by nucleophilic molecules, respectively. The corresponding receptor sites have the opposite electrical properties. The profile of corresponding receptors to those primary odors are shown in Fig. 1.3 and the models described how the primary odor molecules can be sensed by the corresponding receptors are shown in Fig. 1.4, respectively.

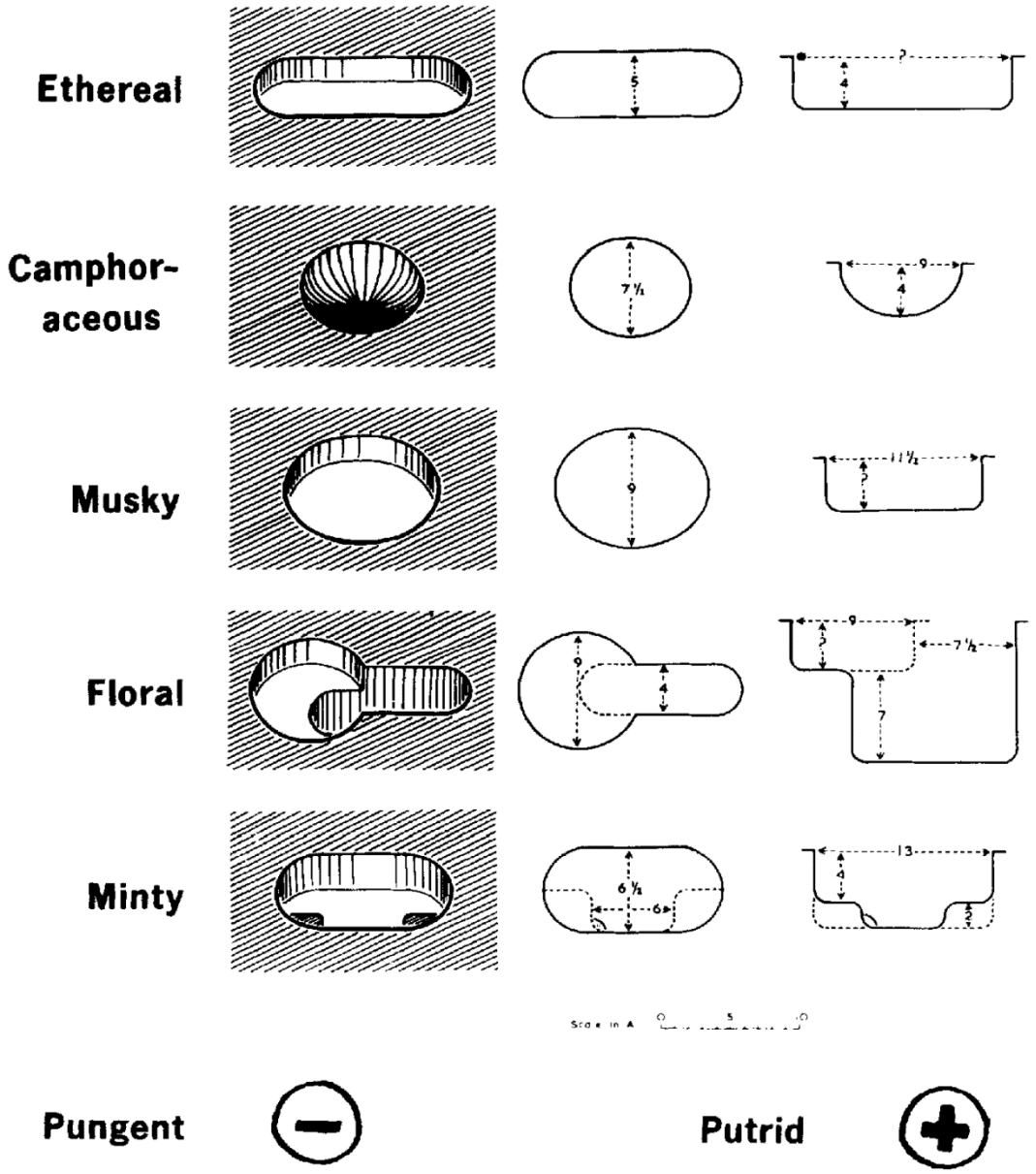


Fig. 1.3 The human olfactory receptors corresponding with the seven primary odors. The left side shows oblique perspective drawings. The center shows the top-viewed images. The right side shows the front-viewed images. The dimensions are in ⊠ units [Amoore1964].

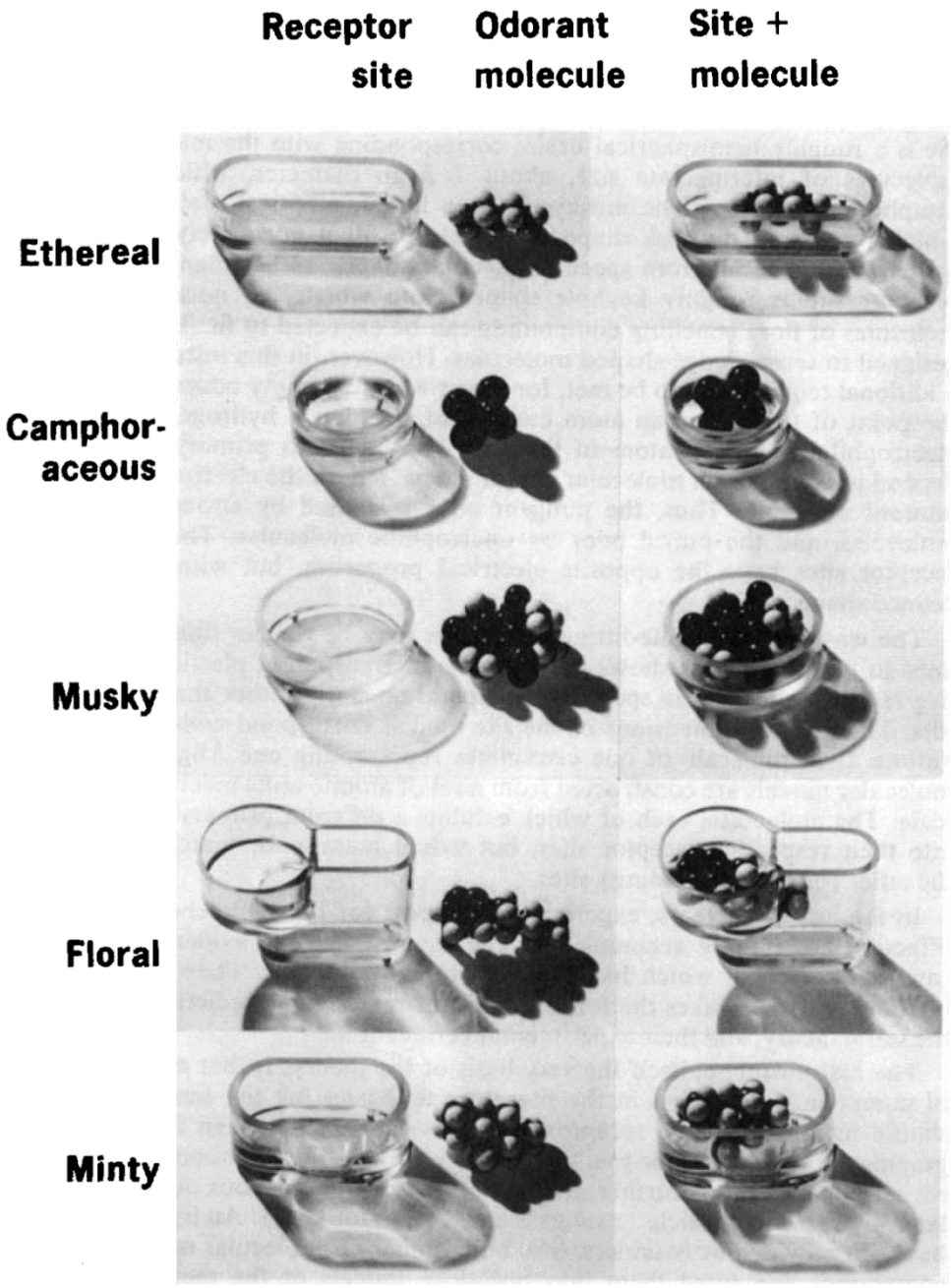


Fig. 1.4 Scale model of olfactory receptor site and odorant molecules [Amoore1964].

At present, Amoore theory remains useful since it can explain more scents and their mechanism. However, the number of primary odors in this theory are not sufficient because it cannot explain some odor phenomena, which are described in the Section 1.2.4. The actual primary odors still have not been discovered nowadays or they might not really exist [Auffarth2013].

1.2.4 Turin's spectroscopic theory

In 1985, Wright's theory [Wright1977] was further extended by Turin. His theory describes that the olfactory receptors respond not to the shape of the molecules but to their vibration as same as in the sense of seeing in which the red, green and blue cones and the gray scale rods in the eyes detect the frequencies of the electromagnetic vibration, and in the sense of hearing in which the organs of the inner ear detect the frequencies of sound waves, respectively [Turin1996]. However, the calculation of the frequencies of the actual molecule vibrations is complex and difficult.

This theory differs from Wright's theory in providing a detailed and plausible mechanism for biological transduction of molecular vibrations. There are a number of different types of receptors responding to different ranges of vibrations. In the eye, millions of colors can be distinguished by only three types of receptors in the retina. In the nose there may be more than three types. In case of olfaction, there might be some smell receptors having overlapping ranges and some uncovered ranges of molecule vibrations having no smell. Turin's vibration theory of smell shows two notably outstanding evidences that Amoore's theory cannot explain as described below.

(1) Most organic molecules contain hydrogen and carbon atoms. Hydrogen exists in three isomeric forms. Its nucleus contain one proton and one electron in a shell surrounding the nucleus. As the proton has a mass about 1800 times larger than the electron, most of the mass is in the nucleus. However, the size of the hydrogen atom is

determined by the electron shell. A second form of the hydrogen atom, called deuterium, has a neutral particle, the neutron, as a nucleus. The size and shape of the deuterium atom is virtually identical to that of the simple hydrogen atom, but the mass is about twice of it. If the simple hydrogen atoms in a molecule are replaced by deuterium atoms then the molecule's shape is unaffected but its vibration frequencies are decreased significantly. In this case, the smell of synthesized deuteriated molecules differ from that of the ordinary version. Amoore's theory cannot describe this mechanism.

(2) Another definitive bit of evidence for vibration theory is that Turin found two molecules with the same vibration but different shapes that smell the same. Turin mentioned that sulfur compounds, which have a distinctive unpleasant smell, was believed that that distinctive character came from the sulfur-hydrogen bond which has a wave number of 2500 cm^{-1}. He also found a boron compound that had that same vibration had the same sulfurous smell even though its shape was completely different from that of sulfur compound. This evidence is also difficult to be explained by Amoore's theory.

Even though Turin's theory can explain molecular structure and mechanism of odors, his empirical has been criticized by some scientists that they did not achieve the same experimental results when they performed the experiments under the same conditions to technically double check his proposed theory [Keller et al.2004]. For the day-to-day purpose and simple explanation, Amoore's theory is still recommended as a simple method, even though it cannot explain some mechanism of odors [Kaye2001].

1.2.5 Proposed theories on primary smells

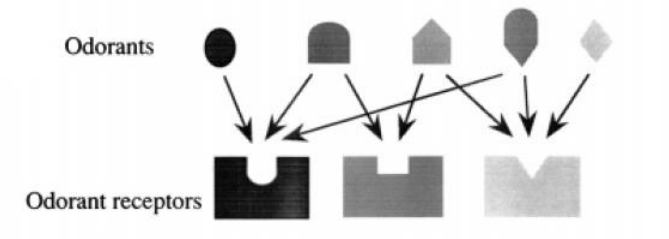
The olfactory system can discriminate among enormous chemical stimulus with different properties using approximately three hundred types of the olfactory receptors. In order to explain the coding of odor in the olfactory system, the model for the

formation of activation pattern in olfactory bulb by a combinatorial mechanism of olfactory receptor was proposed by Touhara et al. [Touhara2001] as shown in Fig. 1.5. Most of odorant molecules are recognized by more than one olfactory receptor and most of receptors recognize several odorants as shown in Fig. 1.5 (a). The structural epitopes in odorant molecules would determine the type of receptors that recognize the particular odorant. The olfactory receptor neurons with a given odorant receptor converge onto defined glomeruli in the olfactory bulb as shown in Fig. 1.5 (b). Then, the activation of the multiple receptors for the particular odorant elicits a specific spatial activation pattern in the olfactory bulb as shown in Fig. 1.5 (c).

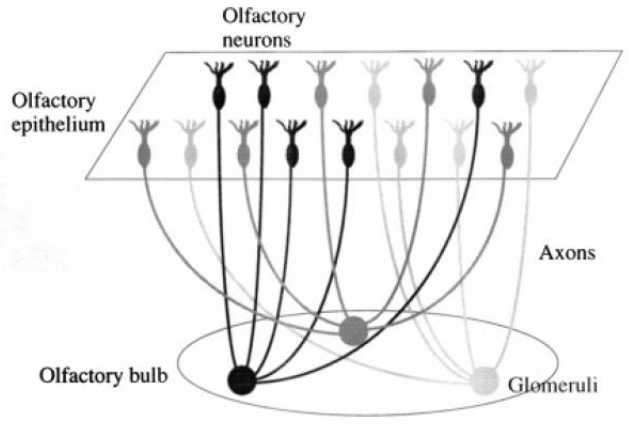
Although the odor detection mechanism of the olfactory system becomes a little known, the relationship between signals obtained from multi-olfactory receptors and molecular properties of odorants still cannot be understood due to the complicity of the olfactory system. Therefore the set of primary smells, where any impressions of smells can be expressed based on their combinations, still cannot be discovered. There were many proposed theories about the interaction mechanism between the olfactory receptors and stimuli odorant as shown in Table 1.1.

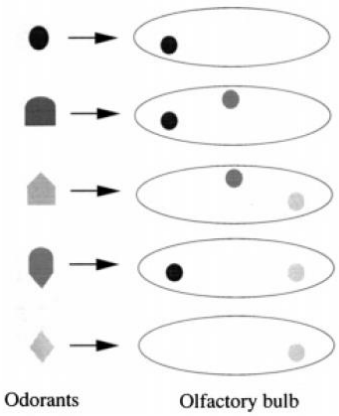
Table 1.1 Theories of olfaction.

Researcher	Theory	Reference
G.M. Dyson et al.	Molecular vibration	[Dyson1938]
J.E. Amoore et al.	Molecular shape	[Amoore1952]
J.T. Davies et al.	Diffusion pore	[Davies1959]
B. Rosenberg et al.	Piezo-effect	[Rosenberg1968]
L. Turin et al.	Nose as a spectroscope	[Turin1996]



(a)





(b) (c)

Fig. 1.5 Model for the formation of activation pattern in olfactory bulb by combinatorial mechanism of odorant-receptor interaction. [Touhara2001].

Although it somehow seems to be possible to utilize this proposed method for prediction the relationship between odorants and their response patterns of olfactory cells, this theory is still at the preliminary stage with very few consistencies. Therefore, a set of primary odors still cannot be discovered.

1.3 Importance of Smells

We have perceived the countless information via our sensory system and utilized it in many ways. At the very beginning of life, despite of any advanced knowledge or training, a newborn baby can immediately perceive information from his/her sensory system and utilize it to interact with a surrounding. After all senses such as audition, vision, touch, gustation and olfaction are well improved by learning process, human can intentionally select and utilize their senses suitable for each situation. Moreover, the integration of information from several senses is performed to deal with more complicated tasks.

In many cases, sense of olfaction is essential and takes advantage over the other senses. For example, we can examine the ripeness as well as the expiration of food by sniffing its emitted smell. We also use the olfactory information perceived from ambient atmosphere to acknowledge a leakage of gas or burning. Moreover, there are also many applications of olfactory information in medical field. Many odors known as biomarker are generally used to diagnose patient's symptoms in medical check up [Gardner2000, Fleisher2002, Natale2003]. In addition, the utilizations of odor in medical therapy called aromatherapy have been used to improve physical and mental status of the patients [Bastard2006, Imura2006, Atsumi2007].

Furthermore, not only the sufficient information for survival of life, the olfactory information also provides the unique sense of pleasure. These benefits can be obviously expressed by a large number of odorants used in food, beverage, cosmetics and daily life appliances. Due to a variety of its own unique virtues, the olfactory information is still required even though much information in audio and video formats is available.

In contrast to its importance and benefits, the olfactory information has been so far excluded from multimedia technology, while video and audio signals can be recorded and broadcasted through the communication media in real time. Moreover, image and voice recorder with satisfied recordable ranges have long been commercially available

while recording smell with limited range is still under developed. Therefore, many applications related to olfaction in multimedia still cannot be realized.

One of the main problems in realization of recording olfactory information is to mimic a function of a human olfactory system with high complexity. In the human olfactory system, more than three hundred types of receptors located in nasal mucus [Buck1991] respond to chemical stimulus, whereas only a few types of receptors contribute to the sense of vision. According to this complexity, a complete set of primary odor components still cannot be discovered while only three primary components (RGB) are sufficient for recording vision signals. Thus, recording olfactory information is still in limited range and it seems difficult to realize it based on the available systems.

Nowadays, although recording wide range of odor is still unpractical, many applications concerned about introduction of olfactory information have been growing up. For example, NTT Communication Company has started sending olfactory information to end users via internet network and a prototype model of an odor player is now commercially available. If recoding wide range of odor can be practically realized, the countless applications in many fields such as e-commerce, telemedicine, virtual environment, etc [Keller1995, Davide2001, Hirose 2002] will be induced.

1.4 Human Olfactory System

Odors are sensations that occur when odorant molecules dissolved in the air stimulate the specialized receptors in the olfactory epithelium in the top of nasal cavity. Fig. 1.6 describes how odorants are detected by sensory neurons in the olfactory epithelium of the nose and how olfactory signals are transmitted to the brain. The odorant receptors are localized on olfactory sensory neurons (OSNs), which occupy a small area in the upper part of the nasal epithelium. Every olfactory receptor (OR) cell expresses only one odorant receptor. On activation, signals from OR cells are relayed in the glomeruli.

Receptor cells of the same type are randomly distributed in the nasal mucosa but converge on the same glomerulus. In the glomerulus, the receptor nerve endings excite mitral cells that forward the signal to higher regions of the brain.

1.4.1 Odorant receptor

A decade ago, Linda Buck and Richard Axel discovered and published the mammalian family of odor receptors [Buck1991]. ORs are G-protein coupled receptors (GPCRs) similar to those known to be important in neurotransmission, photoreception (rhodopsin is a GPCR) and many other cellular processes. They found that there are as many as 1,000 genes for ORs in the mammalian genome, making it by far the largest family of GPCRs, and probably the largest gene family in the entire genome.

Humans have a poor sense of smell. Human evolution was characterized by the gradual ascendance of vision and reduction of smell [Jones1992]. Recent genetic studies show a decrease in the number of functional ORs through primate evolution to humans [Rouquier2000, Gilad2004]. Mice have approximately 1,300 ORs, of which some 1,100 are functional [Young2002, Zhang2002], whereas humans have some only some 350 functional genes of approximately 1,000 [Glusman2001, Zozulya2001]. The small number of functional ORs in humans compared with rodents is directly correlated with the evolutionary decline in the human sense of smell [Shepherd2004].

The receptor proteins are members of a well known receptor family called the 7-transmembrane domain GPCRs. Fig. 1.7 illustrates a schematic view of the three-dimensional structure of the receptor [Pilpel1999]. The hydrophobic regions (the

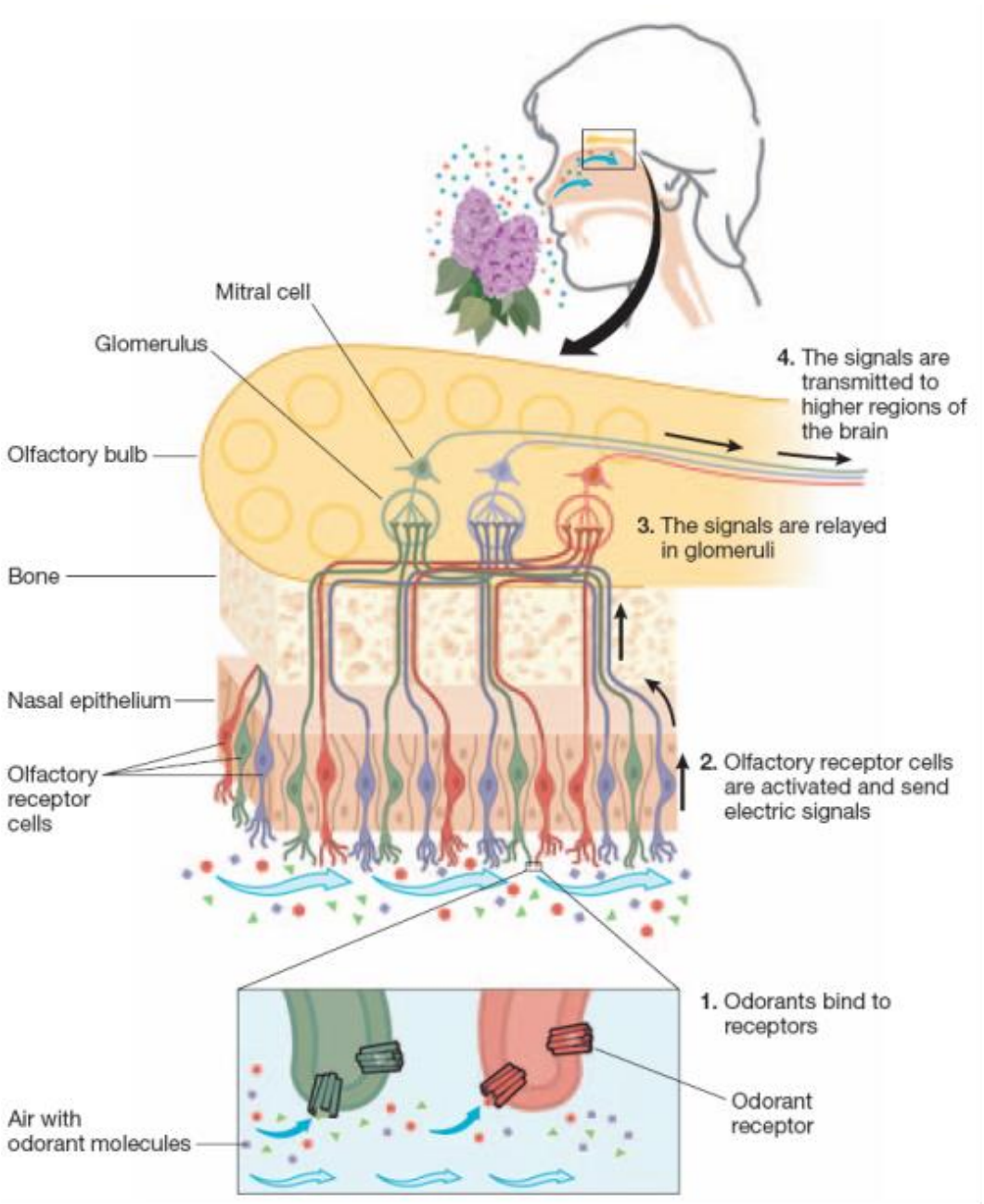


Fig. 1.6 Human olfactory system. The odorant receptors are localized on olfactory sensory neurons, which occupy a small area in the upper part of the nasal epithelium. Every olfactory receptor cell expresses only one odorant receptor. On activation, signals from olfactory receptor cells are relayed in the glomeruli. Receptor cells of the same type are randomly distributed in the nasal mucosa but converge on the same glomerulus. In the glomerulus, the receptor nerve endings excite mitral cells that forward the signal to higher regions of the brain [Rinaldi2007].

transmembrane parts) contain maximum sequence homology to other members of the G-protein linked receptor family. There are some notable features of these olfactory receptors, like the divergence in sequence in the 3rd, 4th and 5th transmembrane domains, which suggest how a large number of different odorants may be discriminated. Rodriguez et al. found Vomeronasal-like receptors (V1RL1) in the human olfactory epithelium [Rodriguez2000]. In theory, this could give humans sensitivity to pheromones. Liberles et al. discovered TAARs, a new type of receptor, in the mouse that detects volatile amines [Liberles2006]. These are found in mouse urine and convey information about stress and gender. One has been reported to be a pheromone.

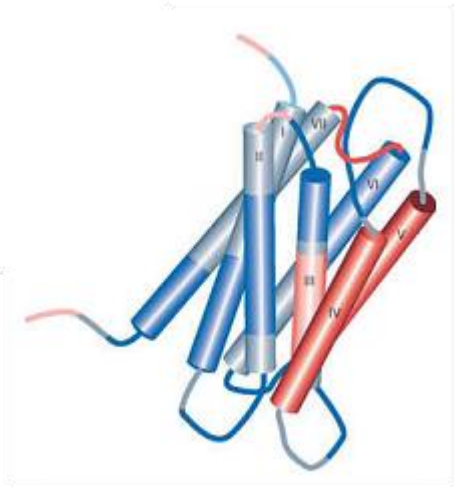


Fig. 1.7 Schematic view of the three-dimensional structure of the receptor. Each of the transmembrane regions is numbered according to that model [Firestein2001]. Red portions are hyper variable which probably determine molecular specifications.

1.4.2 Signal transduction

Once the receptor has bound an odor molecule, a cascade of events is initiated that transforms the chemical energy of binding into a neural signal. That is a change in the membrane potential of the OSN.

Fig. 1.8 illustrates the transduction of the binding of an odorant molecule to a receptor into an electrical signal that can be transmitted to the brain, within the compact cilia of the OSNs. The ligand-bound receptor activates a G-protein just close to the receptor, which in turn activates an adenylyl cyclase (AC) leading to generation of cAMP. The cAMP binds to a cyclic nucleotide-gated (CNG) channel, enabling it to conduct cations such as Na^+ and Ca^{2+} [Firestein1991]. The influx of Na^+ and Ca^{2+} ions causes the cell to reach threshold and generate an action potential in turn. The action potential then propagates along the axon and into the forebrain.

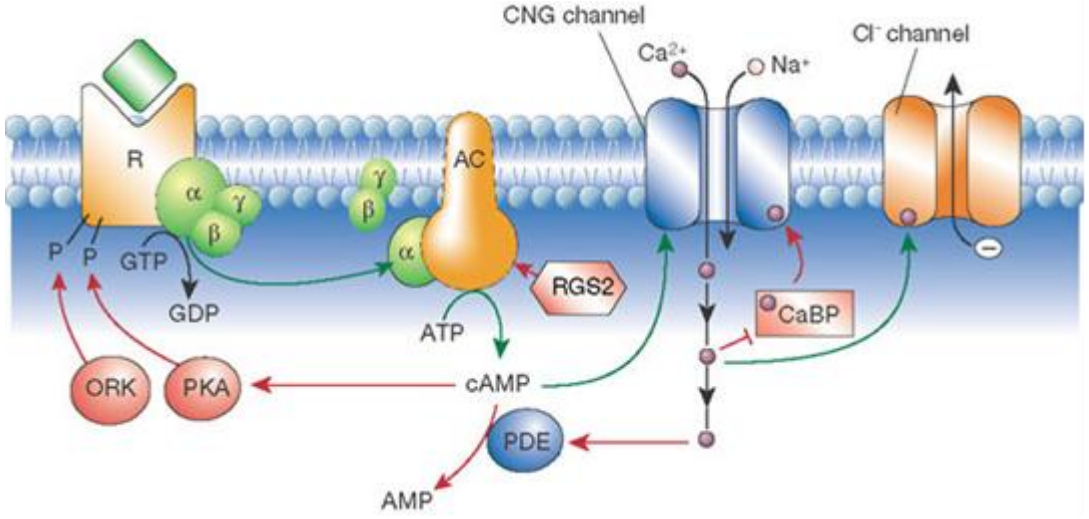


Fig. 1.8 Sensory transduction. Within the compact cilia of the OSNs a cascade of enzymatic activity transduces the binding of an odorant molecule to a receptor into an electrical signal that can be transmitted to the brain. AC, adenylyl cyclase; CNG channel, cyclic nucleotide-gated channel; PDE, phosphodiesterase; PKA, protein kinase A; ORK, olfactory receptor kinase; RGS, regulator of G proteins (but here acts on the AC); CaBP, calmodulin-binding protein. Green arrows indicate stimulatory pathways; red indicates inhibitory (feedback). [Firestein2001].

The second-messenger cascade of enzymes provides amplification and integration of odor-binding events. One membrane receptor activated by a bound odor

can in turn activate tens of G-proteins, each of which will activate a cyclase molecule capable of producing about a thousand molecules of cAMP per second. It seems that a single odor molecule can produce a measurable electrical event in an OSN and just a few channels opening together could pass sufficient current to induce action-potential generation [Lynch1989, Menini1995].

1.4.3 Sensory test

Sensory test or olfactory test is the conventional method for evaluation of odor. Although many analytical techniques such as GC/MS (Gas chromatography/mass spectrometry) etc. are available, the sensory test is necessary because human impression and human detection limit to the tested odor can be expressed in the form of sensory-test result. There are many methods of sensory test as shown in Table 1.2 [Sato1978]. These sensory tests are selected and used in several purposes. For example, the triangle test is used to evaluate the similarity between odor samples. In this sensory test, 3 bags; 1 with sample A and 2 with sample B in them are given to a subject as shown in Fig. 1.9. Then he/she is requested to select one bag different from the other two. This method also can be used to measure threshold concentration of odor.

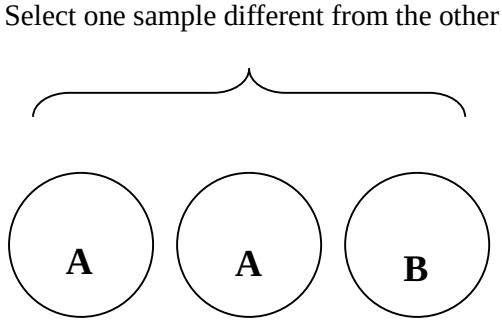


Fig. 1.9 Triangle test method.

Table 1-2 Sensory test methods [Sato1978].

Purpose	Representative methods
Description of characteristics	SD (semantic differential) method, Profile method, QDA (quantitative descriptive analysis) method
Difference test	Triangle test, Paired difference test, Duo-trio test, Dual-standard test, Single-sample test, Sorting test, Matching test
Preference test	Paired preference test, Triangle preference test
Method of choice	Method of choice
Ranking	Ranking method
Rating	Rating method
Scoring	Scoring method
Paired comparison	Paired comparison method
Psychophysical constant	Psychophysical methods
Distance scale	Method of composite standard, Method of successive categories
Ratio scale	Method of magnitude estimation, Method of fractionation
Search for data structure	Factor analysis, Multidimensional scaling method
Classification	Factor analysis, Multidimensional scaling method, Cluster analysis
Estimation	Regression analysis, Multiple regression analysis
Discrimination	Fisher's discriminant function
Search for optimal value	Rank correlation coefficient method, Composite design, Simplex lattice design

In the case of threshold concentration measurement, 3 bags; 1 with a sample in it and 2 without sample (odor-free air) are given to a subject. The subject was asked to choose the odorous bag. If the subject can correctly identify the bag with the sample, the odor is then diluted and the test is continued until it becomes impossible to identify the bag with odor.

Nowadays, Quantitative Descriptive Analysis (QDA) method is frequency used for evaluation of the industrial products [Murray2001, Jacobsson2004, Krumbein2004]. The goal of this method is to provide a quantitative specification of the important sensory aspects of the product. The panelists for QDA methodology were recruited and were screened with olfactory test and questionnaires. The panelists who had successfully passed standardized tests for olfactory, taste and color sensitivity as well as for memorization, verbal abilities were selected. The language source in QDA is non-technical, everyday language, to avoid biasing response behavior. The panel is trained over a period of perhaps 10–15 hours to understand the meaning of the attributes. Results of successful QDA strategy indicate that the panelists are calibrated with respect to the relative differences between samples. The design for QDA is based on repeated measurements and the statistical analysis is generally conducted using analysis of variance. Often the cobweb or spider diagram is used to graphically represent the data.

The sensory test conducted to characterize the properties of tomato by means of QDA [Krumbein2004] is shown here for the example. Whole tomato samples were presented to the panelists individually and in random order, and then were assessed using unstructured line scales with the anchor points 0—not perceptible and 100—strongly perceptible. The sensory profile included 57 descriptive attributes. According to the results of the evaluation of fresh and stored tomatoes, the following characteristics were focused on odor of the cut fruit (eight attributes), flavors (11

attributes) and after-taste (eight attributes). Fig 1.10 shows the profile analysis of flavor for these three tomatoes and Table 1.3 shows the change in sensory odor attributes in fresh and stored tomatoes based on QDA method. The attributes such as intensive, sweet, sweetish, mouldy etc. were used to characterize the properties of tomato samples.

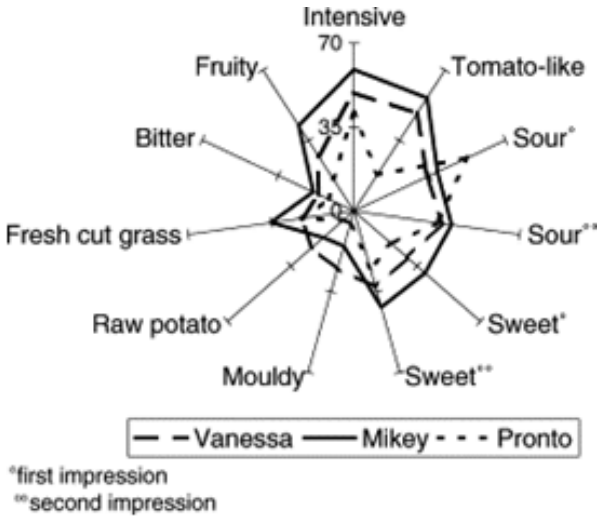


Fig. 1.10 Quantitative descriptive analysis of flavor in fresh tomatoes of the cultivars 'Vanessa', 'Mickey' and 'Pronto'. Panelists made scores about sweet and sour impressions during the first bite (marked with one circle in figure), and their second impression during mastication of the tomato pieces (marked with two circles in tables and figures). [Krumbein2004]

Then, smell presentation techniques in sensory test are described. In sensory test, there are two techniques for introduction odor to the panel such as static olfactometry and dynamic olfactometry [Cometto2002]. In static olfactometry, the odor containers are typically gas or odorless plastic. A series of dilutions of the substance of interest are prepared in individual vessels using the appropriate odorless solvent. The examples of this method are shown in Fig 1.11.

Table 1.3 Changes in sensory odor attributes in fresh and stored tomatoes of the cultivars 'Vanessa' (V), 'Mickey' (M) and 'Pronto' (P) [Krumbein2004].

Sensory attributes	Cultivar	Storage period (days)*				
		0	4	7	10	21
Intensive	V	59.5a	62.6b	61.6ab	61.2ab	64.4c
	M	58.8a	65.0bc	63.7b	66.1c	
	P	31.4a	36.0a	40.5b		
Tomato-like	V	54.8a	60.6bc	58.9b	59.2bc	61.6c
	M	54.1a	63.2c	59.7b	63.5c	
	P	18.8a	25.3b	23.3b		
Sweetish	V	29.0a	32.0a	30.6a	31.6a	29.7a
	M	32.2a	35.7a	34.5a	37.3a	
	P	16.4a	23.1b	22.7b		
Fruity	V	38.9a	39.8a	38.2a	40.9a	41.3a
	M	43.1a	46.5ab	45.2a	48.8b	
	P	15.2a	18.6a	19.4a		
Mouldy	V	17.6a	22.5b	21.5ab	21.9ab	19.3ab
	M	12.8a	12.2a	14.0a	16.4b	
	P	9.4a	10.6a	16.9a		
Raw potato	V	23.4a	24.7a	28.4ab	30.0b	23.7a
	M	17.9a	20.2ab	19.9a	23.0c	
	P	10.8b	7.2a	5.8a		
Fresh-cut grass	V	30.2a	37.3b	35.4ab	36.0b	44.5c
	M	38.1a	45.1b	46.5b	45.4b	
	P	19.2a	18.4a	12.2a		

*Values in the same row with the same letters mean similar values.

In dynamic olfactometry, the chemical stimulus flows continuously in a carrier gas stream. The various concentrations of the substance tested are typically achieved by diluting the substance by a carrier gas. The example of dynamic olfactometry is shown in Fig 1.12.

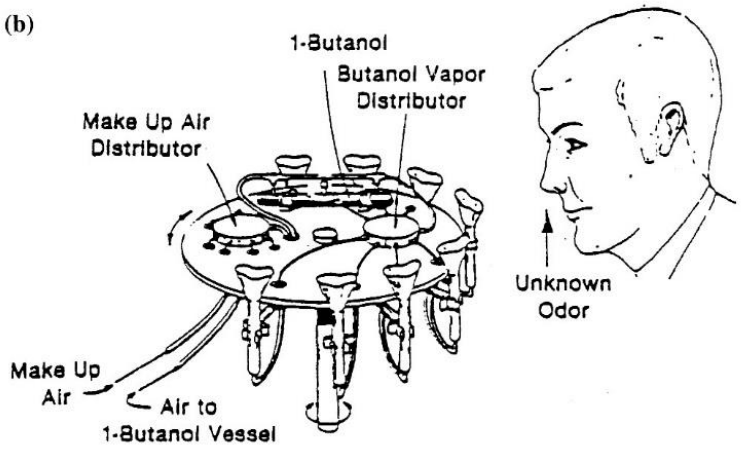


Fig. 1.11 Static olfactometry. [Cometto2002].

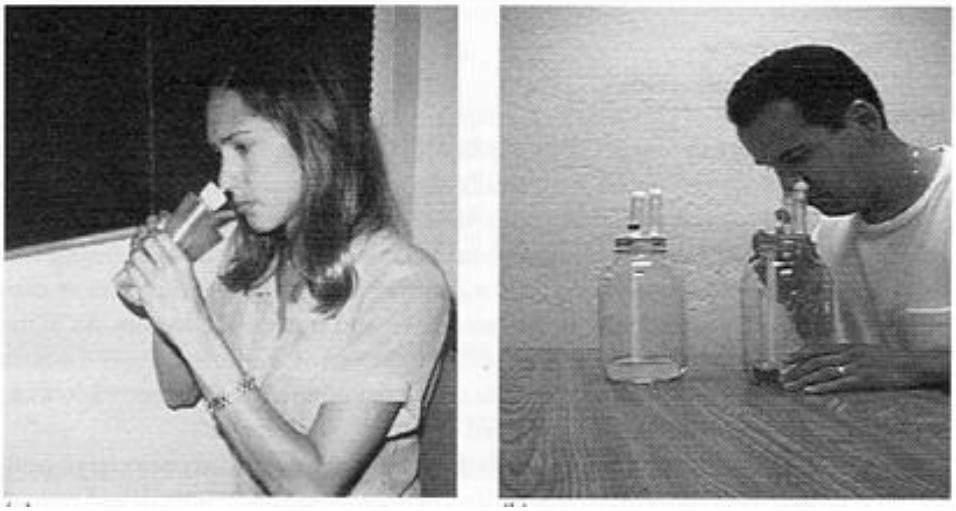


Fig. 1.12 Dynamic olfactometry. [Cometto2002].

1.5 Basics of Olfactory Display

In general the term "display" refers to the visual display, for example the computer screen that presents texts, images, or animations, however, "olfactory display" refers to the odor presenting device that presents smells to users. It might be able to connect with a computer or a smart device so that the user can control the odor presentation including the odor intensity as he or she need. However, the fact that olfaction is chemical sense unlike visual and auditory which are physical senses, cause the development of the olfactory display more difficult and slower than the displays for other kind of senses. For example, a pleasant smell might turn to be a very bad smell when its concentration is increased.

In recent years, olfactory displays based on various methods have been developed. Their structure and mechanism for releasing smells are different, however, the simplified structure of the olfactory display in general can be demonstrated by a diagram shown in Fig. 1.13. Even though, the explanation of olfactory display structure can be made in various ways, the methodology to classify the structure in this dissertation is adopted from that proposed by Yanagida [Nakamoto2012].

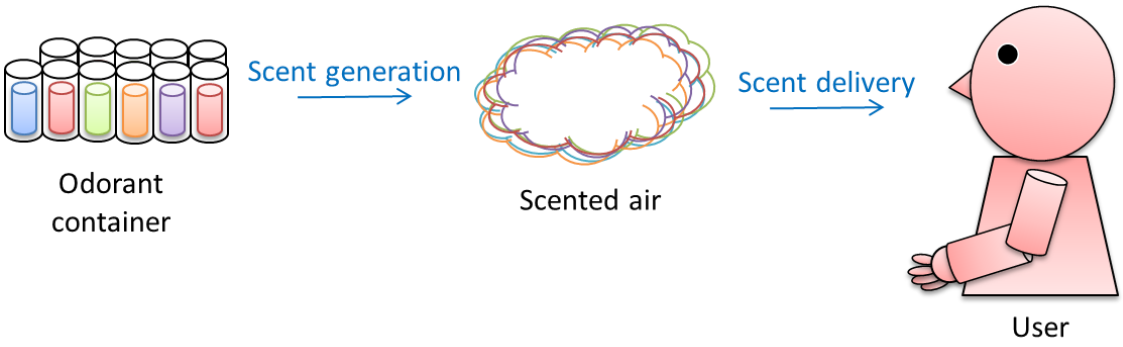


Fig. 1.13 General Structure of the olfactory display

As shown in Fig. 1.13, odorants are stored in containers. The odorants might be in simple liquid or solid form, or it might be a porous material soaked with some liquids

or a capsule with odorants encapsulated inside or a gel. Due to the fact that primary smells have not been discovered or they might not exist unlike three primary colors, the more odorants are used, the more smells can be presented. However, using too many odor components increase the size of the device unavoidably. As a consequence, the study on finding the minimum of odor components needed for achieving an acceptable range of presentable smells is also conducted by some researchers [Nakamoto2009].

To present smells to users, the odorants stored in containers needed to be vaporized into the air. Various scent generation techniques can be used to perform this task. The generated vapor can be delivered to the user's nose through various methods. Other technologies might be also utilized to realize some additional capabilities for some specific applications, for example the capability to transmit scents to a remote area, the capability to control the direction of the travelling scents, or the capability to present scents that were recorded by an odor sensing system. The details about these technologies are described in the next section.

1.6 Fundamental Technologies in Olfactory Display

As mentioned in the previous section, olfactory displays have been developed based on various techniques. The process to present odors are separated into two steps; scent generation and scent delivery. Besides, additional technologies might also be included to realize some specific capabilities. In this section, the details about scent generation methods and scent delivery method are introduced, whereas the contents about additional technologies are included in the detail described in Section 1.7.

1.6.1 Scent generation method

Smells of odorants stored in containers can be vaporized by various methods. The

possible methods are reviewed in this section.

1.6.1.1 Natural evaporation

In this method, odorants are stored in containers having a contact with air so that they can naturally evaporate into smell. An example of the odor presenting device using this technique is aroma diffusers which spread fragrances around the space in which they are placed. This technique is widely used in inexpensive commercial decorative-aroma diffusers due to its simple structure and low price. Even though, the odor release can be stopped by closing the container, the device using this technique still lacks more complicated capabilities, such as the capability to control the amount of odors released. Another problem is that this method is not suitable for presenting scents of low-volatile substances as their odors are hardly evaporated.

1.6.1.2 Vaporization using airflow

In this method, odorants are stored in containers which is connected to a fan, air pump, or air compressor. Odors can be generated by blowing the air passing through the surface of the odorants. Thus, the intensity of odors can be roughly adjusted by varying the airflow speed. Many olfactory displays are based on this technique. However, it still has a difficulty to present scents of low-volatile substances.

1.6.1.3 Heating

Another method to release scents is heating. This method have been generally used in many countries since the ancient time. This method is simple and able to vaporize scents with low volatility by increasing the temperature. Nevertheless, the difficulty is that

amount of odors released by heating is hard to be controlled accurately within a short time. As a consequence, the device using this method is generally difficult to rapidly control the start and stop of the odor generation. Besides, high temperature also affects the nearby circumstance if the appropriate countermeasure technique is not prepared.

1.6.1.4 Atomizaton using airflow

In this method, a nozzle is inserted into a container filled with liquid odorants. The mist can be released by blowing the tip of the nozzle with a high speed airflow generated from another nozzle due to the reduction of atmospheric pressure in the former nozzle that causes the liquid to be soaked up based on Bernoulli's law. The finer mist can be generated by treating the nozzle surface. Even though, this technique can emit fine mist of odorants rapidly, several problems are needed to be solved, such as the complexity of the structure that causes the device difficult to be constructed and miniaturized.

1.6.1.5 Direct atomization

In this method, the structure in which a liquid odorant can compressed to pass through a tube or a small hole is prepared. If the pressure applied to push the liquid is high enough, fine droplets are emitted from the tip of the hole. This method also includes the use of an inkjet device in which a liquid odorant is filled instead of an ink. This method can produce tiny size of droplets whose amounts are approximately in the range of hundred picolitres. This technique is not only able to inject droplets rapidly but also can control amount of the droplets. However, some problems are still difficult to be avoided, such as the difficulty to control the size of all injected droplets to be in the same range. This problem causes users to feel unpleasant liquid droplet enter their nose directly instead of vapor or smell if a big droplet is emitted.

1.6.1.6 Ultrasonic atomization

Fine particles of odorants are also made by ultrasonic atomization. In this method, high frequency voltage is applied to a piezoelectric device that converts the electrical energy into vibration. Thus, if the piezoelectric device is put in a container filled with liquid odorants, the vibration can causes ultrasonic waves to be generated inside the liquid. When the ultrasonic waves reach the interface between liquid and air, most of them are reflected and cause the collision of the liquid near the surface. If its energy is more than the surface tension of the liquid, it causes the liquid to be atomized in to the air. A mist of odorant particles can be emitted by this mechanism. This method has an advantage that it can atomize even liquid odorants of substances with low volatility. However, there is a disadvantage that the deterioration of the transducer after many times of usages. The structure of odor presenting device using ultrasonic atomization can be developed in various manner. An example structure is shown in Fig. 1.14. The atomization using SAW device used in this study can be classified into this category as well.

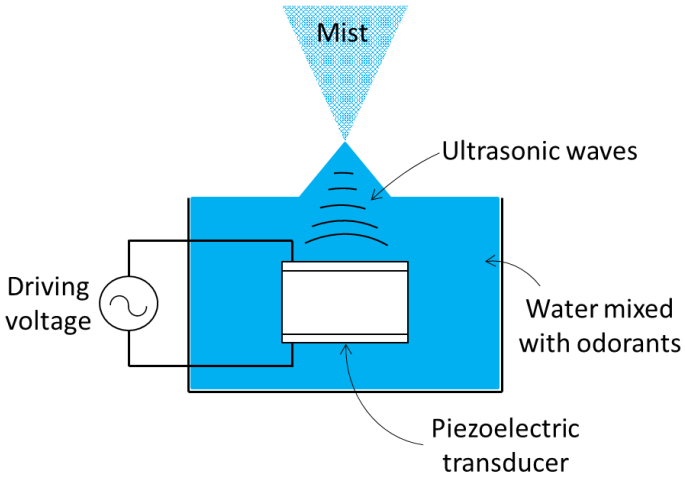


Fig. 1.14 Example mechanism of ultrasonic atomization

1.6.1.7 Discussion

Advantages and disadvantages of odor generation methods can be summarized as shown in Table 1.4. However, this table was created based on the method individually. By using some additional technique together, some capabilities may be capable. For example, odor intensity cannot be controlled by only heating the odorants but it can be realized if some additional techniques are used to drop liquid odorants with controlled size onto the heater.

Table 1.4 Comparison of odor generation methods

	Rapid odor presentation	Presenting smells of low volatile substances	Controlling amounts of released odors	Miniaturization possibility	Presenting scents without small liquid particles
Natural evaporation	X	X	X	O	O
Vaporization using airflow	O	△	△	O	O
Heating	△	△	X	△	O
Atomization using airflow	O	O	O	X	X
Direct atomization	O	O	△	O	X
Ultrasonic atomization	O	O	△ or O	O	X or △

According to the table, natural evaporation technique lacks of many capabilities due to its basic mechanism. Presenting scents using heating technique also has a difficulty to control odor intensity and deal with high temperature. The technique of vaporization using airflow has many capabilities in general but it cannot present scents of low volatile substance at a sufficient speed.

The technique of atomization using airflow possesses many capabilities, however, using this method will confront a difficulty to miniaturize the device's size. As a consequence, the techniques of direct atomization or ultrasonic atomization were compared in detailed to be chose for using in this research. The direct atomization technique is suitable for some applications that require wearable olfactory display as the device using this technique injects tiny droplets of odorants directly into user's nose whereas the ultrasonic atomization is useful in more situations as the odor vapor is released. Therefore, ultrasonic atomization was chosen.

Among ultrasonic atomization techniques, atomization using SAW device has a comparatively advantage in miniaturization the device's dimension, therefore, it was selected to be utilized in this study. Even though this technique has a disadvantage that it may present unpleasant feeling to the user if the large-size droplet enter his or her nose directly, this problem can be reduced by increasing the working frequency of the SAW device.

1.6.2 Scent delivery method

Scents of odorants vaporized by the odor generation method can be delivered to users' nose by various ways. The possible methods are reviewed in this section.

1.6.2.1 Natural diffusion

This method utilizes the diffusion characteristic of the gas by letting scents to diffuse gradually from a high concentration area to the low concentration area. Thus, the scents



Fig. 1.15 Commercial aroma diffuser using natural diffusion to deliver smells [http://in-a-box.com.au]

can spread around the area slowly. This is the simplest method that is mostly used in commercial aroma generator whose example is shown in Fig. 1.15 due to the inexpensive price and its simple concept that does not require other additional device.

1.6.2.2 Scent delivering by wind

This method using the wind or airflow to blow odors to the users' nose. It allows the olfactory display to be able to present smells to the users who are away from the device. Olfactory displays using this method are also able to present smells roughly into some specific directions. However, the disadvantages are that the scents blown by wind are spread around if the distant is too long and it is nearly impossible to send the smell into some specific area. Moreover, scents presented to users' nose by this method also includes the feeling of wind which may be undesirable in some applications as well.

1.6.2.3 Scent delivering by tubes

In this method, tubes are used to convey scents generated from the odorants to the users' nose. This method is a comparatively effective way to deliver smells duo to a lot of advantages, for example the scents are not spread around and can be adjusted to be released only at the specific area. However, the presented scents might remain on the inner wall or the tip of tubes and cause users to feel smell unintentionally or cause cross-contamination when different odors are presented through the same tube.

1.6.2.4 Direct injection

In this method, scents injecting device, such as inkjet devices or atomizers are placed under the nostrils so that the mist or vapor of odorants generated from the devices can be sniffed into the users' nose directly. This method is generally used in wearable olfactory displays because they would not require other devices to deliver scents. Using this technique can only present scents to the limited space, however, it is sufficient for some applications that needs wearable odor presenting device.

1.6.2.5 Scent shooting

This method transmits scents to the far location by shooting scents encapsulated in some shapes so that it would not spread out in accordance with distance unlike delivering using wind or airflow. An example of olfactory display using this method is an air cannon developed by Yanagida [Yanagida2003] which shoots scents encapsulated in vortex ring shape. The detail about this air cannon is described Section 1.7.6. However, this delivering method encounters some problems such as the impropriety to present scents continuously and wind that affects the direction of shot scents if it is strong enough.

1.6.2.6 Discussion

Advantages and disadvantages of odor delivery methods can be summarized as shown in Table 1.5. According to the table, natural diffusion technique lacks of many capabilities for advanced application. Scent delivering by wind can present scents to distant location but it is overcome by scent shooting technique due to the capability to maintain odor intensity in accordance with distance. However, sending scents into distant location is not in the scope of this research. Scent delivering by tubes has a disadvantage that odors will remain in the inner wall and tip of the tube. In this study, basic scent delivering by wind (using a small fan) was considered to be utilized first (in Chapter 4), however, it was then found that the SAW device can release the odor vapor sufficiently to the user's nose nearby without the need of a fan (in Chapter 5). Thus, direct injection method was used instead.

Table 1.5 Comparison of odor delivery methods

	Presentation without smell remaining on device	Presenting smells precisely to some specific areas	Presenting scents to distant location	Presentation without distortion in accordance with distance	Miniaturization possibility
Natural diffusion	△	XO X	O	X	O
Delivering by wind	△	△	O	X	O
Delivering by tubes	X	O	△	N/A	△
Direct injection	X	O	X	N/A	△
Scent shooting	△	△	O	O	X

1.7 Case Studies of Olfactory Displays

Human efforts to release fragrances of incenses so that they could enjoy satisfactory smells have started since the ancient time. For example, people in ancient Egypt society carried a little cone made of a solid perfume on their head and Japanese have used incense burners so that they can experience aromas from the fragrant wood.

The advancement of technologies in the recent years allows researchers to develop odor presenting device with more capabilities. As a consequence, olfactory displays based on various methods have been developed. The details are described in this section.

1.7.1 Magnum opus Sensorama

This machine proposed by Morton Heilig in 1960s is considered as a predecessor of modern odor presenting device [Heilig1962]. It was an immersive multimodal system that could provide 3D virtual experience of riding a motorcycle on the streets to the player. The prototype consisted of stereoscopic 3D screen with a wide-angle view, stereo speaker, nine fans, and a vibrating seat as shown in Fig. 1.16.



Fig. 1.16 Sensorama [Heilig1960]

The feeling of wind including with aromas of jasmine and hibiscus or smells of baking pizza were presented to the driver's face when they drove pass a flower garden or an Italian restaurant in Brooklyn, respectively [Rheingold1991]. Even though, it was impressed and considered as the possible future of cinema, unfortunately Heilig was unable to obtain sufficient financial support to scale up to commercial production [Heilig1969, Heilig1971].

1.7.2 iSmell

iSmell is the first odor presenting device which utilizes the concept of computer-controlled system proposed by DigiScents [Plat1999].



Fig. 1.17 iSmell [DigiScents2001]

The prototype was designed to connect to a computer through a serial or universal serial bus (USB) to emit smells when the user visited a web site or opened an email. According to DigiScents marketing material, the device contained a cartridge with 128 "primary odors" which could be blended together to create thousands of everyday scents. However, it raised a question regarding the existence of the primary smells which might not exist. The article stated that "DigiScents plans to begin taking

beta-user orders by Christmas and aims to make the gadgets generally available by Spring", however, the devices were not available even to developers and the company then declared bankruptcy in April 2001.

1.7.3 Olfactory display using high speed switching solenoid valves

The olfactory display using high speed switching solenoid valves was developed by Nakamoto et al [Nakamoto2002]. The basic concept of this olfactory display is shown in Fig. 1.18. This olfactory display utilizes an air pump to blow an airflow through the surface of odorants filled in bottles to evaporate them into smells. Additionally, high speed solenoid valves were used to improve the capability to control amount of odors released of the device. The solenoid valve used in this device has only two states; ON and OFF. When the solenoid valve is turned on, air flow from the air pump passed through the surface of the odorant is delivered to the user's nose through a tube. When the solenoid valve is turned off, the odor presentation is stopped. Thus, intensity of odors to be presented can be precisely controlled by adjusting the switching ratio of the solenoid valve.

The odor presented by olfactory display was evaluated by using a gas sensor. The sensor response is shown in Fig. 1.19 in which the abrupt and controllability sensor response can be observed. The result clearly demonstrated that the olfactory display can present smell rapidly and can control intensity of the released odor vapor precisely. Besides, by presenting many odors simultaneously, the device can blend multiple smells at any arbitrary recipes and present it to the user's nose. The actual images of the two olfactory displays developed based on this concept are shown in Fig. 1.20 and 1.21, respectively.

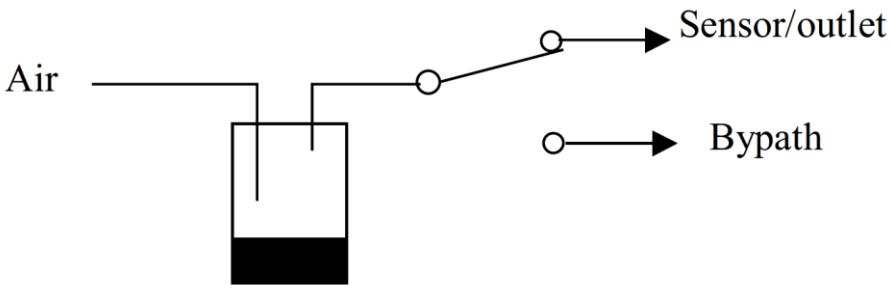


Fig. 1.18 Basic concept of the olfactory display using solenoid valve [Nakamoto2007].

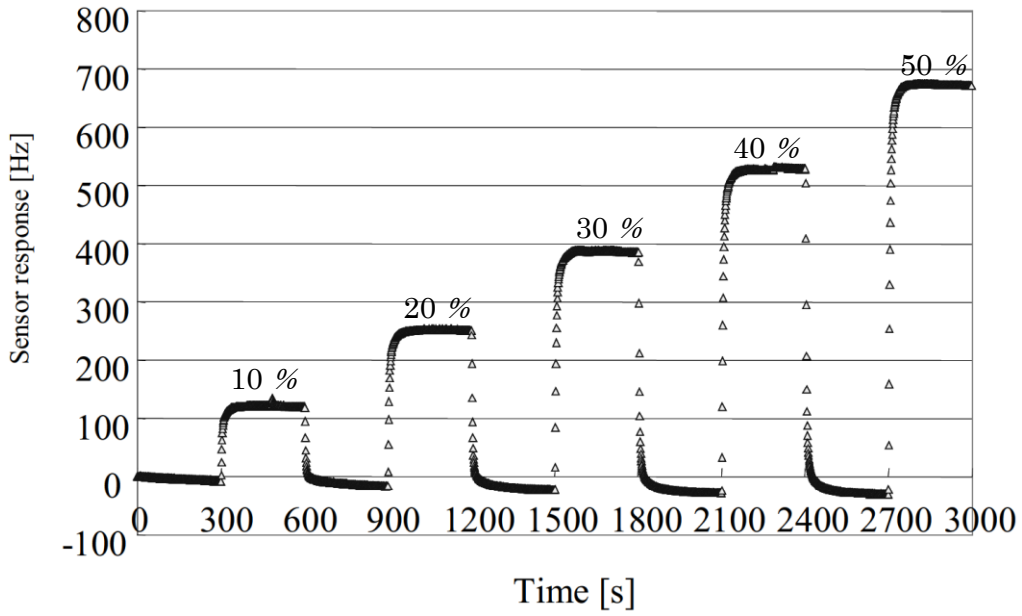


Fig. 1.19 Sensor response from a QCM sensor to an odor vapor of 2-hexanone [Nakamoto2007].

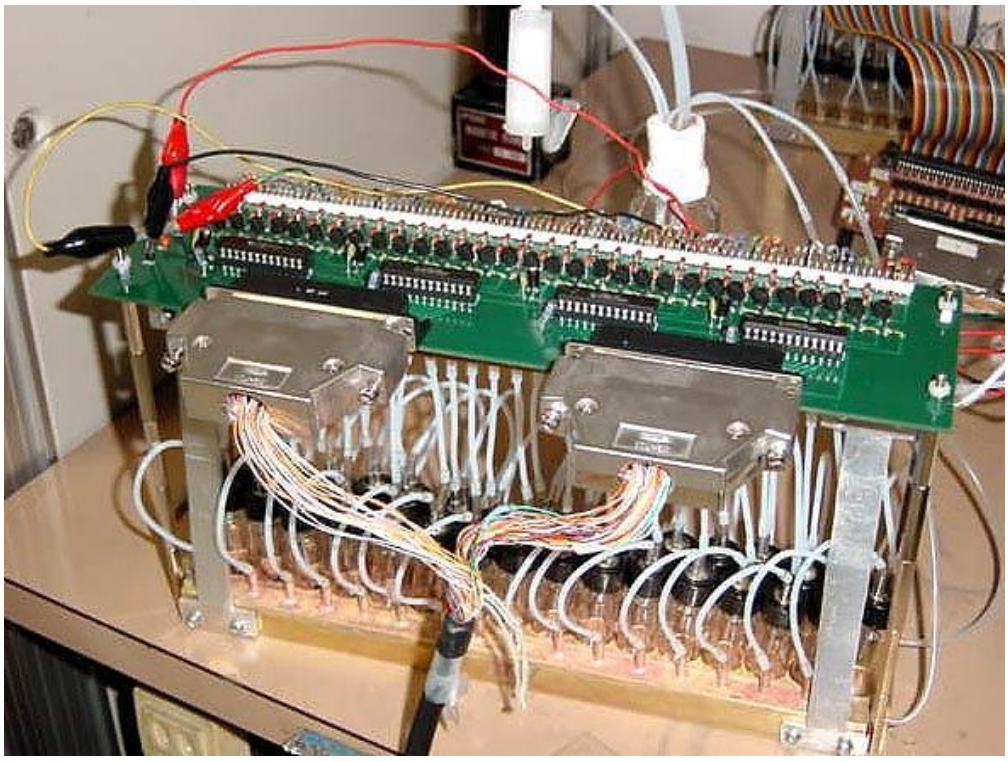


Fig. 1.20 Actual image of the thirty two-component olfactory display [Nakamoto2007].



Fig. 1.21 Actual image of the thirty-two-component olfactory display [Nakamoto2009].

1.7.4 Olfactory display using inkjet devices

An olfactory display using inkjet devices was developed by Okada et al. in collaborating with Cannon Inc. [Okada2008]. Odorants are filled into inkjet devices instead of ink so that the olfactory display could employ an inkjet mechanism to eject a jet of odorant particle to the users' nose.

This olfactory display can emit small volume of odor in the range of pL for a very short time. This advantage allows this device to avoid "olfactory adaptation", the mechanism where sensory nerve activity of olfactory detector is decreased by continuous stimulation of odor molecules causing people not to feel smell after they sniff that smell for some period of time. An actual image and structure of the olfactory display using inkjet device are shown in Figs. 1.22 and 1.23, respectively.



Fig. 1.22 Actual image of the olfactory display using inkjet device [Okada2010].

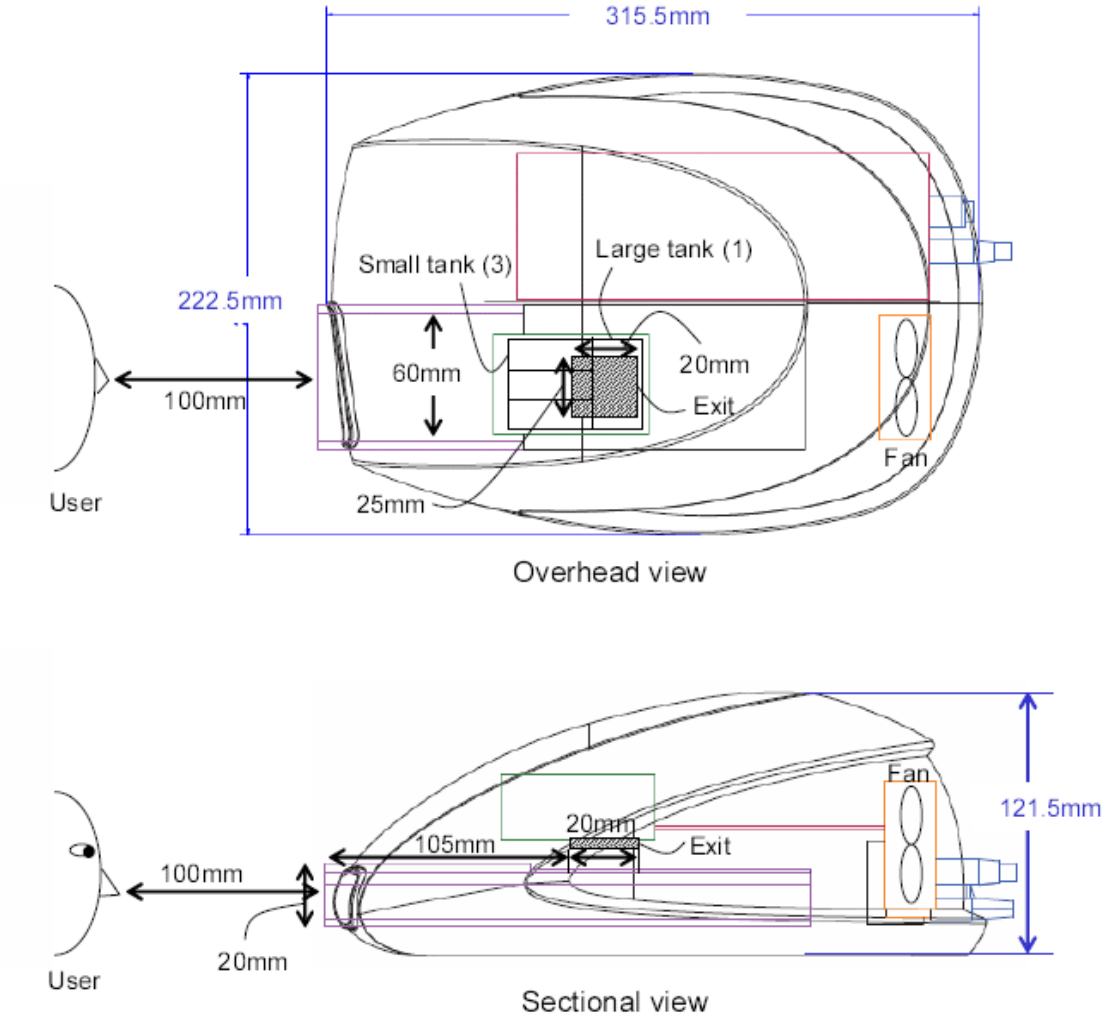


Fig. 1.23 Structure of the olfactory display using inkjet device [Okada2010].

1.7.5 Olfactory display using temperature responsive gel

This olfactory display was developed by Kim et al. [Kim2006]. In this device, the powder of methoxy poly(ethyleneglycol)-block-poly (ε-caprolactone)diblock copolymers (MPEG-PCL) was added to distilled water at concentration ratios of 30 % to produce a temperature-responsive hydrogel. The sol-gel phase transition is demonstrated by simple temperature stimulation, as shown in Fig. 1.24. When the mixture of aroma is added into the gelation and a Peltier module is coupled with it. It was confirmed that the

release of the aroma can be controlled by increasing or decreasing the temperature of the Peltier device. When the temperature is increased more than 60 ℃ the gelation turns into sol from which aroma is released. When the temperature is decreased lower than 25 ℃ the gelation turns into gel which does not release any smell.

Based on this technique, an aroma chip made of a micro cover glass was developed. A temperature-responsive hydrogel was placed in a microsyringe and was applied on the micro cover glass. An actual image of the device is shown in Fig. 1.25. The advantage of this olfactory display is that it can present odors soundlessly [Kim2009], however, the experimental result showed that it takes about 10 *s* since the odor presentation starts until the user can recognize the smell. The experimental result is shown in Fig. 1.26.

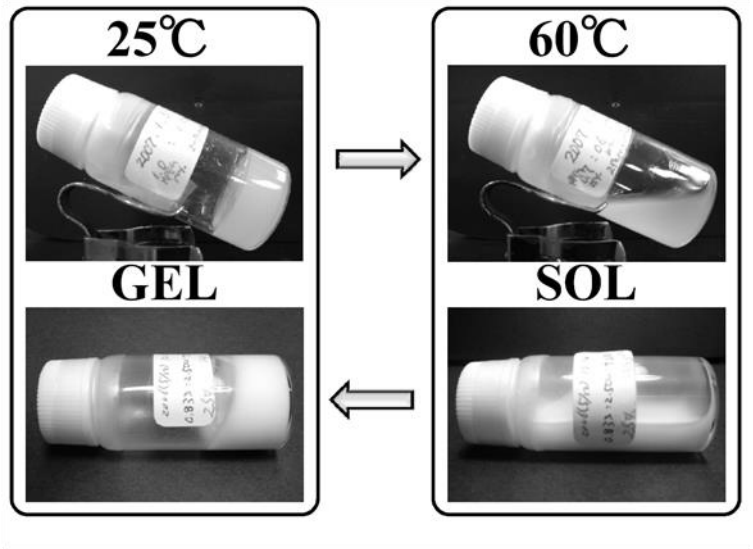
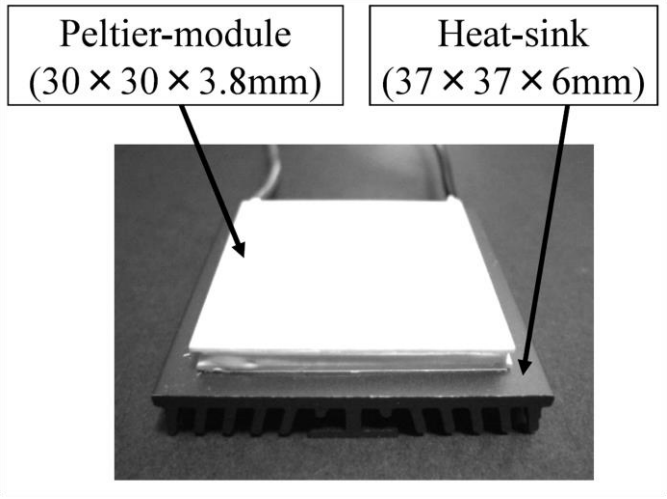
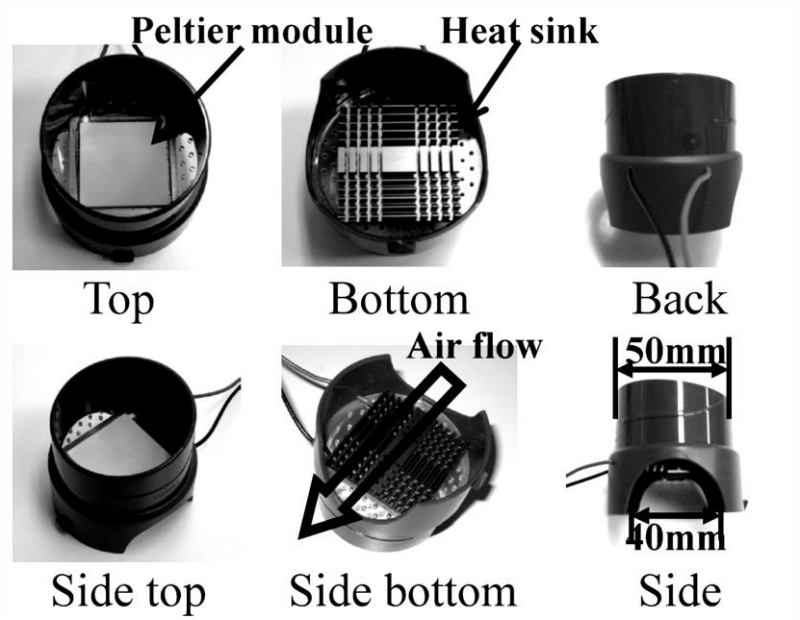


Fig. 1.24 Reversible phase transition between sol and gel [Kim2006].



(a)



(b)

Fig. 1.25 (a) aroma chip, (b) olfactory display [Kim2006].

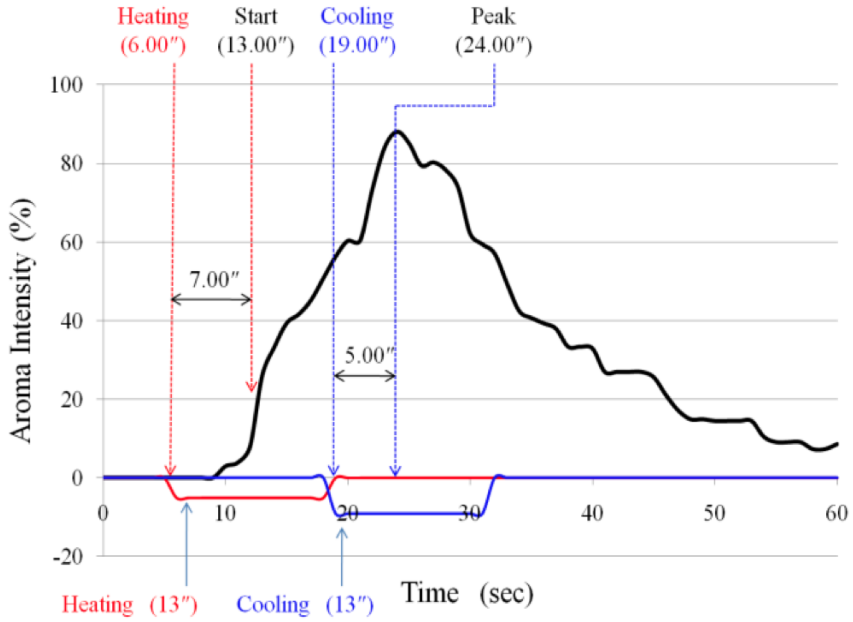


Fig. 1.26 Experimental result [Kim2006].

1.7.6 Olfactory display using air cannon

This kind of olfactory display was developed by Yanagida et al. [Yanagida2003]. The scent emitted by this scent projector is encapsulated in the vortex ring as shown in Fig. 1.27. The vortex ring can reach a relatively long distance as long as the flying vortex keeps its shape. An actual image of the vortex ring is shown in Fig. 1.28.

To launch the vortex ring, the device called an “air cannon”, which is a vessel with a circular aperture is used. A photograph of an air cannon is shown in Fig. 1.29. By instantaneously reducing the inner volume of the air cannon, the air is pushed out of the aperture and forms a vortex ring. The scents encapsulated in the vortex ring can be travel in free space. In contrast to a wind that is a continuous airflow, the use of vortex ring can be considered as discrete method of scent delivery.

Yanagida and his group also improved this scent delivery system to be able to deliver smells to the user’s nose by using a camera. It can detect the positions of both eyes and a nose of the user as shown in Fig. 1.30. Based on this concept, the device can

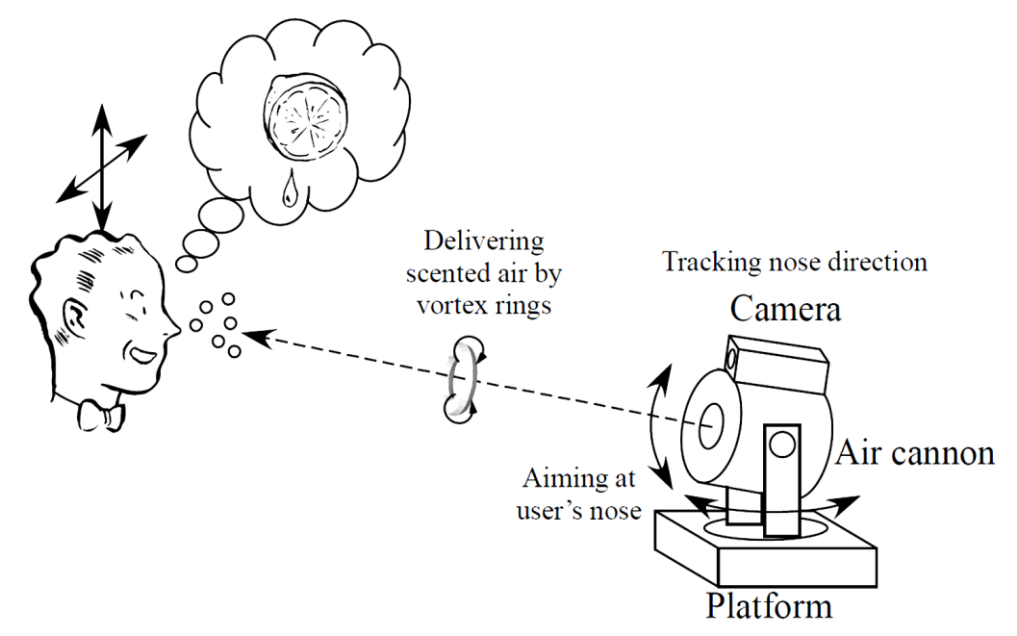


Fig. 1.27 Schmatic of scent projector [Yanagida2003].



Fig. 1.28 Vortex ring [Yanagida2003].

present smells to the user's nose accurately even when he or she is walking [Yanagida2011].

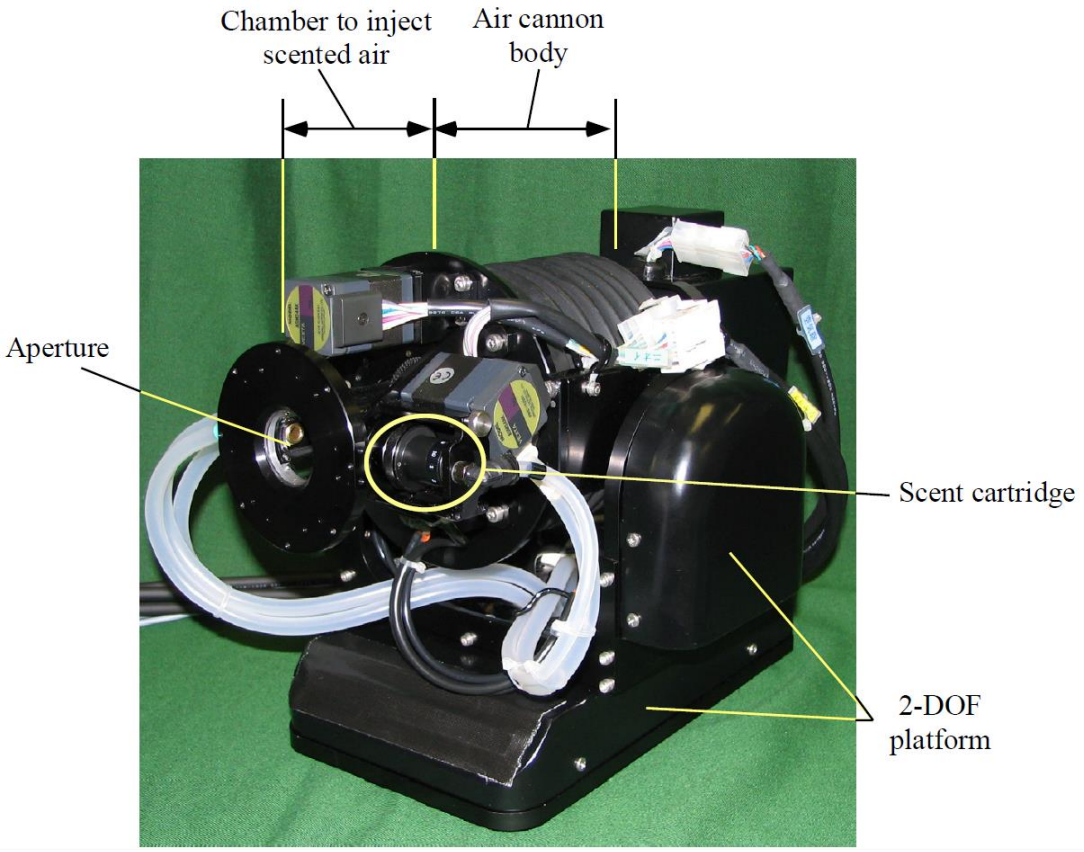


Fig. 1.29 Air cannon [Yanagida2003].

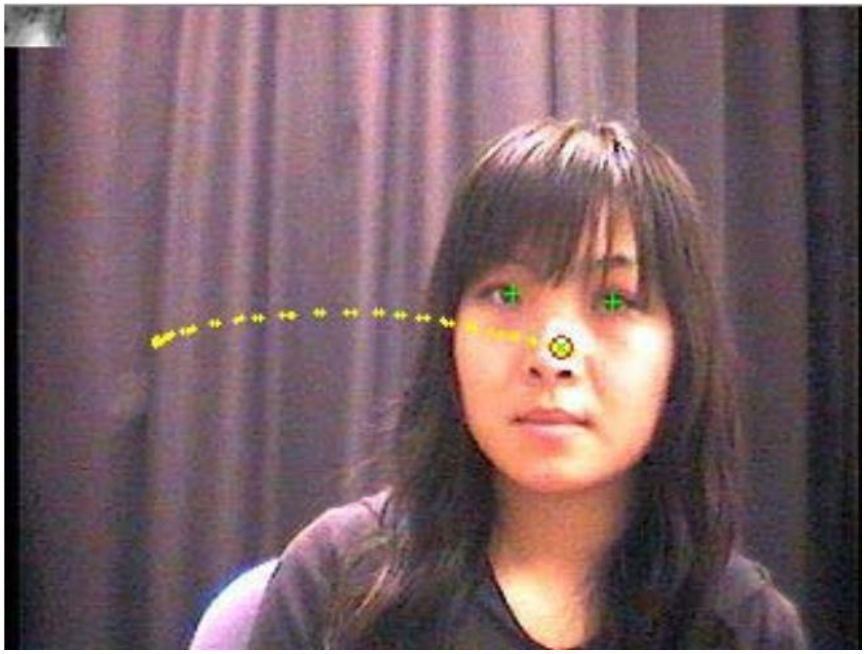


Fig. 1.30 Vision-based nose tracker used in this system [Yanagida2004].

1.7.7 Wearable olfactory

Hirose and his group developed a wearable olfactory display composed of air pumps. The concept of odor presenting unit is shown in Fig. 1.31. It is composed of air pumps and odor filter containing odorant materials. When the air pump is turned on, the air flow through the odor filter to generate an odor. The odor filter was placed as close as possible to the user's nose to avoid effects from nearby wind. An actual image when the device is wore by a user is shown in Fig. 1.32.

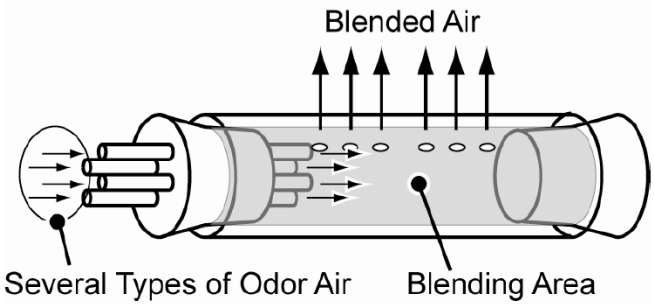


Fig. 1.31 Odor presenting unit [Hirose2006].

This olfactory display can present scents spatially according to the position of the user in the virtual world by connecting with a computer which works as an odor controlling unit. An example of variation of the odor strength according to the position is shown in Fig. 1.33.



Fig. 1.32 A user wearing a wearable olfactory display [Hirose2006].

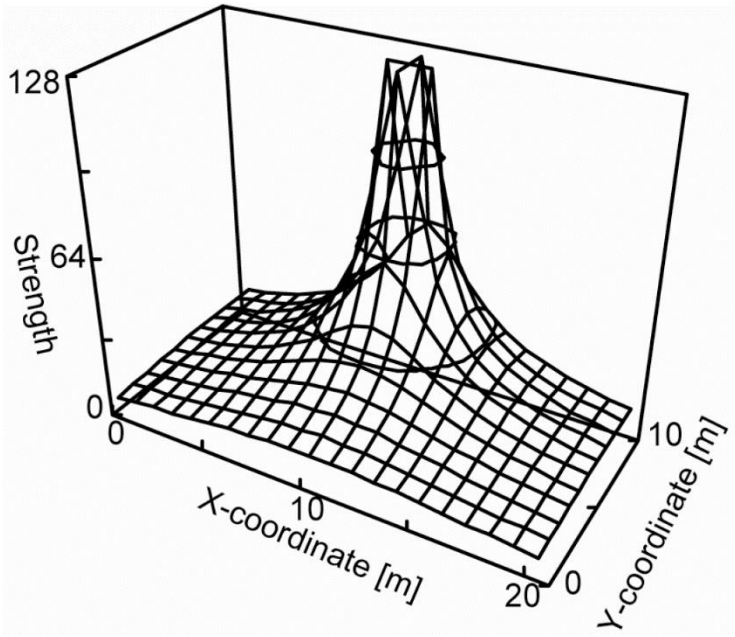


Fig. 1.33 3D graph of odor field [Hirose2006].

Due to the fact that the size of olfactory display composed of odor presenting

unit shown in Fig. 1.31 becomes bigger when the number of odors are increased, Hirose and his group also developed the wearable olfactory display using direct injection technique to overcome that problem. The schematic diagram of an olfactory display using direct injection method is shown in Fig. 1.34. This olfactory display presents smells by injecting tiny odorant droplets into user's nose directly as described in Section 1.6.2.4.

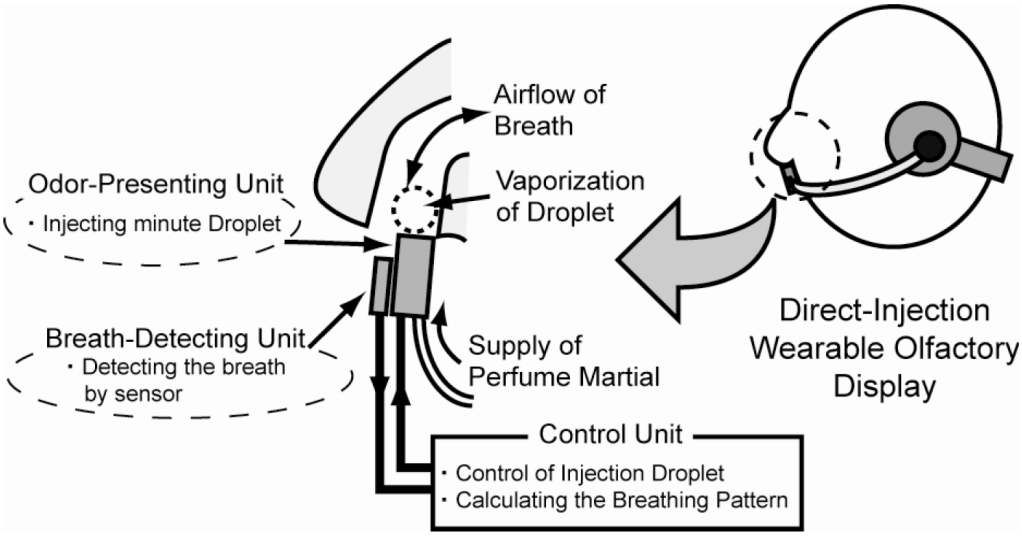


Fig. 1.34 Schematic diagram of direct injection wearable olfactory display [Hirose2006].

1.7.8 Scent Collar

Another wearable olfactory display was developed by the researchers at the University of Southern California's ICT, in collaboration with AnthroTronix, Inc. The actual image of the prototype device is shown in Fig. 1.35. This device is composed of four scent cartridges and fits around a user's neck. Each cartridge can produce one kind of smell, however, the number of cartridges can be increased. The device can be controlled by a wireless such as BlueTooth to work with some games or VR applications [Morie2003].



Fig. 1.35 Scent Collar [Morie2003].

1.7.9 Odor presentation on a LCD screen

This olfactory display named “smelling screen” was proposed by Matsukura and Ishida [Matsukura2013]. It can generate a localized odor distribution on a two-dimensional display screen. The schematic diagram of the device is shown in Fig. 1.36. A pair of axial fans were attached on the lower and upper ends of the screen. When the airflow are generated by the fans, they can be merged into a single stream of airflow coming out of the screen to the user’s nose. Thus, the user can feel the odor as if an odor source had been placed on the position of the screen. An actual image when a user is using a smelling screen as a digital signage of peaches is shown in Fig. 1.37.

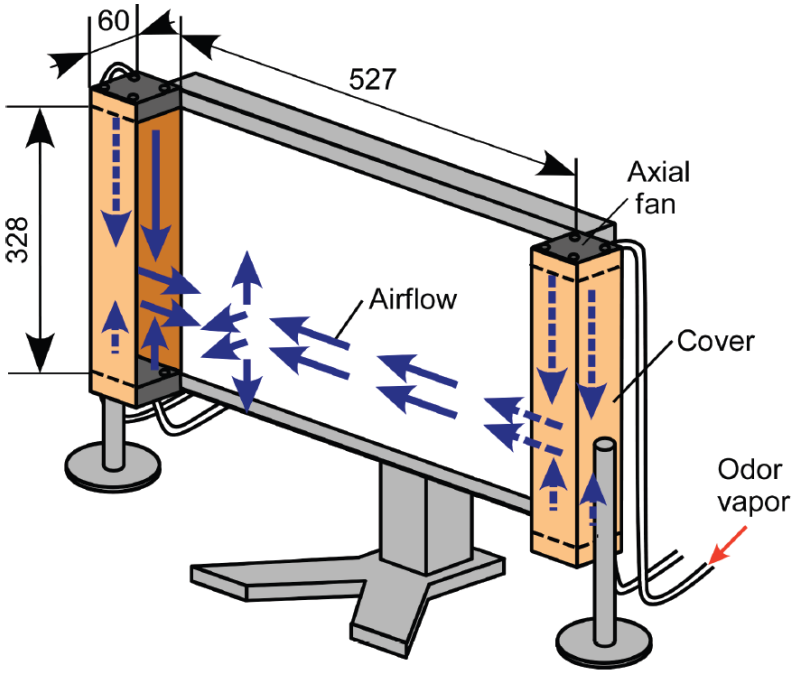


Fig. 1.36 Structure of smelling screen (unit : *mm*) [Matsukura2013].

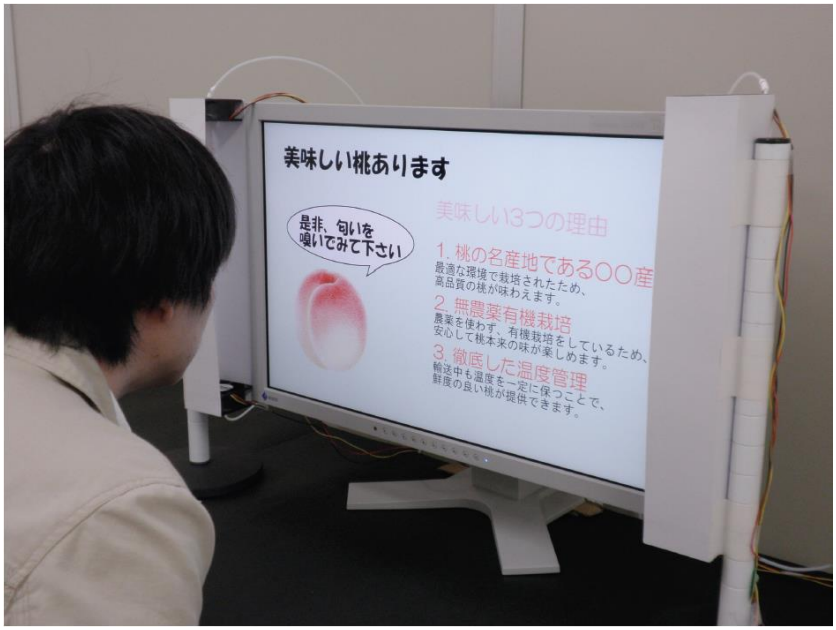


Fig. 1.37 User is using a smelling screen as a digital signage [Matsukura2013].

1.7.10 Micro aroma shooter (MAS)

This olfactory display was developed by Kim and his group [Kim2010]. The actual image of the device is shown in Figure 1.38 and 1.39. MAS is a compact cubic device filled with odorants and connected with an air pump. Thus, when the air pump is turned on, the air flow force odors in the cubic to be shot from the small hole like a jet to the user's nose. The porous material soaked with odorants was used in this olfactory display instead of the liquid odorant to solve the problem that the liquid might evaporate and the spatial control of odor presentation is difficult in case of using liquid.

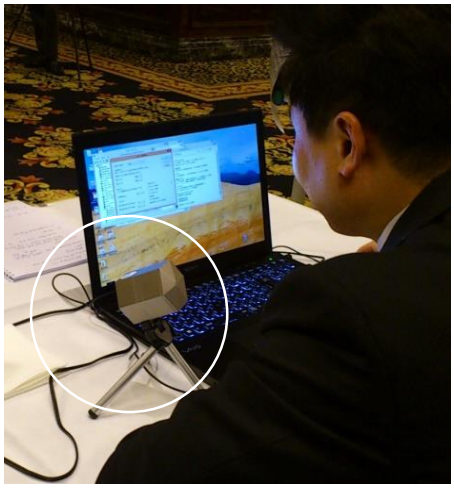


Fig. 1.38 Micro aroma shooter.

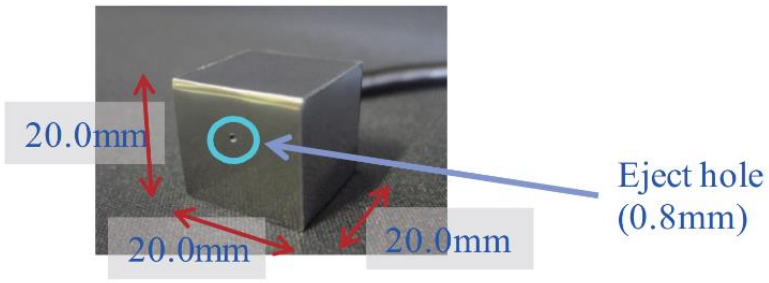


Fig. 1.39 Dimensions of micro aroma shooter [Kim2010].

1.7.11 Olfactory display connected with smartphone

Chakuperf Inc., a company in Japan, proposed the first olfactory display that can be connected with a smartphone as shown in Fig. 1.40. The device utilizes atomization technique to present an odor of the odorant stored in the cartridge. The company also developed the application on the iOS platform so that users can start and stop the odor presentation conveniently.

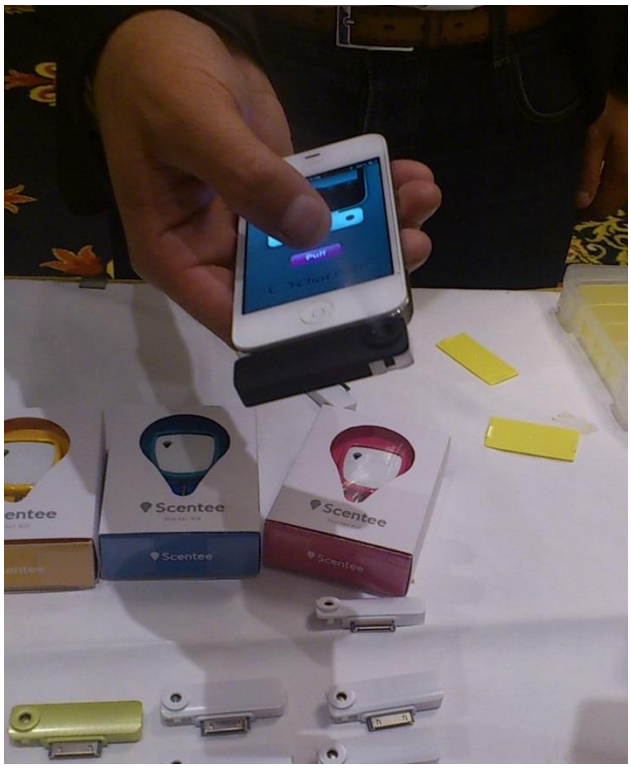


Fig. 1.40 Olfactory display proposed by Chakuperf.

1.7.12 Olfactory display using on-off switchable device

The olfactory display using on-off switchable device was developed by Kim and his group [Kim2011]. They employed a stable polymer, polydimethylsiloxane (PDMS) to create a chamber containing odorants as shown in Fig. 1.41. Each chamber has a

thermally induced volume that can open a tiny exit hole on the top of the container to release gas. The chambers are arranged in X-Y matrix with rows and columns of electrical heating lines, in which only the intersecting cells is forced to be open the cell gate for odor release. They utilizes gas detection tubes to confirm that this olfactory display can control amount of the odor released. Besides, due to the fact that the individual cells can be filled with different odorants, they concluded that this olfactory display has the potential to greatly improve the quality of virtual reality systems.

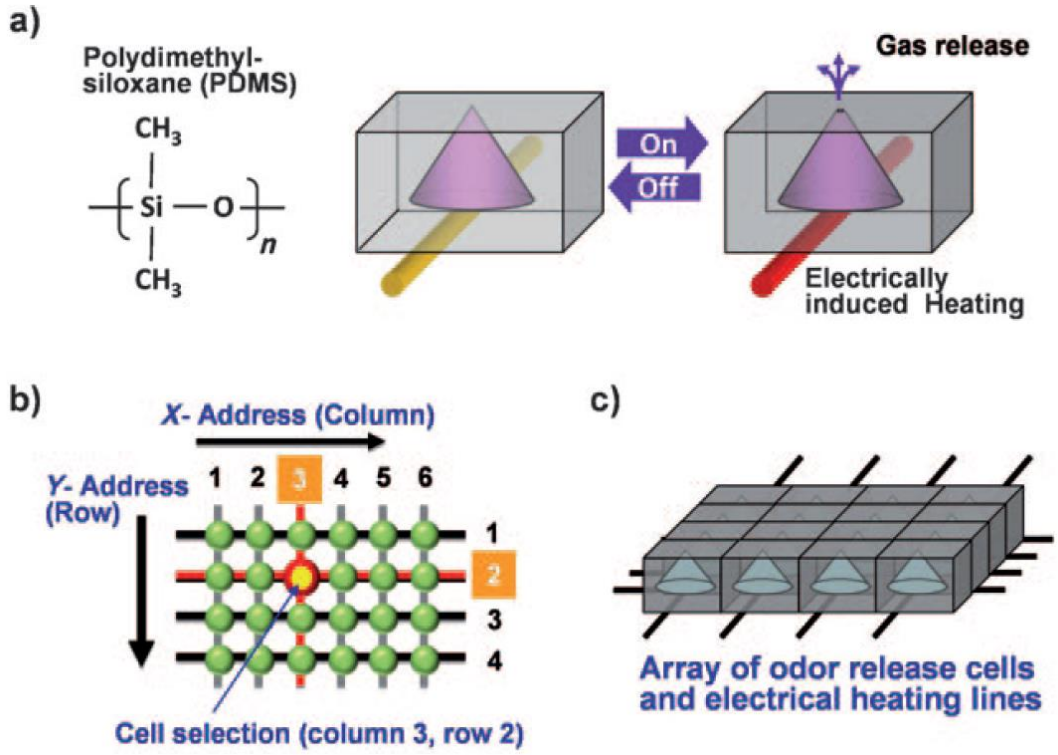


Fig. 1.41 a) odor release device based on an elastic chamber material, (b) a diagram illustrating the x-y coordinate cell-selection method, and (D) a X-Y matrix structure odor releasing system with 4 x 4 cells [Kim2011].

1.7.13 Olfactory display using MEMS actuator

Kashiwagi utilized MEMS technology to develop an olfactory display whose structure is shown in Fig. 1.42. The device is composed of a liquid inlet, micro valve, reservoir, and heater. As shown in Fig. 1.43, the odor presentation can be started by opening the valve and turning on the heater, and vice versa. Based on this concept, they proposed an olfactory display using MEMS technology and electroosmotic pumps whose structure is shown in Figure 1.44. According to the experimental result, this olfactory display possesses the capabilities to control odor intensities and to blend smells [Kashiwagi2012].

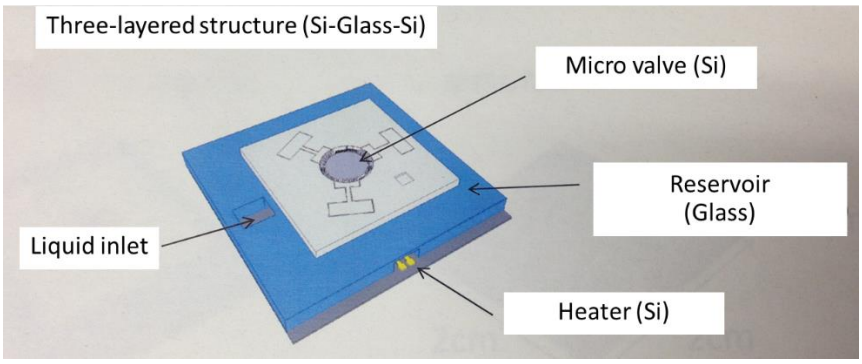


Fig. 1.42 Olfactory display using MEMS technology [Kashiwagi2012].

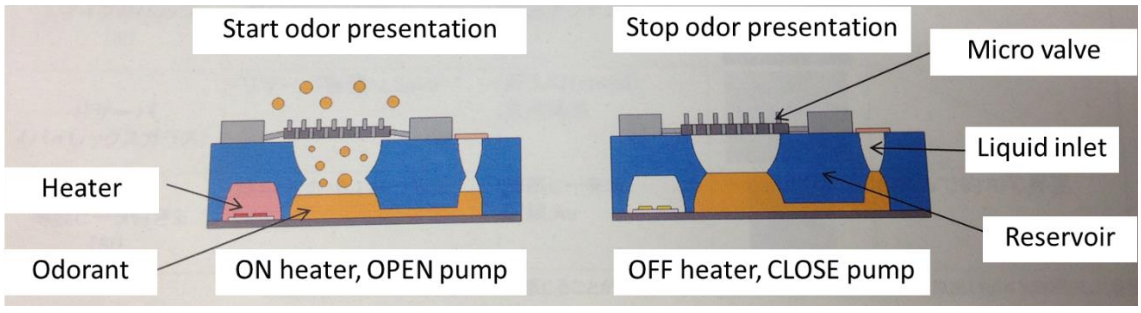


Fig. 1.43 Mechanism of olfactory display using MEMS technology [Kashiwagi2012].

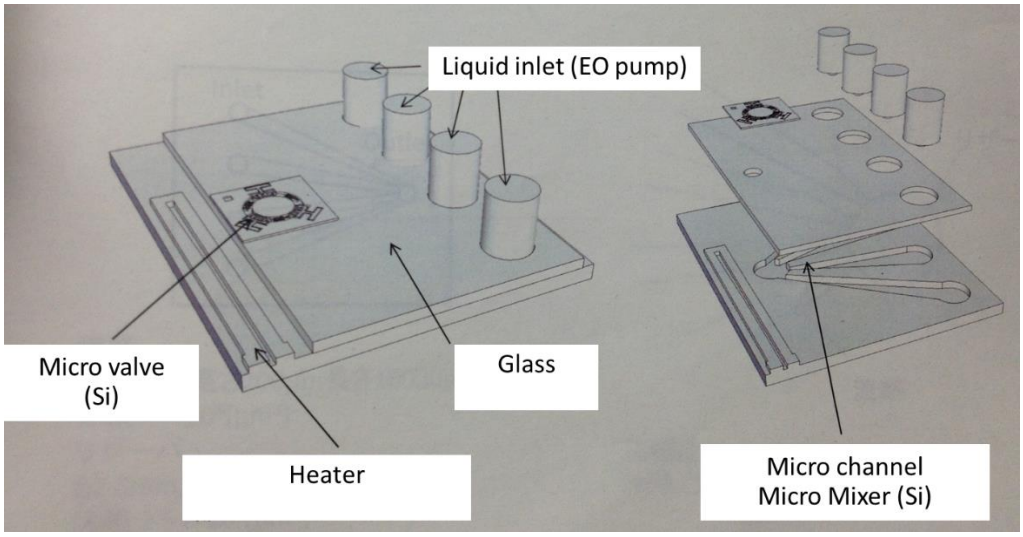


Fig. 1.44 Olfactory display using MEMS technology and electroosmotic pumps [Kashiwagi2012].

1.7.14 Comparison

Olfactory displays described in the above reviews can be summarized as shown in Tables 1.6 and 1.7.

Table 1.6 Comparison of existing olfactory displays (1).

	Odor generation method	Odor delivery method
Olfactory display using solenoid valves	Air blowing	By tube
Olfactory display using inkjet devices	Direct atomization	Direct injection
Olfactory display using temperature responsive gel	Heating	Natural diffusion
Olfactory display using air cannon		Scent shooting
Wearable olfactory display using air pump	Vaporization using air flow	By tube
Wearable olfactory display using direct injection	Direct atomization	Direct injection
Scent Collar		Natural diffusion
Odor Presentation on a LCD screen	Air blowing	By wind
Micro aroma shooter	Air blowing	By wind
Olfactory display connected with smartphone	Ultrasonic atomizer	Natural diffusion
Olfactory display using on-off switchable device	Heating	Natural diffusion
Olfactory display using MEMS actuator	Heating	Natural diffusion

Table 1.7 Comparison of existing olfactory displays (2).

	Fast odor presentation	Low volatile odor presentation	Controllability of odor concentration	Odor blending	Size
Olfactory display using solenoid valves	O	△	O	O	△
Olfactory display using inkjet devices	O	O	O	X	O
Olfactory display using temperature responsive gel	X		X	X	
Olfactory display using air cannon	O	O	X	O	X
Wearable olfactory display using air pump	O	△	X	△	△
Wearable olfactory display using direct injection	O	O		X	O
Scent Collar					△
Odor Presentation on a LCD screen	O	X	O	O	
Micro aroma shooter	△			△	O
Olfactory display connected with smartphone	△	△	X	X	O
Olfactory display using on-off switchable device					
Olfactory display using MEMS actuator			O	O	O

1.8 Research Purpose

Taking the current situation into account, olfactory displays based on several techniques and standards have been so far studied. Even though they are useful in certain situations, in my point of view the olfactory display for general usage should fulfill the following requirements.

(1) It should be able to present all kinds of smells vividly and reproducibly. It also should possess the sufficient speed to start and stop the odor presentation as fast as possible even in the case of low volatile compound.

(2) It should be able to adjust the intensity and amount of the presented odor precisely and in real time.

(3) It should be able to blend smells to present a variety of odors from a limited number of odor components.

(4) It should be small and thin enough.

(5) It should not create any disturbance such as noise or heat.

Indeed, no existing device at the moment could fulfill all of these requirements as shown in Table 1.7. Thus, the objective of this research is to develop the olfactory display that satisfies all of the above requirements and can be used effectively in all situations. To realize the olfactory display that can present all kinds of scents equivalently, a SAW (Surface Acoustic Wave) device whose SAW streaming can atomize a liquid droplet into a vapor forcibly was utilized. Thus, when a droplet of liquid odorant is supplied onto the SAW device, it is atomized into a smell suddenly. If the atomization performance is sufficient, even the droplet of odorant with low volatility can be atomized abruptly and completely without any residue. Thus, the odor presentation can be started and stopped rapidly and reproducibly. To realize the olfactory display that can control the odor intensity, a kind of miniaturized liquid pump called electroosmotic pump was utilized as a liquid tank and supplier that conveys the odorant droplets to the

SAW device. Since the flow rate of the pump can be adjusted conveniently by varying the amplitude of the driving voltage, the intensity or amount of the released odor can also be controlled easily by adjusting the amount of liquid droplets in the same way. By using a number of electroosmotic pumps filled with different odorants, an odor blending is possible. Both electroosmotic pump and SAW device are tiny and do not create any disturbance to the nearby circumstance when they are working. Thus, the olfactory display based on this concept can have a compact size and is safe enough to be applied to many systems.

The structure of this dissertation is shown in Fig. 1.45. In Chapter 2, the development of SAW devices for liquid droplet atomization is described. In Chapter 3, the study on conveying liquid odorant using electroosmotic pump is explained. The basic development of an olfactory display composed of the SAW device and the electroosmotic pump is described in Chapter 4. The development of a higher atomization SAW device included with the development of miniaturized six-component olfactory display is described in Chapter 5. In Chapter 6, the development of a further higher atomization SAW device included with the development of wearable eight-component olfactory display is described. The evaluation of the olfactory display using sensory evaluation is described in Chapter 7. In Chapter 8, the conclusion of the study is described.

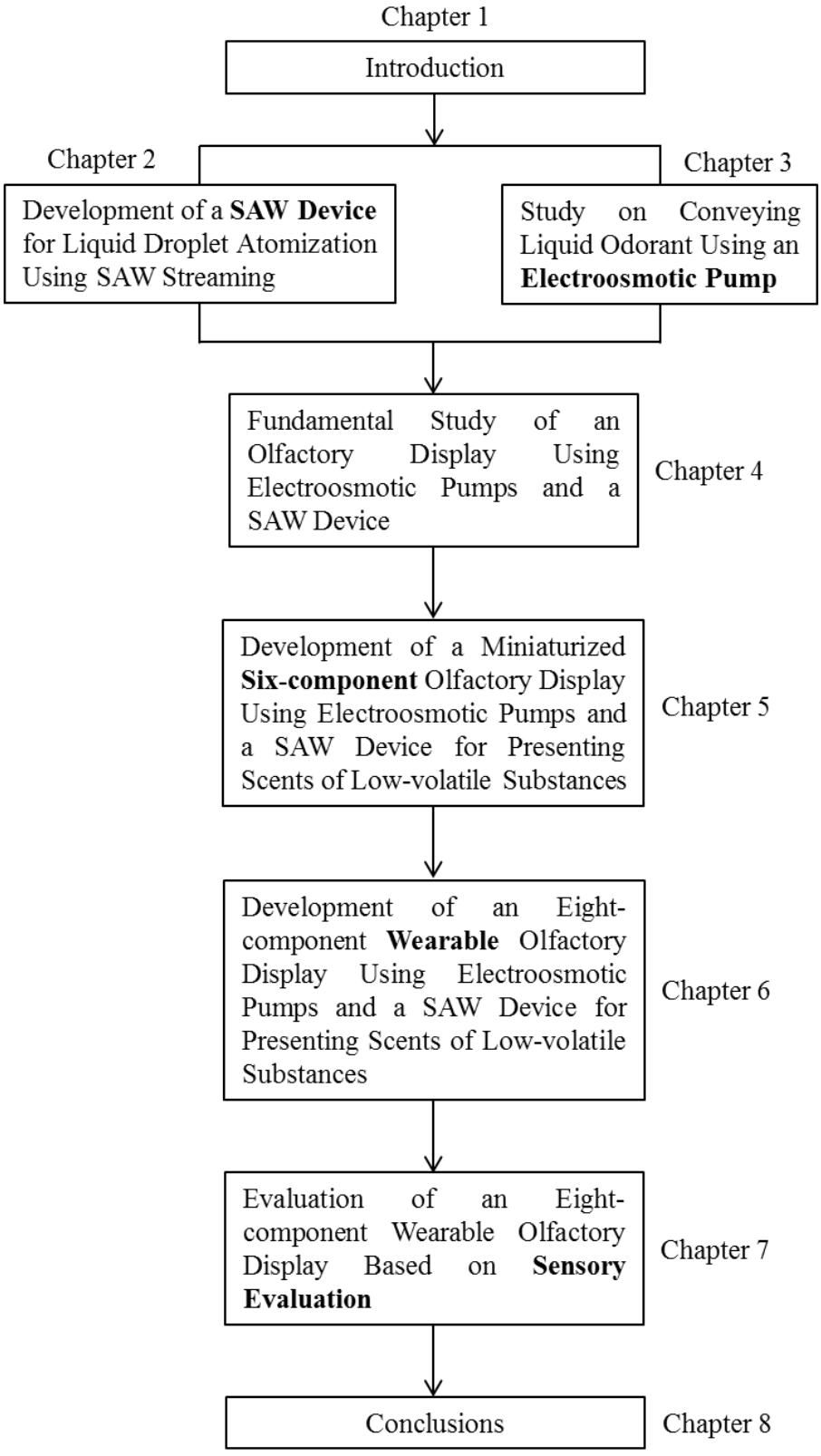


Fig. 1.45 Structure of this dissertation.

Chapter 2

Development of a SAW Device for Liquid Droplet Atomization Using SAW Streaming

2.1 Introduction

SAW devices are one of the crucial components in the field of electronics for many decades. They are ubiquitous in various electronic devices due to their identifying electro-acoustic characteristic and their feature allowing the miniaturized system to be realized. Their capability to excite small amount of liquid that was discovered recently is applied in various fields of liquid manipulation. As mentioned in Section 1.8, the SAW device was used in this study as an atomizer to atomize the target odorants into smells. The atomization is based on SAW streaming phenomenon in which acoustic energy transferred into liquid droplets can atomize the liquids if that energy exceeds some certain value. Therefore, the problem, mentioned in Section 1.8 that the odors of some substances with low volatility cannot be presented within a short time and without odor residue after presentation, was expected to be solved by developing an olfactory display composed of the SAW atomizer. Besides, the olfactory display to be proposed was expected to be miniaturized as the SAW device is tiny.

This chapter presents details on the development and evaluation of the first two SAW devices fabricated in this research for liquid droplet atomization. Starting with an explanation about fundamentals of SAWs, basics of SAW devices, and mechanism and applications of SAW streaming in Section 2.2. Details on the design of two SAW devices are described afterwards in Sections 2.3 and 2.5, included with explanations about experiments performed to evaluate the atomization performance of the fabricated SAW devices in Sections 2.4 and 2.6. Finally, the chapter is summarized in Section 2.7.

2.2 Principles of SAW Device

This section starts with the introduction to SAW in Section 2.2.1, followed by the descriptions about SAW device in Section 2.2.2, and SAW streaming in Section 2.2.3, respectively.

2.2.1 Surface acoustic wave (SAW)

Acoustic (or elastic) waves involve time-varying deformations or vibrations of the atoms in material media [Auld1990]. Acoustic waves propagating in a solid material can be roughly divided into two main categories: bulk waves and surface waves. Bulk waves propagate through the interior of the medium with a character unaffected by boundaries, as opposed to surface waves that travel along the medium's surface. The existence of the basic type of surface acoustic wave (SAW) propagating over the free surface of an elastic half-space was first demonstrated by Lord Rayleigh in 1885 [Rayleigh1885], and hence the wave is often referred to as a Rayleigh wave. The deformation of the medium through which the Rayleigh wave travels is shown in Fig. 2.1.

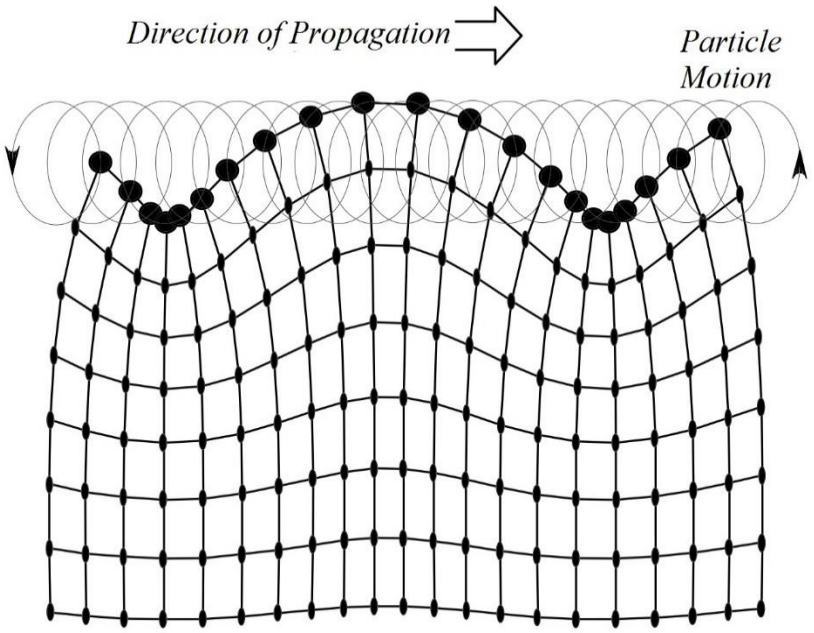


Fig. 2.1 A Rayleigh wave traveling through a medium.

As shown in the figure, Rayleigh wave which includes both longitudinal and transverse motions causes the surface particles to move in ellipses in planes normal to the surface and parallel to the direction of propagation. Amplitude of the wave decreases exponentially with depth and the wave entirely disappears within the depth of four to five wavelengths under the propagation surface. Material returns to its original shape after the wave passes. Among the attractive characteristics of acoustic waves are the low velocities (approximately 4000 *m/s* which is approximately 100,000 times slower than electromagnetic (EM) wave) resulting in a compact size compared with other competitive devices for a given frequency.

2.2.2 SAW device

In the 1960s, Rowen and Mortley first suggested independently that surface acoustic waves (SAWs) might be useful [Rowen1963, Mortley1963], however the required key was to understand some means for generating and detecting the waves, in a plane surface,

which were discovered subsequently by White and Voltmer in 1965 [White1965]. They demonstrated the interdigital transducer (IDT) that consisted of interleaved metal electrodes connected alternatively to two bus bars as shown in Fig. 2.2. With this component fabricated on a piezoelectric substrate such as quartz or lithium niobate as shown in Fig. 2.3, a SAW device can convert electrical signal applied to an IDT to acoustic wave that propagates over the substrate and vice versa. Relationship between velocity of the SAW and resonant frequency can be expressed as

$$f_0 = \frac{v_R}{\lambda} = \frac{v_R}{4d} \tag{2.1}$$

where f_0 is the resonant frequency (Hz), v_R is the Rayleigh velocity (m/s), λ is its wavelength (m), and d is the length of distance between two fingers of the IDTs (m), respectively. In addition to the IDT, other important components were developed, especially reflecting gratings that are widely used in surface-wave resonators [Ash1970]. Both IDT and reflector are shorted metal electrodes which can be fabricated conveniently and inexpensively using lithographic techniques originally developed by semiconductor manufacturers.

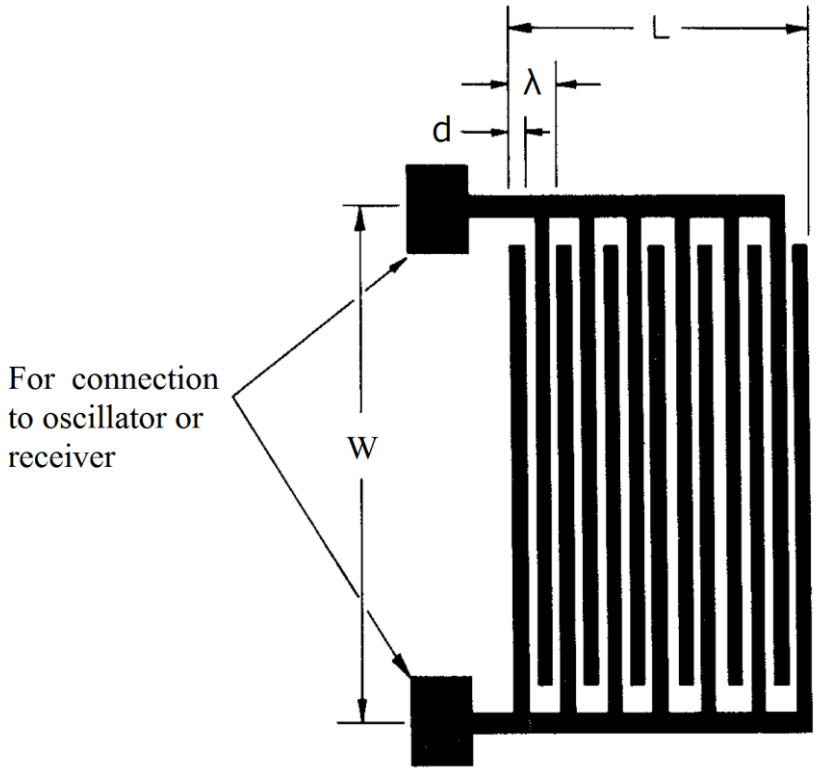


Fig. 2.2 Pattern of interdigital transducer for piezoelectric surface wave transduction [White1965].

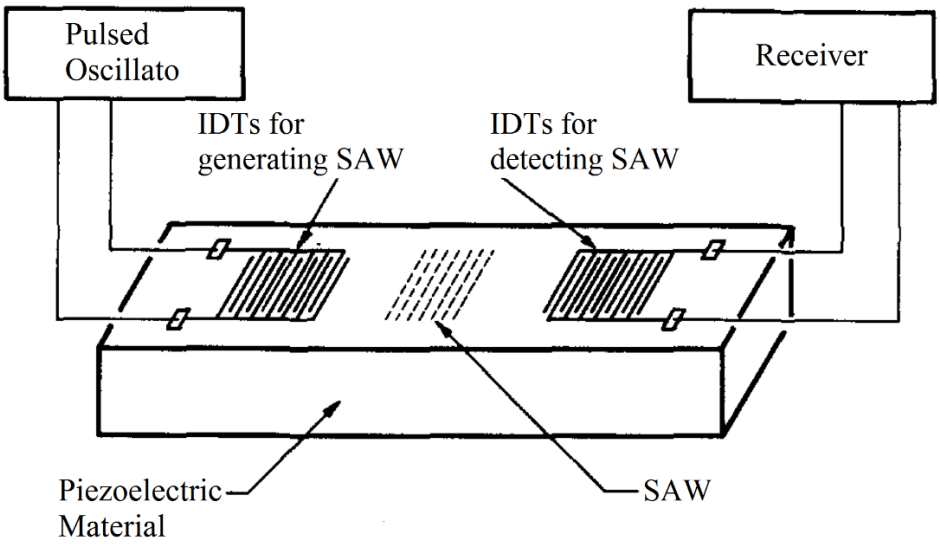


Fig. 2.3 Arrangment for surface-wave transduction by IDTs on a piezoelectric substrate [White1965].

Due to these benefits, various devices based on a wide variety of different forms of SAW devices have been developed in the subsequennt years, including delay lines [Smith1969], bandpass filters [Tancrell1974], matched filters [Costanza1969], oscillators [Lewis1974] and resonators [Coldren1979]. These devices are now ubiquitous in applications ranging from professioanl radar [Solie1981] and communications systems [Panasik1992] to consumer applications such as television [Takahashi1978] and mobile phones [Tsubouchi1992]. In the last two decades, many researches have been conducted in the area of SAW sensors. Due to the fact that surface waves can be easily influenced by physical interference unlike electrical signal, SAW devices can be used as sensors as well. The applications include all area of sensing [Benes1998], for example, pressure, strain, torque, temperature, accumulation of mass on a surface, chemical vapor, biological matter, humidity, magnetic fields, and viscosity. Recently, the studies on applications of SAW devices in microfluidic field by using SAW streaming have also been widely conducted. The detail relating with this issue is described in the next section.

2.2.3 SAW streaming

When an acoustic wave travels through media, if the acoustic intensity is not high, the acoustic energy propagates through the media under linear phenomenon in which the media does not moved by the wave travelling. However, as the wave amplitude increases, the nonlinear behavior, such as, steady motion of the media, appears. Such a nonlinear phenomenon is called “acoustic streaming” [Nyborg1958, Nyborg1965]. Similarly, when a SAW with high intensity reach the boundary between a liquid and solid, the transmission mode is changed from the Rayleigh mode to the leaky Rayleigh mode that radiates longitudinal wave into the droplet at the Rayleigh angle

$$\theta_R = \sin^{-1}(\frac{c_l}{c_s}) \tag{2.2}$$

due to the difference acoustic-wave velocities in the liquid c_l and solid c_s, where c_s is a complex number when the attenuation of leaky SAW is considered. However, it is real value here since the attenuation is not included in c_s. The radiated longitudinal wave induces nonlinear and chaotic recirculation in the droplet, as shown in Fig. 2.4.

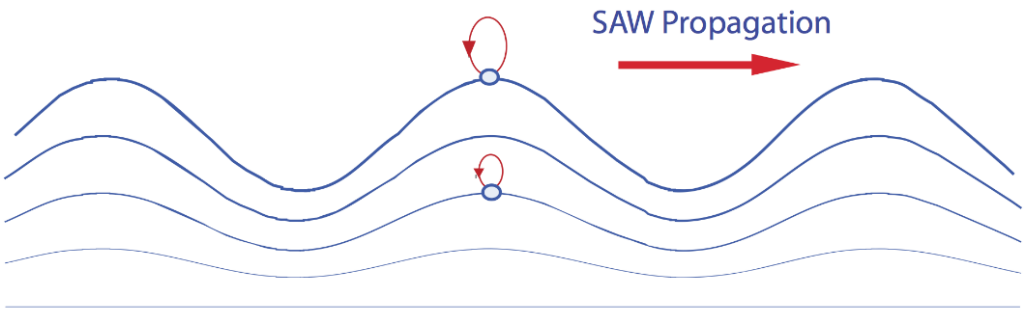


Fig. 2.4 Recirculation in the liquid droplet driven by SAW [Aisha2009].

At high acoustic power, the particle velocity at the surface as the SAW passes is on the order of 1 *m/s* regardless of the excitation frequency. Thus, at excitation frequencies on the order of 10 *MHz*, the displacement of the surface and the amplitude of the acoustic wave are expected be only around 10 *nm*. However, the acceleration of the surface is incredibly high, at around 10^7 m/s^2. Such huge surface acceleration is transmitted into a liquid drop placed upon it, inducing strong acoustic waves within the drop. If amount of the liquid droplet is small enough and the acoustic energy is above a certain threshold, it can destabilize the free surface of liquid, leading to capillary wave breakup as shown in Fig. 2.5 [Aisha2009]. Meanwhile, the liquid droplet is driven to move in some patterns, such as, vibration, flow, soaring, or atomization [Kurosawa1995-1, Kurosawa1995-2}, showing the SAW energy flow. Such a phenomenon is called "SAW streaming" because the phenomenon involves essentially

the same physics as the "acoustic streaming" [Shiokawa1988].

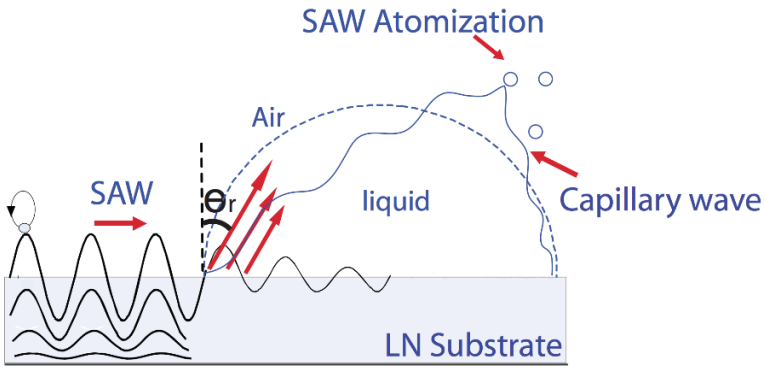


Fig. 2.5 Mechanism of SAW streaming [Aisha2009].

Based on the pumping feature of SAW streaming, SAW devices can be utilized as actuators in a variety of microfludic manipulations, for instance, non-contact linear motors [Gu2009], non-contact rotary motors [Zhang2009], and micromanipulators [Renaudin2006]. In the recent years, the use of SAW streaming has been considered as an optional method to release smells by atomizing liquid odorants [Saitoh2008].

The SAW streaming force was derived mathematically based on the acoustic streaming theory as follows. The general equation of hydrodynamics of viscous fluids is [Shiokawa1990]

$$F = -\nabla P + \eta\nabla^2 v + \frac{1}{3}\eta\nabla(\nabla \cdot v) \tag{2.3}$$

where F is the net force per unit volume due to stress, ρ is the density, η, is the shear viscosity coefficient and v is the particle velocity. Based on the continuity equation, one can obtain:

$$\frac{\partial(\rho v)}{\partial t} + \rho(v \cdot \nabla)v + v\nabla \cdot \rho v = F_0 - F_1 \tag{2.4}$$

where

$$F_0 = \frac{\partial(\rho v)}{\partial t} \tag{2.5}$$

and

$$-F_1 = \rho(v \cdot \nabla)v + v\nabla \cdot \rho v \tag{2.6}$$

for acoustic waves vary sinusoidally with time at the frequency ω, in order to obtain a streaming equation from Eqs. (2.4) - (2.6), it needs to retain the terms up to the second order and take the time average over a suitable number of cycles. Noting that the time average of F_0 should be zero in the steady state, then

$$-F_1 = \langle \rho_0(v \cdot \nabla)v + v\nabla \cdot \rho_0 v \rangle \tag{2.7}$$

in $\langle\ \rangle$ means "time average", and F_1 is the exact force of the acoustic streaming.

2.3 Development of 11 x 11 *mm* SAW Device

As described in Sections 1.8, a SAW device is considered to be a key component in this research to realize the olfactory display that can present the scents of low-volatile substances effectively. Before designing a SAW device, there is a trade-off between two important parameters, the resonant frequency and the expected size of the device that needed to be considered. As expressed in Eq. (2.1), the length of an aperture between any adjacent fingers of the IDTs determines the resonant frequency, therefore a tiny SAW device with narrow IDTs' fingers (and narrow apertures between fingers) needs high resonant frequency to be driven, and vice versa.

In this research, the minimum width of IDTs that the present industry can construct conveniently was considered first. As a result, we fixed the width of the IDT at 16 μm, therefore the resonant frequency is $= c_s/\lambda_{SAW} = (3965m/s)/(64\mu m) =$ 61.95 *MHz*. The entire electrode was made of gold/chromium and fabricated, by using photolithography, onto a piezoelectric substrate made of a 128° rotated Y-cut X-propagation $LiNbO_3$. Two IDTs, made up of 10 pairs of fingers per IDT, were designed at left and right sides of the substrate to construct a two-port SAW device. Each port has 100 lines of grating reflectors which are separated by a 2 *mm* SAW propagation path. The device's overall dimension is 11 x 11 *mm*. The SAW wavelength was 16 x 4 = 64 μm. The piezoelectric substrates were designed to be thicker than several wave lengths so that the acoustic wave would not reach the back side of the substrate. The entire electrode pattern is shown in Fig. 2.6 and the actual image of the SAW device is shown in Fig. 2.7. The device was mounted on a copper clad board connected to two BNC connectors. Pieces of aluminum foil, slitted by using a cutter, were pasted on the board, by using a conductive paste to create signal paths. An actual image of the device is shown in Fig. 2.8.

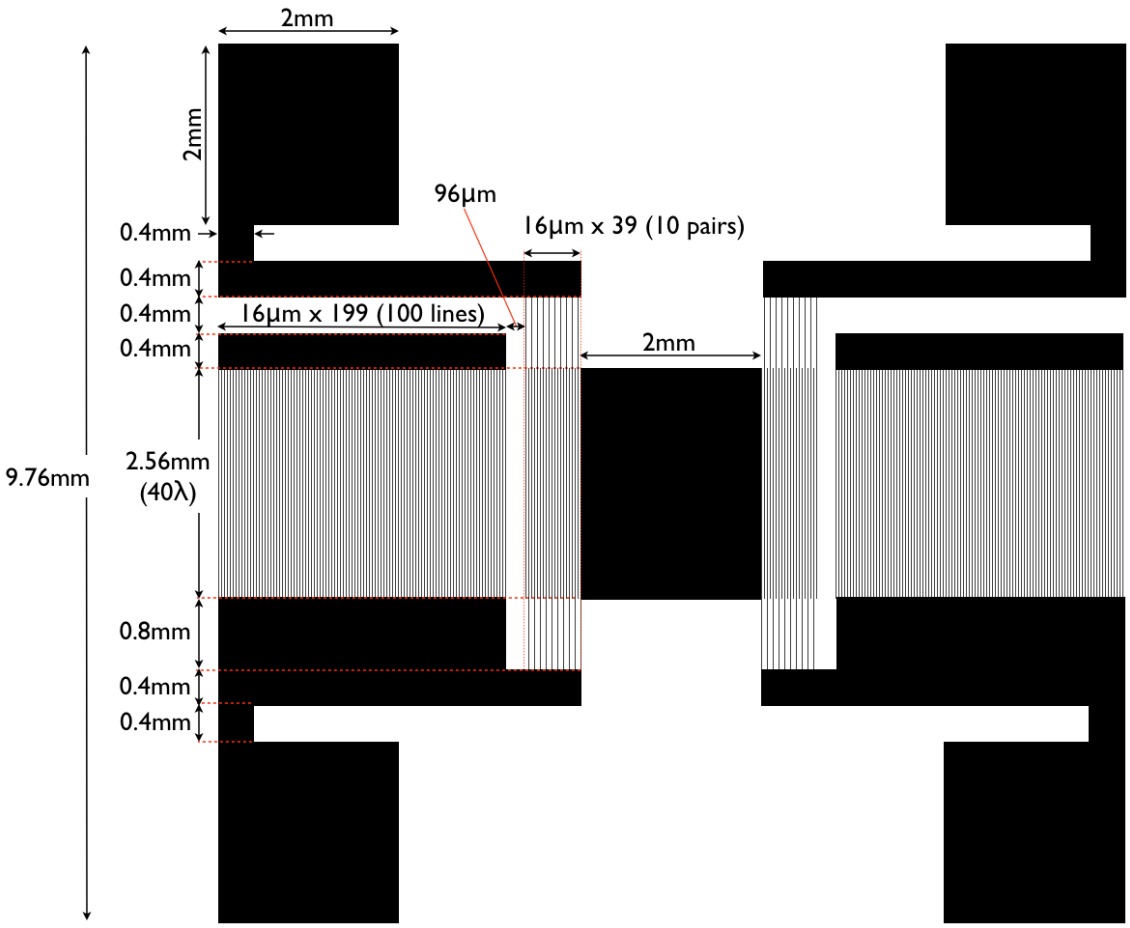


Fig. 2.6 Pattern of the 11 x 11 *mm* SAW device.

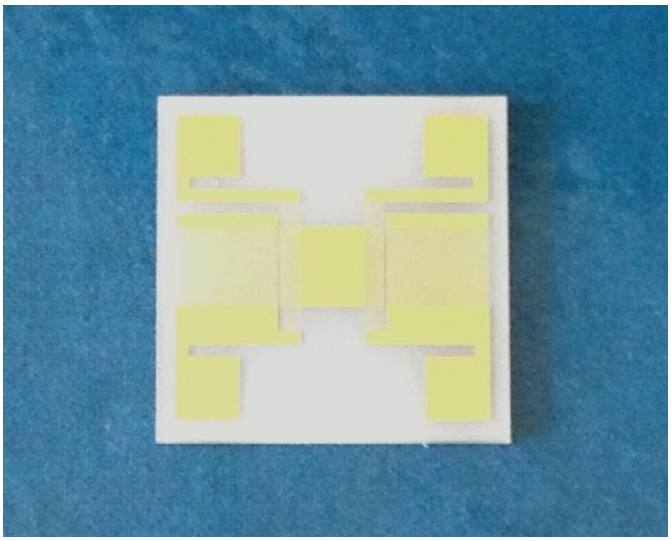


Fig. 2.7 Actual image of the 11 x 11 *mm* SAW device.

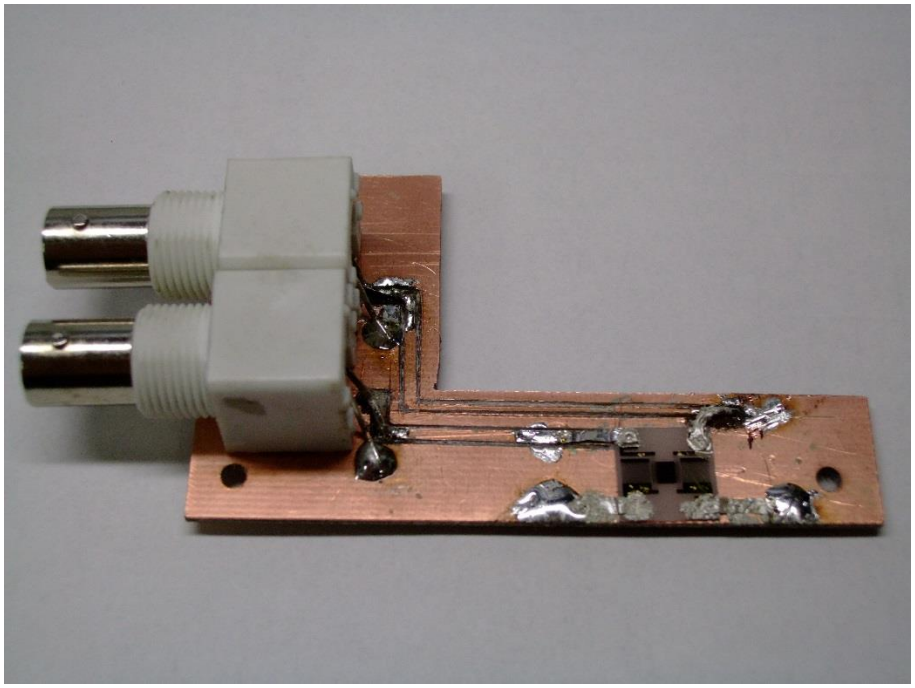


Fig. 2.8 Actual image of the 11 x 11 *mm* SAW device pasted onto a copper clad board.

2.4 Evaluation of 11 x 11 *mm* SAW Device

2.4.1 Resonant frequency measurement

Even though, the resonant frequencies of the 11 x 11 *mm* SAW device was calculated in the previous section, it was also measured by using an impedance analyzer (4291A, Hewlett Packard). The frequency characteristic obtained from the measurement is shown in Fig. 2.9. According to the result, the resonant frequency of the device is approximately 60.7 *MHz*. The difference between the result obtained from calculation and from measurement might be caused by some defect patterns of the IDTs, such as inaccurate shapes or tiny flaws, and parasitic elements in the connection between the SAW device and the connector.

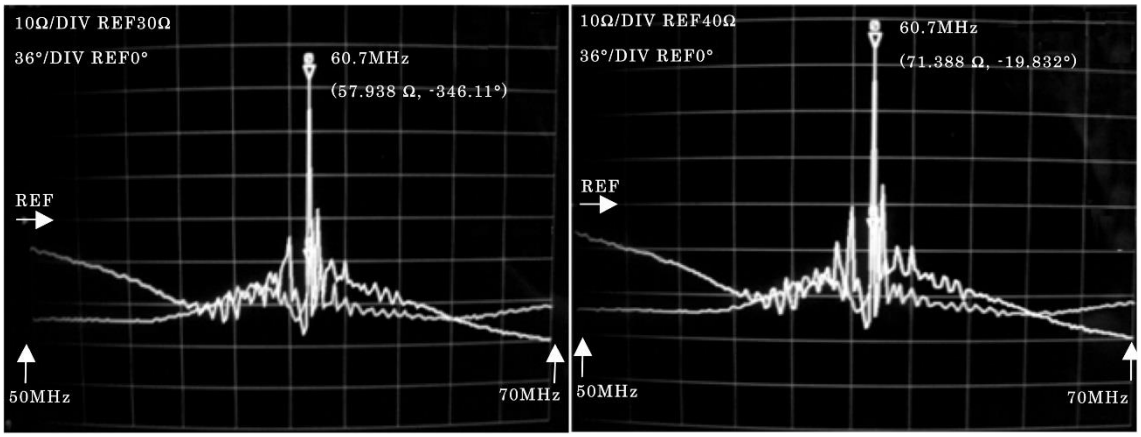


Fig. 2.8 Frequency characteristics of the 11 x 11 *mm* SAW device pasted onto a copper clad board at the left port (left) and right port (right).

2.4.2 Evaluation of the atomization performance

In this section, a result of an experiment to evaluate the atomization performance of the 11 x 11 *mm* SAW device is described. In the experiment, a microsyringe was used to drop an approximate 1.5 μL tiny liquid droplet on to the SAW device. The samples used in this step were water and other liquids which have moderate volatility, including acetone, ethanol, pentane, and hexane. The experimental setup is shown in Fig. 2.9. A 1 W RF amplifer (ZHL-1A, Mini-Circuits) was used to apply an RF square wave at the resonant frequency generated from a function generator (AFG-3251, Tektronix) to the IDTs through the BNC connectors to excite the droplet and its behaviors at any driving conditions were observed. The experiment was done in two cases, one-port driving condition and two-port driving condition in which the RF signal was applied to only one BNC connector and both BNC connectors at the same time, respectively. Amplitude of the applied RF signal was 38 V_{pp} which is the maximum output voltage at that frequency. The experimantal result is shown in Table. 2.1.

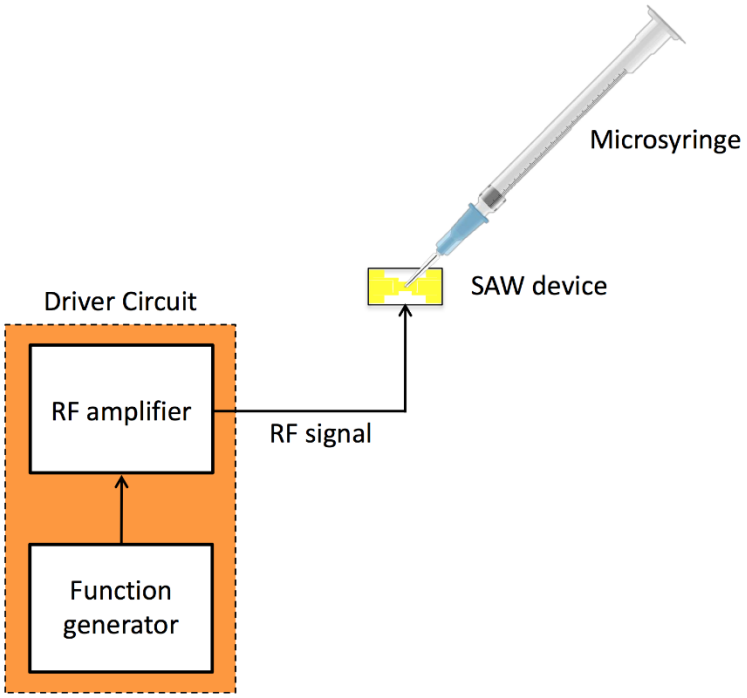


Fig. 2.9 Experimental setup in the experiment to evaluate atomization performance.

Table 2.1 Droplet behavior induced by SAW streaming at different driving conditions.

Liquid	Droplet behavior	
	One-port driving	Two-port driving
Pentane	Flowed (Sometimes) and Atomized	Atomized and Soared (Rarely)
Hexane	Flowed (Sometimes) and Atomized	Atomized and Soared (Rarely)
Acetone	Flowed and Atomized	Atomized
Ethanol	Flowed and Atomized Softly	Atomized (Softly)
Water	Flowed	Atomized (Extremely Softly)

The result confirmed that the 11 x 11 *mm* SAW device can produce SAW streaming that induces various motions of the droplet depending on the driven power. At low power, SAW streaming induces the droplet to vibrate and if the power is further increased, the droplet turns to flow, be atomized, or soar. According to the result, the two-port driving can provide SAW streaming with stronger power to the droplet than one-port driving. It also revealed that pentane (b.p.: 36 ℃) and hexane (b.p.: 62 ℃) can

be atomized easier than acetone (b.p.: 56 ℃), ethanol (b.p.: 78.3 ℃), and water (b.p.: 100 ℃), respectively. This result confirmed that the volatility of liquid affects atomization performance.

However, as the flow occurred simultaneously with the atomization, the droplet was sometimes expelled from the 2 *mm* propagation path before it was atomized entirely. To solve this problem, another SAW device with longer SAW propagation path was developed subsequently. Its development is explained in the next Section.

2.5 Development of 11 x 19 *mm* SAW Device

In this section, the development of a SAW device with 10 *mm* propagation path is described. The minimum width of IDTs and resonant frequency of the device was the same as that of the previous 11 x 11 *mm* SAW device. Therefore, the electrode shape was almost the same as that of the previous device except the length of the SAW propagation path which was lengthened to be 10 *mm*. The entire electrode pattern is shown in Fig. 2.10. The size of the entire device was 11 x 19 *mm*.The actual image of the SAW device is shown in Fig. 2.11 and the image of the SAW device pasted onto a copper clad board with two BNC connectors is shown in Fig. 2.12. Two electrodes were also soldered onto the board for convenient voltage measurement by using oscilloscope's probe.

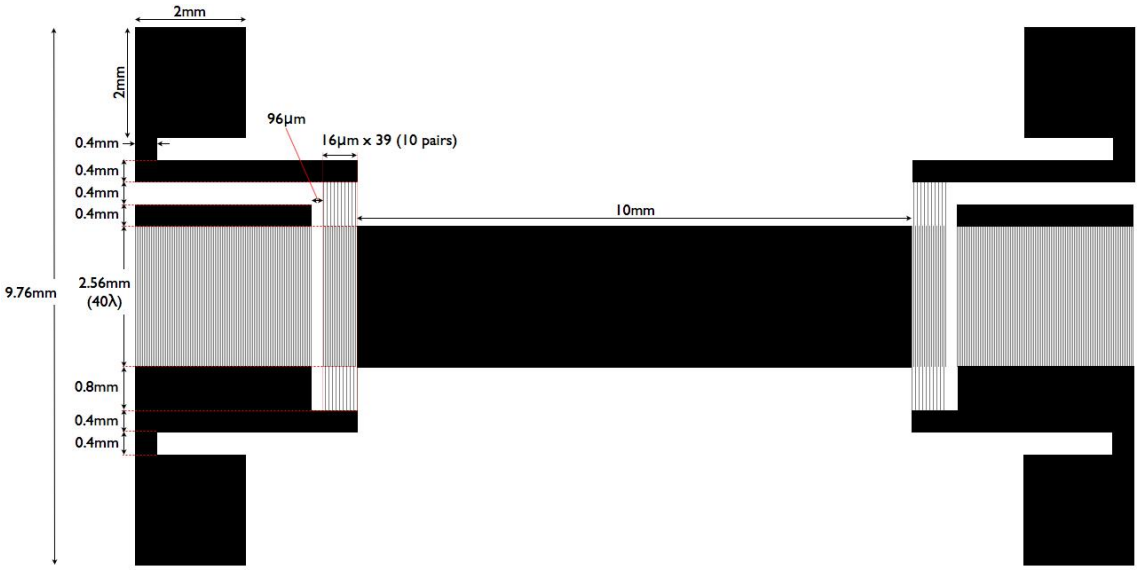


Fig. 2.10 Pattern of the 11 x 19 *mm* SAW device.

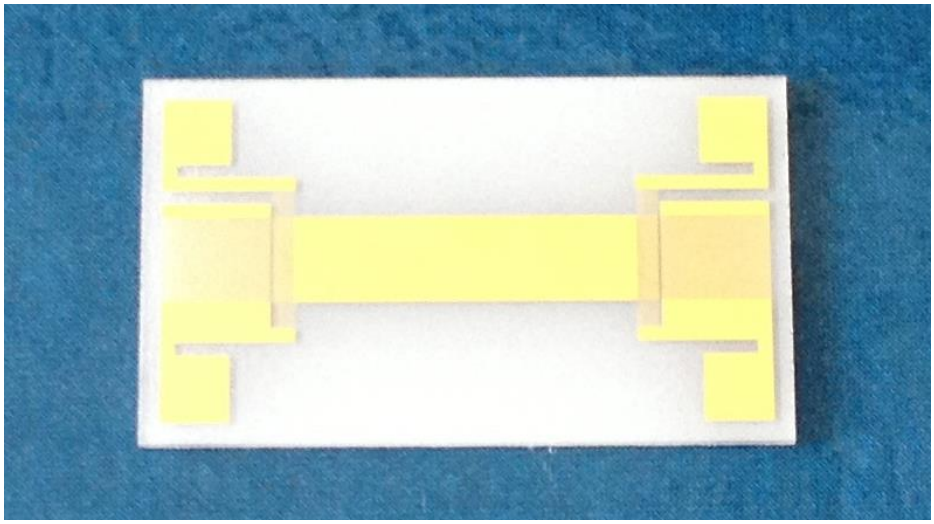


Fig. 2.11 Actual image of the 11 x 19 *mm* SAW device.

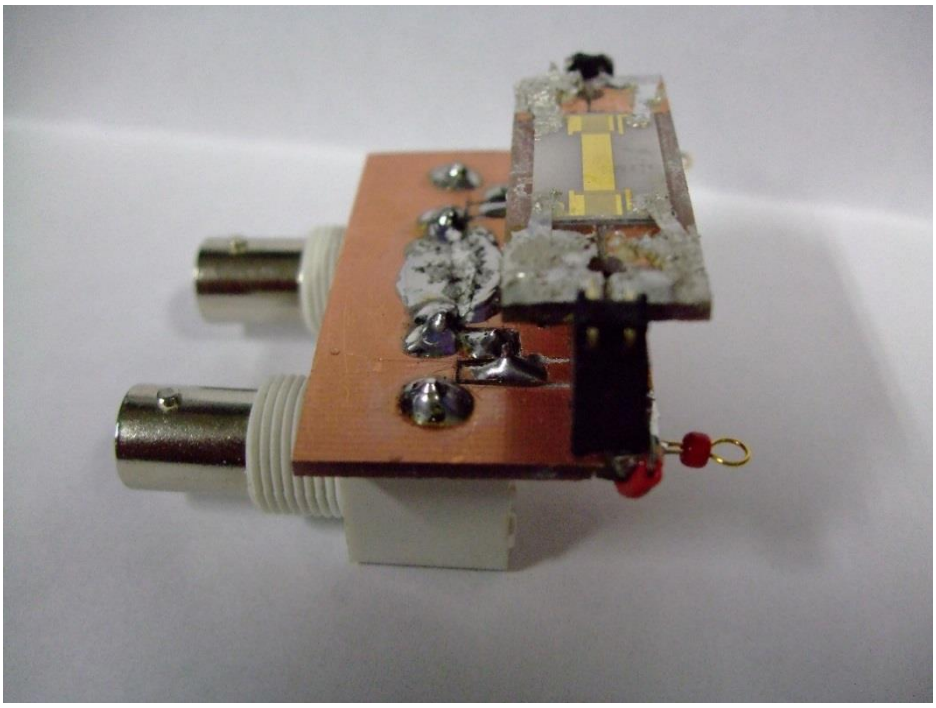


Fig. 2.12 Actual image of the 11 x 19 *mm* SAW device pasted onto a copper clad board.

2.6 Liquid Atomization Using 11 x 19 *mm* SAW Device

Since the transducer pattern of the 11 x 19 *mm* SAW device was almost the same as the previous one, its resonant frequency and frequency characteristic remained the same as the result shown in Section 2.4.1. Thus it is not represented again in this section since the redundancy should be avoided. In Sections 2.6.1 and 2.6.2, experiments on the atomization performance of the 11 x 19 *mm* SAW device in more details is described.

2.6.1 Investigation on threshold voltage of liquid droplet atomization

In this section, pentane, hexane, acetone, and ethanol were prepared to be atomized at the same procedure and almost same condition as the experiment in Section 2.4.2, except that the 11 x 19 *mm* SAW device and a 5 *W* RF amplifier (ZHL-5W, Mini-Circuits) were used instead of the 11 x 11 *mm* SAW device and the 1 *W* RF amplifier. The voltage applied to the SAW device was varied from 0 to the threshold value at which the droplet starts to be atomized rapidly. The threshold voltages required for atomizing the liquid droplets in this experiment are summed up in Table. 2.2

Table 2.2 Threshold voltage of liquid droplet atomization.

Liquid	Threshold voltage (V)	
	One-port driving	Two-port driving
Pentane	30	14
Hexane	36	30
Acetone	30	28
Ethanol	76	55

The table confirmed the result shown in Section 2.4.2 that two-port driving can provide SAW streaming with stronger power to the droplet than one-port driving. However, as the threshold voltage required for atomization of hexane is higher than acetone while the former can be atomized effectively than the latter at the same driving voltage as described in Section 2.4.2, we concluded that the volatility of liquid is a parameter governing the atomization performance but not the only crucial one.

2.6.2 Observation of liquid residue after atomization

As the SAW propagation path of the SAW device was lengthened, the residue remaining on it after atomization became easily to be observed. The photographs of the SAW devices after atomization a 5 μL droplet of pentane, hexane, and acetone by SAW streaming induced by the 40 V_{pp} RF signal are shown in Figs. 2.13, 2.14, and 2.15, respectively.

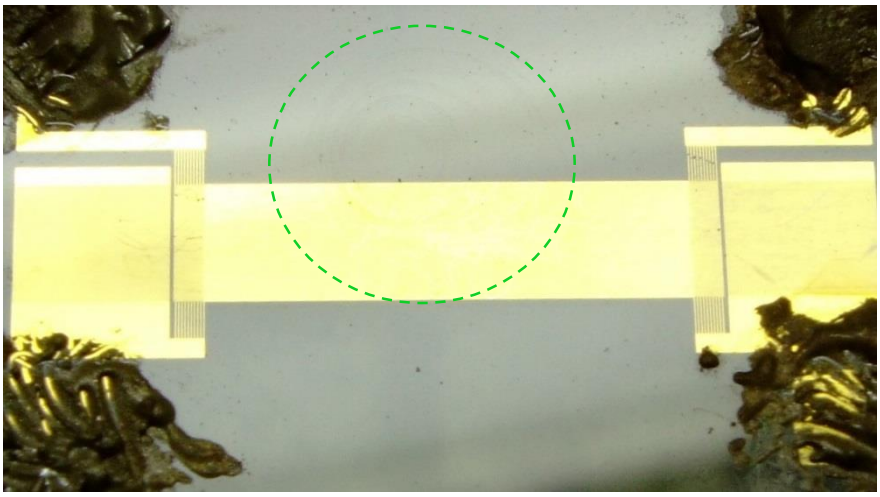


Fig. 2.13 Residue after a 5 μL droplet of pentane is atomized.



Fig. 2.14 Residue after a 5 μL droplet of hexane is atomized.

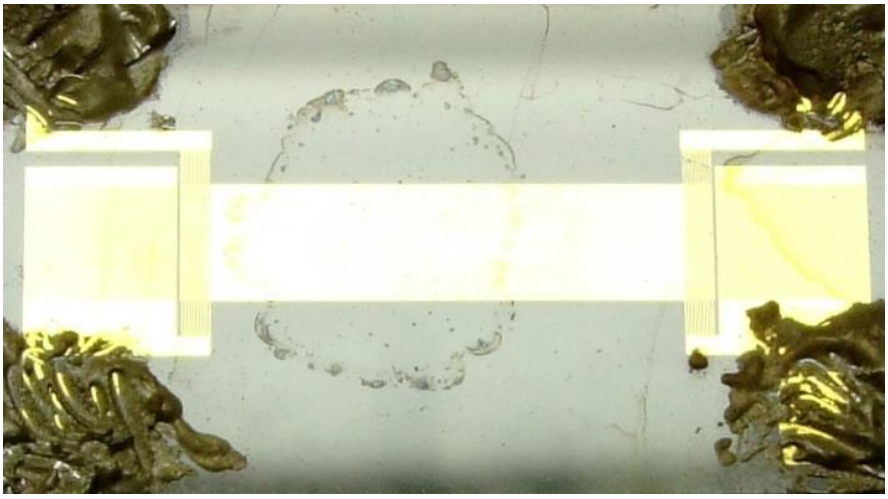


Fig. 2.15 Residue after a 5 μL droplet of acetone is atomized.

Since, the residues can be clearly observed, it was concluded that the SAW device can atomize 5 μL of liquid droplets used in this experiment but not completely even though they have no low volatilities. It was also found that the residue remaining on the SAW propagation path drastically reduces power of the next SAW streaming. Nevertheless, it was found that if the droplet volume is less than approximate 0.5 μL, the residue does not occur. Thus, in order to realize the olfactory display that can present scents of lower volatile substances effectively, the method to increase the atomization performance of the SAW device so that it does not leave any residues at all, or/and the precise method to convey tiny amount of liquid droplet that is smaller than 0.5 μL to the SAW propagation path was required.

The study on using an electroosmotic pump to convey a tiny liquid droplet precisely is described in Chapter 3, and the development of a higher performance SAW device is described later in Chapter 5.

2.7 Summary

In this chapter, the fundamental of SAWs, SAW devices, and SAW streaming were explained. Since the SAW streaming can atomize a liquid droplet if the acoustic energy is sufficient, it was considered to be utilized in the olfactory display to be developed in this study.

This chapter described about the development of two SAW devices with 2 *mm* and 10 *mm* of SAW propagation paths, firstly developed in this research. The resonant frequencies and frequency characteristics of the proposed device were measured. The latter was found to be easier to use than the former due to its longer SAW propagation path. In the experiments, their capabilities to atomize a droplet of liquid with boiling point up to 78.3 ^{o}C rapidly were proved and threshold voltages required for starting rapid atomization of pentane, hexane, acetone, and ethanol were recorded. Regarding the SAW device excitation, according to the result, two-port driving can produce SAW streaming with stronger energy than one-port driving. According to the experimental, the volatility of liquid was considered to be a parameter that governs the atomization performance but not the only crucial one. Even though, the proposed SAW device can atomize a droplet of the liquid in this study rapidly, the residue remaining on the SAW propagation path was founded. Therefore, we conclude that in order to develop the olfactory display that can present scents of low-volatile substances rapidly, the method to increase the atomization performance of the SAW device so that it does not left any residues at all, or/and the precise method to convey a more tiny amount of liquid droplet to the SAW propagation path was required.

Chapter 3

Study on Conveying Liquid Odorant Using an Electroosmotic Pump

3.1 Introduction

An electroosmotic pump is a kind of micro pump which drives liquid based on electroosmotic phenomenon. It has several advantages over other kinds of micro pumps, such as tiny size, soundless operation, low power consumption, and convenient usage. As mentioned in Section 1.7, a number of electroosmotic pumps were used in this research to realize a multi-component olfactory display that can blend smells. Each pump works as a liquid tank and supplier that conveys a liquid odorant to the SAW device so that it can be atomized into a smell.

This chapter focuses on the exploratory study on the use of a single electroosmotic pump to spout liquid droplet and its evaluation. Starting with an overview of electroosmosis and a detail about of its application in electroosmotic pump in Section 3.2, the specification of the electroosmotic pump used in this study is described in Section 3.3. According to the experimental result in Section 2.6.2, volume of a droplet supplied onto the SAW propagation path of the 11 x 19 mm SAW device needs to be in the range of 0.1 μL in order to achieve the atomization. Therefore, the effective approach to use the electroosmotic pump in an olfactory display was investigated, including the appropriate methods to drive the pump and to suppress the

amount of a droplet within the required value. These investigations and the results are described in Section 3.4. In Section 3.5, the measurements of electroosmotic pump's parameters which are important in the application to odor presentation including the start-up time and the droplet's volume are described. Finally, the chapter is summarized in Section 3.6.

3.2 Basics of Electroosmotic Pump

An electroosmotic pump is a kind of micro pump that utilizes electroosmosis to induce a liquid flow. The principles of electroosmosis is described in Section 3.2.1 and detail about the electroosmotic pump is described in Section 3.2.2.

3.2.1 Electroosmotic flow

Electroosmotic flow (or electro-osmotic flow, synonymous with electrokinetic flow, electroosmosis or electroendosmosis) was first reported by Reuss [Reuss1809] in 1809 in experiments that demonstrated that water could be made to percolate through porous clay diaphragms through the application of an electric field. The theoretical aspects of this phenomena were investigated by Kohlrausch in 1897 [Kohlrausch1897]. Hunter, Probstein, Rice and Whitehead are also regarded as fundamental sources for this theory [Hunter1981, Probstein1994, Rice&Whitehead1965].

This phenomenon occurs in a micro-scale channel, such as porous material, capillary tube, or membrane near a two phase interface between solid and liquid. As shown in Fig. 3.1, when a dielectric is in contact with an electrolyte, an immobile charge occurs on the dielectric surface (for the case shown in Fig. 3.1, a negative charge). This immobile surface charge in turn attracts a cloud of free ions of the opposite sign forming a thin layer of mobile charges near it. This thin layer is called Debye layer whose

thickness is approximately 1 – 10 *nm* under typical conditions. The variation of electric potential near a surface is called electric double layer in which the voltage is called zeta (ζ) potential [Hunter1981].

In the presence of an external electric field in parallel direction with the surface (usually via electrodes placed at inlets and outlets), the liquid in this non-zero net charge Debye layer acquires a momentum which is then exerted to adjacent layers of liquid through the effect of viscosity [Sandip2004] as shown in Fig. 3.2. The resulting flow is termed electroosmotic flow.

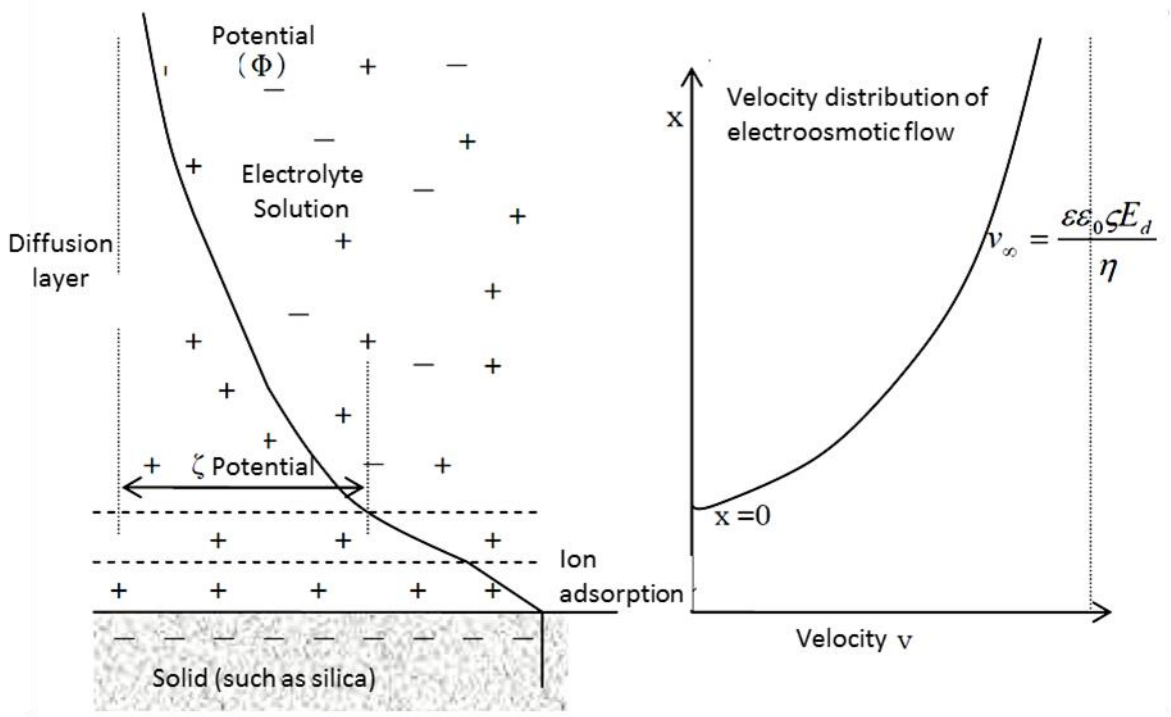


Fig. 3.1 Model illustrating electric double layer and electroosmotic flow [Ichiro2005].

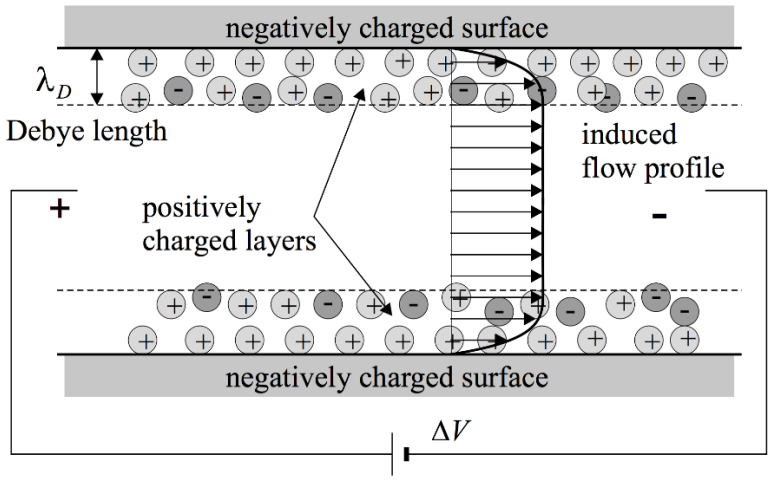


Fig. 3.2 Schematic illustration of electroosmotic flow in a channel [Brask2005].

As the thickness of the electric double layer is extremely thin, this electroosmotic flow does not affect the general liquid flow in macro-scale. If the liquid is incompressible, the flow is governed by the Navier-Stokes (Eq. 3.1) and continuity equations (Eq. 3.2).

$$\rho\left(\frac{\partial v}{\partial t} + \mathrm{v}\cdot\nabla\mathrm{v}\right) = -\nabla\mathrm{p} + \eta\nabla^2\mathrm{v} - \rho_E E_d \tag{3.1}$$

$$\nabla\mathrm{v} = 0 \tag{3.2}$$

where v is the flow rate (*m/s*), η is the viscosity constant (*Pa·s*), p is the liquid pressure (*Pa*), ρ is the density of the liquid ($1/m^3$), ρ_E is charge density (C/m^3), and E_d is electrical potential and charge density in the electric double layer (*V/m*).

The relatively small dimensions and flow velocities of the electroosmosis limit the flow to the strongly laminar and low Reynolds number. Thus, the flow rate of the electroosmosis can be expressed as

$$\eta\nabla^2\mathrm{v} = -\rho_E E_d \tag{3.3}$$

Potential distribution of the mobile ion occurred near the surface can be expressed as

$$\rho_E = -\varepsilon\varepsilon_0\nabla^2\Phi \tag{3.4}$$

where Φ is potential in electrolyte, ε is relative permittervity, ε_0 is dielectric constant of vacuum. If the electrostatic effect persists within the length x, from Eqs. (3.1) and (3.2)

$$\eta\frac{\partial^2 v}{\partial x^2} = -\varepsilon\varepsilon_0 E_d\frac{d^2\Phi}{dx^2} \tag{3.5}$$

where x is the direction of liquid migration. By assuming that the boundary condition is infinity $\frac{dv}{dx} = 0$、$\frac{d\Phi}{dx} = 0$、x=0, v=0、Φ=ς and double integrates Eq. (3.3),

$$v = -\frac{\varepsilon\varepsilon_0\varsigma E_d}{\eta} \tag{3.6}$$

For example, in case of water that $\varepsilon = 88$, $\varsigma = 100$ *mV*, $\eta = 10^{-3}$ *Pa·s* and $E_d = 10000$ *V/m* (10 *V/mm*), the flow rate $v = 7.8 \times 10^{-4}$ *m/s* can be obtained.

If the pressure gradient is neglected, the maximum back pressure of the electroosmotic pump can be calculated from

$$\Delta P = \frac{8\varepsilon\varepsilon_0\varsigma E_d L}{a^2} \tag{3.7}$$

where, a is the radius of circular tube (the pump's outlet).

From Eq. (3.6), it can be observed that the flow rate depends on the viscosity of liquid, the accumulated charge on the solid surface, and the strength of external electric

field and is largely independent of channel size (outsize the double layer). From Eq. (3.7), it can be observed that higher back pressure can be obtained by reducing the dimension of the flow path. Besides, it is clear that both flow rate and back pressure can be controlled by adjusting the voltage. The fact that maximum flow rate and back pressure of the pump can be calculated conveniently from the amplitude of the applied voltage is one of the advantage of the electroosmotic pump.

For example, if the distance between electrodes is constant, in case of water that $\varepsilon = 88$, $\varsigma = 100\ \ mV$, $\eta = 10^{-3}\ \ Pa{\cdot}s$ and $V = 10000\ \ V$ ($E_d = 10\ V/mm$), $a = 100\ \mu m$, distant between electrodes: $L = 10\ mm$, the maximum flow rate $v_m = 1.47$ *μL/min* and maximum back pressure $P_m = 6\ \ Pa$ can be obtained. If the radius of the tube is changed to be $a = 1\ \mu m$, the maximum flow rate $v_m = 0.14\ \ nL/min$ and maximum back pressure $P_m = 62\ \ kPa$ can be obtained.

3.2.2 Electroosmotic pump

Electroosmotic pumps can be mainly categorized into two types. The first one utilizes electroosmotic phenomenon occurred in a capillary or microchannel [Seiler1993]. This kind of electroosmotic pump has a limitation to produce high back pressure due to its shape. The electroosmosis occurs in a microchannel as shown in Fig. 3.2 belongs under this category. Since it has not much driving power, another kind of electroosmotic pump which is called generalized electroosmotic pump was developed. In this case, a porous material is used to be a liquid flow path [Yao2003]. It can provide flow rate in the range of *μL/min* to *mL/min* with back pressure in the range of 100 *kPa* [Paul2000]. The electroosmotic pump used in this research is generalized electroosmotic pump. Its structure is shown in Fig. 3.3.

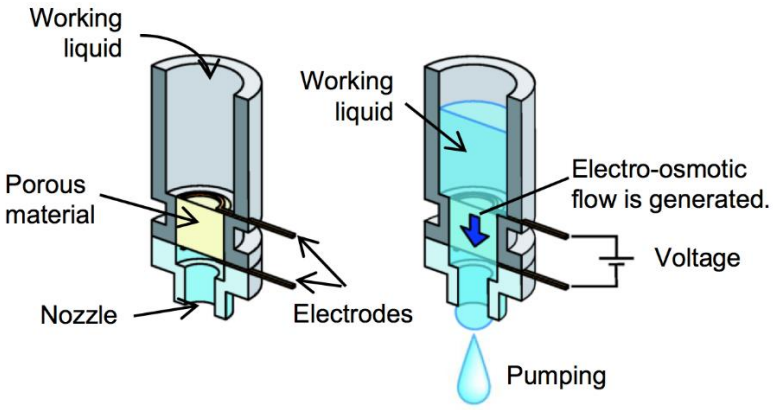


Fig. 3.3 Structure of generalized electroosmotic pump [Nano Fusion Technologies2009]

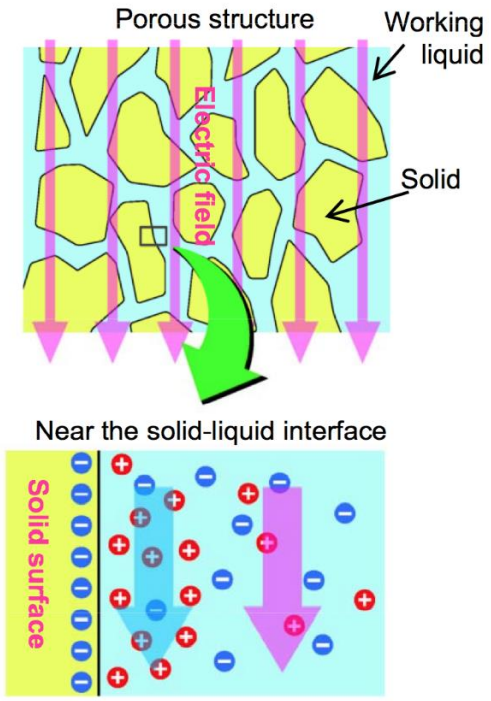


Fig. 3.4 Electroosmosis in porous material [Nano Fusion Technologies2009]

As shown in Fig. 3.3, a hydrophilic porous material is simply placed between two electrodes. When a liquid is filled into the reservoir on the top of the pump, the liquid diffuses into the porous material through capillary action. An enlarged image of the area in the internal structure of porous material is shown in Fig. 3.4. Since each gap

in the porous material is in micro-scale, the porous material can be considered as a number of microchannels that are packed together. Therefore, when the electric field is applied across the material, a number of microchannels like flow structure can produces a large amount of flow rate. Based on this configuration, even though the device's size is tiny and applied power is not so high, a large flow rate can be realized.

In summary, the advantages and disadvantages of electroosmotic pumps compared with other types of micropumps are shown below.

Advantages

1. Its implementation is simple.
2. The simplicity of its structure enables low production cost.
3. It can perform fluidic handling in picoliter scale simply and precisely.
4. It does not contain any moving parts and can produce a silent non-pulsating flow.
5. Its performance is not affected from a bubble or a particle inside the flow path unlike some kinds of micropumps and a widely used inkjet device.

Disadvantages

1. The efficiency of the pump is very low, typically less than 1 %. It needs relatively high applied voltage to generate a significant flow rate. For example, a potential of 1000 V is required to produce a flow rate of 100 $\mu m/s$ in a 10 cm channel.
2. The requirement of the high potential may cause a difficulty to develop a portable device.
3. The high electric field can cause significant damage to transported living organisms whose internal elements tend to exhibit different mobility.
4. It is only compatible with only some types of liquids which are aqueous solutions with low ionic concentration.

The electroosmotic pump was selected to be used in this study due to all of the advantages listed above. Since the odorants used in this research do not contain a living organism, this disadvantage can be neglected. To overcome other disadvantages, some experiments were performed to investigate the effective approach to drive the pump and the appropriate type of solvent used in this study. The details are described in Sections 3.4 and 4.3.3, respectively.

3.3 Characteristics of Electroosmotic Pump in This Study

The electroosmotic pump used in this study was obtained commercially from Nano Fusion, a company in Tokyo. Its model number is RP3-N2. Its actual image and dimension are shown in Figs. 3.5 and 3.6 respectively. According to the datasheet, its power consumption is 6 mW, maximum flow rate and maximum back pressure tested at 30 V of driving voltage are 10 $\mu L/min$ and 90 kPa, respectively. There is a reservoir on the top of the pump for storing a targeted liquid. The capacity of a reservoir is 100 μL. Diameters of the inner and outer outlets of the pump are 0.6 and 2 mm respectively. The relationship between driving voltage, back pressure and flow rate of the liquid is shown in Fig. 3.7.

Due to the fact that the flow rate at maximum driving voltage written in the datasheet (30 V) as shown in Fig. 3.7 is not sufficient for the use in this study, various investigations and experiments, such as the application of a 30 V exceed potential, were performed to obtain the appropriate condition to drive the pump. The details about those investigations and experiments are described in the later Sections in this chapter.

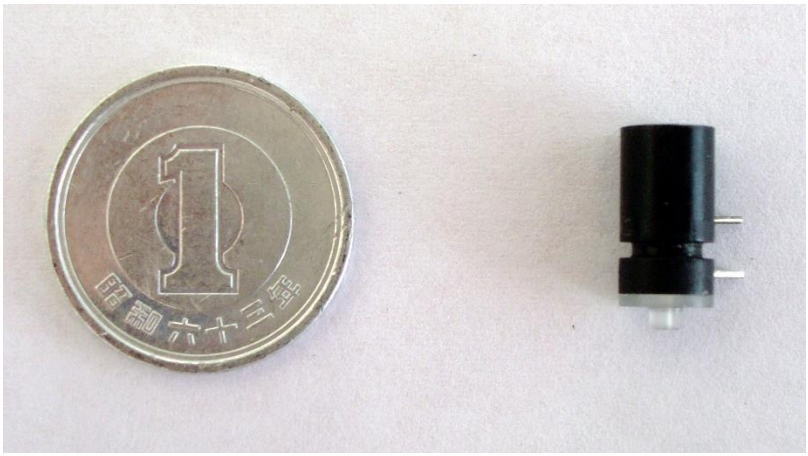


Fig. 3.5 Actual image of the electroosmotic pump used in this study.

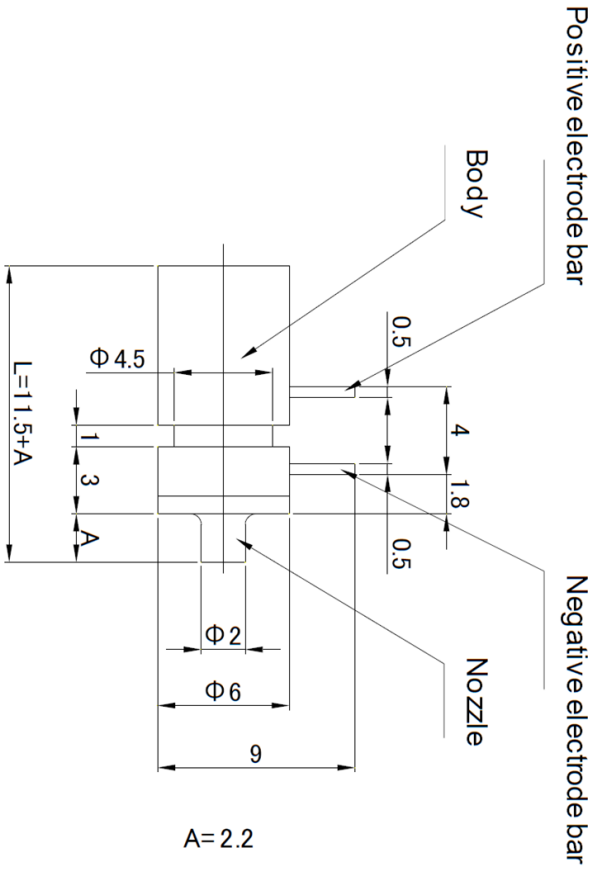


Fig. 3.6 Structure of an electroosmotic pump (unit: *mm*) [Nano Fusion Technologies2009].

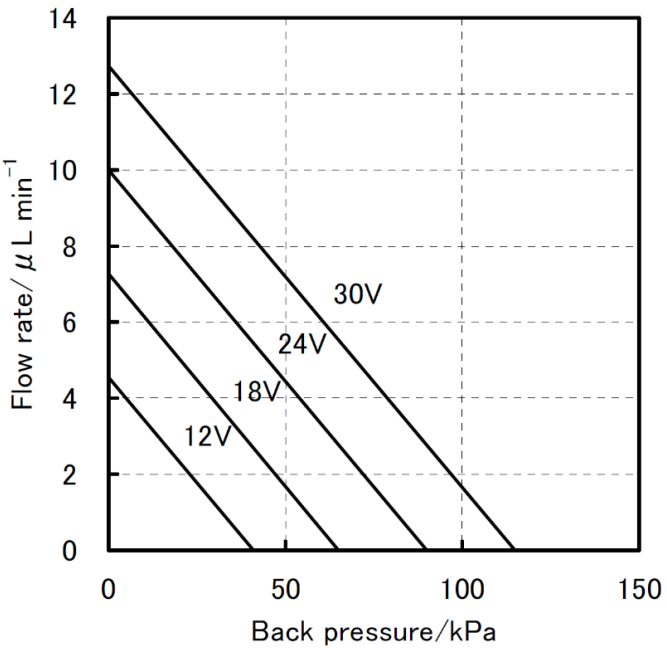


Fig. 3.7 Structure of an electroosmotic pump [Nano Fusion Technologies2009].

3.4 Investigation on Effective Approach to Use Electroosmotic Pump in Olfactory Display

The electroosmotic pump is considered to be an essential component in this research. It conveys the odorant droplet onto the SAW propagation path of the SAW device so that the droplet can be atomized into a vapor of odor. According to the result of an experiment in Section. 2.6.2, the volume of a droplet spouted from the electroosmotic pump is one of the important parameters that determine whether the atomization can occur. Therefore, it needs to be controlled strictly.

Thus, the investigations on the approach to drive an electroosmotic pump so that it can spout a liquid droplet effectively were done. In Section 3.4.1, the investigation on a suitable driving approach is described. In Section 3.4.2, a method to limit the amount of a droplet spouted from the electroosmotic pump so that it will not be exceed the required value is described.

3.4.1 Investigation on pump driving method

As mentioned in Section 3.2, the velocity of electroosmotic flow depends on the electrical energy applied to the pump. Thus, by varying the electrical energy in some ways, the volume of a liquid droplet can be adjusted. According to the result from an experiment in Section 2.6.2, the volume of a liquid droplet needs to be in the range of 0.1 μL in order that the atomization can occur. Therefore, an investigation to determine the appropriate approach to drive the pump effectively was conducted. It is described in this section.

In my consideration, the approach to drive an electroosmotic pump and control the volume of a liquid droplet can be categorized into three ways;

1) Driving an electroosmotic pump by a pulse signal and adjusting the number of pulse to control the amount of a droplet.
2) Driving an electroosmotic pump by a one shot pulse and adjusting the pulse width to control the amount of a droplet.
3) Driving an electroosmotic pump by a DC voltage and adjusting the amplitude to control the amount of a droplet.

Since the electroosmotic flow depends on the electrical power applied to the pump, the velocities of liquid flows resulted from three different driving manners above are not different if the driving power are equal. However, adjusting the number of pulse in the first approach takes longer time to provide the same electrical power to the pump than that of the other two method. Thus, it was considered as an inefficient manner and was used only one time in this research (in an experiment in Section 4.4.3). The second and third method were determined to be used throughout this study. However, as the olfactory display to be developed is for abrupt odor presentation, the pulse width less than 5 s was normally adjusted. Since the electroosmotic flow is not too strong, the high driving voltage up to 100 - 150 V was applied in most of experiments. For this reason, to

avoid using the very high voltage amplitude, the driving voltage was adjusted not to exceed about 150 V (even though a 200 V driving potential was used in some experiments) and the droplet size was mainly adjusted by varying the pulse width.

3.4.2 Investigation on method to suppress droplet volume

As mentioned in Section 2.6.2, to atomize the liquid droplet by using the 11 x 19 *mm* SAW device, the volume of a liquid droplet needs to be in the range of 0.1 μL. However, when an electroosmotic pump is driven, the droplet is accumulated in the outlet of the pump first as shown in Fig. 3.8 due to the surface tension between the liquid and the inner surface of the pump outlet. The liquid is accumulated until its weight is more than the surface tension, then a droplet in the range of 10 μL is dropped as shown in Fig. 3.9. As the droplet with this volume is larger than that the 11 x 19 *mm* SAW device can atomize, some method to suppress the volume of the droplet spouted from the pump is strongly required.

I considered that the crucial parameter that determine the size of the droplet spouted from the pump is the outlet diameter. Besides, the thickness between inner and outer of the outlet is also important. It should be as thin as possible so that it can be handled conveniently.

As a consequence, the electroosmotic pump was connected with a tiny stainless tube (inner diameter: 0.1 *mm*, outer diameter: 0.5 *mm*, INZA0402054K, Lee) through two silicone and a Teflon tubes as shown in Fig. 3.10. The measurement of a droplet volume spouted from this tiny tube is described in Section 3.5.2. This form of connection had been used in all experiments in the early stage of this research until the new structure of the olfactory display was developed (in Chapter 5).

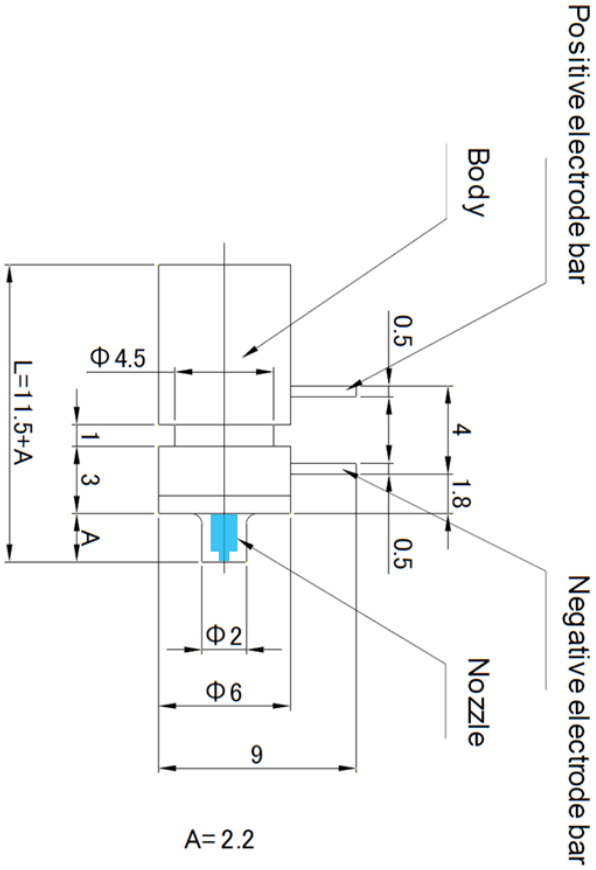


Fig. 3.8 Structure of an electroosmotic pump (unit: *mm*) (the blue area indicates the liquid accumulation in the pump outlet).

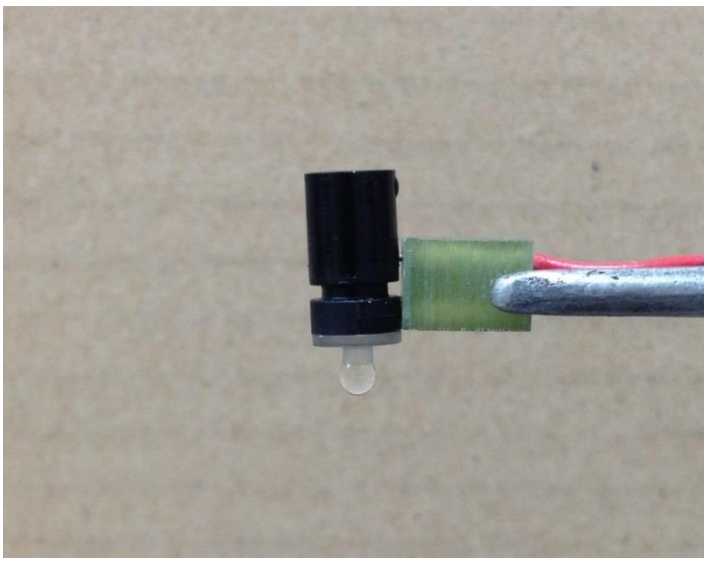


Fig. 3.9 A liquid droplet in the range of 10 μL spouted from an electroosmotic pump.



Fig. 3.10 An electroosmotic pump connected with a tiny stainless tube through two silicone and a Teflon tubes.

3.5 Measurement of Parameters Affecting Odor Presentation

Parameters of the electroosmotic pump connected with a tiny stainless tube as shown in Fig. 3.10 were evaluated by various experiments. First, the experiment that was performed to measure the start-up time of the pump is described in Section 3.5.1. Another experiment that was performed to measure the volume of a spouted droplet is described in Section 3.5.2.

3.5.1 Measurement of start-up time

As explained in Section 3.2, the flow rate induced by electroosmosis is in the order of *μL/min* that is not so high. Besides, the liquid diffuses into the porous material at slow speed. As a consequence, the electroosmotic pump takes a considerably long time since

the pump is driven until the first droplet appears at the outlet of the tube. This period was named "start-up time" in this study.

To understand the relationship between this start-up time and the applied voltage in order to propose some technique to shorten that period, an experiment was performed. The experimental setup is shown in Fig. 3.11. The pulse was generated by a functional generator (33120A, Hewlett Packard) and amplified by a MOSFET amplifier whose schematic diagram is shown in Fig. 3.12.

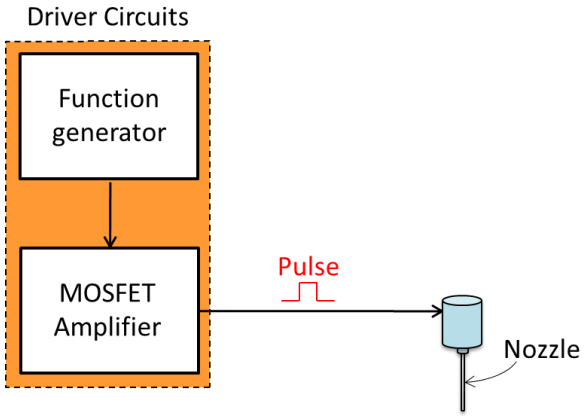


Fig. 3.11 Experimental setup.

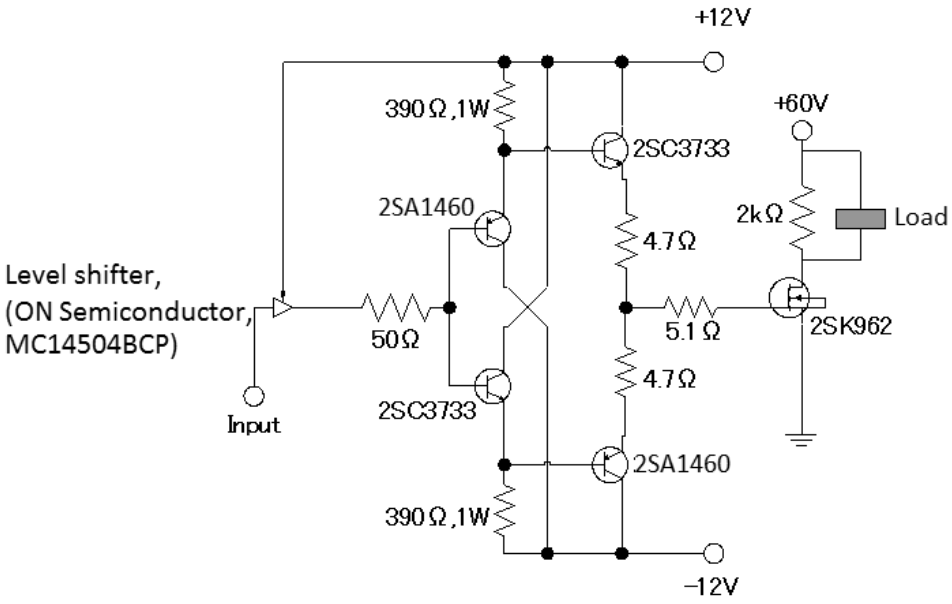


Fig. 3.12 A MOSFET amplifier used in this study [Takigawa2004]

The experiment and obtained result are described in this section. In the experiment, an electroosmotic pump filled with ethanol was driven under four conditions in which the DC driving voltage was adjusted to 25, 50, 100, 150, 200 *V*, respectively. The outlet of the stainless tube connected with the pump was put on the filter paper that can absorb liquid well so that the liquid can be observed suddenly when it reaches the tube's outlet. Time period since the driving is started until the first droplet appears on the filter paper was recorded. The result of this experiment is shown in Fig. 3.13.

From the result, it was understood that the raising of the flow rate, by increasing the driving voltage, results in the shortening of the start-up time. For example, the continuous driving voltage at 200 *V* can drive the first droplet to reach the tube's outlet within 16 *s*. Therefore, in this study, about 200 *V* of DC voltage was driven first until the first droplet appears in all experiments. Even though applying higher voltage can further shorten this period, it was not done in this study to avoid too high voltage.

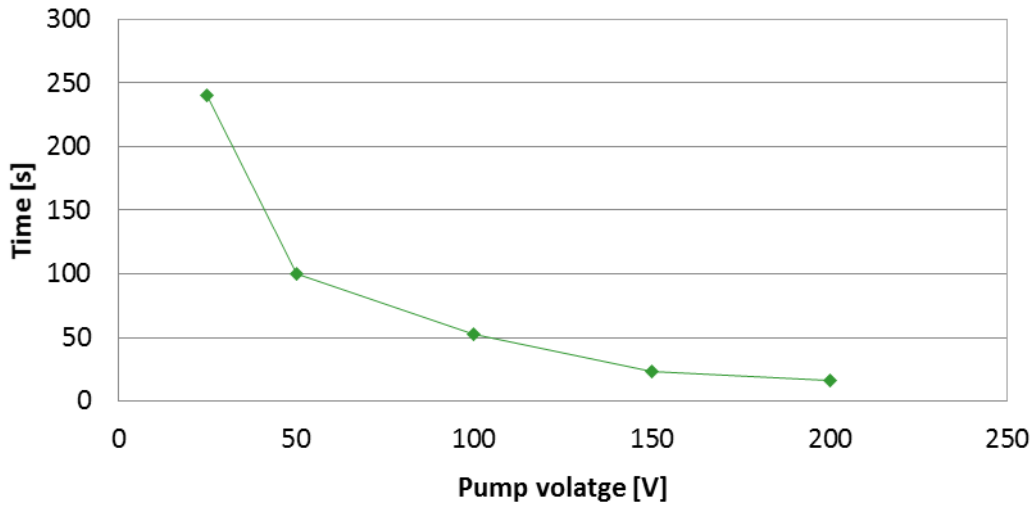


Fig. 3.13 Relationship between the DC voltage applied to an electroosmotic pump and the start-up time.

3.5.2 Measurement of droplet's volume

This section describes the measurement of the volume of a droplet spouted from the tube's outlet as described in Section 3.4.2 at different pulse widths of driving conditions as described in Section 3.4.1. In the experiment, an electroosmotic pump filled with ethanol was driven by a 75 V pulse generated from a function generator () under four conditions that the pulse width was varied to 1, 2, 3, and 4 s, respectively. The outlet of the stainless tube connected with the pump was put on the filter paper so that spouted droplet was then completely absorbed into the paper. The different weight of the paper before and after the dropping was measured by using an electronic balance. The amount of a droplet spouted from the pump in each case was then obtained by calculation. The experimental result is shown in Fig. 3.14.

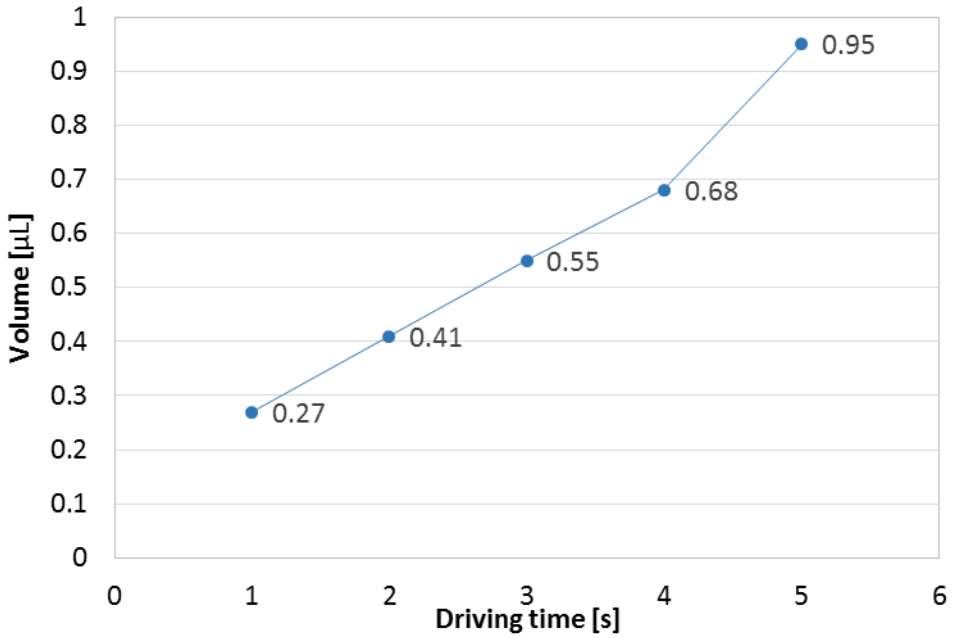


Fig. 3.14 Relationship between the pulse width of a driving voltage applied to an Electroosmotic pump and the amount of the spouted ethanol droplet.

The experimental result proved that a liquid droplet in the range of 0.1 μL can be successfully spouted if the pulse width of a driving signal is short enough. Besides, it was proven that the amount of a droplet can be adjusted by varying the pulse width of the driving pulse. Thus, this driving method and the configuration in which a tiny tube is connected with the pump's outlet were then used in all experiments throughout this research.

3.6 Summary

In this chapter, the fundamental of electroosmosis and its application in an electroosmotic pump were explained. Since the electroosmotic phenomenon can convey liquid precisely, it is suitable to be used to spout droplet to be atomized by the SAW device in this study.

This chapter also described the detail of the electroosmotic pump used in this study including dimensions, flow rate, back pressure, and relationship between those parameters and the driving voltage. The approach to use the electroosmotic pump effectively in olfactory display was investigated. It was found that the pump should be driven by a one shot pulse or DC voltage so that the amount of a droplet can be adjusted by varying the pulse width or amplitude of the applied voltage. Moreover, in order to limit the amount of liquid droplet not to exceed the value that the SAW device can atomize, a tiny stainless tube was connected with the electroosmotic pump. An experiment was then performed to measure the volume of a droplet spouted from the tube's outlet. The experimental result confirmed that this configuration can decrease the amount of a droplet from the range of 10 μL to be in the range of 0.1 μL. However, as the flow rate of electroosmotic flow is not high, the time since the pump is firstly driven until the first droplet is spouted from the tube's outlet is considerably long. In an experiment, it was confirmed that by applying a high voltage at start, that time can be

shortened. Therefore, this approach was used throughout all experiments in this study.

Chapter 4

Fundamental Study of an Olfactory Display Using Electroosmotic Pumps and a SAW Device

4.1 Introduction

The objective of this research is to develop the olfactory display using electroosmotic pumps and a SAW device. The development of SAW devices is described in Chapter 2 and the study on method to convey a liquid droplet using an electroosmotic pump is described in Chapter 3. The olfactory display based on this configuration was expected to be compact and able to present all kinds of scents vividly and reproducibly, control the odor intensity, and blend smells. In this chapter, the preliminary development of an olfactory display based on this configuration is explained. Since it is in the preliminary stage, the size and dimension of the proposed olfactory display were not mainly concentrated in this chapter.

This chapter starts with the explanation of the concept of the olfactory display using an electroosmotic pump and SAW device in Section 4.2. The preliminary development of the olfactory display is then described in Section 4.3. In this section, the investigation of the method to drive the SAW device appropriately and the

consideration of the suitable solvent for diluting odorants used in this study are reported. Subsequently, the arrangement of the proposed preliminary olfactory display is described. The proposed olfactory display was evaluated its capability to present smells through SAW atomization by using an odor sensing system. That issue including with the principle of an odor sensing system and investigation on the method to control intensity of a present smell are described in Section 4.4.

The odor sensing system was then improved to be more suitable for measuring the intensity of an odor vapor released from atomization. Investigation on atomization performance at different positions, evaluation of method to control intensity of odor vapor, and measurement of odor vapor of substance with low volatility generated from SAW atomization are described in Section 4.5. In Section 4.6, this chapter is summarized.

4.2 Concept of Olfactory Display Using Electroosmotic Pump and SAW Device

This section describes a basic concept of the olfactory display composed of an electroosmotic pump and a SAW device. The schematic diagram of this olfactory display is illustrated in Fig. 4.1.

First, the odorant of the target odor to be presented is dissolved into a solvent that can be driven by electroosmotic phenomenon (ex. ethanol, de-ionized water) whose mechanism is explained in Section 3.2 and then filled into the reservoir on the upper side of an electroosmotic pump. The pump is connected with a driver circuit which applies a DC voltage or a one shot pulse as described in Section 3.4.1 to induce electroosmotic flow. A droplet of a solvent mixed with the target odorant is spouted from the pump onto the SAW propagation path of a SAW device located below. The SAW device is connected with an RF amplifier that applies RF signal in need to induce

SAW streaming whose mechanism is explained in Section 2.2.3. If the power of the SAW streaming is sufficient, the spouted droplet is atomized forcibly into a smell which is then blown to the user's nose by a tiny fan. The primary development of the olfactory display using an electroosmotic pump and a SAW device is described in detail in Section 4.3.4 and its capability to present smell based on SAW streaming was evaluated by using an odor sensing system whose principle is described in Section 4.4.1 and the experimental result is described in Section 4.4.2.

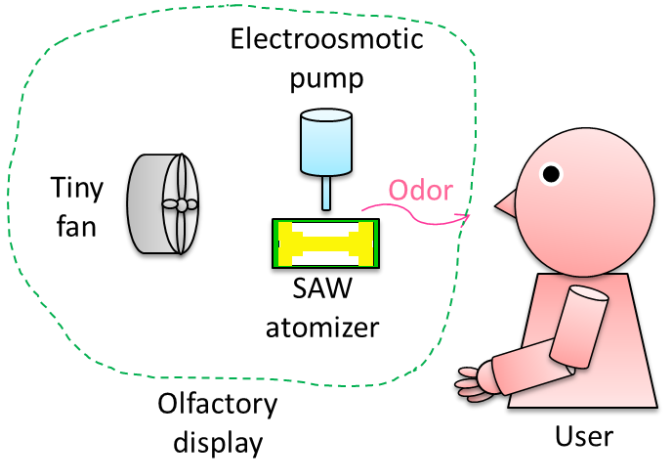


Fig. 4.1 Schematic diagram of the olfactory display using electroosmotic pump and SAW device.

Based on this configuration, the volume of a droplet can be controlled by adjusting amplitude of the voltage applied to the electroosmotic pump or by adjusting pulse width if the driving signal is a pulse. By adjusting the volume of a droplet spouted from an electroosmotic pump in these ways or by adjusting energy of the SAW streaming, the intensity of the odor vapor released from atomization was considered to be able to be controlled. Two experiments were conducted to verify this idea. The details about those experiments are described in Sections 4.4.3 and 4.5.3.

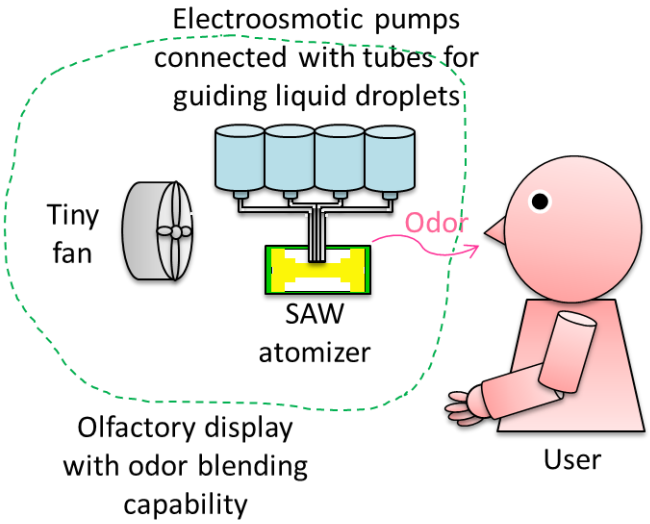


Fig. 4.2 Schematic diagram of the olfactory display using multiple of electroosmotic pumps and a SAW device for odor blending.

Besides, when many electroosmotic pumps filled with solvents mixed with different odorants are used to spout different kinds of droplets together to be atomized by a SAW device simultaneously as shown in Fig. 4.2, the blended odor was expected to be able to be presented. An experiment to verify this idea was conducted and described in Section 4.5.5. The electroosmotic pumps are connected with tubes to guide multiple droplets to be spouted onto the adjacent location to achieve the same level of atomization energy. The experiment which was then carried out to verify whether the atomization performance of the SAW streaming varies by the position on the SAW propagation path is described in Section 4.5.2.

4.3 Preliminary Development of Olfactory Display Using Electroosmotic Pump and 11 x 19 *mm* SAW Device

The preliminary development of the olfactory display using an electroosmotic pump and a SAW device which were investigated individually as described in Chapters 2 and 3 respectively is explained in this section. This section starts with description about the preparation of the 11 x 19 *mm* SAW device for use in the olfactory display in Section 4.3.1. The consideration on appropriate methods to drive the SAW device and to dilute the odorants are described in Sections 4.3.2 and 4.3.3, respectively. The arrangement of electroosmotic pumps and a SAW device in this preliminary olfactory display is then described in Section 4.3.4.

4.3.1 Preparation of 11 x 19 *mm* SAW device

In this section, the preparation of the 11 x 19 *mm* SAW device for use in the olfactory display is described. As the signal routes on the copper clad board shown in Fig. 2.12 was roughly created, it was considered to be a bottle neck of the system that reduced the atomization performance due to its parasitic elements. Besides, the device should be recreated to be more compact so that it will be more convenient to be integrated into the olfactory display. Thus, the copper clad board was replaced with a PCB designed by using Protel 99 SE. The layout of the PCB is shown in Fig. 4.3 and the actual image of the device is shown in Fig. 4.4. The SAW device was pasted onto the PCB by using a conductive paste. The SMB connectors were used instead of the BNC connector. The overall size of the device is 20 x 53 *mm*.

Frequency characteristic of the SAW device was measured by using an

impedance analyzer (4291A, Hewlett Packard). The result is shown in Fig 4.5. According to the result, the working frequency is approximately 60.65 *MHz*.



Fig. 4.3 Layout of a PCB designed for the 11 x 19 *mm* SAW Device (red: top layer, blue: bottom layer, yellow: top overlay, olive: bottom overlay, white: through hole).

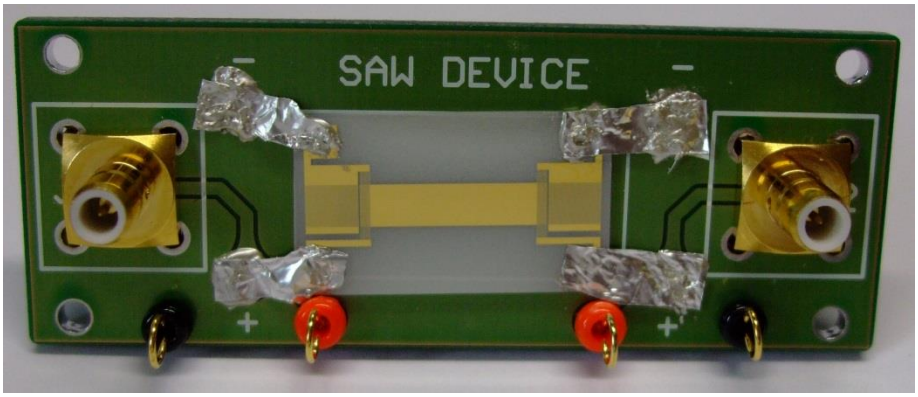
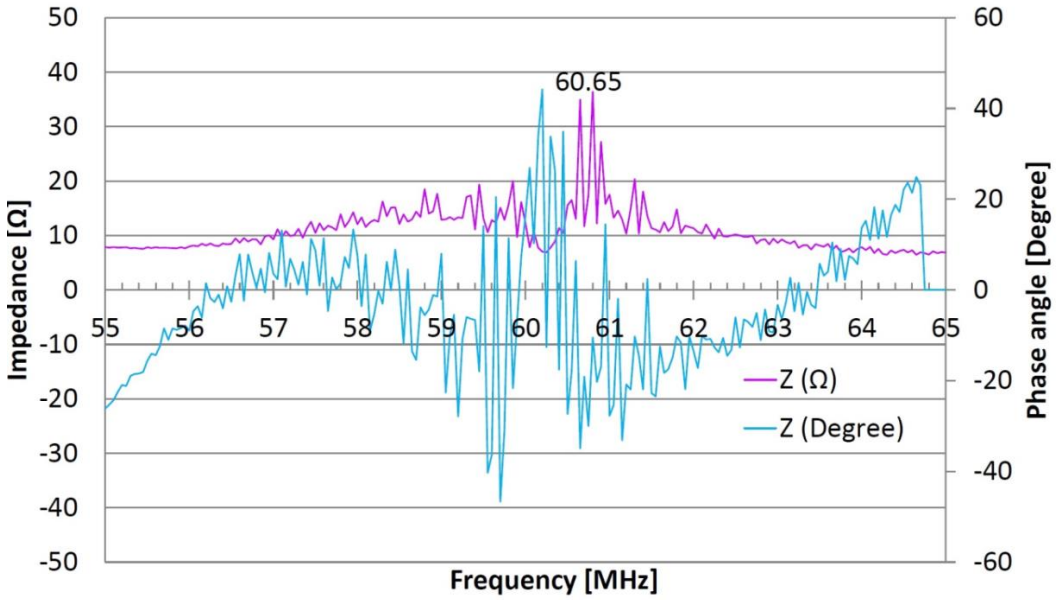
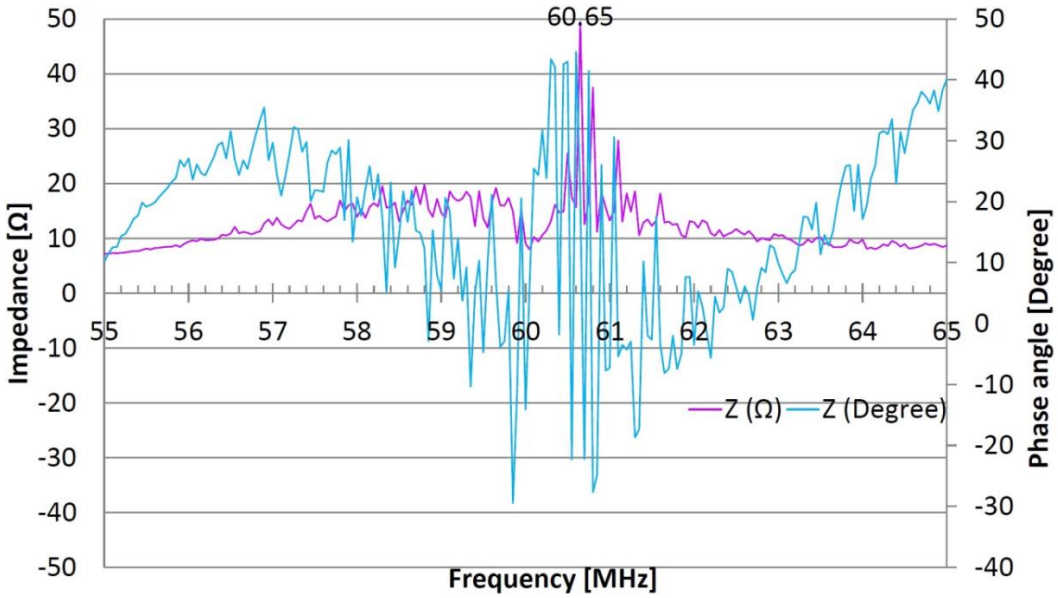


Fig. 4.4 Actual image of the 11 x 19 *mm* SAW device pasted onto a PCB.



(a)



(b)

Fig. 4.5 Frequency characteristics of the 11 x 19 *mm* SAW device pasted onto a PCB at (a) the left port and (b) right port.

4.3.2 Consideration on method to drive the SAW device

In the experiments described in Sections 2.4.2, 2.6.1, and 2.6.2, the SAW devices were driven by a continuous RF signal for observation the droplet behavior at the maximum driving power condition. However, continuous driving might cause SAW devices to be fractured. Thus, the RF burst wave should be used. This section explains the consideration on the appropriate parameters of the RF burst wave as a SAW device driving signal.

As shown in Fig. 4.6, RF burst wave is a wave with on and off states repetitively over a period of time. The burst is determined by a pulse repetition period (T_2) and duty cycle ($d = \frac{T_1}{T_2}$). These parameters govern the electrical energy transferred to the SAW device to be converted into a SAW whose energy determines the strength of the SAW streaming.

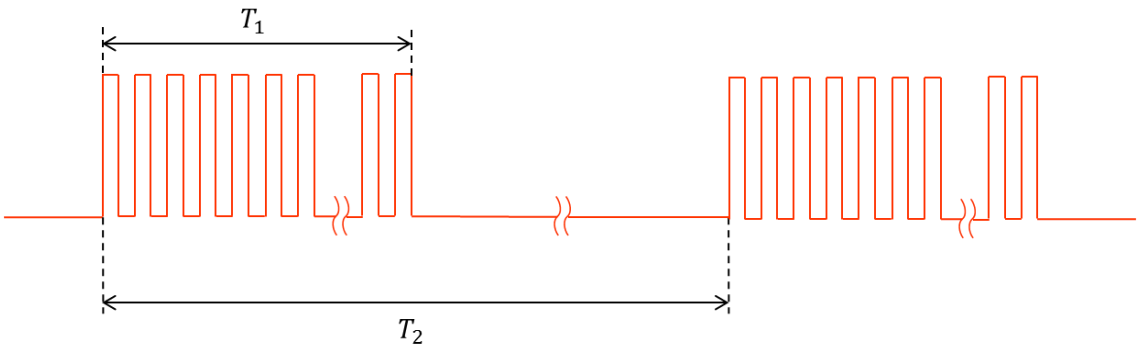


Fig. 4.6 Burst wave.

Based on my assumption, the parameter that directly affects the energy transferred to the SAW device is "the number of pulses in a repetition period (n)" expressed as

$$n = T_1 f \tag{4.1}$$

$$n = \left(\frac{T_1}{\tau}\right) T_2 f = dT_2 f \tag{4.2}$$

Therefore, the larger n is, the stronger SAW streaming is. Various driving conditions were then considered, such as:

- Condition 1: $T_2 = 10\ \mu s,\ d = 50\ \%$ resulting in n = 300,
- Condition 2: $T_2 = 20\ \mu s,\ d = 50\ \%$ resulting in n = 60,650
- Condition 3: $T_2 = 1\ ms,\ d = 1\ \%$ resulting in n = 60,650,
- Condition 4: $T_2 = 0.1\ s,\ d = 1\ \%$ resulting in n = 6,065,000

In PWM application in which the burst wave is mostly used, the duty cycle is generally used to describe the power of the burst wave. However, in this case even though the duty cycles in condition 1 and 2 are equal, the atomization performance in condition 2 is incomparably stronger than that in condition 1 and approximately equal with that in condition 3. However, the duty cycle is still important to be considered as it determines the interval in which the SAW device works and stops for a rest. Therefore, if the duty cycle is too high, the SAW device can be stressed and then broken when its limitation is exceeded. Based on observations, the 11 x 19 *mm* SAW devices start being fractured at about 14 % of duty cycle. Therefore, the parameters need to be balanced.

In this study, the T_2 was fixed at 0.1 *s* first. This gives the opportunity to raise the duty cycle above when compare with the lower repetition period value. The duty cycle was then set to 1 % (thus n = 6,065,000) as shown in condition 4. Subsequently, an experiment was performed in which an RF burst at the resonant frequency was applied to the 11 x 19 *mm* SAW device with these parameters for a minute. As a result, the SAW device was not broken. Thus, this driving condition had been used in the experiments throughout this chapter.

4.3.3 Consideration on solvent for odorant dilution

This section describes the consideration on the solvent that is suitable for diluting odorants. As most of pure odorants' smells are too strong to a human's sensation, in general, they are diluted by mixing with some solvent before use. In this research, criteria to define the solvent that is suitable for diluting the odorants to be presented by the SAW atomization were considered as the follows:

1. It must not harm sniffers' health.
2. It must be drivable by electroosmotic flow.
3. It must be a targeted odorants-dilutable solvent.
4. It must be atomizable by SAW streaming (its viscosity should be low).
5. Its volatility should not be too high to avoid rapid and unintentional evaporation.
6. It should have no smell or have a smell as weak as possible.

After the consideration, ethanol was examined to be used as the solvent in this study since it meets the all above requirements.

4.3.4 Arrangement of electroosmotic pumps and SAW device in preliminary olfactory display

In this section, the arrangement of electroosmotic pumps and a SAW device in the preliminary olfactory display is described. The SAW device described in Section 4.3.1 was placed by an artificial holding hand in vertical direction as shown in Fig. 4.7. Three electroosmotic pumps (RP3-N1, Nano Fusion Technologies) were set on the upper side of the SAW device. Each of the pump was connected with a small Teflon tube (inner diameter: 0.85 *mm*, outer diameter: 1.2 *mm*, Hermatocrit) so that the droplet spouted

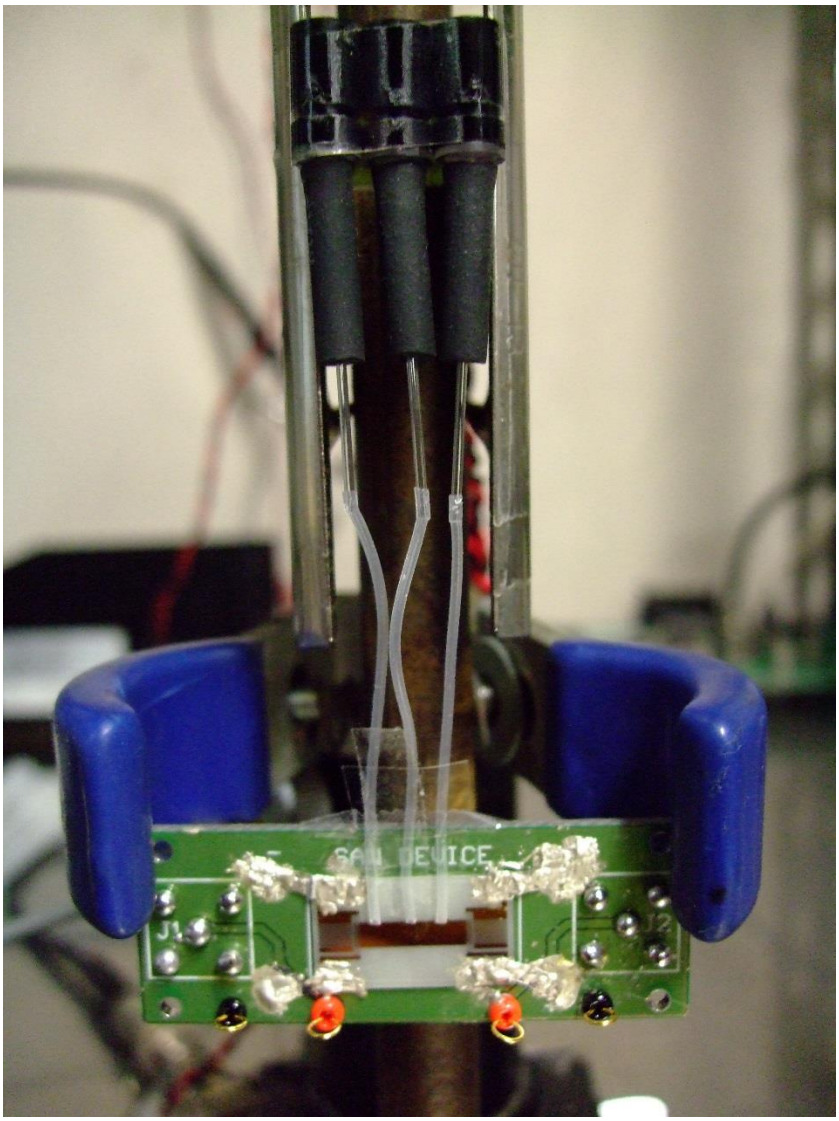


Fig. 4.7 Arrangement of electroosmotic pumps and a SAW device in the preliminary olfactory display.

from the pump would be conveyed on to the SAW propagation path of the SAW device to be atomized. As this experiment was performed before the investigation described in Section 3.4.2, the Teflon tube whose size is larger than the tiny stainless tube in Section 3.4.2 was used. Even though three electroosmotic pumps were prepared, only the pump in the center was used in the rest of the experiments in this chapter (except the experiment in Section 4.5.2). The system was constructed in vertical direction so that the droplet spouted from the electroosmotic pump would be fallen onto the SAW

propagation path by the gravity. If the system was built in the horizontal direction, there was a possibility that the droplet would percolate reversely on to surface of the tube due to the surface tension. As the olfactory display shown in Fig. 4.7 is in preliminary stage, the tube needed to be assisted by hand so that the droplet will be completely conveyed onto the SAW propagation path of the SAW device as described again in Section 4.4.2.

4.4 Evaluation of Olfactory Display Using Electroosmotic Pumps and 11 x 19 *mm* SAW Device Based on Improved Odor Sensing System

This section describes the experiments on evaluation of the preliminary olfactory display whose development is described in Section 4.3.5. As human's olfactory perception is influenced by adaptation as described in Section 1.8 and varies from person to person, an odor sensor was used in the experiments to obtain more objective result. The principle of an odor sensing system used for measuring an intensity of the odor vapor released from the SAW atomization is described in Section 4.4.1. An experimental setup and experimental result of the measurement is described in Section 4.4.2. Subsequently, an investigation on methods to control intensity of odor vapor is described in Section 4.4.3.

4.4.1 Principle of odor sensing system using QCM gas sensor

The structure of a basic odor sensing system used in this study is shown in Fig. 4.8.

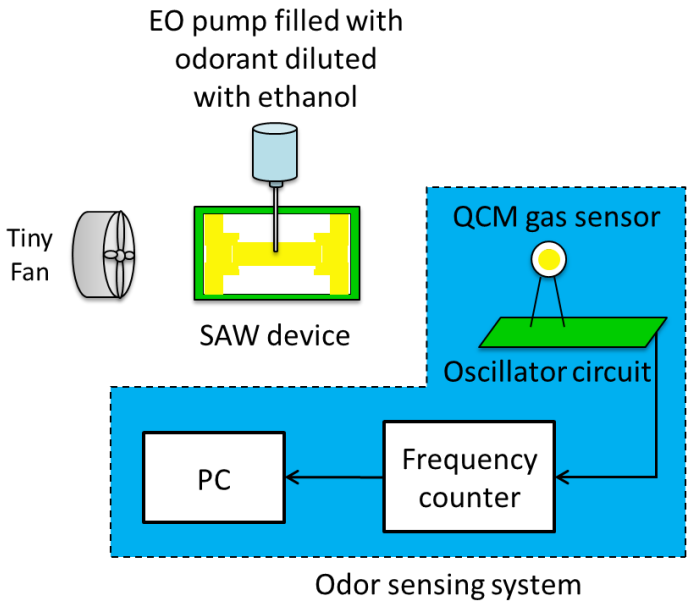


Fig. 4.8 Schematic diagram of the odor sensing system using a QCM gas sensor.

An AT-CUT quartz crystal microbalance (QCM) gas sensor with 20 *MHz* of resonant frequency was connected with an oscillator circuit. The electrodes of the sensor is made of gold and their surface were coated with a thin film of Siponate DS-10, a commercial name of sodium dodecylbenzene sulfonate, to increase the sensitivity. A tiny fan was used to blow the odor vapor released from the SAW atomization to the QCM sensor. When molecules of an odorant in the odor vapor reaches the QCM sensor' surface, they are adsorbed onto the sensing film. Meanwhile, the mass change occurs on the QCM sensor resulting in the resonance frequency shift due to mass loading effect, expressed as

$$df = -f_r \frac{dM}{M} \tag{4.3}$$

where f_r is the resonant frequency and M is the mass of quartz crystal under electrodes. Based on this technique, intensity of the odor molecule can be converted to the frequency shift which is then measured by the frequency counter. The measured data were transferred to a computer via serial interface and were stored as a text file.

4.4.2 Measurement of intensity of odor vapor released from SAW atomization

In this section, a result of the experiment that was carried out to evaluate the capability

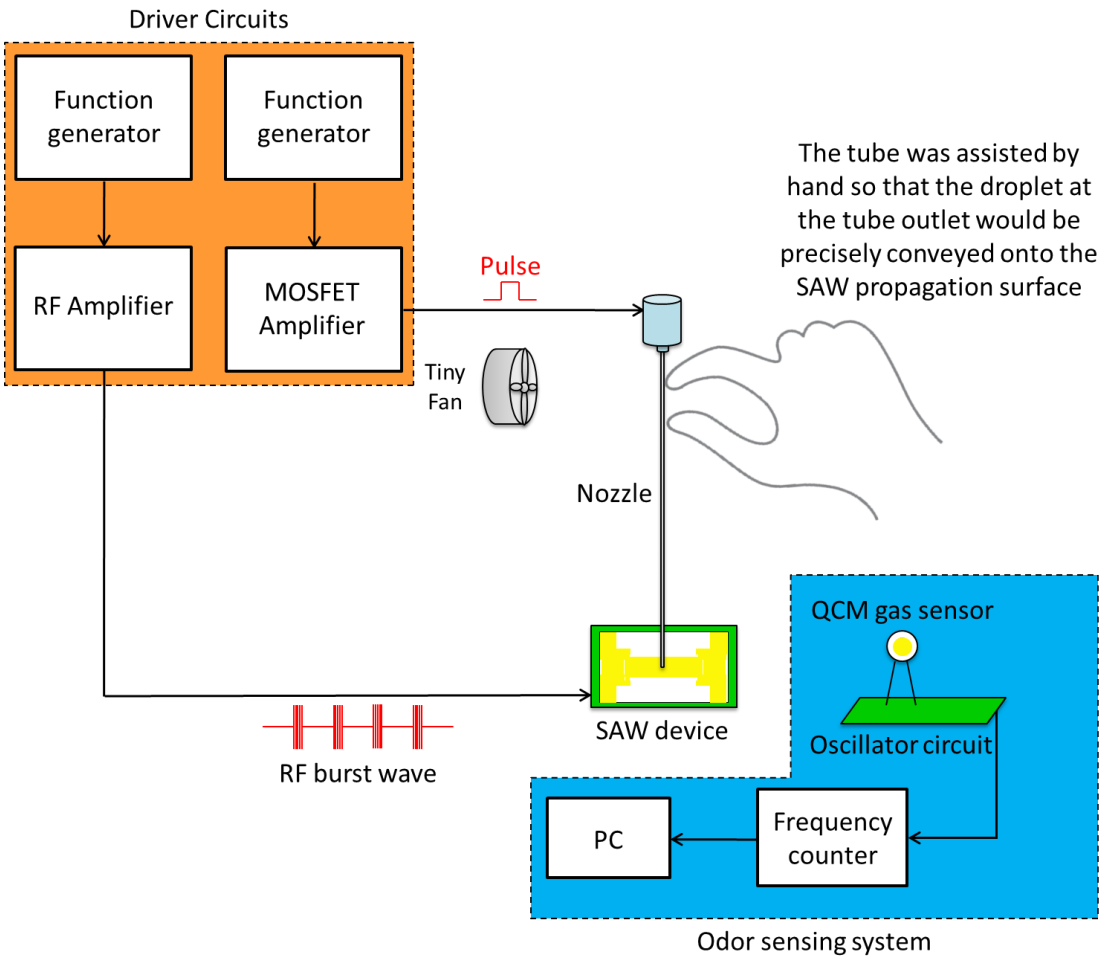


Fig. 4.9 Experimental setup in the experiment to evaluate the ability to present smells.

of the preliminary olfactory display to present a smell of substance with moderate volatility is described. The experimental setup is shown in Fig. 4.9.

In the experiment, the SAW device was driven by a 60 V_{pp} of burst wave at the resonant frequency with 0.1 *s* of repetition period and 1 % of duty cycle. The signal was generated by a functional generator (AFG 3251, Textronix) and was amplified by an RF amplifier (ZHL-5W-1, Mini-Circuits). The electroosmotic was connected with a glass capillary tube (inner diameter: 0.85 *mm*, outer diameter: 1.65 *mm*, Hermatocrit) and then driven by an electrical pulse through the method described in Section 3.4.1 to drive an approximate 0.5 μL of liquid droplet to the tube' outlet. As this experiment was performed before the investigation described in Section 3.4.2, the glass capillary tube whose size is larger than the tiny stainless tube in Section 3.4.2 was used. The pulse was generated by a functional generator (33120A, Hewlett Packard) and amplified by a MOSFET amplifier whose schematic diagram is shown in Fig. 3.12. The tube was assisted by hand in order that the tiny spouted droplet on the outlet of the glass capillary tube would be completely conveyed on to the SAW propagation path to be atomized.

A tiny fan (F1517AP-01YCV, Shincoh) was used to blow the odor vapor released from the SAW device to the QCM gas sensor described in the previous section. The distance between the tiny fan and the atomization position of the SAW device was set to 2 *cm*, and the distance between the atomization position and the QCM sensor was set to 2.5 *cm*, respectively. Wind speed was approximately 0.67 *m/s*. It was obtained by using a thermal anemometer (ISA-12, Shibata). The temperature control was not performed. The frequency shift of the QCM sensor was measured by a frequency counter implemented into a FPGA. The air pump used in the odor sensing system was a diaphragm pump (N86KT.18, Neuberger).

The liquid sample used in this experiment was 10 % of 2-hexanone (MW: 100.2, b.p.: 127 ℃) diluted with ethanol. Since 2-hexanone was typical compound with moderate volatility, its sensor response can imply both whether the olfactory display can

present a smell and whether the odor sensing system works correctly. The sensor response is shown in Fig. 4.10.

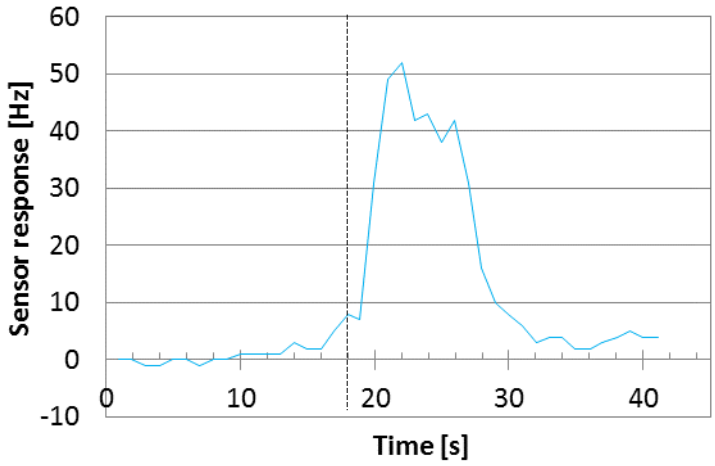


Fig. 4.10 Sensor response to vapor of 10 % of 2-hexanone diluted with ethanol released from SAW atomization.

The dashed line shows when the droplet was put onto the SAW propagation path. The abrupt peak of the sensor response was obtained as a result. It means that the odorant of 10 % of 2-hexanone diluted with ethanol could be atomized into smell and was detected by the QCM sensor. Therefore, the capability to present smell by SAW atomization of the olfactory display as well as that to measure the smell intensity of the odor sensing system was confirmed.

Next, another experiment was carried out to confirm whether the sensor response did not occur due to the natural evaporation of the liquid but from the SAW atomization. Therefore, 10 % of β-ionone (MW: 192.3, b.p.: 239 ℃), a compound with relatively low volatility, diluted with ethanol was used as the liquid sample in this experiment. In the experiment, 0.5 μL of droplet was put onto the SAW propagation path to be atomized. The SAW device was driven by a burst wave whose duty cycle was adjusted to 0, 10, 20, 30, 40, and 50 %, respectively. The repetition period was set to 10 μs.

The released odor was then measured by the QCM sensor. The measurement in each condition was performed five times. The relationship between the duty cycle of the RF burst wave and the average value of the sensor response peaks is shown in Fig. 4.11.

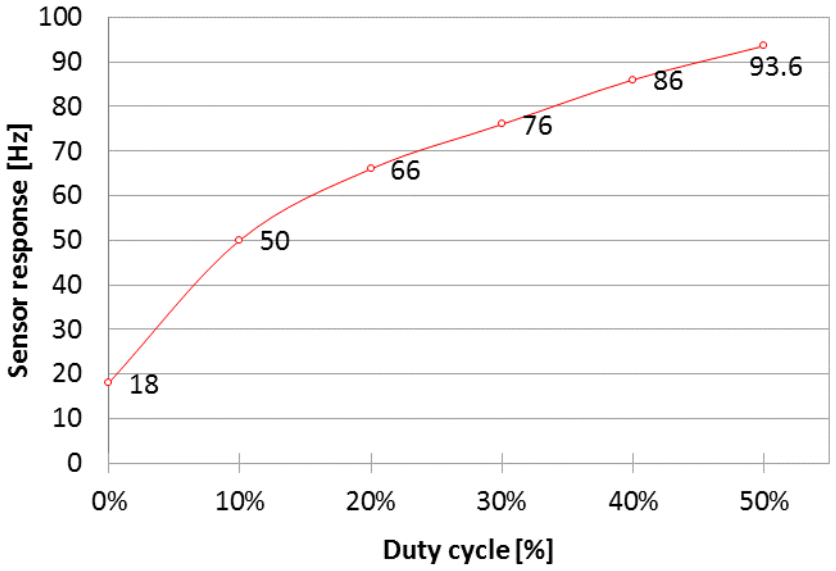


Fig. 4.11 Relationship between the duty cycle and the peak of the sensor response.

After the experiment in each case, a residue was observed. The detail about the residue after atomization of the odorant of low volatility substance is described later in Section 4.5.4. According to the result in Fig. 4.12, the peak of sensor response increased monotonously to the duty cycle. It implies that the odor sample in this experiment could be slightly atomized and the atomization performance increases at higher duty cycle. Nevertheless, the sensor response at non-driving condition (0 % of duty cycle) was not zero but a low value. Thus, it can be concluded that the sensor response obtained from the measurement mostly expresses the intensity of an odor vapor released from atomization, with some minor offset from intensity of the odor released from its natural evaporation.

4.4.3 Investigation on methods to control intensity of odor vapor

As stated in Section 4.2, the olfactory display developed in this study was expected to have an ability to adjust intensity of the presented smell. This section describes an experiment which was conducted to confirm that capability.

The experiment was done under the almost same environment described in the previous section except that the volume of a liquid droplet to be atomized was varied by changing the number of pulses applied to the electroosmotic pump. The number of pulses was adjusted to 4, 10 and 14, respectively. Time between the pulses was approximately a second. Each pulse applied to an electroosmotic pump is a 5 V signal with 10 ms of pulse width and the volume of one droplet was about 0.4 μL. The measurement in each condition was performed five times. The relationship between average value of the peak of the sensor response and number of pulses applied to the electroosmotic pump is shown in Fig. 4.12.

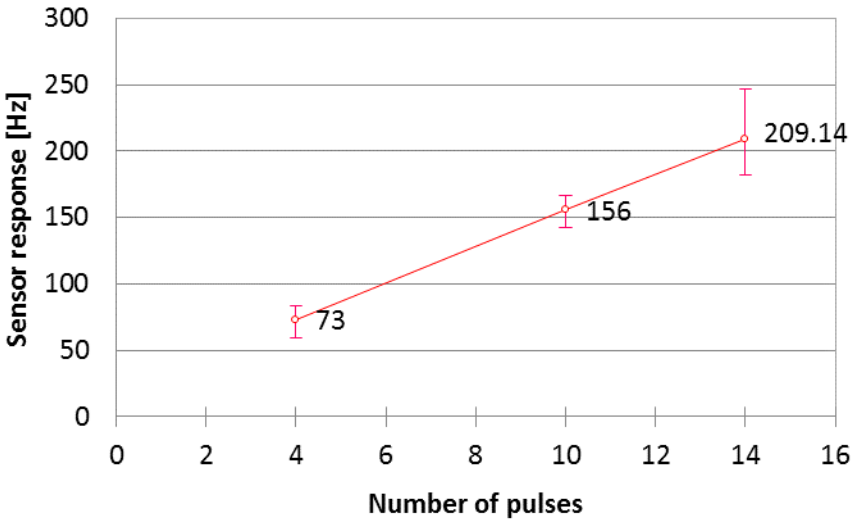


Fig. 4.12 Relationship between the peak of the sensor response and duty cycle.

According to the result, the peak of sensor response increases proportionally to the number of pulses. Thus, the capability to control intensity of the odor vapor was confirmed. However, the difference of obtained data in each case is remarkably large. I considered that this large difference was caused by the unstable performance of the SAW device or the inefficient capability to measure odor vapor released from atomization of the odor sensing system. Subsequently, the investigation was conducted to describe the cause of this problem. I observed that the mist released from atomization blown by the tiny fan was sometimes spread out around and only a part of it that reached the surface of the QCM sensor. Therefore, to assure the reliability of the obtained data from measurement, the odor sensing system was improved to be more suitable to measure the intensity of an odor vapor released from atomization. The detail about improvement of the odor sensing system is explained in Section 4.5.1.

4.5 Evaluation of Olfactory Display Using Electroosmotic Pumps and 11 x 19 *mm* SAW Device Based on Improved Odor Sensing System

As described in Section 4.4.3, the odor sensing system in which a tiny fan is used to blow an odor vapor into a QCM gas sensor cannot measure intensity of the odor vapor released from atomization effectively. Therefore, the improvement of odor sensing system was performed. The detail about the improvement is described in Section 4.5.1. Subsequently, the use of the improved odor sensing system to evaluate the atomization performance at different points on the SAW propagation path is described in Section 4.5.2. The use of the improved odor sensing system to evaluate the capability to control intensity of an odor vapor released from atomization is described in Section 4.5.3. An experiment that was performed to evaluate the capability to present an odor of the

substance with low volatility is described in Section 4.5.4.

4.5.1 Improvement of odor sensing system using QCM gas sensor

As stated in Section 4.4.3, when the odor sensing system described in Section 4.4.1 is used to measure the intensity of an odor released from atomization, the tiny fan sometimes blows the released vapor to spread out around. In this case, only a part of the vapor can reach the QCM sensor. This behavior was considered to be the cause of the high tolerance of the data shown in Section 4.4.3. Therefore, the odor sensing system was improved to be more suitable to measure the intensity of an odor vapour released from atomization. The structure of an improved odor sensing system used in this study is shown in Fig. 4.13.

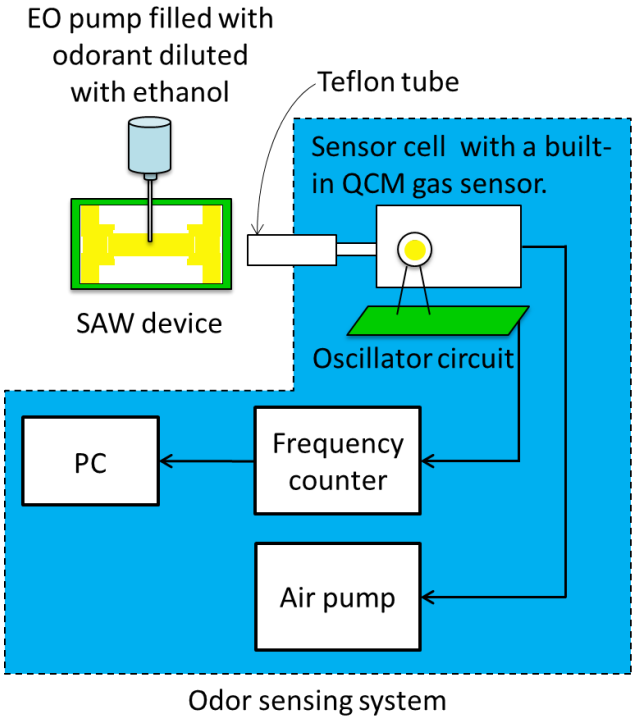


Fig. 4.13 Schematic diagram of the improved odor sensing system.

In the improved system, the QCM gas sensor was built-in to a sensor cell connected with an air pump. When the air pump is turned on, the odor vapor around the inlet of the sensor cell is then sucked in to the cell in order that the intensity of the odor is measured by the QCM sensor. A tube with 1 *cm* diameter was connected to the inlet of the sensor cell to increase the area in which the vapor can be sucked. The tube was made of Teflon so that molecules of the odorant could not remain on the tube's inner surface. The fan is not required in this improved system. The distance between the inlet of the Teflon tube and the atomization position of the SAW device was set to 1 *cm* and the wind speed at the inlet of the tube was adjusted to be about 0.45 *m/s* that is sufficient to suck most of the vapor around the inlet of the Teflon tube into the cell. This improved odor sensing system had been used in the experiments in all of the rest of this thesis. A photograph of the improved odor sensing system when it was used in an experiment is shown in Fig. 4.14.

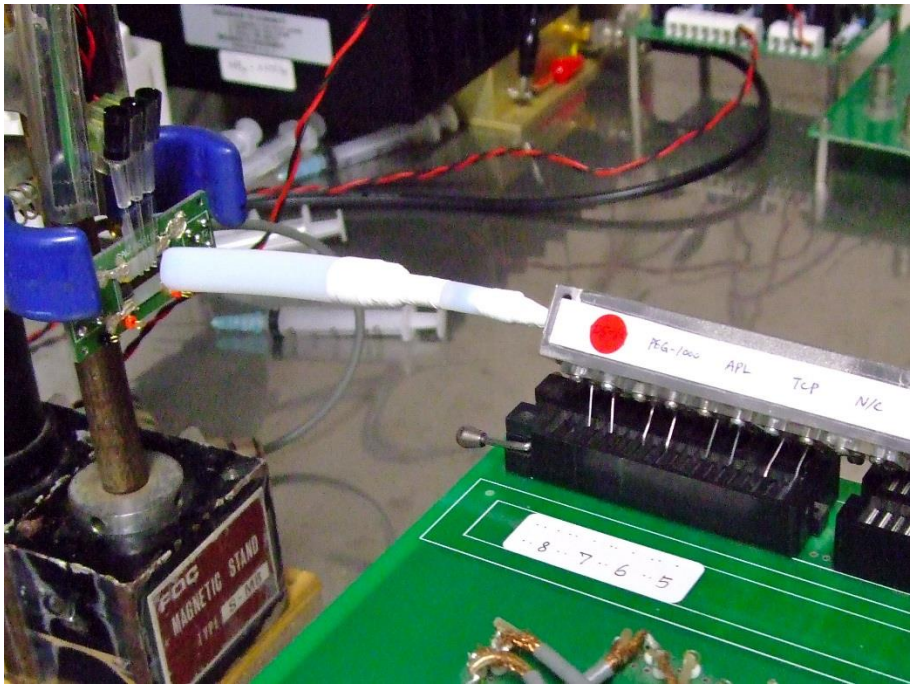


Fig. 4.14 Photograph of the improved odor sensing system when it was used in an experiment.

4.5.2 Investigation on atomization performance at different positions

As stated in Section 4.2, the olfactory display developed in this study was expected to have an ability to blend smells. However when many electroosmotic pumps are used at the same time, the atomization area increases proportionally. Thus, before trying to blend smells, the atomization performance at the different position on the SAW propagation path was studied. This section describes an experiment conducted to verify that issue.

This experiment was done under the almost same environment described in Section 4.4.1 except that the SAW propagation path was roughly divided into three regions; left, center, and right as shown in Fig. 4.15. A droplet of the 10 % of 2-hexanone diluted with ethanol was put on the SAW propagation path to be atomized. The amount of a droplet was controlled to be 0.27, 0.41, 0.55, 0.68, and 0.95 μL by adjusting pulse width of the driving signal. The measurement was done twice for each conditions. The average peaks of the sensor responses in each conditions are shown in Fig. 4.16.

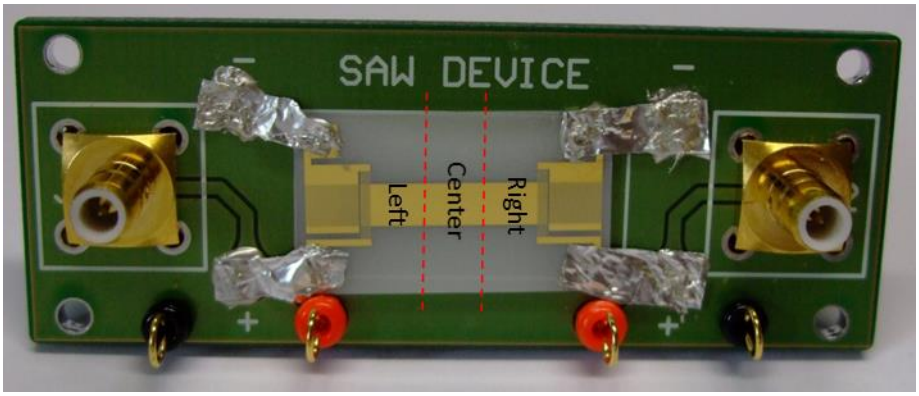


Fig. 4.15 Three atomization positions on the SAW device in the experiment to evaluate atomization performance at difference positions.

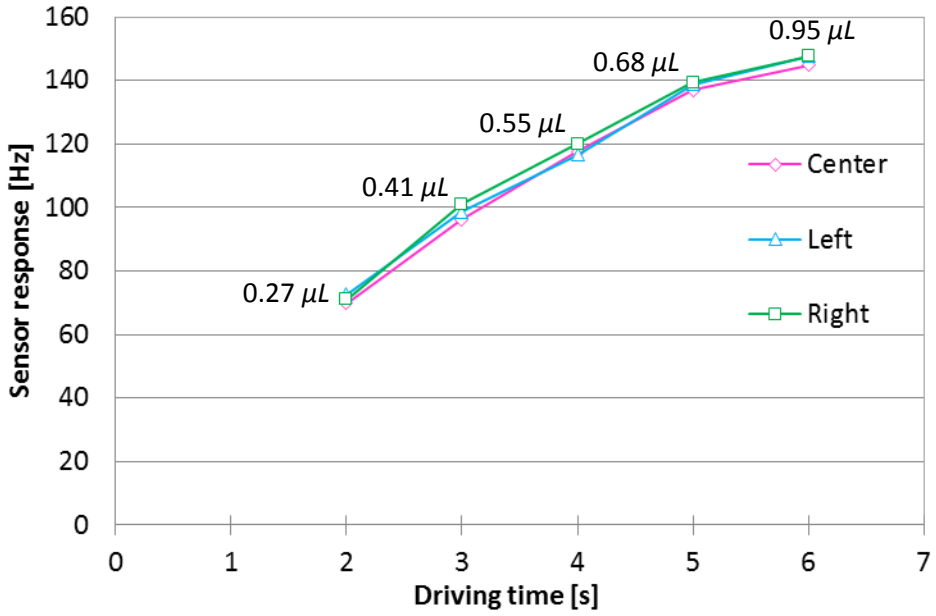


Fig. 4.16 Comparison of the sensor responses when droplets were put onto the center and the right side of the SAW device.

From the result, it was found that only slight differences of the sensor responses at different positions occurred. Therefore, it can be concluded that the atomization performance does not change noticeably due to the atomization position. Thus, it is possible to blend multiple odors. Moreover, this result also indicates the improved performance of the odor sensing system because of only slight difference among the responses at these atomization positions.

4.5.3 Evaluation of method to control intensity of odor vapor

The evaluation of the capability to control intensity of the released smell was performed as stated in Section 4.4.3. However, since the obtained data had large tolerance, the experiment was conducted again by using the improved odor sensing system to obtain more reliable result. In Section 4.4.3, the intensity of the released smell was controlled

by adjusting number of pulses applied to the electroosmotic pump, however in the experiment in this section, a one shot of the pulse was used and the intensity was controlled by adjusting the pulse width due to the reason mentioned in Section 3.4.1. The detail about that experiment is described in this section.

The experiment was done under the almost same environment described in Section 4.4.3 with some exceptions. First, the improved odor sensing system was used instead of the conventional one. Second, a one shot of the pulse was used and the odor intensity was controlled by adjusting the pulse width instead of varying the number of pulses. In the experiment, an electroosmotic pump was driven by a 75 V electric pulse in four conditions that the pulse width was adjusted to 1, 2, 3, and 4 *s*, respectively. A 0.14, 0.27, 0.41, and 0.55 μL droplet of 10 % of 2-hexanone diluted with ethanol was put onto the SAW propagation path to be atomized in each condition. The sensor response obtained from each condition is shown in Fig. 4.17.

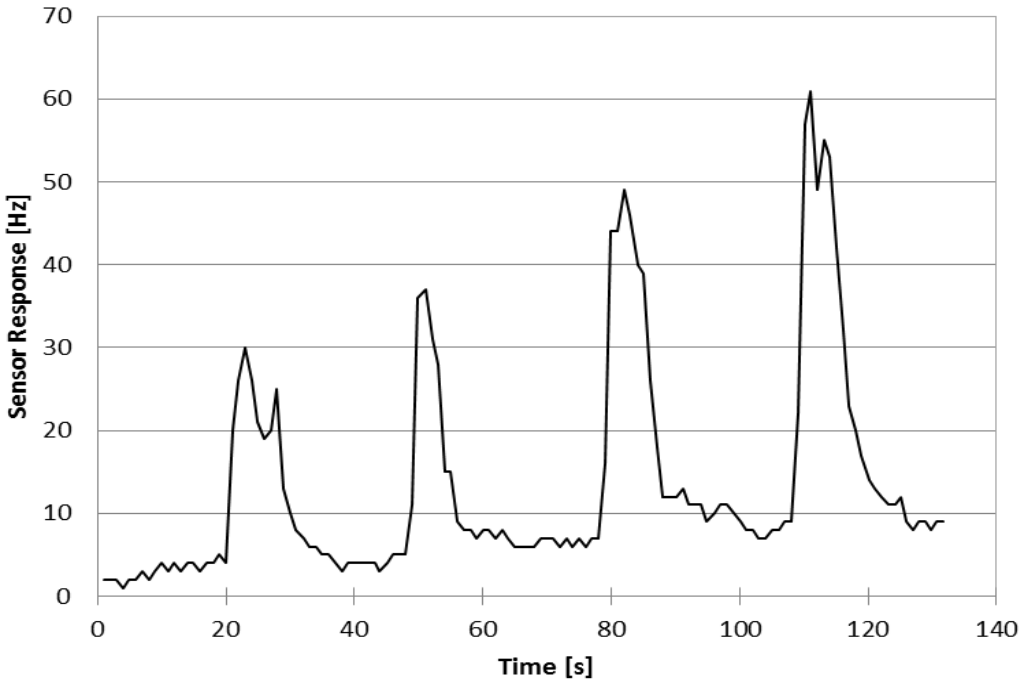


Fig. 4.17 Temporal change of sensor response when pulse width of electroosmotic pump is varied.

According to the result, when the droplet volume increases by applying longer pulse width, the sensor response also increases. Therefore, the intensity of a released odor can be controlled in this way.

4.5.4 Measurement of odor vapor of substance with low volatility generated from SAW atomization

As stated in Section 1.8, an objective of this study is to develop an olfactory display that can present scents of low-volatile substance within a short time. Thus, an experiment that was carried out to confirm that capability is described in this section.

The experiment was done under the almost same environment described in Section 4.4.2 except that the improved odor sensing system was used instead of the conventional one, and β-ionone which is a low volatile substance was used instead of 2-hexanone. In the experiment, an electroosmotic pump was driven by an electrical pulse to drive an approximate 0.27 μL of droplet to the glass capillary tube' outlet. A droplet was put on the SAW propagation path to be atomized. The released odor vapor was then sucked into the sensor cell so that its intensity is measured. The sensor response obtained from the measurement is shown in Fig. 4.18. For comparison, the sensor response to the same sample presented by the conventional solenoid valve based olfactory display is shown in Fig. 4.19. However, the sensing film of the QCM sensor was different (the film used in that previous experiment was Versamid900).

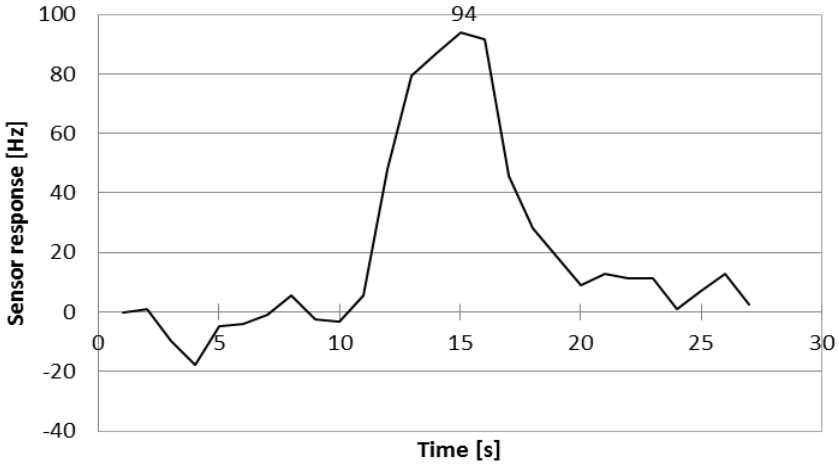


Fig. 4.18 Sensor response to vapor of 10 % of β-ionone diluted with ethanol released from SAW atomization.

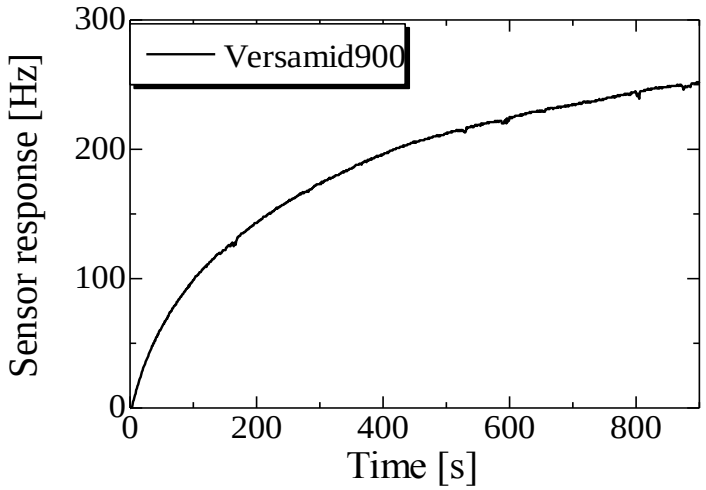


Fig. 4.19 Sensor response to 10 % of β-ionone diluted with ethanol released from the solenoid valve type olfactory display (Flow rate: 1350 *L/min*).

As a result, the abrupt peak of the sensor response to the 10 % of β-ionone diluted with ethanol was obtained as well as the previous experiment in Section 4.4.2 in which the 2-hexanone was used. Besides, when both response time and recovery time of the result was much faster than that in Fig. 4.19. It indicates that the olfactory display using atomization technique developed in this study can present even the scents of

low-volatile substances and the scents around the sensor then disappear in a short time while the conventional device requires very long time to reach the steady state and also a very long time until the scents disappear due to the natural evaporation characteristic of the substance and the smell persistence inside the tube.

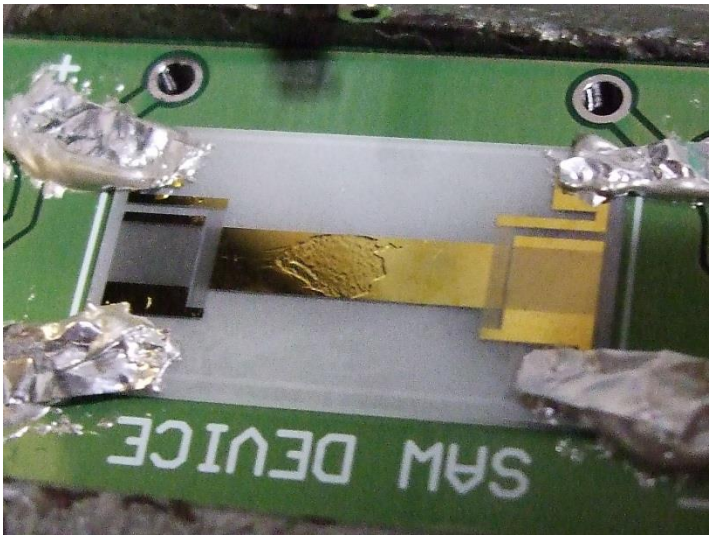


Fig. 4.20 Residue after a 0.27 μL droplet of 10 % of β-ionone diluted with ethanol is atomized.

Nevertheless, after the atomization of a droplet of 10 % of β-ionone diluted with ethanol, a residue remaining on the SAW device was observed as shown in Fig. 4.20. As stated in Section 2.6.2, the residue drastically reduces power of the next SAW streaming. Thus the voltage of RF burst signal applied to the SAW device was increased. However, even though the voltage was raised up to 200 V_{pp} that can break the SAW device suddenly if the duty cycle is too high, the residue still be left after the atomization. Therefore, it is clear that the SAW device with more atomization performance is required. The development and evaluation of the improved SAW device including with the development and evaluation of the next developed olfactory display using that improved device is described in Chapter 5.

4.6 Summary

In this chapter, the preliminary olfactory display was developed using the SAW device and electroosmotic pump whose investigation were described in Chapter 2 and 3, respectively. The consideration on method to drive the SAW device and consideration on suitable solvent for odorant dilution were done. The preliminary olfactory display was then proposed. Its capability to present odor using SAW atomization was confirmed through an odor sensing system. The odor sensing system was then improved to be more suitable to measure the intensity of a vapor released from SAW atomization. An experimental result showed that the atomization performance at different location on the SAW propagation path are slightly equal. It means that the odor blending is possible. Subsequently, the capability to control odor intensity by adjusting pulse width of the driving pulse applied to the electroosmotic pump was confirmed. However, it was found that the atomization performance was still not sufficient to atomize a droplet of an odorant with low volatility completely. Thus, the improvement of a SAW device was required which is described in the next chapter.

Chapter 5

Development of a Miniaturized Six-component Olfactory Display Using Electroosmotic Pumps and a SAW Device for Presenting Scents of Low-volatile Substances

5.1 Introduction

In Chapter 4, the developments of a preliminary olfactory display using an electroosmotic pump and the 11 x 19 *mm* SAW deice are described. According to the experimental results, the proposed olfactory display can present smells by utilizing SAW streaming and its concept to control intensity of the odor vapor was verified. However, it was found that the atomization performance of the 11 x 19 *mm* SAW device was still not sufficient to atomize a droplet of the odorant with low volatility. Moreover, the olfactory display structure was not completed. As a consequence, it needed to be assisted by hand during all experiments.

Those limitations were solved by improving the structure of the olfactory display and developing the higher-performance SAW device. The details about these improvements are described in Sections 5.2 and 5.3, respectively. The investigation on appropriate condition to drive a proposed SAW device was then performed. The detail is described in Section 5.4. Subsequently, other experiments carried out to evaluate the proposed olfactory display by using the odor sensing system are described in Section 5.5. Finally, the chapter is summarized in Section 5.6.

5.2 Development of Miniaturized Six-component Olfactory Display Using Electroosmotic Pumps and SAW Device

A SAW device and an electroosmotic pump were used together to realize a preliminary olfactory display as described in Chapter 4. The experimental results confirmed that it can atomize a droplet of liquid odorant to present smell. However, since the olfactory display deals with a very tiny liquid droplet in the range of 0.1 μL, the outlet of the tube connected with the electroosmotic pump needs to be placed closely on the SAW propagation path. If the outlet of the tube is not placed closely enough, the tiny droplet is not conveyed on to the path but accumulated at the tip of the outlet until its size becomes larger enough to touch the path. This issue causes two problems in the preliminary basic olfactory display, which are;

- The fact that the droplet is not atomized sometimes causes low repeatability of the odor presentation
- If volume of the accumulated droplet is too large to be atomized, a residue remains on the SAW propagation path.

Therefore, in order to avoid these problems, a tube was assisted by hand to make sure

that its tip was placed closely to the SAW propagation path in all experiments in Chapter 4. Thus, in order to enhance the completeness of the device, a new structure of the olfactory display which does not need manual handling was developed, subsequently. The design and development of the new structure are described in this section.

In order to place the tube closely to the SAW propagation path, two pieces of metal blocks were designed and constructed. The dimensions of those two structures are shown in Figs. 5.1 and 5.2, respectively. The configuration when they are assembled together is shown in Fig. 5.3. The metal block shown in Fig. 5.1 was made of aluminum. The six square holes and a shallow cavity were made for inserting the electroosmotic pumps' connector and for placing the SAW device, respectively. Therefore, up to six electroosmotic pumps can be equipped with the metal block to realize the six-component odor blender. The circular holes were made for inserting screws.

The metal block shown in Fig. 5.2 was made of brass. Six holes were drilled at one side of the block in order that it could be inserted by the six stainless tube with 2 *mm* outer diameter and 1 *mm* inner diameter. At another side of the block, other six holes were drilled in order that it could be inserted by the six tiny stainless tube with 0.31 *mm* outer diameter and 0.13 *mm* inner diameter. The tiny tubes were inserted through the brass block and the bigger tubes as shown in Fig. 5.4. The gap between each pair of tubes were sealed by using silicone and the bigger tubes were soldered into the block as shown in Fig. 5.5. It was confirmed that there is no leak and all parts are not dissolved into ethanol. The six tiny stainless tubes were used as the final outlets at which tiny droplets are spouted. The bigger tubes were connected with the outlet of the electroosmotic pumps by silicone tubes.

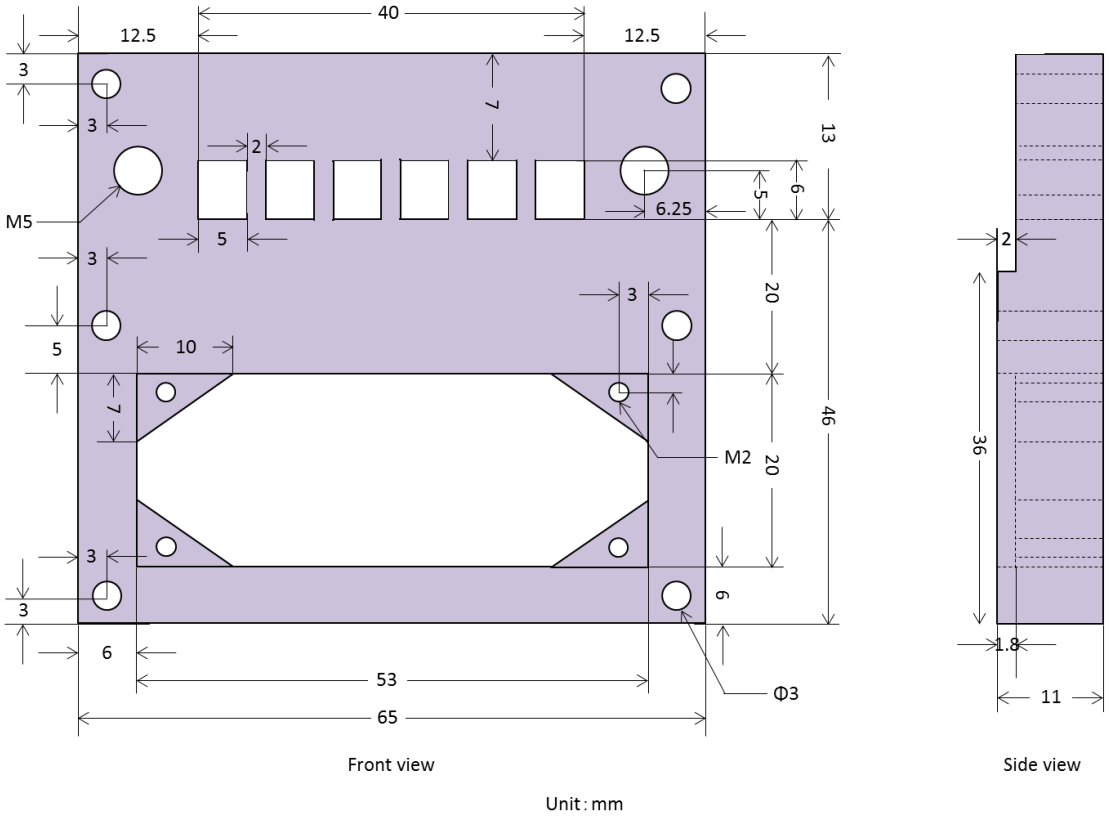


Fig. 5.1 Part of miniaturized six-component olfactory display designed for placing a SAW device.

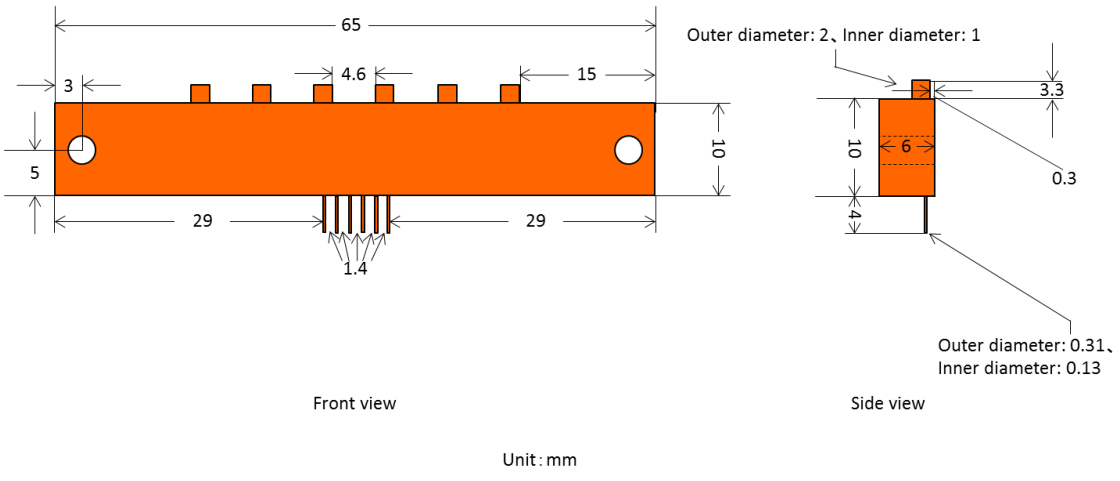


Fig. 5.2 Part of miniaturized six-component olfactory display designed for guiding liquid droplets.

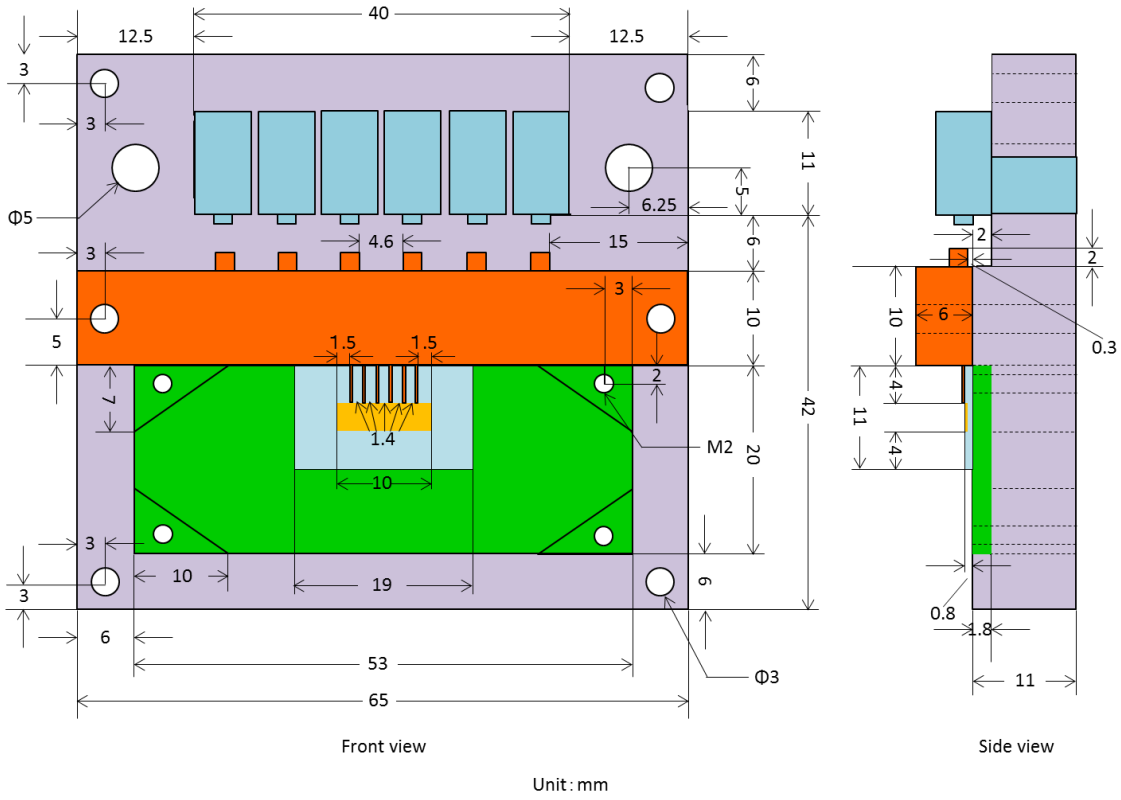


Fig. 5.3 Complete structure of miniaturized six-component olfactory display.

As shown in Fig. 5.3, the PCB at which the SAW device is pasted (green) was placed on the cavity of the aluminum block (purple). The brass block with stainless tubes (orange) was then put on the SAW device carefully so that the SAW device would not be broken. Subsequently, six electroosmotic pumps (blue) were inserted into the square holes in the aluminum block. Six silicone tubes were used to connect between outlet of the pump and the inlet of the bigger stainless tube. The actual image of the completed device is shown in Fig. 5.6. Its dimension is 65 x 59 x11 *mm* which is rather smaller than any other multi-component olfactory displays developed by using other techniques.

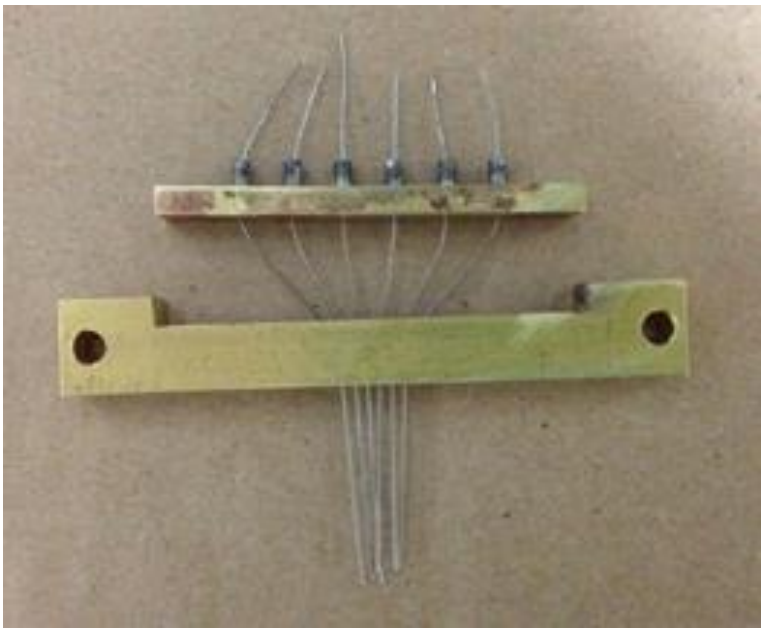
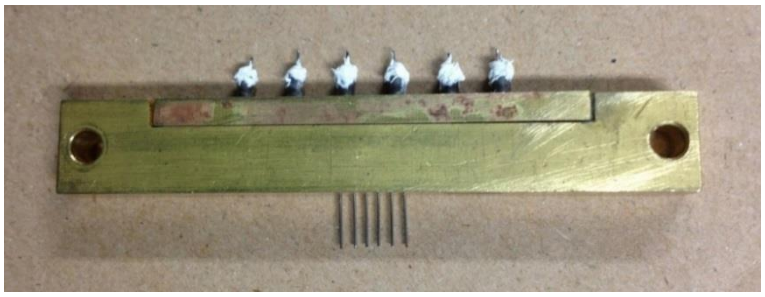
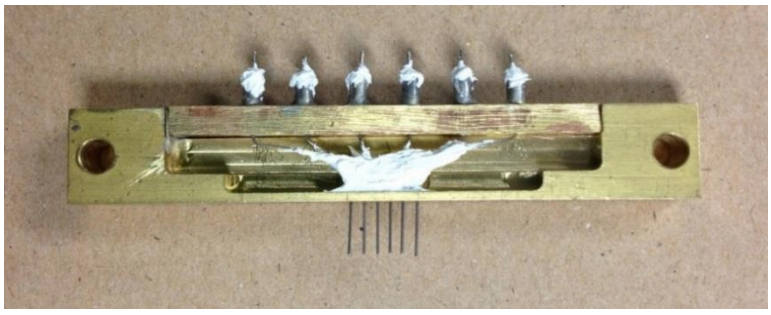


Fig. 5.4 Six thin tubes are inserted through the brass block and the bigger tubes.



(a)



(b)

Fig. 5.5 Actual image of a part of miniaturized six-component olfactory display for guiding liquid droplets taken from (a) front view, (b) back view.

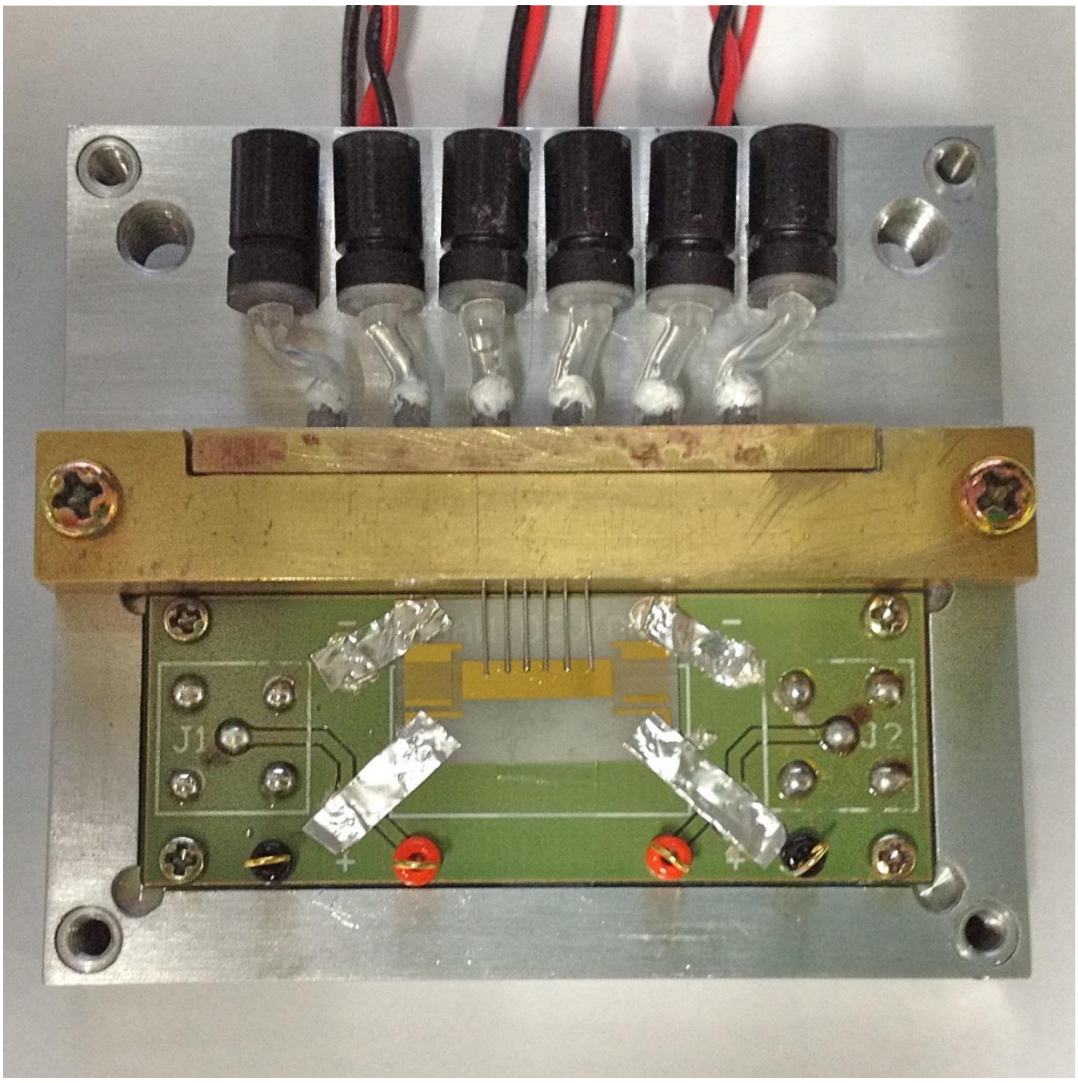


Fig. 5.6 Actual image of the miniaturized six-component olfactory display using electroosmotic pumps and 11 x 19 *mm* SAW device.

This proposed olfactory display should be more reproducible than the previous one that is described in Chapter 4. However, as improvement of the atomization performance was also another problem to be solved. The 11 x 19 *mm* SAW device was then replaced by the higher performance SAW device. The development of that SAW device is described in the next section. Subsequently, the experiments that were performed to evaluate capabilities to present smells of the proposed olfactory display are described in Section 5.5.

5.3 Development of 14 x 25.5 *mm* SAW Device

As described in Section 4.5.1, the 11 x 19 *mm* SAW device that was previously developed can atomize liquid with moderate volatility, such as pentane, hexane, acetone, or ethanol. However, its performance was not sufficient to atomize liquid with low volatility even though the amplitude of the applied RF signal was increased upto 200 V_{pp} at which the device might be broken suddenly. Therefore, in order to enhance the performance of SAW streaming to realize atomization of the scents of low volatile substances, it was necessary to redesign the SAW device. The detail about development of the new SAW device is described in this section.

As stated in Section 2.3, the minimum width of IDTs that the manufacturer can construct conveniently nowadays is about 16 μm. Therefore, the IDTs of the new SAW device was not changed from that 16 μm of the previous one. As a result, the resonant frequency was also same as 61.95 *MHz*. In order to increase the atomization performance, the IDTs' finger was increased from 10 to 30 pairs. The length of SAW propagation path was increased from 10 *mm* to 14.132 *mm*. Other parameters except the number of finger's pair and the length of the SAW propagation path were the same as those of the 10 x 19 *mm* one. The entire electrode pattern is shown in Fig. 5.7.

A new PCB connected with two SMB connectors was also developed for this SAW device. The layout of the PCB is shown in Fig. 5.8. The SAW device was pasted onto the PCB by using a conductive paste. The actual image of the SAW device passed on the PCB is shown in Fig. 5.9. The overall size of the device is 20 x 53 *mm*.

Frequency characteristic of the SAW device pasted on the board was measured by using an impedance analyzer (4291A, Hewlett Packard). In this measurement, both left and right ports of the SAW device were connected together. The result is shown in Fig 5.10. According to the result, the working frequency is 60.88 *MHz*.

This SAW device was then used in the olfactory display expressed in the previous

section instead of the 11 x 19 *mm* one. To evaluate its capability to atomize a liquid droplet of substances with low volatility, 10 % of β-ionone diluted with ethanol was filled into the reservoir on the top of an electroosmotic pump. A 150 V pulse with 5 s of pulse width was applied to the electroosmotic pump to drive an approximate 1.35 μL liquid droplet onto the SAW propagation path. The SAW device was driven by a 80 V_{pp} burst wave with 17 % duty cycle and 1 *ms* repetition period (the reason for using these parameters are described in the next section). As a result, the droplet was atomized suddenly as shown in Fig. 5.11.

Thus, the improved performance of the SAW device was proven. Even a liquid droplet of substance with low volatility was also able to be atomized within a short time. Besides, maximum volume of a droplet that can be atomized also increased. The experiments were carried out to confirm whether the new configuration of the olfactory display and the new SAW device can enhance atomization performance and repeatability from the previous preliminary olfactory display. The detail about this experiment is described in Section 5.5.

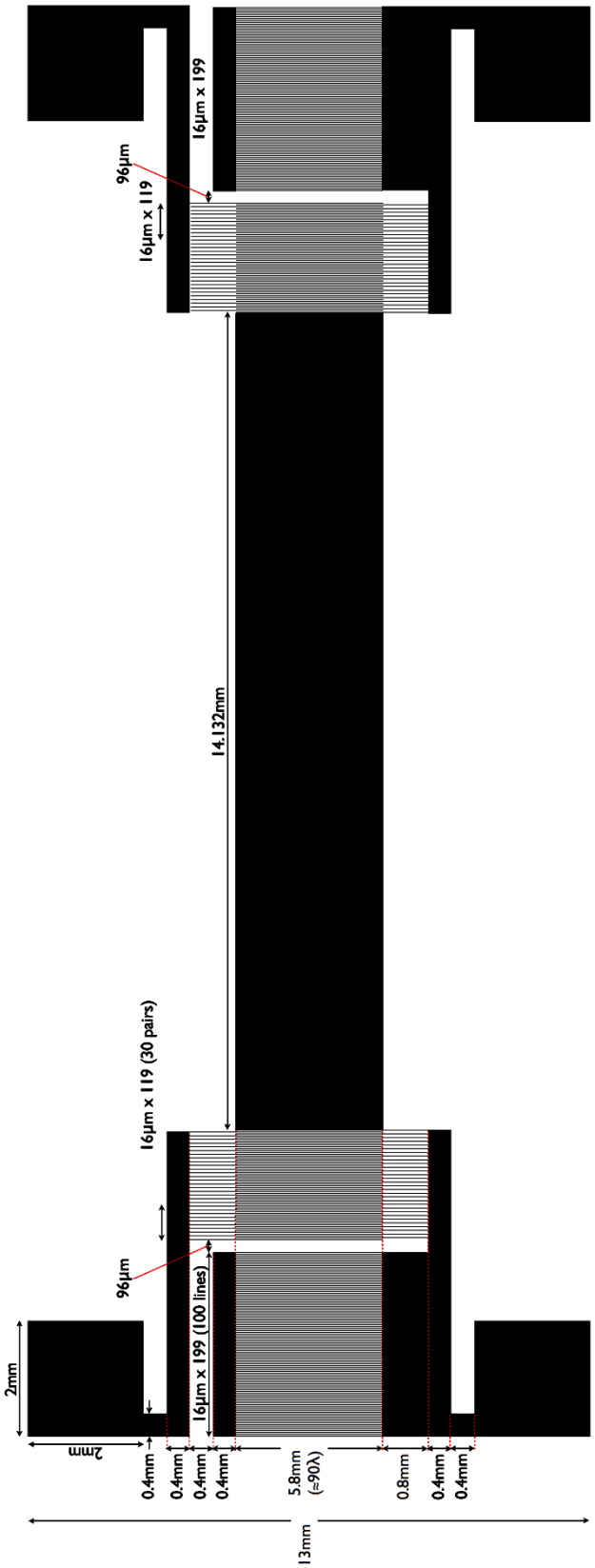


Fig. 5.7 Pattern of the 14 x 25.5 *mm* SAW device.



Fig. 5.8 Layout of a PCB designed for 14 x 25.5 *mm* SAW Device (red: top layer, blue: bottom layer, yellow: top overlay, olive: bottom overlay, white: through hole).



Fig. 5.9 Actual image of 14 x 25.5 *mm* SAW device pasted onto a PCB.

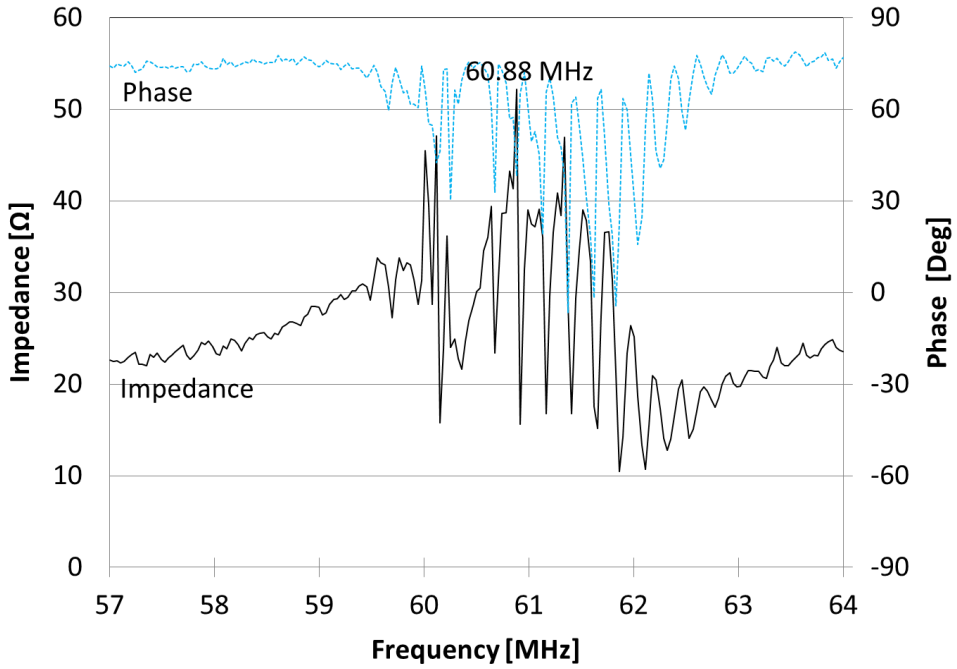


Fig. 5.10 Frequency characteristics of 14 x 25.5 *mm* SAW device (both left and right ports were connected together in parallel).

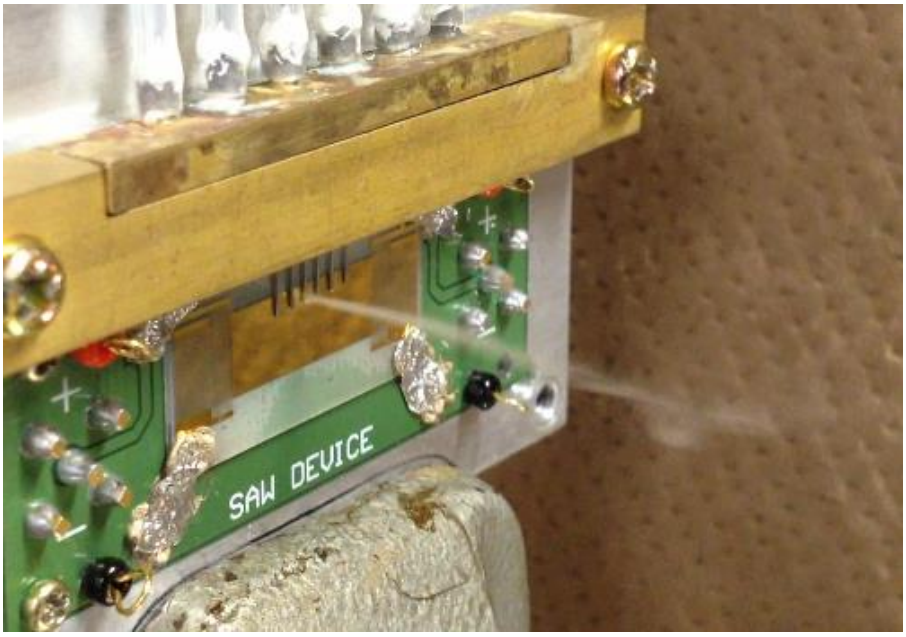


Fig. 5.11 Droplet of a 10 % of β-ionone diluted with ethanol was being atomized by miniaturized six-component olfactory display with 14 x 25.5 *mm* SAW deice.

5.4 Investigation on Appropriate Condition to Drive SAW Device

As described in Section 4.3.2, two parameters including duty cycle and repetition period need to be balanced to meet the driving condition that can acquire the highest atomization performance without breaking the SAW device. In Chapter 4, the duty cycle and repetition period were adjusted at 1 % and 0.1 s, respectively. It was confirmed that the 11 x 19 *mm* SAW device was not broken at that driving condition. However, it did not guarantee that highest atomization performance can be obtained with that driving condition. An experiment was performed to understand the required parameters that does not break the SAW device and produce atomization performance as high as possible. The detail is described in this section.

In the experiment, the 14 x 25.5 *mm* SAW device was driven with 80 V_{pp} of burst wave whose repetition period was fixed to 1 *ms*. Duty cycle was first adjusted to 1 %. The SAW device was driven under this condition for 40 s and if it was not broken the duty cycle was then raised by 1 %. The experiment was done repeatedly until the SAW device was broken.

As a result, the SAW device can be driven for 40 *s* without broken until the duty cycle was set to 17 %. At 18 % of the duty cycle, the SAW device was broken within 8 *s*. These parameters (duty cycle = 17 % and repetition period = 1 *ms*) were then used in all of the experiments described in the next section and the SAW device was not broken at all. Therefore, the driving condition for the 14 x 25.5 *mm* SAW device that can provide atomization performance as high as possible without breaking the SAW device was understood.

5.5 Evaluation of Olfactory Display Using Electroosmotic Pumps and 14 x 25.5 *mm* SAW Device Based on Improved Odor Sensing System

A lot of experiments were performed to evaluate capabilities of the miniaturized six-component olfactory display with the 14 x 25.5 *mm* SAW device. The capability to control intensity of the odor was evaluated in an experiment described in Section 5.5.1. The capability to blend multiple of smells was evaluated in an experiment described in Section 5.5.2. Resolution and dynamic range of the olfactory display were evaluated in an experiment described in Section 5.5.3.

5.5.1 Evaluation of capability to control odor intensity

A measurement for evaluating the capability to control odor intensity of the preliminary olfactory display was described in Section 4.5.3. The experimental result revealed that the olfactory display using an electroosmotic pump and a SAW device possesses the capability to control intensity of an odor to be presented. However, as an odorant sample used in that experiment was 2-hexanone which has moderate volatility, it needed to be confirmed whether the olfactory display still possesses that capability even if the odorant sample is low volatile substance. An experiment performed to confirm this issue is described in this section.

The experimental setup was almost similar with that done in Section 4.5.3 except that the miniaturized six-component olfactory display was used to present a smell instead. In the experiment, volume of the liquid droplet to be atomized was varied by changing the pulse width of the one shot pulse applied to an electroosmotic pump. The electroosmotic pump was driven by a 100 V electric pulse in five conditions that the

pulse width was adjusted to 1, 2, 3, 4 and 5 *s*, respectively. 0.18, 0.36, 0.55, 0.73 and 0.9 μL droplets of 10 % of β-ionone diluted with ethanol were then conveyed onto the SAW propagation path to be atomized. The sensor response obtained from each condition is shown in Fig. 5.12. Subsequently, another experiment was performed under the almost similar condition except that 2-hexanone was used as a sample instead. The sensor response obtained from the experiment is shown in Fig. 5.13.

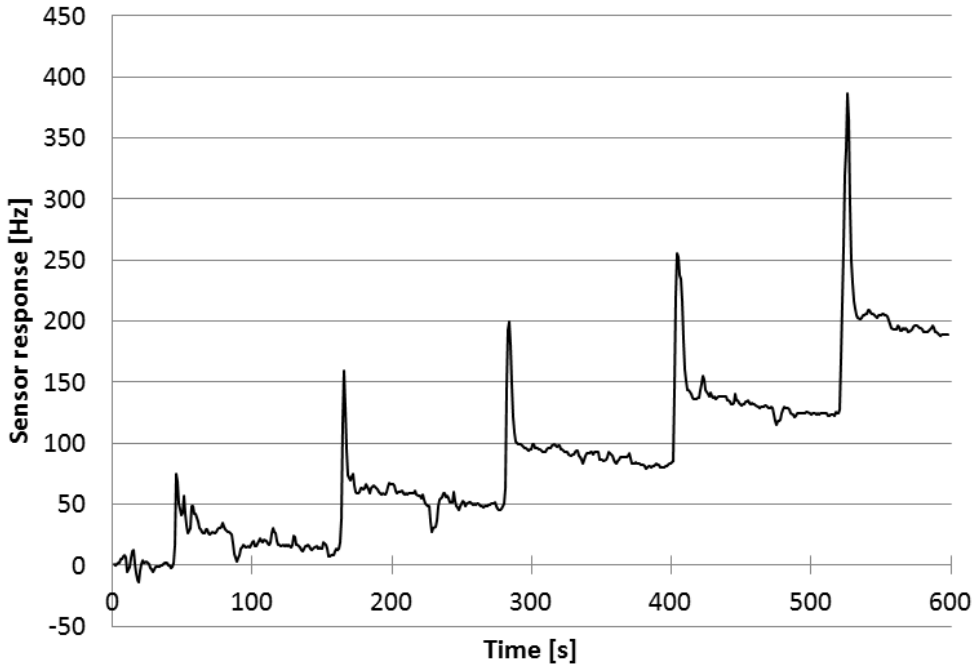


Fig. 5.12 Temporal sensor response to vapor of 10% of β-ionone diluted with ethanol atomized for 1 – 5 seconds.

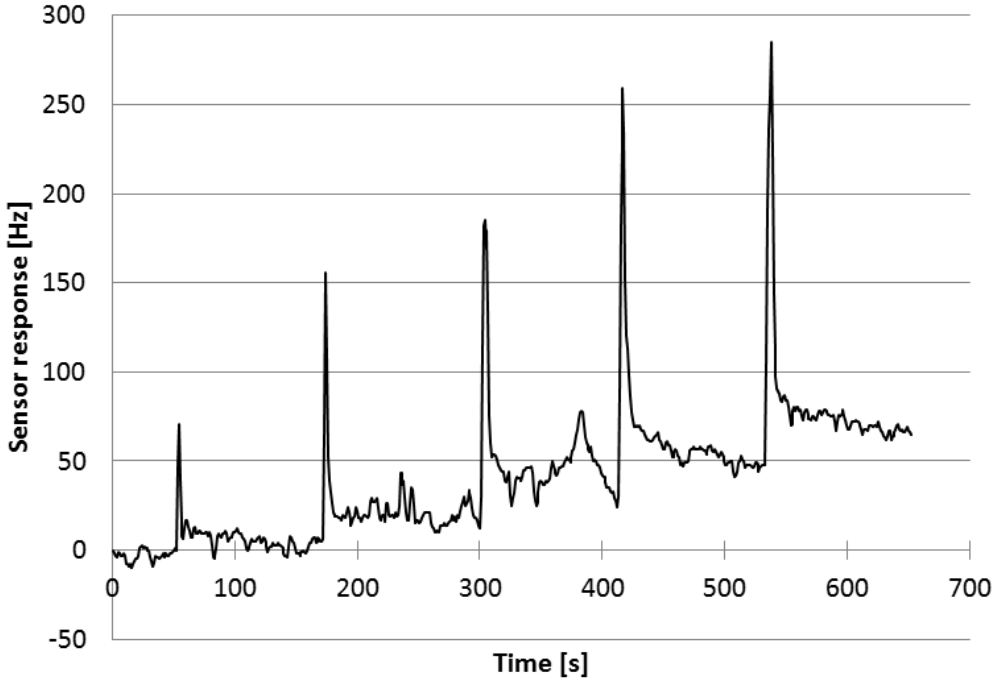


Fig. 5.13 Temporal sensor response to vapor of 10% of 2-hexanone diluted with ethanol atomized for 1 – 5 seconds.

Abrupt peaks of sensor responses can be observed in the results. They demonstrate that even the scents of low volatile substances can be atomized as rapid as the scents with moderate volatility. Besides, when the droplet volume increases by applying longer pulse width, the sensor response also increases proportionally. Therefore, the capability to control intensity of an odor with low volatile substance was also confirmed. However, baseline frequency shifts appeared every time after the atomization. I observed that the shifted sensor response did not return completely into the previous value even though the long time passed. Thus, I supposed that the shifts were caused by some odor molecule which was permanently adsorbed on the surface of the QCM sensor. If this assumption is correct, this problem occurred due to the limitation of the measurement system, not the olfactory display. However, the fact that the baseline frequency shift did not occur in the previous experiment in Section 4.5.3 might be

because the liquid droplet was not absolutely atomized in those experiments. Thus, the amount of liquid droplet was larger than that in the Section 4.5.3 since it was completely atomized. This assumption is supported by the peak of sensor response in Fig. 5.12 which is relatively higher than that in Fig. 4.16.

In order to confirm this issue, the experiments based on sensory evaluation were performed. The details are described in the next chapter.

5.5.2 Evaluation of capability to blend multiple of odors

As described in Section 1.8, one of the goals of this research is to realize the olfactory display that can blend multiple of smells with various volatilities. In this case, a lot of odorant droplets are conveyed on to the SAW propagation path at the same time, so the total amount of droplet volume is relatively large compared with only one odor presentation. Another difficulty is that the olfactory display needs to be able to atomize all odorant droplets simultaneously without delay even though the droplets of substances with high and low volatilities are conveyed onto the SAW propagation path together. As a consequence, the SAW device with sufficient atomization performance is indispensable to realize this odor blender. An experiment was performed to verify whether that miniaturized six-component olfactory display with the 14 x 25.5 *mm* SAW device possesses the capability to blend multiple of odors with different volatility at the same time.

The experimental setup was almost similar to that done in Section 4.5.3 except that two electroosmotic pumps were used together for odor blending. The pumps were filled with 10% of 2-hexanone and 5% of β-ionone diluted with ethanol, respectively. Each pump was driven for the duration of $1 - 5$ *s* separately to obtain the sensor responses. Then, two samples were atomized together for the same duration and condition to obtain the sensor responses of binary mixtures. The measurement was

performed 4 times in each case. The summarized average sensor responses to the vapors of all conditions are shown in Fig. 5.14.

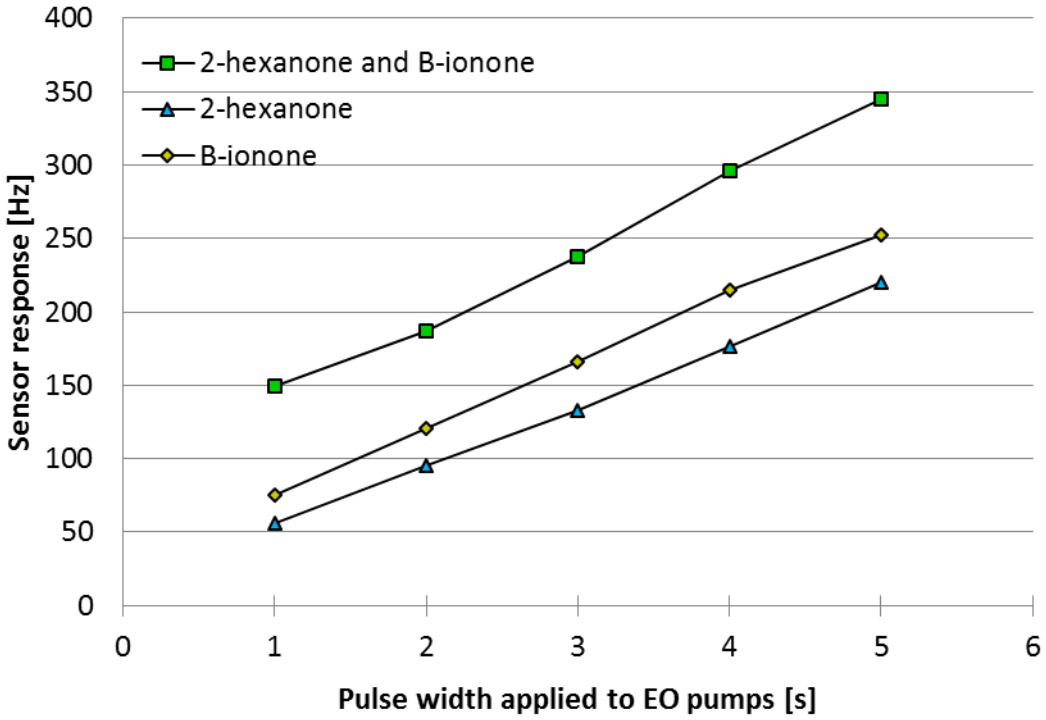


Fig. 5.14 Sensor responses to the binary mixture of odor components.

The superposition characteristic when the binary odor mixtures were presented can be observed in the result. It demonstrates that the miniaturized six-component olfactory display with the 14 x 25.5 *mm* SAW device has high atomization performance enough to atomize multiple of odorants with different volatility which are spouted on to the SAW propagation path abruptly and simultaneously. Thus, the odor blending capability of the device was also confirmed.

5.5.3 Evaluation of dynamic range and resolution

The experimental results in the previous section in this chapter confirmed that the six-component olfactory display possesses the abilities to present scents of low volatile substances, to control odor intensity, and to blend multiple of smells. Based on the olfactory display's configuration, intensity of the odor can be controlled by varying the pulse width of a one shot pulse applied to the electroosmotic pump.

In the previous experiments, an electroosmotic pump was driven for at least 1 *s* to drive a liquid droplet. However, it is useful to know the minimum time that the pump can drive a liquid droplet with the minimum size that can be conveyed on to the SAW propagation. Besides, the minimum time also implies dynamic range of the odor intensity that can be presented. Thus an experiment was performed to investigate this issue. The detail is described in this section.

The experimental setup was similar to that in Section 5.5.1 except that 10 % of 2-hexanone diluted with ethanol was used instead of that of β-ionone. In the experiment, volume of the liquid droplet to be atomized was varied by changing the pulse width of a one shot pulse applied to the electroosmotic pump. An electroosmotic pump was driven by a 150 *V* electric pulse in six conditions that the pulse width was adjusted to 10, 5, 1, 0.5, 0.1, and 0.08 *s*, respectively. A droplet was then conveyed onto the SAW propagation path to be atomized in each condition. The measurement was performed 5 times. The sensor responses obtained from each condition which the pulse width was adjusted to 10, 5, 1, 0.5, and 0.1 *s* are shown in Figs. 5.15, 5.16, 5.17, 5.18, and 5.19, respectively. The thin lines demonstrate the time that the driving pulse was applied to the electroosmotic pump. In case of driving by a pulse with 0.08 *s* pulse width, no sensor response appeared. Thus, it is not shown in a figure.

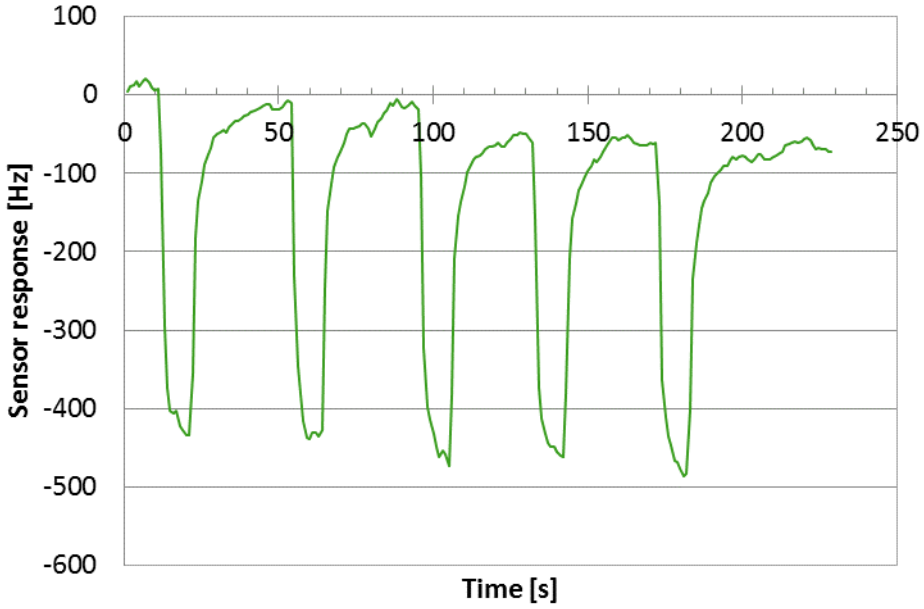


Fig. 5.15 Sensor response to vapor of 10% of 2-hexanone diluted with ethanol atomized for 10 seconds.

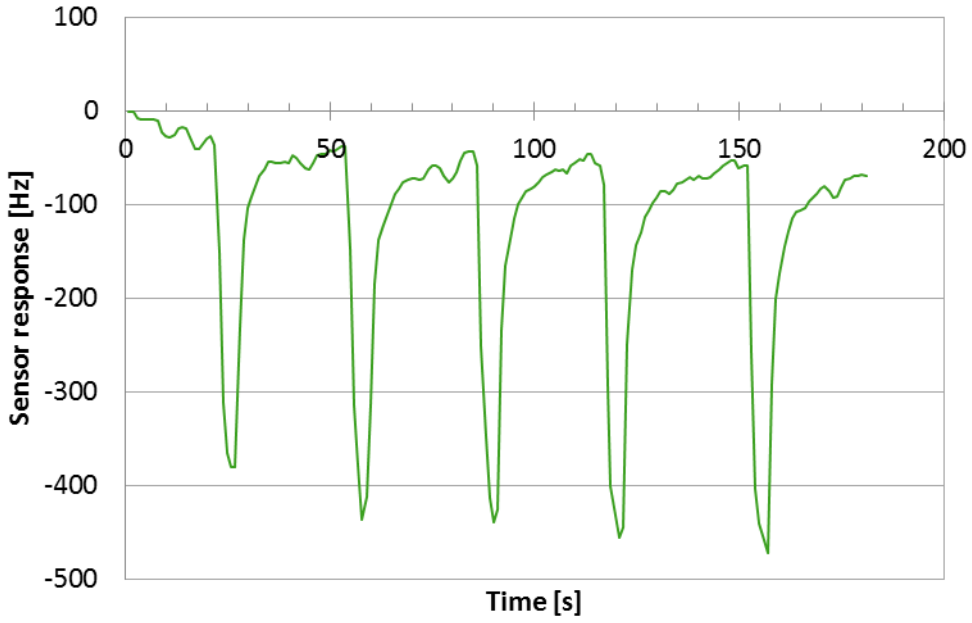


Fig. 5.16 Sensor response to vapor of 10% of 2-hexanone diluted with ethanol atomized for 5 seconds.

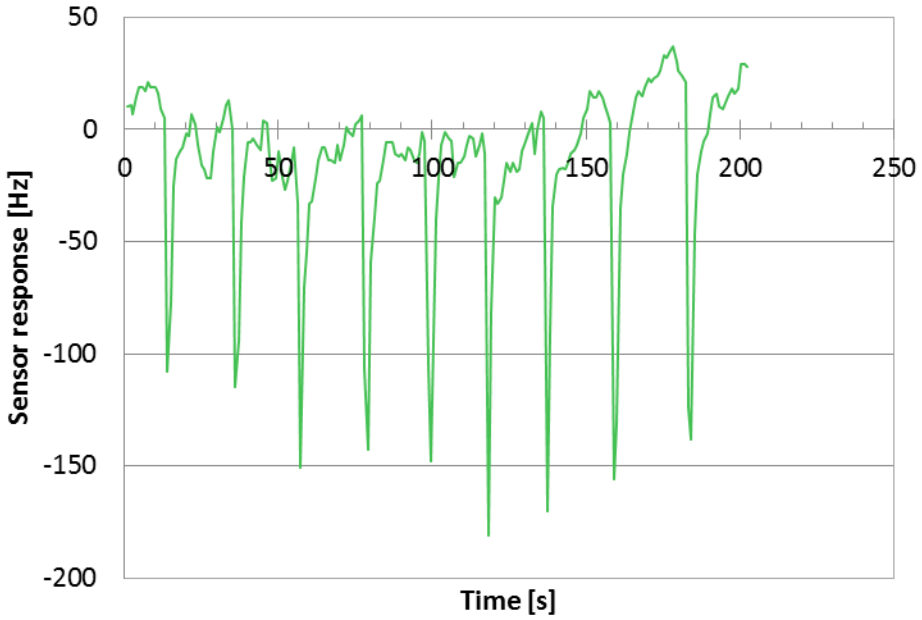


Fig. 5.17 Sensor response to vapor of 10% of 2-hexanone diluted with ethanol atomized for 1 seconds.

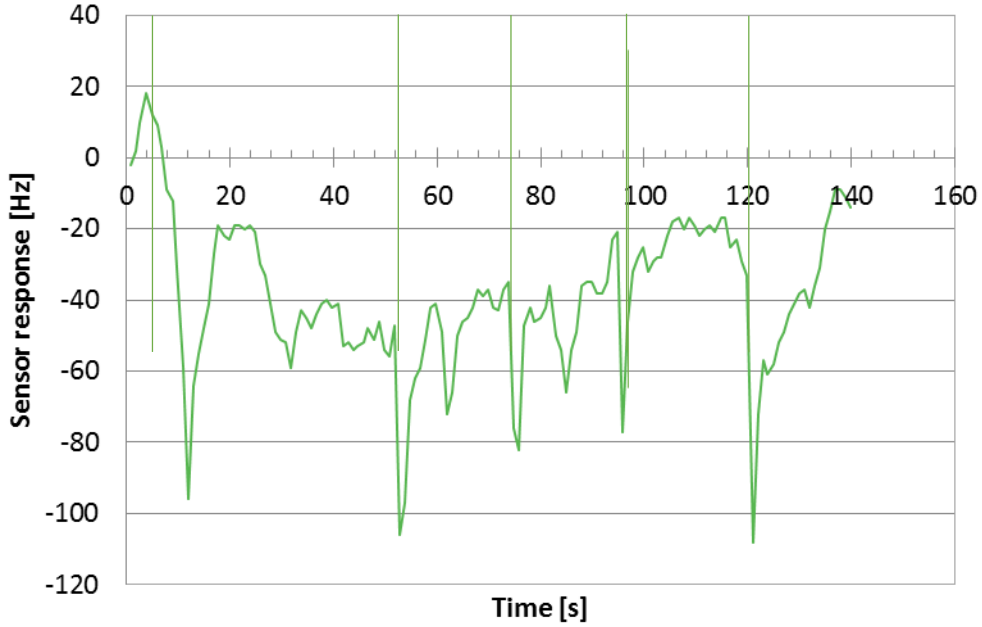


Fig. 5.18 Sensor response to vapor of 10% of 2-hexanone diluted with ethanol atomized for 0.5 seconds.

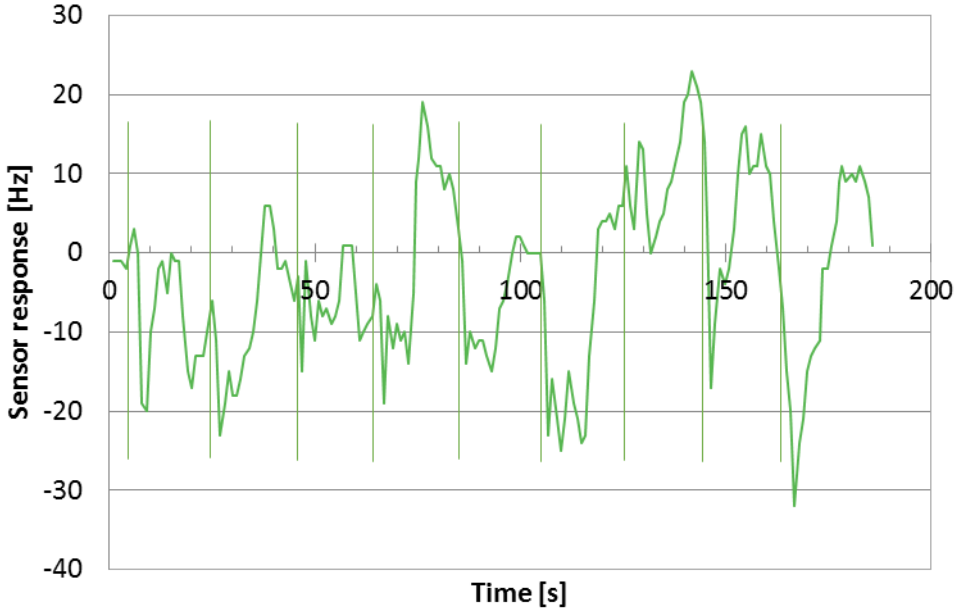


Fig. 5.19 Sensor response to vapor of 10% of 2-hexanone diluted with ethanol atomized for 0.1 seconds.

From the results shown in Figs. 5.15 – 5.19, it can be seen that the minimum time that the olfactory display can present odor is 0.1 *s* in case that the voltage applied to an electroosmotic pump was adjusted to 150 *V*. If the voltage is varied this minimum time is expected to be changed slightly as well. Besides, resolution of the odor presentation by using this olfactory display is approximately 20 Hz, according to the experimental result. The ratio of peak of the sensor response in Fig. 5.19 to that in Fig. 5.15 is approximately 20. This value indicates the dynamic range of odor presentation.

5.6 Summary

In this chapter, the development and evaluation of the miniaturized six-component olfactory display were explained. Its structure is composed of two metal blocks made of brass and aluminum. Very thin stainless tubes were placed closely to the SAW propagation path to supply the liquid droplets to be atomized. Based on this

configuration, the repeatability of the released odor was improved from the previous device described in Chapter 4 in which the tube needed to be manually assisted by hand.

Besides, a 14 x 25.5 *mm* SAW device with more atomization performance was developed to realize the atomization of a droplet of the odorant with low volatility. It was then found that 17 % of duty cycle is the appropriate condition for this SAW device to realize the highest SAW atomization performance without breaking the device in case that the repetition period is 1 *ms*. Subsequently, various experiments were performed by using the odor sensing system. From the experimental results, the capabilities to present even the scents of low volatile substances and to control the intensity of the released odor were confirmed. Moreover, two electroosmotic pumps were used to spout droplets with different volatility simultaneously to blend smells. In this case, the superposition characteristic of the sensor responses could be observed. It demonstrates that the olfactory display also possesses the capability to blend smells. Finally, the experiments performed to investigate the dynamic range and resolution of the intensity of released smell is described. As a result, it was clear that the pulse width of the signal applied to the electroosmotic pump that can convey the smallest amount of droplet onto the SAW propagation path is 0.1 s, in case that the pulse amplitude is 150 *V*. The 20 times difference between the highest and lowest sensor responses obtained in the experiments implies the dynamic range of the odor presented from this six-component olfactory display.

Chapter 6

Development of an Eight-component Wearable Olfactory Display Using Electroosmotic Pumps and SAW Device for Presenting Scents of Low-volatile Substances

6.1 Introduction

The miniaturized olfactory display composed of six electroosmotic pump for blending odors from up to six components was developed as described in Chapter 5. It can present even the scents of low volatile substance rapidly, can control odor intensity, and can blend smells. However, there were some problems that still needed to be solved. The problems are described in this chapter.

To overcome the problem, a new SAW device which possesses higher atomization performance was developed. The detail about the development including with the content about the investigation of an appropriate method to drive the SAW

device are described in Sections 6.3 and 6.4, respectively. Subsequently, the eight-component olfactory display was developed to realize a wearable odor blender. The detail is described in Section 6.5. Some experiments were done by using odor sensing system to evaluate the proposed wearable olfactory display. The detail is then described in Section 6.6. Finally, the chapter is summarized in Section 6.7.

6.2 Problem of Insufficient Atomization Performance

As described in Section 1.8, the objectives of this research is to develop an olfactory display that can present scents with low volatility within a short time and does not leave any residue after the presentation. Whether those objectives can be realized depends on the SAW device's atomization performance which can be enhanced by increasing the number of IDT finger pairs as described in Section 5.3.

The 14 x 25.5 *mm* SAW device described in Section 5.3 can atomize β-ionone, a low-volatile substance, into vapor abruptly without residue on the SAW propagation path. However, when it is used to atomize some liquid odorants whose volatility are lower than that it can deal with, the atomization does not occur. For example, in an experiment, a droplet of 10 % of butter flavor diluted with ethanol was dropped onto the SAW propagation path under the same driving condition as previous experiments described in Chapter 4. The SAW device can atomize it into smell with some residue. After five times of atomization, the amount of residue could be obviously seen as shown in Fig. 6.1.

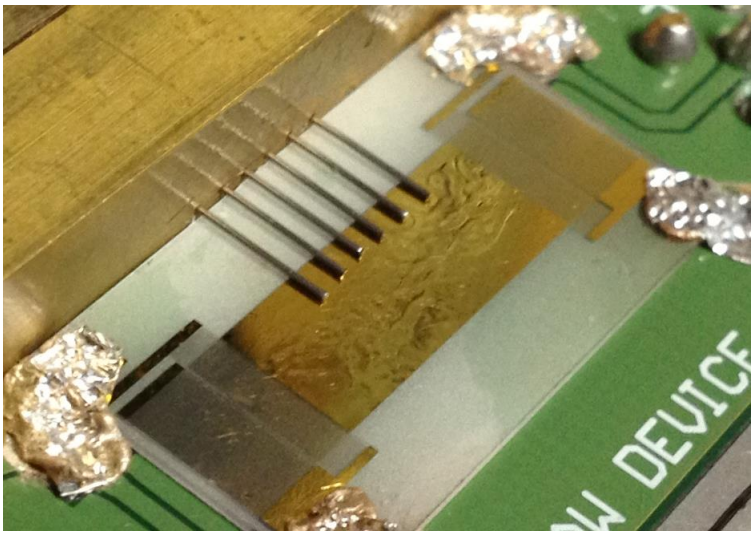


Fig. 6.1 Residue after five 0.27 μL droplets of 10 % of butter flavor diluted with ethanol are atomized.

The result implies that the atomization performance of the proposed 14 x 25.5 *mm* SAW device is still not sufficient to atomize some odorants with very low volatility absolutely without reside remaining after the atomization. Besides, as stated in Section 2.6.2, the residue remaining on the SAW propagation path drastically reduces power of the next SAW streaming. Thus, it does not allow the SAW device to atomize more droplets.

It is clear that the more atomization performance the SAW device has, the more possibility to release many kind of odors. Therefore, the SAW device with higher atomization performance was further developed to broaden the range of odor types that can be released by the olfactory display. The development of the new SAW device is described in the next section.

6.3 Development of 14 x 27.5 *mm* SAW Device

As described in the previous section, the SAW device with higher atomization performance was developed to broaden the range of odor types that can be presented.

To raise the atomization performance, the number of IDTs' finger pair of the SAW device was increased from 30 to 45. Other parameters were the same as those of the 14 x 25.5 *mm* one. The entire electrode pattern is shown in Fig. 6.2. An actual image of the SAW device is shown in Fig. 6.3. The size of the SAW device is 14 x 27.5 *mm*. The SAW device was pasted onto the same PCB designed for the previous 14 x 25.5 *mm* by using a conductive paste. The actual image of the device is shown in Fig. 6.4.

Frequency characteristic of the SAW device pasted on the board was measured by using an impedance analyzer (4291A, Hewlett Packard). In this measurement, both left and right ports of the SAW device were connected together. The result is shown in Fig 6.5. According to the result, the working frequency is 61.21 *MHz*.

A basic experiment was then performed and the experimental result showed that the proposed 14 x 27.5 *mm* SAW device can atomize more odorants with low volatility such as vanilla flavor, chocolate flavor, curry flavor, butter flavor, and other odorants in perfume whereas the previous 14 x 25.5 *mm* SAW device cannot atomize them without residue. Moreover, a droplet of water which can be only vibrated by using the previous SAW devices can be atomized by using this device. Therefore, it can be concluded that the range of odors that can be presented by the olfactory display was successfully broadened. The experiments showing the capability to present this kind of scents abruptly and does not leave any residue is described in Section 6.7.

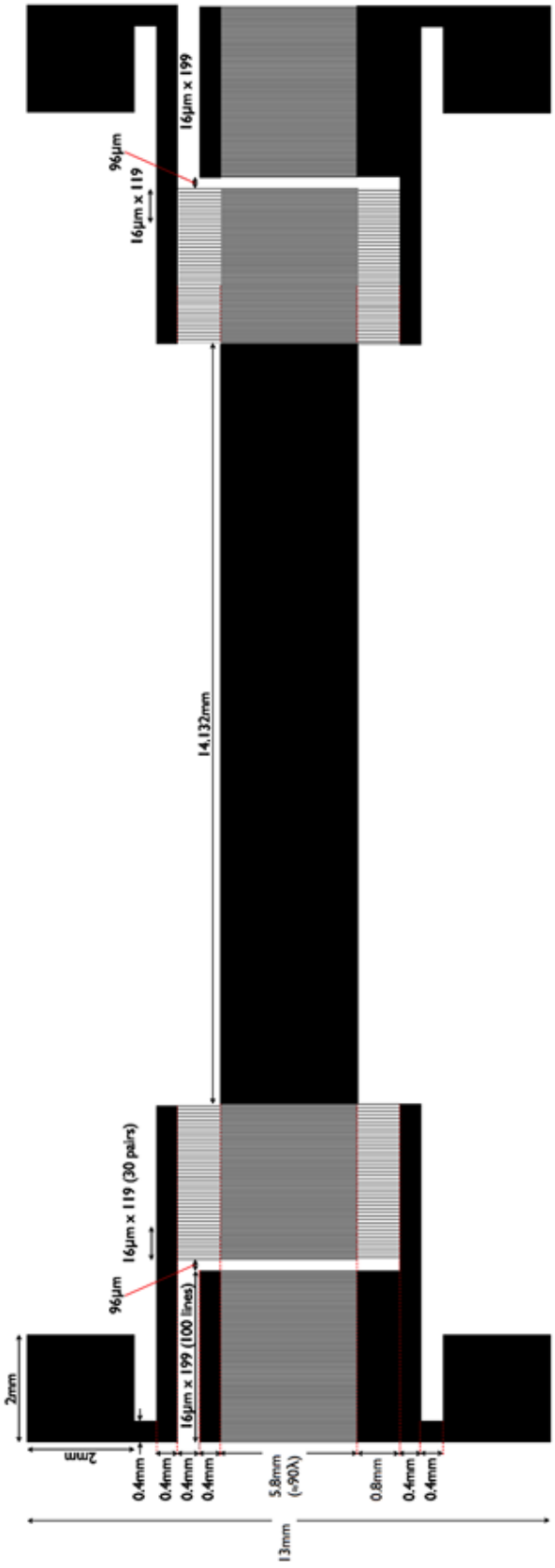


Fig. 6.2 Pattern of 14 x 27.5 *mm* SAW device.

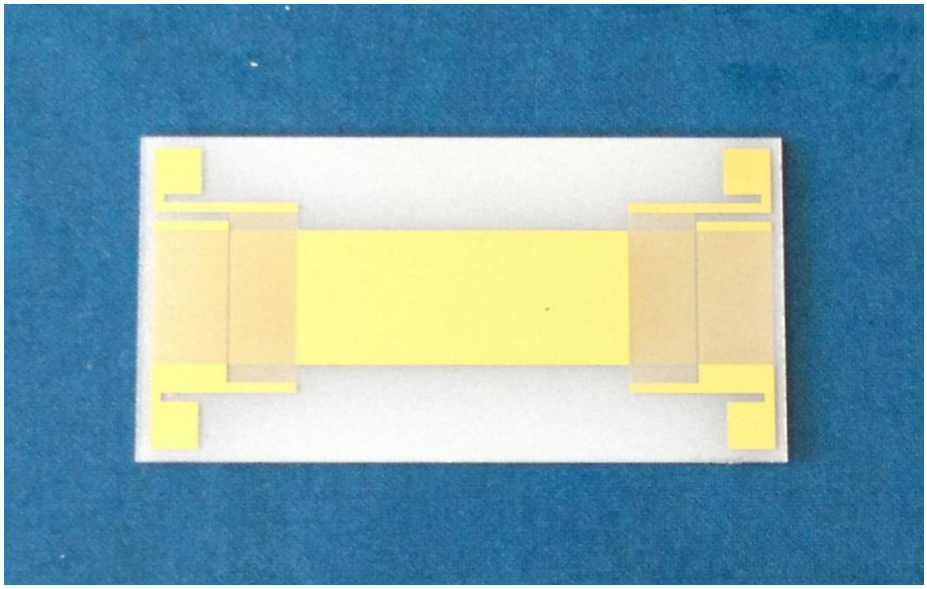


Fig. 6.3 Actual image of 14 x 27.5 *mm* SAW device.

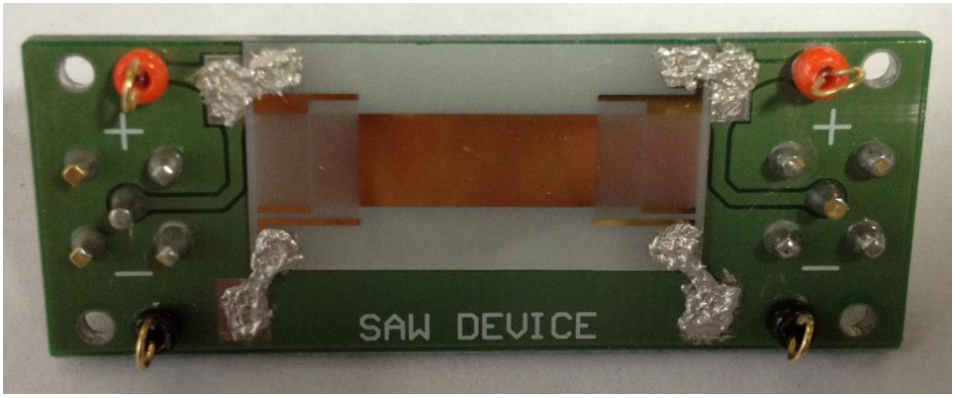


Fig. 6.4 Actual image of 14 x 27.5 *mm* SAW device pasted onto a PCB.

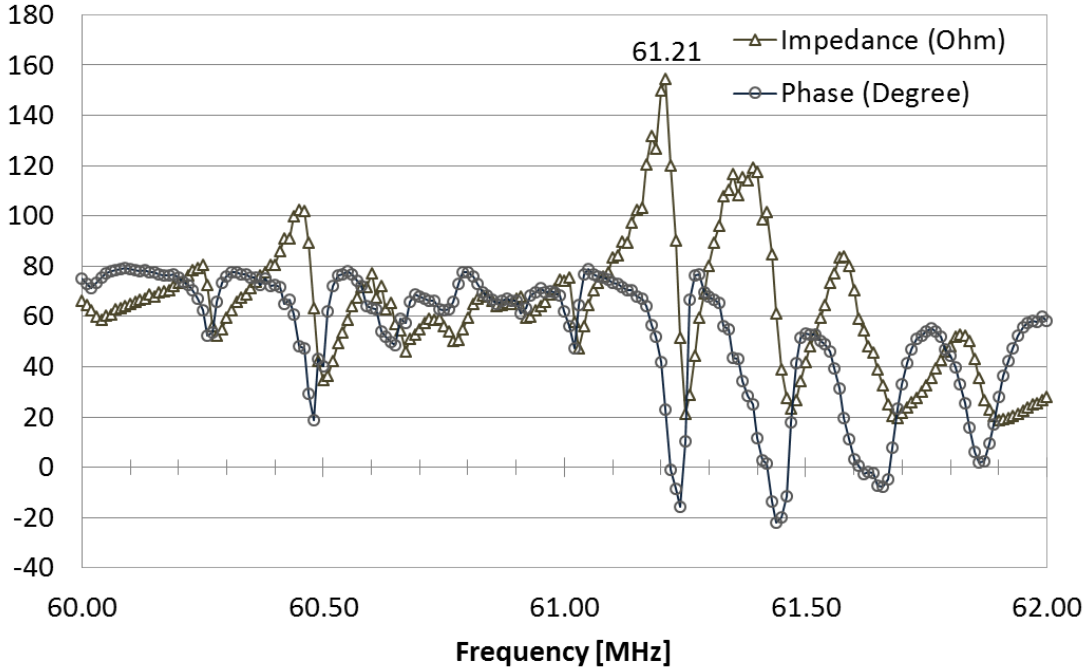


Fig. 6.5 Frequency characteristics of the 14 x 27.5 *mm* SAW device (both left and right ports were parallel connected together in the measurement).

6.4 Investigation on Appropriate Condition to Drive SAW

In Section 5.4, it was investigated that the 14 x 25.5 *mm* SAW device can be driven by the RF burst wave with the duty cycle up to 17 *%* at 1 *ms* of repetition period. An experiment was also performed to verify the same maximum driving condition for the 14 x 27.5 *mm* SAW device. The detail is described in this section.

In the experiment, the 14 x 25.5 *mm* SAW device was driven with 80 V_{pp} of RF burst wave whose repetition period was fix to 1 *ms*. Duty cycle was first adjusted to 1 *%*. The SAW device was driven under this condition for 20 s and if it was not broken the duty cycle was then raised by 1 *%*. The experiment was done repeatedly until the SAW device was broken.

As a result, the SAW device can be driven for 20 *s* without damage until the

duty cycle was set to 28 %. At 29 % of the duty cycle, the SAW device was broken within 10 *s*. As a result, the driving condition for the 14 x 27.5 *mm* SAW device that can provide atomization performance as high as possible without damaging the SAW device was understood.

6.5 Development of Wearable Eight-component Olfactory Display Using Electroosmotic Pumps and SAW Device

The miniaturized olfactory display composed of six electroosmotic pump for blending odors from up to six components was developed as described in Chapter 4. In this section, an attempt to further reduce the size of the olfactory display to realize the wearable multi-component olfactory display was described.

In order to further reduce the entire size of the device, all space should be used as useful as possible. Therefore, the olfactory display basis structure was not then divided into 2 parts; a PCB and a metal structure like that of the previous six-component olfactory display but all parts were integrated on a single PCB. The layout of the PCB is shown in Fig. 6.6.

In Fig. 6.6, the lower half area of the PCB is a space for a SAW device. The SAW device was pasted on the area by using conductive paste. The upper half area of the PCB is a space for a SMB connector that is connected with the SAW device's electrode via a signal route on a PCB. There are also eight-pair holes for eight electroosmotic pumps. The electroosmotic pumps were inserted into the holes to fit their pins tightly to avoid soldering. There are eight soldering pads on the bottom side of the PCB for connecting with eight electrical lines for driving the electroosmotic pumps by soldering. Lastly, the yellow frame shown between the area for SAW device

and electroosmotic pumps is an area for an aluminum block for guiding a liquid droplet. The layout of that block is shown in Fig. 6.7.

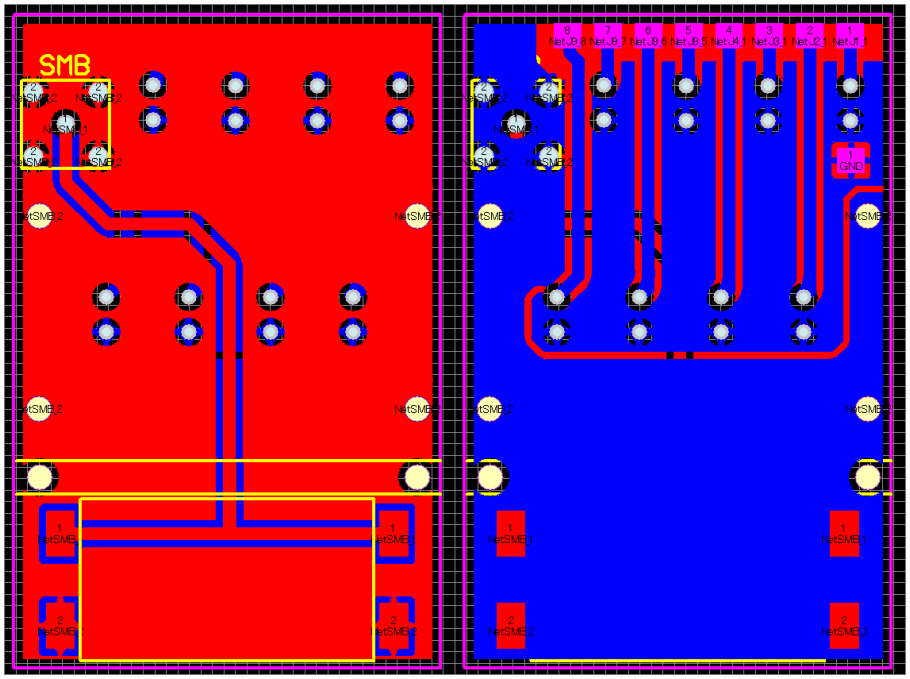


Fig. 6.6 Layout of an on-board olfactory display (left: top view, right: bottom view), (red: top layer, blue: bottom layer, yellow: top overlay, olive: bottom overlay, white: through hole).

The liquid guiding block shown in Fig. 6.7 was made of brass with eight very thin stainless tubes (outer diameter: 0.31 *mm*, inner diameter: 0.09 *mm*) inserted through. The outlet tubes were arranged to be placed closely to the surface of the SAW device to avoid problem that liquid droplet cannot be conveyed on to the SAW propagation path as described in Section 5.2. The inlet tubes were connected with the outlet of the electroosmotic pumps by using the cut micro-chips shown in Fig. 6.8 and silicone tubes. Fig. 6.9 illustrates how the connection was made.

An actual image of the eight-component olfactory display is shown in Fig. 6.10. The entire dimension is 37.4 x 56.7 *mm*. Frequency characteristic of the SAW device in

this olfactory display was measured by using an impedance analyzer (4291A, Hewlett Packard). In this measurement, both left and right ports of the SAW device were connected together. The result is shown in Fig 6.11. According to the result, the working frequency is 60.79 *MHz*.

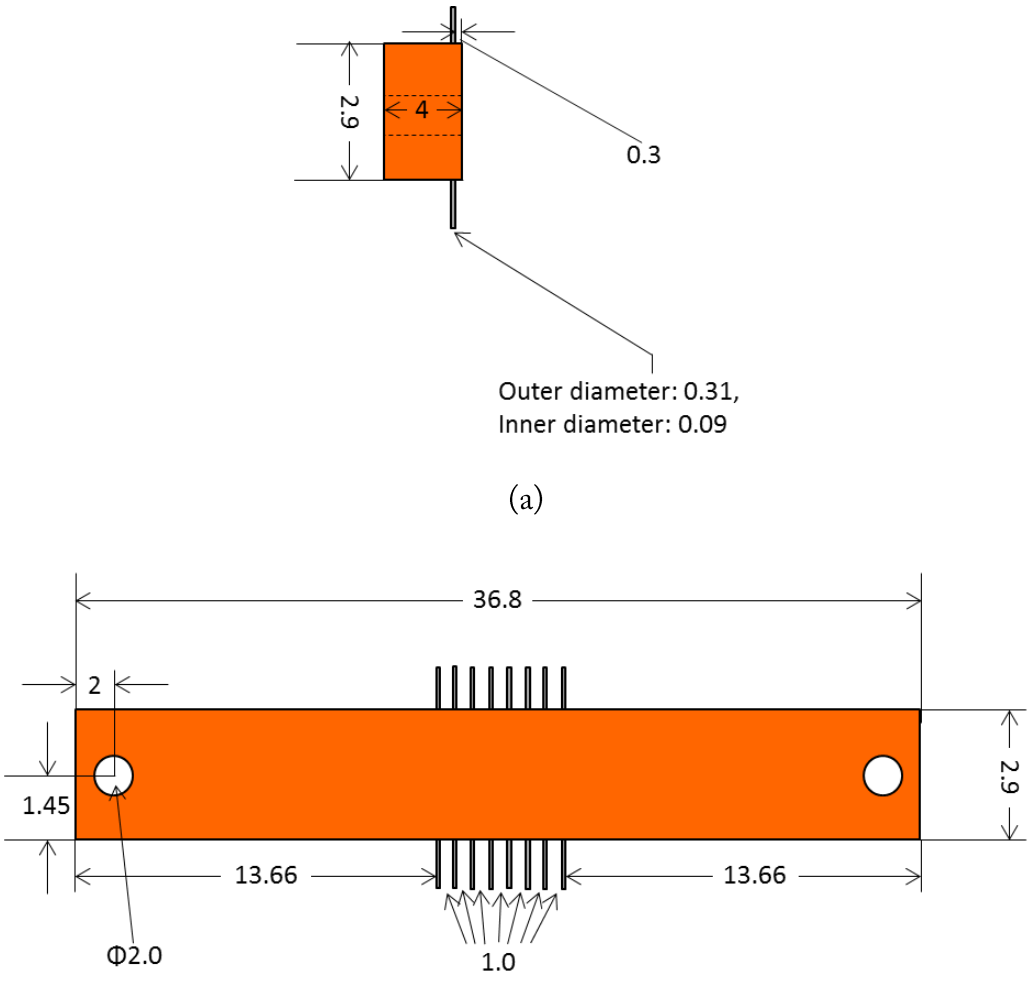


Fig. 6.7 Part of the miniaturized eight-component olfactory display designed for guiding liquid droplets (unit: *mm*); (a) front view, (b) side view.



Fig. 6.8 Micro-chip used in a connection between an electroosmotic pump and an inlet of a droplet guiding unit (the red line shows the plane that was cut by using a cutter).



Fig. 6.9 Example of a connection between an electroosmotic pump and an inlet of a droplet guiding block.

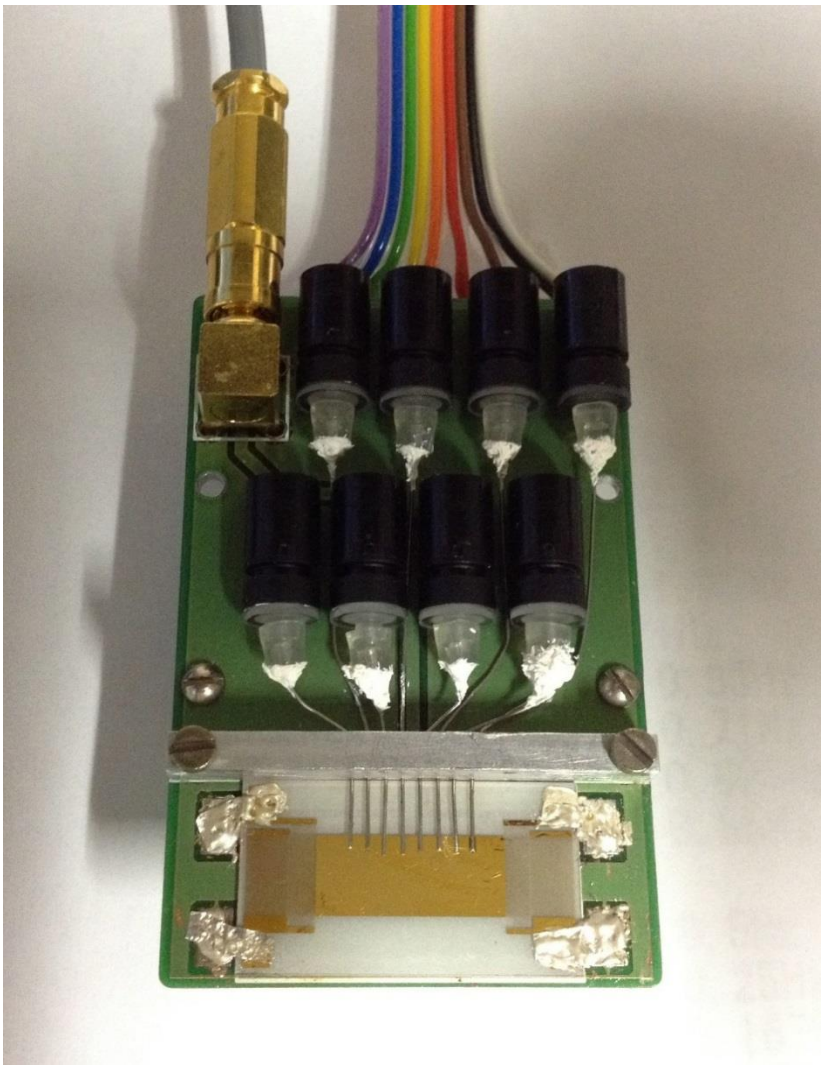


Fig. 6.10 Actual image of miniaturized eight-component olfactory display using electroosmotic pumps and 14 x 28.5 *mm* SAW device.

As shown in Fig. 6.10, the miniaturized multi-component olfactory display was realized. Its dimension is rather smaller than any other odor blender. As the size is miniaturized, the device can be equipped with a headset as shown in Fig. 6.12. In the figure, the olfactory display was placed on the headset mic and then locked by binding using a wire. When a user wears the headset, it is just in front of the user's nose. Thus, it becomes possible to express the sense of smell to the user abruptly. A photograph when it was worn by a user is shown in Fig. 6.13.

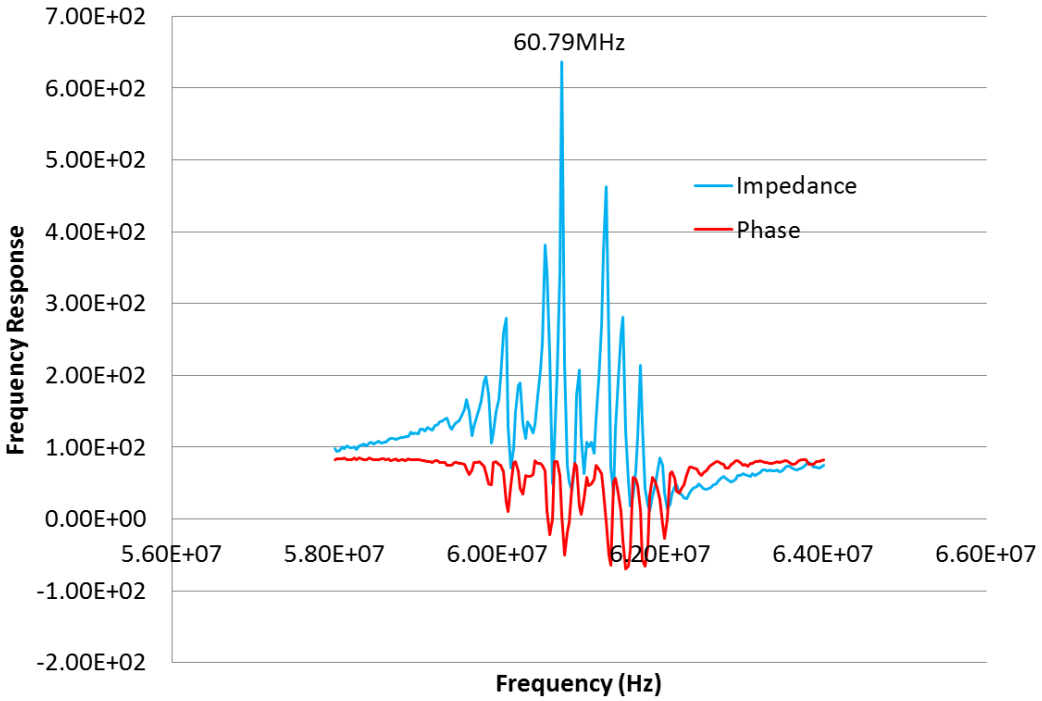


Fig. 6.11 Frequency characteristics of 14 x 28.5 *mm* SAW device (both left and right ports were connected together in parallel in the measurement).

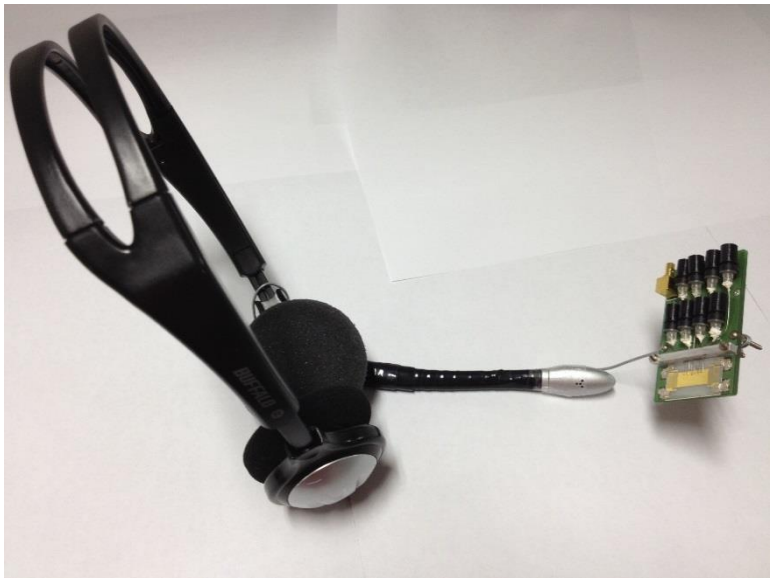


Fig. 6.12 Configuration of eight-component olfactory display equipped on a head set.

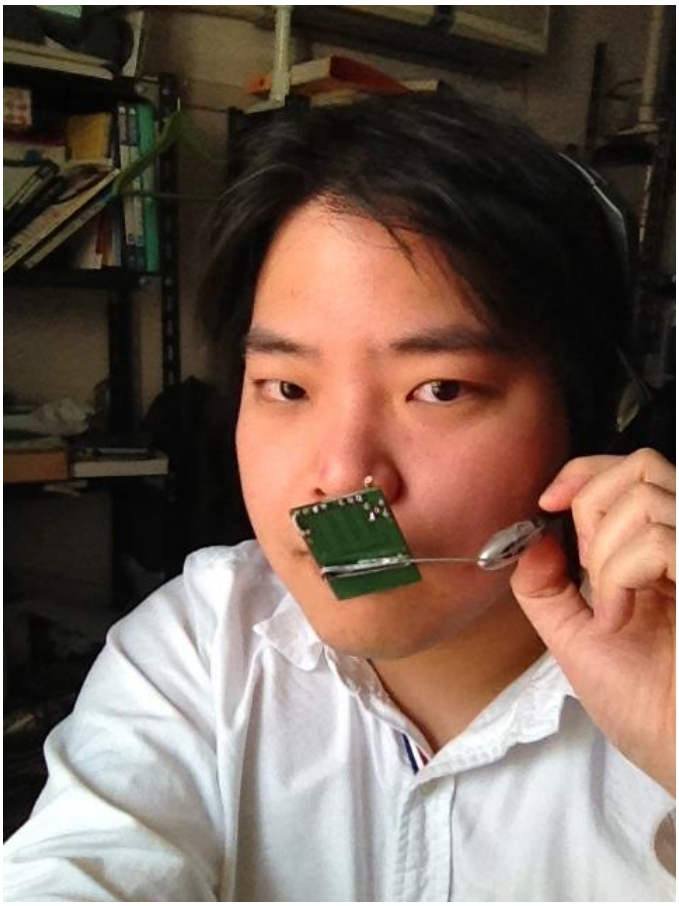


Fig. 6.12 A user wearing headset equipped with a miniaturized olfactory display.

Subsequently, the experiments that were performed to evaluate capabilities to present smells of the proposed olfactory display based on the odor sensing system and sensory evaluation are described in Section 6.6 and 6.7, respectively.

6.6 Evaluation of Olfactory Display Using Electroosmotic Pumps and 14 x 27.5 *mm* SAW Device Based on Improved Odor Sensing System

To evaluate capabilities of the miniaturized eight-component olfactory display with the 14 x 27.5 *mm* SAW device, three experiments were performed by using the odor sensing

system whose structure is described in Section 4.5.1. Sections 4.5.2 and 4.5.3 describe the first and second experiments which were carried out to evaluate the dynamic range and resolution of the moderate-volatile and low-volatile odor presentation, respectively. Lastly, Section 6.6.3 describes the third experiment which was performed to evaluate the capability to blend odors.

6.6.1 Evaluation of dynamic range and resolution of moderate-volatile odor presentation

To evaluate the dynamic range and resolution of the moderate-volatile odor presentation of the eight-component olfactory display, an experiment was performed. The detail is described in this section.

The experimental setup was almost similar to that done in Section 5.5.3. In the experiment, volume of the liquid droplet to be atomized was varied by changing the pulse width of a one shot pulse applied to the electroosmotic pump. The SAW device was driven by 80 V_{pp} RF signal with 14 % duty cycle and 1 ms repetition period. An electroosmotic pump was driven by a 150 V electric pulse in five conditions that the pulse width was adjusted from 0.1 to 10 s. A droplet of 10 % of 2-hexanone diluted with ethanol was then conveyed onto the SAW propagation path to be atomized in each condition. Sensor response obtained when the pulse width was 5 s is shown in Fig. 6.13 and the summary of sensor responses is shown in Fig. 6.14.

From the result, it can be observed that the olfactory display can start presenting the odor with moderate volatility by only 0.1 s of driving period in case that the voltage applied to an electroosmotic pump was adjusted to 150 V. The device was also able to atomize a rather large droplet spouted from up to 10 s of driving period. The difference between those two values are in two-orders of magnitude that can be

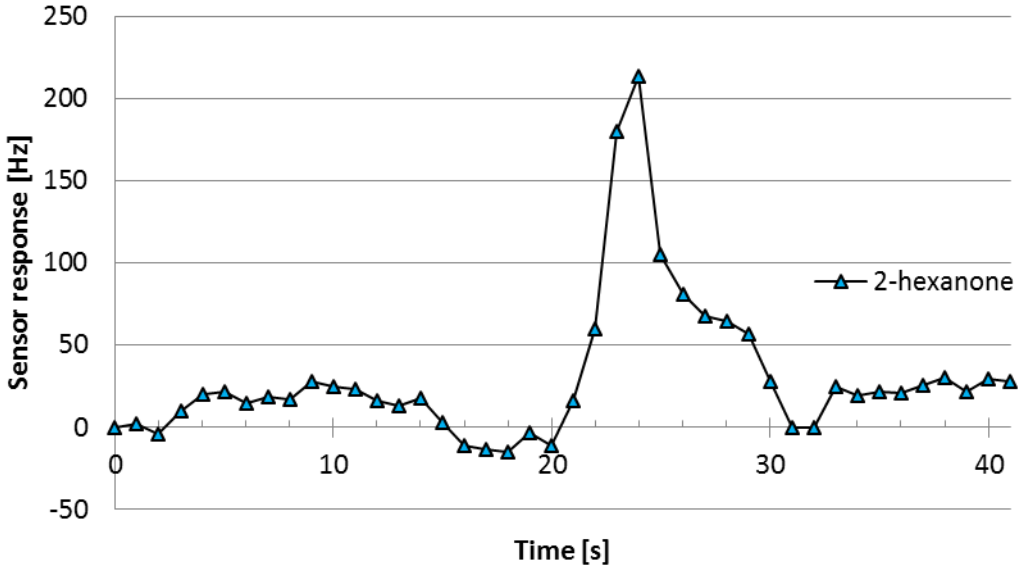


Fig. 6.13 Sensor response to vapor of 10% of 2-hexanone diluted with ethanol atomized for 5 seconds.

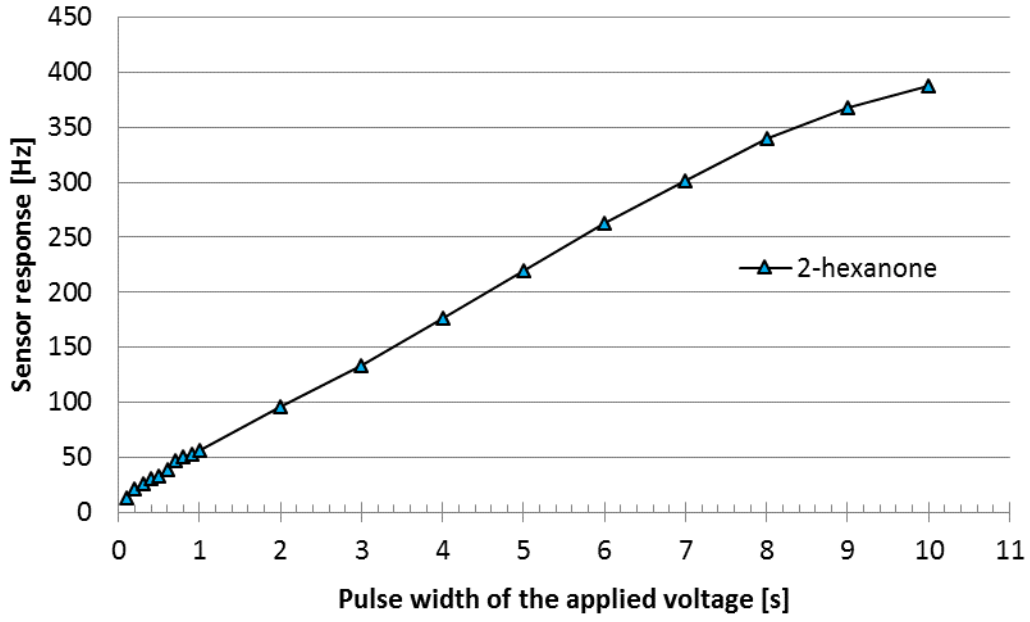


Fig. 6.14 Peak of sensor response to vapor of 10% of 2-hexanone diluted with ethanol atomized for 0.1 – 10 seconds.

considered as 0 – 100 % of odor-intensity variation span which was greatly improved from the span of the previous device shown in Section 5.5.3. The result also implies the high atomization performance of the proposed 14 x 27.5 *mm* SAW device. This wide dynamic range allows a variety of application on odor presentation. The experiments based on the practical application by which the odor is actually presented and evaluated by human's nose is then described in Chapter 7.

6.6.2 Evaluation of dynamic range and resolution of low-volatile odor presentation

The dynamic range and resolution of the moderate-volatile odor presentation of the eight-component olfactory display is described in the previous section. In this section, another experiment that was performed to evaluate the same qualification in case of the low-volatile odor presentation is described.

The experimental setup and procedure were almost similar to that done in Section 6.6.1 except that β-ionone was used instead of 2-hexanone. Sensor response obtained when the pulse width was 5 *s* is shown in Fig. 6.15 and he summary of sensor response from all conditions is shown in Fig. 6.16.

From the result, it can be concluded that even the scent of low volatile substance can also be released when the pulse width of driving signal was adjusted from 0.1 to 10 *s* as same as that of the scent with moderate volatility. This result shows the high atomization performance of the proposed 14 x 27.5 *mm* SAW device. However, it can be observed from Fig. 6.15 that the sensor response did not return completely to the

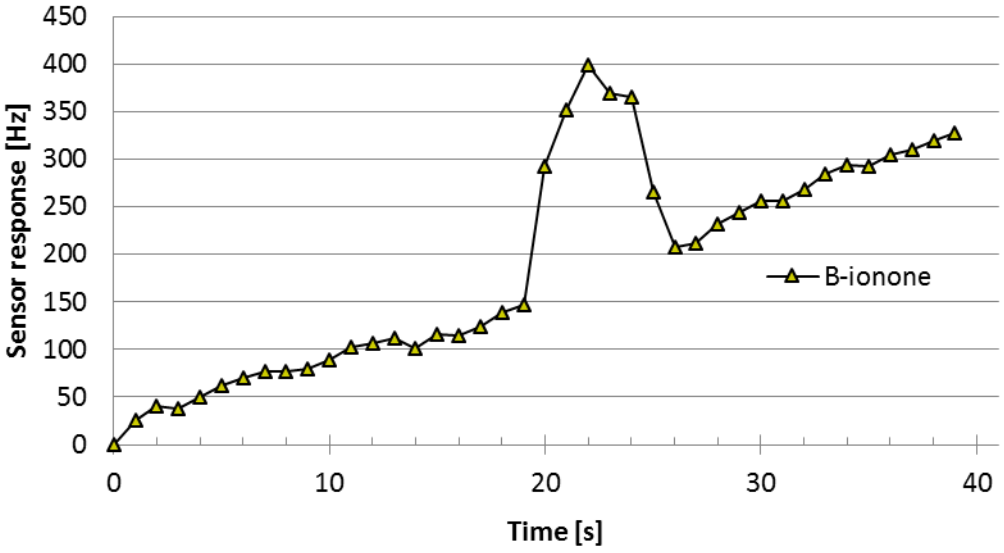


Fig. 6.15 Sensor response to vapor of 10% of β-ionone diluted with ethanol atomized for 5 seconds.

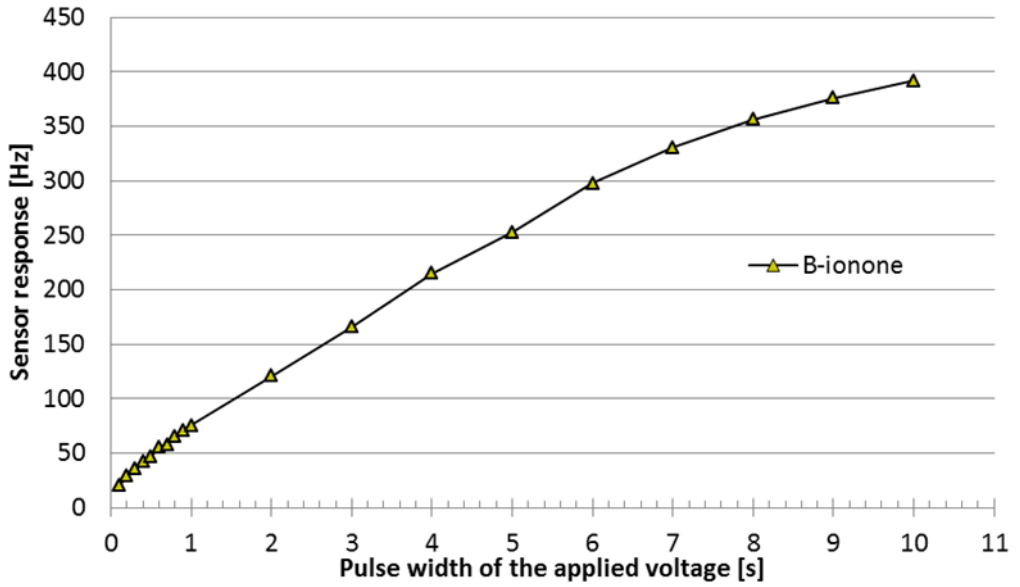


Fig. 6.16 Peak of sensor response to vapor of 10% of β-ionone diluted with ethanol atomized for 0.1 – 10 seconds.

baseline before the measurement. It might be duo to the odor residue on the SAW propagation surface or the adsorption of the odor molecule onto the QCM sensor

surface. The former case implies the insufficient of atomization performance of the olfactory display while the latter implies the limitation of the sensing system using QCM gas sensor. Thus, an experiment using a sensory evaluation was performed to verify the cause of this issue. It is described in Chapter 7.

6.6.3 Evaluation of capability to blend multiple of odors

As described in Section 1.8, one of the goals of this research is to realize the olfactory display that can blend smells. In case of the six-component olfactory display, it was confirmed that the device can blend binary-mixture of odors as demonstrated in Section 5.5.2. As the eight-component olfactory display is composed of the 14 x 27.5 *mm* SAW device that possesses higher atomization performance, its capability to blend up to ternary mixtures of odors was evaluated. The detail is described in this section.

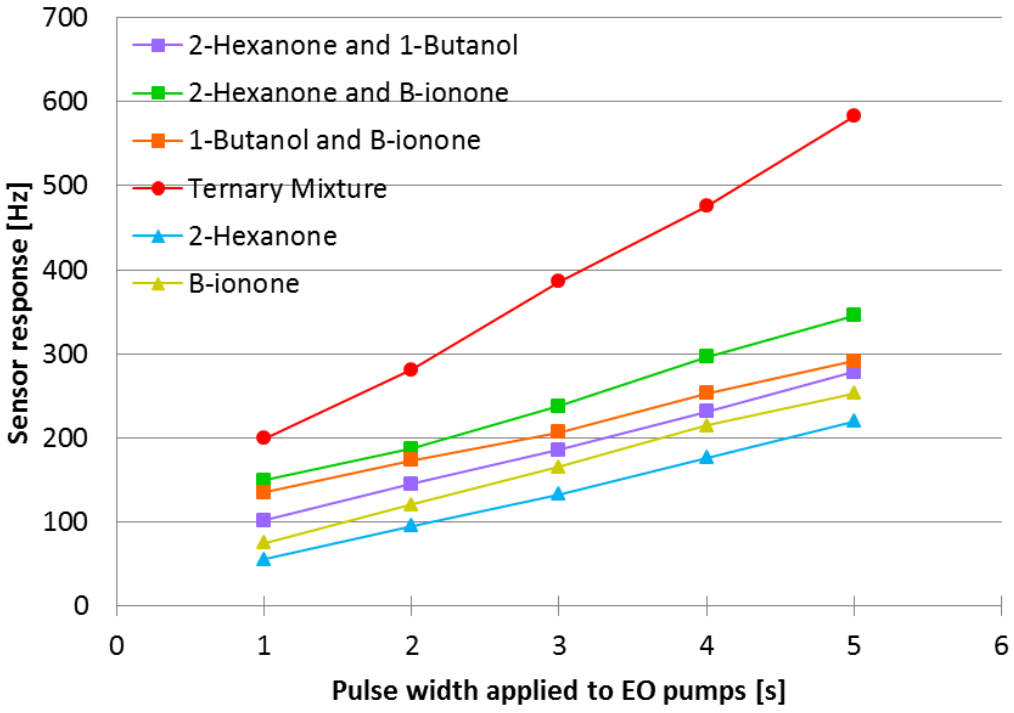


Fig. 6.15 Peak of sensor response to vapor of 10% of β-ionone diluted with ethanol atomized for 0.1 – 10 seconds.

The experimental setup was almost similar to that done in Section 5.5.2 except that three electroosmotic pumps were used together for odor blending. The pumps were filled with 10% of 2-hexanone, 1-butanol, and 5% of β-ionone diluted with ethanol, respectively. Each pump was driven for the duration of 1 – 5 seconds separately to obtain the sensor responses of each sample. Then, two and three pumps were used to spout odorant droplets to be atomized simultaneously. The measurement was performed 4 times in each case. The summarized average sensor responses to the vapors of all conditions are shown in Fig. 6.15.

The superposition characteristic when the binary and ternary odor mixtures were presented can be observed in the result. Thus, the odor blending capability of the miniaturized eight-component olfactory display was confirmed.

6.7 Summary

In this chapter, the insufficient performance of the miniaturized six-component olfactory display to present a smell of very low volatile substance without residue was indicated. To solve that problem the 14 x 27.5 *mm* SAW device with more pairs of IDT fingers than the previous device was developed. An experiment was performed to investigate the appropriate method to drive the proposed SAW device. Its higher atomization possibility was then confirmed by atomizing some odorants that the previous olfactory display cannot, such as, vanilla flavor, chocolate flavor, butter flavor, and some odorants in perfumes.

Subsequently, in order to further miniaturize the dimension of the entire device, the new structure of the olfactory display was developed on a single PCB. The device is rather smaller than any other odor blender and compact enough to be equipped on a headset. The experiments based on odor sensing system were performed to evaluate capabilities of the proposed device. The results showed that the eight-component

olfactory display has wider dynamic range than the previous devices.

The difference between minimum and maximum intensities of odors that the device can present is in two-orders of magnitude that can be considered as 0 – 100 % of dynamic range which was broadened from the previous device obviously. However, the sensor response did not completely return to the baseline after the measurement. Thus, an experiment using a sensory evaluation was performed to verify the cause of this issue. It is described in the next chapter.

Chapter 7

Evaluation of an Eight-component Wearable Olfactory Display Using Electroosmotic Pumps and a SAW Device Based on Sensory Evaluation

7.1 Introduction

According to the experimental result measured by the odor sensing system, the miniaturized eight-component olfactory display can present scents of substances with low volatility rapidly, can control odor intensity, and can blend multiple components as described in Chapter 6. Besides, the dynamic range of odor type that can be presented was also broadened.

However, as the olfactory display is an odor presenting device that release odors to the human's nose, evaluating the device based on not only odor sensing system but also sensory evaluation is indispensable. Therefore, the experiments based on sensory test were performed to further evaluate the proposed olfactory display. The experiments that were done to evaluate the smell persistence on the device is described in Section 7.2.

Subsequently, the experiment that was performed to evaluate the timing of the odor presentation is described in Section 7.3. The device was also integrated into a visual-olfactory presentation system to verify its capability in practical use. The detail is described in Section 7.4 and its evaluation is described in Section 7.5, respectively. Finally, the chapter is summarized in Section 7.6.

7.2 Evaluation of Smell Persistence Using Sensory Evaluation

Even though the capability to present odors, control odor intensities, and blend smells of the proposed olfactory display were confirmed by using an odor sensing system as described in Chapter 5 and 6, Sections 5.5.1 and 6.6.2 indicates that the sensor responses obtained in the measurement did not return to the baseline. This issue might be caused by two reasons; odor remaining on the SAW propagation path or odor molecule adsorption on the surface of QCM gas sensor. The former implies the insufficient capability to completely atomize an odorant droplet whereas the latter implies the limitation of the odor sensing system. Thus, the experiment using human sensory evaluation was performed to verify this issue. The detail is described in this section.

Before the experiment, the proposed eight-component olfactory display was equipped with a headset as shown in Fig. 6.12. The experiment was performed in a room equipped with air conditioning facilities. . The SAW device was driven by 80 Vpp RF signal with 14 % duty cycle and 1 ms repetition period. The temperature was set to 26 ˚C. Since sensory test is influenced by physical and mental condition, i.e. health, memory, experience, the test was conducted with participants as many as possible. However, to further increase the reliability of the result, a preliminary experiment was

conducted first. The detail about the preliminary experiment is described in Section 7.2.1 and the details about the main experiment are described in Section 7.2.2, respectively.

7.2.1 Preliminary experiment

In the two experiments described in Sections 7.2.2 and 7.2.3, 10 % of pineapple flavor and 10 % of β-ionone diluted with ethanol were used as representatives of odorants with moderate and low volatilities, respectively. Since sensory test is influenced by physical and mental condition, a preliminary experiment was conducted first to verify whether the participants can discriminate the difference between pineapple and β-ionone odors. The detail is described in this section.

In the preliminary experiment, participants were asked to sniff the 10% of β-ionone diluted with ethanol filled in a bottle and remember it. They were then asked to wear a head set equipped with the olfactory display and sit on a chair. Subsequently, the vapor of pineapple odorant was presented for 5 *s*. After that they were inquired whether the odor presented by the olfactory display have something similar to the odor in the bottle that they sniffed before. If they says 'yes', it implies that they cannot discriminate the difference between pineapple and β-ionone odors. The procedure of this preliminary experiment is demonstrated in Fig. 7.1. The results of 64 subjects are tabulated in Table 7.1.

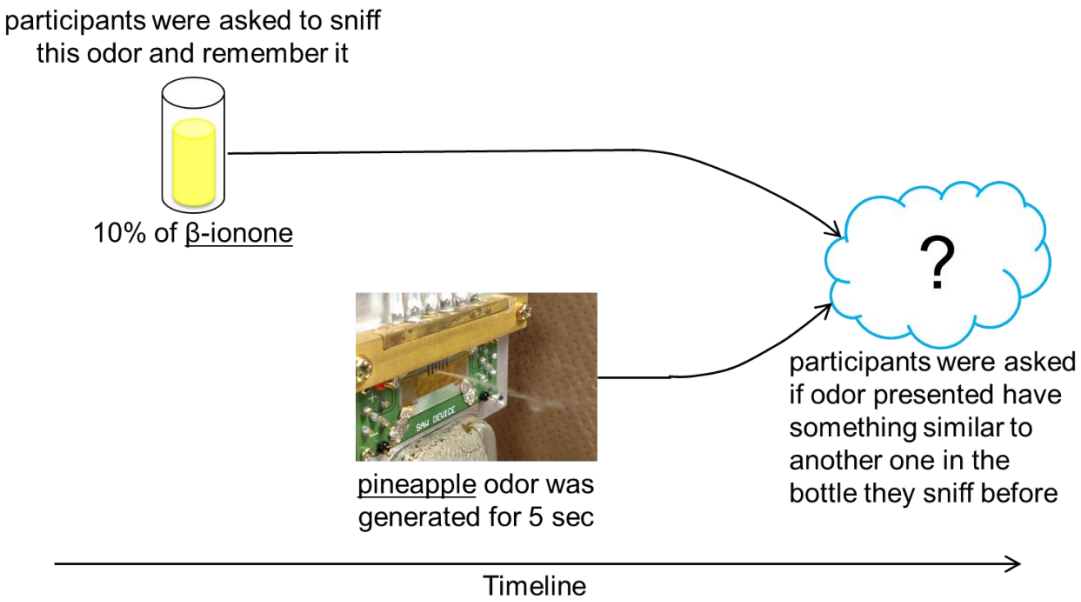


Fig. 7.1 Procedure of preliminary experiment.

Table 7.1 Number of participants' answers in preliminary experiment.

Answer	Yes	No	N/A
Number	3	58	3

According to the result, 3 participants cannot discriminate the difference between pineapple and β-ionone odors. It means that the rate of discrimination between these two scents exceeds 90 %.

7.2.2 Main experiment

In the previous section, the validation of using pineapple and β-ionone odors as representative odor samples for the sensory evaluation was approved as the discrimination rate exceeds 90 %. Thus, they were used in the sensory test to evaluate the olfactory display. The detail of the first sensory evaluation is described in this section.

In the experiment, 10 % of β-ionone and 10 % of pineapple odorants diluted with ethanol were filled into two electroosmotic pumps. Firstly, the vapor of β-ionone was released for 6 *s* without presenting to the participants. After that, participants were asked to sniff the 10 % of β-ionone diluted with ethanol filled in a bottle and remember it. Next, they were asked to wear a headset equipped with the olfactory display and sit on a chair. The vapor of pineapple odorant was then presented for 5 *s*. The experiments were done within 30 *s* after the first time that β-ionone was presented. After that they were inquired whether the odor presented by the olfactory display have something similar to the odor in the bottle that they sniffed before. If they says 'yes', it may imply that β-ionone still remained on the device after the atomization. The procedure of this preliminary experiment is demonstrated in Fig. 7.2. The results of 64 subjects are tabulated in Table 7.2.

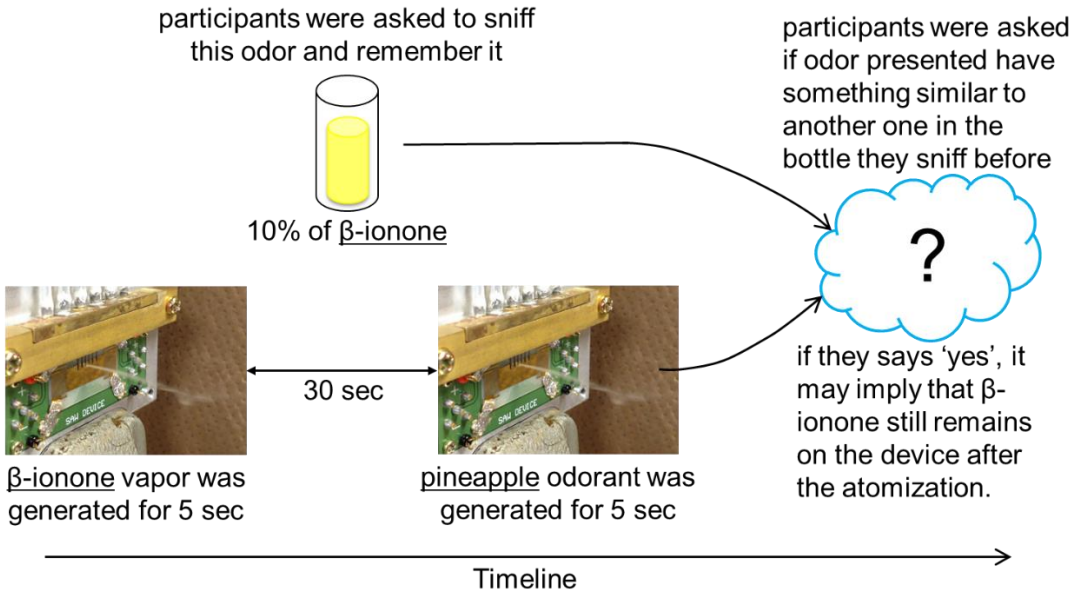


Fig. 7.2 Procedure of experiment using sensory evaluation to verify odorant remaining on olfactory display after presentation.

Table 7.2 Number of participants' answers in experiment on smell persistence.

Answer	Yes	No	N/A
Number	3	61	0

From the result, the number of negative answers is almost equal to the negative answers in the preliminary test. It means that the proposed eight-component olfactory display can present even the scents of low-volatile substance and remove it quickly after the atomization. Therefore, the sensor responses in experiments described in Sections 5.5.1 and 6.6.2 that did not return to the baseline were considered to be due to the limitation of the odor sensing system not the insufficient performance of the olfactory display.

7.3 Evaluation of Timing of Odor Presentation Using Sensory Evaluation

According to the experimental results in Chapter 5 and 6, the sensor responses appeared suddenly approximately within 1 *s* after the presentation start. However, it is also necessary to evaluate the actual timing that the participants can feel smells after the odor releasing by using sensory evaluation. An experiment was performed to verify this issue. The detail is described in this section.

Before the experiment, 10 % of β-ionone diluted with ethanol was filled into an electroosmotic pump. Before the experiment, participants were asked to wear a headset equipped with the olfactory display and sit on a chair. They were requested to close their eyes and say something when they start feeling any odor and say something again when they feel that the odor disappears. In the experiment, the pump was driven for 5 *s* to

present the vapor of β-ionone odorant. A timer was used to record the time that participants said something. This experiment was conducted with 11 subjects. The result is shown in Table 7.3.

Table 7.3 Participants' answers in experiment 3.

Participant No.	Time starting feeling an odor [*s*]	Time feeling the disappear of an odor [*s*]
1	3.8	12.1
2	1.4	6.1
3	5.1	12.6
4	2.7	16.7
5	2.5	8.9
6	3.6	5.7
7	2.3	6.2
8	3.6	10.8
9	3.1	6.7
10	2.6	8.0
11	2.7	6.8
Average	3.0	9.1

As a result, we can see that the participant with the most sensitive sense of smell could feel the smell within 1.4 *s* and could identify the absence of odor presentation within 6.1 *s* after the atomization finished while other participants took longer time. After the experiments, all participants were interviewed about the experiment.

According to the interview result, several participants said that they needed to

think for a while to make sure whether they really felt an odor or the odor really disappeared. Some participants also tried to sniff 3 – 4 times to make sure that the odor really disappeared and thus it took 5 – 7 *s* to determine before their answer.

Due to the fact that the person with strong olfactory perception (participant No. 2) could feel the odor presentation rapidly and the results obtained from odor sensing system described in Chapter 4 and 5 also indicate the rapid presentation, it can be considered that the olfactory display can present smells within that short time and other answers in case of other participants which took longer times were caused by the inconstancy of human olfactory perceptions. Even if the time delay mentioned above really occurs, this time is negligible compared with that of the conventional olfactory displays shown in Fig. 4.19 where it lasts for a few tens of minutes.

7.4 Development of Visual-olfactory Presentation System

The capability of the proposed eight-component olfactory display to present the odor rapidly was confirmed by both the odor sensing system and sensory evaluation as shown in Chapter 4, 5 and the previous section, respectively. Thus, an application was developed to verify that capability in practical use. The detail is described in this section.

One of the applications that requires rapid odor release is odor presentation with media since the presentation must be synchronized with the media scene which is normally less than 1 *s*. Thus, a visual-olfactory presentation system was developed to evaluate the proposed eight-component olfactory display in practical use. The schematic diagram of the system is shown in Fig. 7.3.

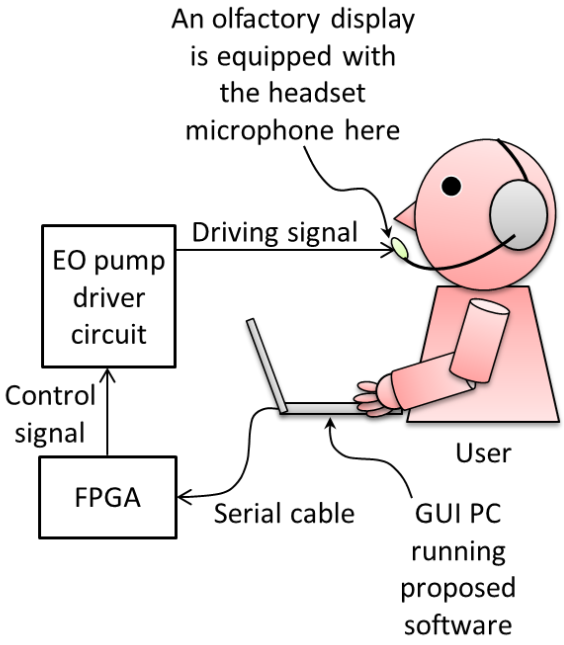


Fig. 7.3 Schematic diagram of the visual-olfactory presentation system using wearable multi-component olfactory display.

In the system, the miniaturized eight-component olfactory display was mounted on a headset so that it would be close to the user's nose. The user can interact with the system via a GUI PC that sends data synchronously with a movie on the platform of Windows Media Player to the FPGA board (Altera, ACM-012) via serial interface. The FPGA board generates a pulse with specified duration time to the EO pump driver circuit corresponding with the content in the media scene. The program that runs on a PC was written in Visual Basic 6.0.

7.5 Evaluation of Visual-olfactory Presentation System Based on Sensory Evaluation

An experiment was performed to evaluate the proposed visual-olfactory presentation system. The detail is described in this section.

In the experiment, a sensory test was used to evaluate the proposed system. The movie used in this study consists of 4 static scenes of fragrance bottles as shown in Fig. 7.4. Each scene continues for 5 *s*. Scene 1, 2 and 4 were played without the smell while scene 3 was played with the presentation of 10 % of a fragrance named Eau de Givenchy for 1.5 *s*. Eau de Givenchy is a mixture of a lot of odor components with different volatilities: i.e., rose, muguet, musk, jasmin, green, woody, diluted with ethanol. The distance between a SAW substrate and participant's nose was approximately 2.5 – 4 *cm*. Then, the participants were asked whether they feel any smell in each scene. This experiment was conducted with 9 subjects. The summary of the questionnaire survey is shown in Fig. 7.5. As a result, we can see that 100 % of participants can feel the fragrance of Eau de Givenchy presented with the movie in an appropriate scene. According to the result, the capability to present even am odor with very low volatility rapidly was confirmed.



Fig. 7.4 Movie scenes presented to participants.

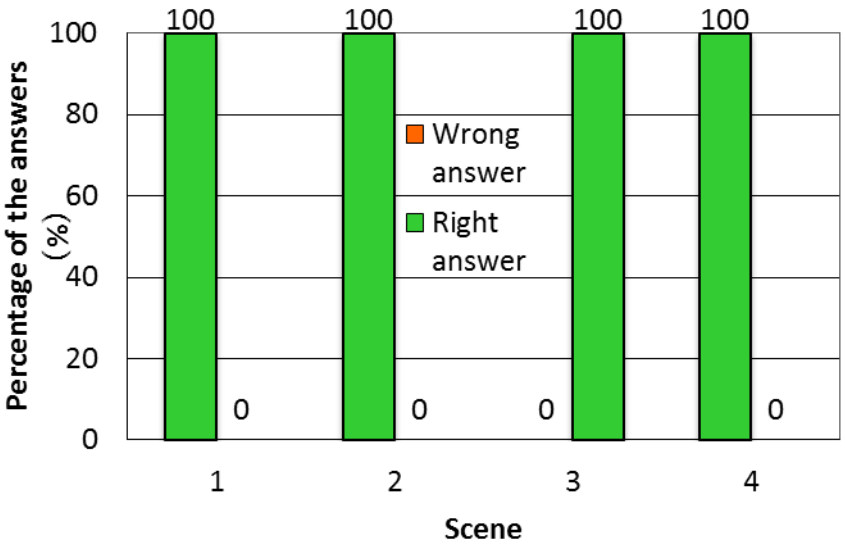


Fig. 7.5 Summary of answers given by 9 participants.

7.6 Summary

In this chapter, the evaluation of the proposed eight-component wearable olfactory display through sensory evaluation is described. Since sensory test is influenced by physical and mental condition, i.e. health, memory, experience, the test was conducted with participants as many as possible. To further increase the reliability of the result, a preliminary experiment was conducted first. According to the preliminary test result, participants more than 90 % can discriminate the difference between the pineapple and β-ionone odors used in the experiment. Thus, the next experiment was performed to evaluate the smell persistence on the device after the odor presentation. According to the device, more than 90 % of participants' answer implies that there was no odor remaining after the atomization. Another sensory test was performed to evaluate the timing of odor presentation. According to the result, the participant with the most sensitive sense of smell could feel the smell within 1.4 *s* and could identify the absence of odor presentation within 0.7 *s* after the atomization finished while other participants took longer time. It was considered that most of the answers were caused by the

inconstancy of human olfactory perceptions. Even if the time delay occurs, this time is negligible compared with that of the conventional olfactory displays where it lasts for a few tens of minutes. Subsequently, the visual-olfactory system was developed to verify the proposed olfactory display in practical use. An experiment was performed to verify whether participants can feel the fragrant of Eau de Givenchy, a perfume with relatively low volatility, presented by the system. The result shows that all participants could feel the smell when it is presented. The validity of the proposed olfactory display was confirmed.

Chapter 8

Conclusions

8.1 Conclusions

In this research, the olfactory displays using electroosmotic pumps and a SAW device were developed. The detail of thesis can be categorized into three main topics as follows.

1. Preliminary study of olfactory display using an electroosmotic pump and a SAW device (Chapter 2 – 4)

A basic olfactory display was developed. Its characteristics are shown below.

1. Structure: It has simple structure which still needs to be hold by a hand during experiments. A 10 x 10 or 10 x 19 *mm* SAW device and an electroosmotic pump are used.
2. Performance: It can present an odor of substance with high or moderate volatility, such as pentane, hexane, acetone, and ethanol.
3. Dynamic range: 30 % (calculated from 2 – 6 *s* of span of pulse width)

2. Development of miniaturized six-component olfactory display using electroosmotic pumps and a SAW device (Chapter 5)

A miniaturized multi-component olfactory display was developed. The atomization

performance was also improved. Its characteristics are shown below.

1. Structure: The structure is reliable and durable since it was made of solid metal blocks. Its dimension is 65 x 59 x 11 *mm*. A 14 x 25.5 *mm* SAW device and six electroosmotic pumps and are used.
2. Performance: It can present an odor of substance with low volatility. Atomization of β-ionone was confirmed.
3. Multiple-odor blending: binary-mixture was confirmed.
4. Dynamic range: 50 % (calculated from 1 – 5 *s* of span of pulse width)

3. Development of wearable eight-component olfactory display using electroosmotic pumps and a SAW device (Chapter 6 – 7)

An improved miniaturized multi-component olfactory display was developed. The atomization performance was also further improved. Its characteristics are shown below.

1. Structure: The structure was made of a PCB. Its dimension is 37.4 x 56.7 x 7.5 *mm*. It is very compact and smaller than a credit card. A 14 x 27.5 *mm* SAW device and eight electroosmotic pumps are used.
2. Performance: It can present an odor of substance with very low volatility, such as curry flavor, vanilla flavor, chocolate flavor, butter flavor, and Eau de Givenchy (fragrance).
3. Multiple-odor blending: ternary-mixture was confirmed.
4. Dynamic range: 100 % (calculated from 0.1 – 10 *s* of span of pulse width)

This research proved the validation of the method to utilize SAW streaming to release odors. Even scents of low volatile substances can be presented rapidly. Another advantage of the olfactory display developed based on this technique is the compact size. Dimension of the eight-component olfactory display developed in this study is 37.4 x 56.7 x 7.5 *mm*. However, most of the area in the device is for liquid tanks and electrical

connections. Moreover, smell persistence can be avoided using this olfactory display.

8.2 Future Perspective

In my perspective, if a liquid tank, made of an appropriate material that does not distort SAW energy, is constructed on a SAW device. The electroosmotic pumps in this research can be omitted. The liquid flow from the tank to the atomization location can be controlled by SAW streaming. Moreover, when multiple of droplets are forced to flow to be mixed and then atomized at the actual same position on the SAW propagation path, the more ideal blending can be expected. By these means, the entire size of the olfactory display can be reduced to be approximately equal with the size of the SAW device.

Based on these concepts, what I name "olfactory display on a chip" can be realized. The multiple-component olfactory display chip which can present various kind of fragrances when it is embedded into other apparatus with power supply for the device can be expected. With that compact size including capabilities to control odor intensity and to blend multiple of smells, the widespread of the olfactory display as one of the daily life apparatus will come in the near future.

Publications

Journal Articles

1. Y. Ariyakul, T. Nakamoto, *Improvement of odor blender using electromotic pumps and SAW atomizer for low-volatile scents*, IEEE SENSORS Journal, 2013 (Accepted)

2. Y. Ariyakul, T. Aizawa, T. Nakamoto, *Tiny olfactory display based on SAW streaming and electroosmosis*, IEEJ Transactions on Sensors and Micromachines (E), Vol. 133, No. 6, pp. 206 – 211, 2013

3. Y. Ariyakul, T. Nakamoto, *Fundamental study of olfactory display using extremely small liquid pump and SAW atomizer*, Transactions of Virtual Reality Society of Japan, Vol. 15, No. 4, pp. 589 - 594, December 2010 (in Japanese)

International Conferences

1. Y. Ariyakul, T. Nakamoto, *Movie with scents generated by olfactory display using SAW device and EO pumps*, ISOEN 2013, Daegu, Korea, July 2013 (to be presented)

2. Y. Ariyakul, T. Aizawa, T. Nakamoto, *Visual-olfactory presentation system using a miniaturized olfactory display based on SAW streaming and electroosmotic pumps*, IEEE Virtual Reality 2013, pp. 155 - 156, Orlando, Florida, United States, March 2013

3. Y. Ariyakul, Y. Hosoda, T. Nakamoto, *Improvement of odor blender using electroosmotic pumps and SAW atomizer for low-volatile scents*, IEEE SENSORS 2012, pp. 1025 - 1128, Taipei, Taiwan, October 2012

4. (Reviewed) Y. Ariyakul, T. Nakamoto, *Improvement of olfactory display using electroosmotic pumps and a SAW device for VR application*, Proc. 21st Intl. Conf. on Artificial Reality and Telexistence (ICAT 2011), pp. 15 - 21, Osaka, Japan, November 2011

5. Y. Ariyakul, T. Nakamoto, *Olfactory display using a miniaturized pump and a SAW atomizer for presenting low-volatile scents*, IEEE Virtual Reality 2011, pp. 195 - 196, Singapore, March 2011

6. T. Nakamoto, M. Kinoshita, K. Murakami, A. Yossiri, *Demonstration of improved olfactory display using rapidly-switching solenoid valves*, IEEE Virtual Reality 2009, Research Demo, pp. 301 - 302, Lafayette, Louisiana, United States, March 2009

Domestic Conferrences

1. Y. Ariyakul, T. Aizawa, T. Nakamoto, *Visual-olfactory presentation system using tiny odor-presenting unit*, Interaction 2013, Information Processing Society of Japan, pp. 719 - 722, Tokyo, Japan, March 2013 (in Japanese)

2. Y. Ariyakul, Y. Hosoda, T. Nakamoto, *Study of odor presenting unit using micro liquid pump and surface acoustic wave device*, IEEJ Annual Meeting 2012, Vol. 3, pp. 198, Hiroshima, Japan, March 2012 (in Japanese)

3. Y. Ariyakul, T. Nakamoto, *Study of olfactory display using electro-osmotic pumps and SAW atomizer*, IEEJ Sensors and Micromachines (E) 2011, Papers of Technical Meeting on Chemical Sensor, pp. 71 - 75, Kanagawa, Japan, July 2011 (in Japanese)

4. Y. Ariyakul, T. Nakamoto, *Fundamental study of olfactory display using extremely small liquid pump and SAW device*, IEEJ Sensors and Micromachines (E) 2010, Papers of Technical Meeting on Chemical Sensor, pp. 1 - 5, Tokyo, Japan, June 2010 (in Japanese)

5. Y. Ariyakul, T. Nakamoto, *Study of odor generator using extremely small liquid pump*, IEEJ Annual Meeting 2010, Vol. 3, pp. 211, Tokyo, Japan, March 2010 (in Japanese)

6. Y. Ariyakul, T. Nakamoto, *Movie with scents generated by olfactory display using SAW device and EO pumps*, ISOEN 2013, Daegu, Korea, July 2013.

Patents

1. Nakamoto, Yossiri, Odor generator, Tokugan 2010-048365, 2010.3.4

2. Nakamoto, Yossiri, Odor generator, PCT/JP2011/54790, 2011.3.2

Award

1. Honorable Mention, Intl. Conf. on Artificial Reality and Telexistence (ICAT 2011)

Bibiography

J. W. Gardner, H. W. Shin and E. L. Hines (2000). An electronic nose system to diagnose illness. Sensors and Actuators B: Chemical, Vol. 70, pp. 19-24.

M. Fleisher, E. Simon, E. Rumpel, H. Ulmer, M. Harbeck, M. Wandel, C. Fietzek, U. Weimar and H. Meixner (2002). Detection of volatile compounds correlated to human diseases through breath analysis with chemical sensors. Sensors and Actuators B: Chemical, Vol. 83, pp. 245-249.

C. Natale, A. Macagnano, E. Martinelli, R. Paolesse, G. D'Arcangelo, C. Roscioni, A. Finazzi-Agro and A. D'Amico (2003). Lung cancer identification by the analysis of breath by means of an array of non-selective gas sensors. Biosens. Bioelectron., 18, pp. 1209-1218.

J. Bastard and D. Tiran (2006). Aromatherapy and massage for antenatal anxiety: Its effect on the fetus. Complementary Therapies in Clinical Practice, Vol. 12, pp. 48-54.

M. Imura, H. Misao and H. Ushijima (2006). The Psychological effects of aromatherapy-massage in healthy postpartum mothers. Journal of Midwifery & Women's Health, Vol. 51, pp. e21-e27.

T. Atsumi and K. Tonosaki (2007). Smelling lavender and rosemary increases free radical scavenging activity and decreases cortisol level in saliva. Psychiatry Research, Vol. 150, pp. 89-96.

L. Buck and R. Axel (1991). A novel multigene family may encode odorant receptors: a molecular basis for odor recognition. Cell, 65, pp. 175-187.

P. E. Keller, R. Kouzes, L. Kangas and S. Hashem (1995). Transmission of olfactory information for telemedicine. Medicine Meets Virtual Reality III, pp. 168-172 (Chapter 27).

T. Davide, M. Holmberg, I. Lundstrom, G. Riva and F. Davide, in: G. Riva, F. Davide (Eds.) (2001). Virtual olfactory interfaces: Electronic noses and olfactory displays in Communications through Virtual Technologies, Amsterdam, IOS, pp. 194-220.

H. Hirose (2002). Sensory info-communications technology and olfactory media. Aroma Research, 10, pp. 60-65 (in Japanese).

Jones, S., Martin, R., Pilbeam, D. (1992). The Cambridge encyclopedia of human evolution. Cambridge Universty Press, New York, 1992.

Shepherd, G. M. (2004). "The human sense of smell: Are we better than we think?". PLoS Biology, Vol. 2, Issue 5, pp. 572–575.

S. Zozulya, F. Echeverri and T. Nguyen (2001). Genome Biol, Vol. 2, pp. 18.1-18.2.

K. Touhara (2001). Functional cloning and reconstitution of vertebrate odorant receptors. Life Science, 68, pp. 2199-2206.

S. Firestein (2001). How the olfactory system make sense of scents. Nature, Vol. 413, pp. 211-218.

L. Turin (1996). A spectroscopic mechanism for primary olfactory reception. Chemical Senses, 21, pp. 779-791.

L. Turin (2002). A method of the calculation of odor character form molecular structure. Journal of theoretical biology, 216, pp. 367-385.

L. Turin and F. Yosshii (2003). Structure-odor relations: a modern perspective. Handbook of Olfaction and Gustation, R. Doty ed., Marcell Dekker, New York.

S. Sato (1978), Sensory Test (Kannou Kensa Nyuumon). NIKKA GIREN (in japanese).

J. M. Murray, C. M. Delahuntyb and I. A. Baxtera (2001). Descriptive sensory analysis: past, present and future. Food Research International, Vol. 34, Issue 6, pp. 461-471.

A. Jacobsson, T. Nielsen, I. Sjoholm and K. Wendin (2004). Influence of packaging material and storage condition on the sensory quality of broccoli. Food Quality and Preference, Vol. 15, pp. 301-310.

A. Krumbein, P. Peters and B. Bruckner (2004). Flavour compounds and a quantitative descriptive analysis of tomatoes (Lycopersicon esculentum Mill.) of different cultivars in short-term storage. Postharvest Biology and Technology, Vol. 32, Issue 1, pp. 15-28.

J. E. Cometto-Muniz (2002). Chemical sensing in human and machines. Handbook of Machine Olfaction, T. C. Pearce, S. S. Schiffman, H. T. Nagle, and J. W. Gardner eds., WILEY-VCH, pp. 33-53.

Dong Wook Kim, Kazushi Nisimoto, and Susumu Kunifuji, An Editing and Displaying System of Olfactory Information for the Home Video, Lecture Notes in Artificial Intelligence 4253: 859-866 2006.

Jiang Yu, Yasuyuki Yanagida, Sinjiro Kawato, Nobuji Tetsutani, Air Cannon Design for Projection-Based Olfactory Display, ICAT 2003, December 3-5, Tokyo, JAPAN.

Masuda Yuichi, Kitano Keiichi, Yasuyuki Yanagida, Trajectory Prediction for Scent Projectors Using Range Imaging 3D-Camera, Technical report of IEICE. Multimedia and virtual environment 108(77), 25-30, 2008 (in Japanese).

T. Yamanaka, R.Matsumoto, T. Nakamoto, Sensors and Actuators B, 87 (2002), 457-463.

Takamichi Nakamoto and Hai Pham Dinh Minh, Improvement of olfactory display using solenoid valves, IEEE Virtual Reality Conference 2007, North Carolina, USA

Junta Sato, Kaori Ohtsu, Yuichi Bannai, Ken-ichi Okada, Pulse Ejection Technique of Scent to Create Dynamic Perspective, ICAT2008, ISSN:1345-1278, 167-174.

Lord Rayleigh, On waves propagation along the plane surface of an elastic solid, in Proc. London Math. Soc., 7, 1885, 4-11

J.H. Rowen, in U.S. patent 3, 289, 114, 1963

W.S. Mortley, in British patent 988, 102, 1963.

R. M. White and F. W. Voltmer, Direct piezoelectric coupling to surface elastic waves, in Appl. Phys. Lett., 7, 1965, 314-316.
E. A. Ash, Surface wave grating reflectors and resonators, in IEEE MIT Symp., 1970, 385-386.

W. R. Smith, H. M. Gaard, J. H. Collins, T. M. Reederd, and H. J. Shaw, Design of surface wave delay lines with interdigital transducers, in IEEE rans., MTT-17, 1965, 865-873.

R. H. Tancrell, Analytic design of surface wave bandpass filters, in IEEE Trans., SU-21, 1974, 12-22.

S. T. Costanza, P. J. Hagon, and L. A. MacNevin, Analog matched filter using tapped acoustic surface wave delay line, in ibd., 1974, 1042-1043.

M. Lewis, The surface acoustic wave oscillator – a natural and timely development of the quartz crystal oscillator, in 28th Ann. Freq. Control Symp., 1974, 304-314.

L. A. Coldren and R. L. Rosenburg, Surface-acoustic-wave resonator filters, in Proc. IEEE, 67, 1979, 147-158.

L. P. Solie and M. D. Wohlers, Use of a SAW multiplexer in FMCW radars system, in IEEE Trans., SU-28, 1981, 141-145.

C. M. Panasik and M. Jurgovan, Programmable transversal filter based adaptive line enhancer, in IEEE Ultrasonics Symp., 1981, 227-230.

S. Takahashim H. Hirano, T. Kodama, F. Mirashiro, B. Suzuki, A. Onoe, T. Adachi, and K. Fujinuma , SAW IF filter on $LiTaO_3$ for colour TV receivers, in IEEE Trans. Consum. Electron., CE-24, 1978, 337-348.

K. Tsubouchi, SAW devices for mobile comm., in Proc. Intl. Symp., 1992, 215-222.

E. Benesm M. Grschl, and F. Seifert, Comparison between BAW and SAW sensor principles, in IEEE Trans. Ultrason. Ferro. Freq. Control 45, 1998, 1314-1330.

M. Kurosawa, T. Watanabe, and T. Higuchi, Surface acoustic wave atomizer with pumping effect, in Proc. IEEE MEMS, 1995, 25-30.
M. Kurosawa, T. Watanabe, A. Futami, and T. Higuchi, Surface acoustic wave atomizer with pumping effect, in Sensors and Actuators A, 1995, 69-74.

S. Shiokawa and Y. Matsui, The dynamics of SAW streaming and its application to fluid devices, in Proc. 9th Symp. Ultrasonic Electronics, Sendai, 1988, Jpn. J. Appl. Phys. 28, 1988, 126-128.

S. Shiokawa, Y. Matsui, and T. Moriizumi, Experiment study on liquid streaming by SAW, in MRS Proceedings, 360, 1995, 53-64.

A. Qi, J. R. Friend, and L. Y. Yeo, Investigation of SAW atomization, in IEEE International Ultrasonics Symposium Proceedings, 2009, 787-790.

H. H. Gu, S. Y. Zhang, L. P. Cheng, D. Ma, F. M. Zhou, Z. J. Chen, and X. J. Shui, Study on non-contact linear motors driven by surface acoustic waves, in Sensors and

Actuators, A155. 2009. 163-167.

H. Zhang and L. P. Cheng, Surface acoustic wave motors and actuators: mechanism, structure, characteristic and application, in Acoustic Waves, 2010, 207-232.

A. Renaudin, P. Tabourier, J. C. Camart, and C. Druon, Surface acoustic wave two-dimensional transport and location of microdroplets using echo signal, in Journal of applied Physics, 100, 2006, 116101.

T. Monji, A. Saitoh, and T. Nomura, Development of odor supplying device using surface acoustic wave device, in Proc. Sensor Symposium, IEEJ, 2008, 167-170.

J. G. Santiago, Anal. Chem., 73, 2353-2365, 2001

Fumio Kitahara, Watanabe Shou, electrocapillarity, Kyouritu, 1978 (in Japanese)
Yanagisawa ichiro, Electroosmotic Pump, Electronic Material, vol. 44, 2005 (in Japanese)

K. Seiler, D.J.Harrison, and A. Manz, Anal. Chem. 1993, 65, 1481

P.H.Paul, D.W.Arnold, D.W.Neyer, K.B.Smith, A. Van den Berg (Ed.), μ TAS
Kluwer Academic, Dordrecht, 2000, 583

S. Yao, D. E. Hertzog, S. Zeng, J. C. Mikkelsen Jr., and J. G. Santiago, J. Colloid Interface Sci., 268, 143-153, 2003

Titus Lucretius Carus, De rerum natura (On the Nature of Things), 47 BC.

Philip de May, Lucretius: Poet and Epicurean, Cambridge University Press, 2009.

Robert Hamilton Wright, Odor and Molecular Vibration: The Far Infrared Spectra of

Some Perfume Chemicals, Annals of the New York Academy of Sciences, Vol. 116, pp. 552 – 558, 1964.

Robert Hamilton Wright, The Science of Smell. George Allen & Unwin, Ltd. London, England & Basic Books, Inc. New York, N. Y, 1964.

Robert Hamilton Wright, Odor and molecular vibration: neural coding of olfactory information, Journal of Theoretical Biology, Vol. 64, pp. 473 – 502, 1977.

John E. Amoore, Stereochemical theory of olfaction". Nature 198 (4877), pp. 271 – 272, 1963.

John E. Amoore, Current Status of the Steric Theory of Odor, Annals of the New York Academy of Sciences, Vol. 116, pp. 475 – 476, 1964.

John E. Amoore, Molecular Basis of Odor. Thomas, 1970. ISBN 0398000395.

John E. Amoore, How Smells Shape Up. American Chemical Society, 1977.

Benjamin Auffarth, Understanding smell—The olfactory stimulus problem, Neuroscience & Biobehavioral Reviews, Vol. 37, Issue 8, September 2013, pp. 1667–1679.

Luca Turin, A Spectroscopic mechanism for primary olfactory reception, Chemical Senses, Vol 21/ 6 pp. 773 – 791, 1996.

Andreas Keller and Leslie B. Vosshall, Testing a radical theory, NATURE NEUROSCIENCE, Vol. 7, Num. 4, pp. 337, 2004.

Joseph Nathaniel Kaye, Symbolic Olfactory Display, Master Thesis, Massachusetts Institute of Technology, 2001.

Takamichi Nakamoto and Keisuke Murakami, Selection Method of Odor Components for Olfactory Display Using Mass Spectrum Database, IEEE Virtual Reality Conference, pp.159 – 162, 2009.

F. F. Reuss, Sur un nouvel effet de l'électricité galvanique, Mémoires de la Société Impériale des Naturalistes de Moscou, 1809, 2, 327-337.

F. Kohlrausch, Uber Concentrations-Verschiebungen durch Elektrolyse im Inneren von Losungen und Losungsgemischen. Ann. Phys. Chem. (Leipzig), 1897, 62, 209-239.

R.J. Hunter, Zeta Potential in Colloidal Science: Principles and Applications, Academic Press, London, 1981.

R.F. Probstein, Physicochemical Hydrodynamics, An Introduction 2nd Edition, John Wiley and Sons, Massachusetts Institute of Technology, 1994.

C.L. Rice and R. Whitehead, J. Phys. Chem., 1965, 69, 4017.

S. Ghosal, Fluid mechanics of electroosmotic flow and its effect on band broadening in capillary electrophoresis, Electrophoresis, 2004, 25, 214–228.

Yanagisawa Ichiro, Electroosmotic Pump, Electronic Material, vol. 44, 2005 (in Japanese).

A. Brask, Electroosmotic micropumps, Ph.D. dissertation, Dept. Micro. Nanotechnol., Tech. Univ. Denmark, Copenhagen, Denmark, 2005.

Nano Fusion Technologies, Inc, Micro Electro-osmotic Pump - Summary -, March 2009.

K. Seiler, D. J. Harrison, and A. Manz, Anal. Chem., 1993, 65, pp. 1481-1488.

S. Yao, D. E. Hertzog, S. Zeng, J. C. Mikkelsen Jr., and J. G. Santiago, J. Colloid Interface Sci., 2003, 268, 143-153.

P. H. Paul, D. W. Arnold, D. W. Neyer, K. B. Smith, Electrokinetic pump application in micro-total analysis system mechanical actuation to HPLC, in Micro Total Analysis Systems' 2000 (eds A. W. Van Den Berg, P. Olthuis, and P. Bergveld), Kluwer, Boston MA, 583-590.

H. Takigawa, Study on odor recorder composed of odor presenting device using inkjet devices, Master thesis, Dept.Physical Electronics, Tokyo Institute of Technology, Tokyo, Japan, 2004 (in Japanese).

Nakamoto, Human Olfactory Displays and Interfaces Odor Sensing and Presentation, IGI Global, 2012.

Yasuyuki Yanagida , Shinjiro Kawato , Haruo Noma , Akira Tomono , and Nobuji Tetsutani, Projection-Based Olfactory Display with Nose Tracking, Proceedings of IEEE Virtual Reality 2004, pp. 43 – 50.

Heilig ML. Stereoscopic-television apparatus for individual use. US2955156, 1960.

M. Heilig, Sensorama simulator, U.S.Patent # 3050870, 1962.

M. Heilig, Experience theater, U.S.Patent # 3628829, 1971.

T. Nakamoto, Interactive Odor Playback Based on Fluid Dynamics Simulation, IEEE Virtual Reality 2009 poster, 255-256.

Sayumi Sugimoto, Daisuke Noguchi, Yuichi Bannnai, Kenichi Okada, Ink jet olfactory display enabling instantaneous switches of scents, Proceeding MM '10 Proceedings of the international conference on Multimedia, pp. 301-310.

Dong Wook Kim, Yeong Hee Cho, Nishimoto, K., Kawakami, Y., Kunifuji, S., Ando, H., Development of aroma-Card based soundless Olfactory Display, Electronics, Circuits, and Systems, 2009. ICECS 2009, pp.703 - 706, 2009.

K. Murai, T. Serizawa, Y. Yanagida, Localized scent presentation to a walking person by using scent projectors, R Innovation (ISVRI), 2011 IEEE International Symposium on , pp. 67 - 70, 2011.

Tomoya Yamada, Satoshi Yokoyama, Tomohiro Tanikawa, Koichi Hirota, Michitaka Hirose, Wearable Olfactory Display: Using Odor in Outdoor Environment, vr, pp.199-206, IEEE Virtual Reality Conference (VR 2006), 2006.

Morie J. F., lyer, K., Valanejad, K., Sadek, R., Miraglia, D., Milam, D., Williams, J., Luigi, D-P., Sensory design for virtual environments, Proceeding of ACM SIGGRAPH, Sketches, San Diego.

H. Matsukura, T. Yoneda, H. Ishida, Smelling Screen: Development and Evaluation of an Olfactory Display System for Presenting a Virtual Odor Source, IEEE Transactions on Visualization and Computer Graphics, vol. 19, no. 4, pp. 606-615, April 2013.

Dong Wook Kim, Hiroshi Ando, Development of directional olfactory display, VRCAI '10 Proceedings of the 9th ACM SIGGRAPH Conference on Virtual-Reality Continuum and its Applications in Industry, pp. 143-144.

Kim, H., Park, J., Noh, K., Gardner, C. J., Kong, S. D., Kim, J. and Jin, S., An X–Y Addressable Matrix Odor-Releasing System Using an On–Off Switchable Device. Angew. Chem. Int. Ed., 50: 6771–6775, 2011.

Kashiwagi Kenta, Tech. Digest of IEEJ Sensor Symposium, 2012, SPLN-9.

ABOUT THE AUTHOR

Yossiri Ariyakul has pursued his Ph.D. in the Department of Physical Electronics at the Tokyo Institute of Technology, Japan, since 2010. He received his B.E. (Hons.) degree from the Department of Electronics Engineering, King Mongkut's Institute of Technology Ladkrabang, Bangkok, Thailand, in 2006. In 2010, he received his M.E. degree from the Department of Physical Electronics, Tokyo Institute of Technology, Tokyo, Japan. He worked for Sony Device Technology (Thailand) Co., Ltd. and PTT Chemical Public Company Limited in 2005 and 2006, respectively.